

**Development of a new therapeutic regime for
the treatment of glioblastoma multiforme
(GBM)**

Joshua Rory Day Pearson

N0660672

A thesis submitted in partial fulfilment of the requirements of Nottingham Trent
University for the degree of Doctor of Philosophy

This research was carried out in collaboration with the University of Portsmouth

October 2019

COPYRIGHT STATEMENT

This work is the intellectual property of the author. You may copy up to 5 % of this work for private study, or personal, non-commercial research. Any re-use of the information contained within this document should be fully referenced, quoting the author, title, university, degree level and pagination. Queries or requests for any other use, or if a more substantial copy is required, should be directed to the owner of the Intellectual Property Rights.

ABSTRACT

Glioblastoma multiforme is the most frequently occurring primary brain tumour and it carries a dismal prognosis. Despite surgical intervention and aggressive chemo-radiotherapy the median survival of patients is just under 15 months. Very little progress has been made with regards to improving patient survival therefore novel therapeutic interventions are required.

Vaccination offers an attractive option for the therapeutic treatment of GBM, with activated T-cells previously being shown to access tumours located within the brain resulting in improved survival in pre-clinical murine models of GBM. Several vaccine platforms have been developed and tested in GBM patients, however many of these therapies fail during clinical trials and as of 2019 no immunotherapeutic treatments have been approved for use in the GBM setting. One major obstacle to overcome when using the immune system to treat GBMs is the highly immunosuppressive phenotype these cancers have. GBMs frequently express immunosuppressive checkpoints that prevent anti-tumour T-cell activity. Immune checkpoint blockade has recently gained approval for the treatment of malignant melanoma, lung cancer, head and neck cancer, lymphoma, bladder cancer and kidney cancer. The utilisation of immune checkpoint blockade as a monotherapy improves survival in small subsets of patients however it is not a completely curative treatment modality. Therefore it is of great interest to see if combining immune checkpoint blockade with vaccine therapy can boost anti-tumour immunity by stimulating T-cells and preventing the inhibitory signals from tumour cells that prevent T-cell killing.

Examination of GBM tumour tissues and cell lines revealed that a large proportion of GBMs express the immunogenic antigens Tyrosinase-related protein-2 (TRP-2) and Wilms' tumour 1 (WT-1). It was also revealed that these tumours expressed several immunosuppressive proteins with PD-L1, HLA-E and HLA-G expression being observed in tissues and cell lines studied. It was also revealed that when GBM cell lines were treated with the immune stimulating cytokine IFN γ they up-regulated the immunosuppressive proteins PD-L1 and IDO.

The ImmunoBody[®] DNA plasmid vaccination encodes an IgG antibody molecule that acts as a carrier protein for the peptide targets of interest, these peptides are engrafted into the complementarity determining regions of the antibody. This method of vaccination generates a strong-immune response via direct and cross-presentation. Pre-clinical testing using the humanised HHDII/DR1 C57BL/6 mouse model revealed that a HLA-A2 specific TRP-2 and a HLA-A2 specific WT-1 directed ImmunoBody[®] vaccine generated a strong peptide specific immune response. When both vaccinations were given simultaneously this strong TRP-2 and WT-1 directed immune response was

equivalent to when each vaccine was given alone meaning that epitope dominance is not a factor when targeting these two antigens.

Using the HHDII/DR1 humanised mouse the effects of this dual ImmunoBody® vaccination regime was tested both prophylactically and therapeutically. In these proof of concept experiments the B16 HHDII/DR1 Luc2 cell line was utilised. This cell line expresses both TRP-2 and WT-1 antigens and it has the chimeric HLA-A2 HHDII/DR1 MHC molecule meaning it presents HLA-A2 specific peptides. When the dual ImmunoBody® vaccination regime was used prophylactically it significantly improved the survival of mice intracranially implanted with B16 HHDII/DR1 Luc2 cells compared to sham vaccinated mice. In the therapeutic setting the addition of an anti-PD-1 blocking antibody to the dual vaccination regime improved survival of B16 HHDII/DR1 Luc1 tumour bearing mice when compared to dual vaccinated mice receiving PD-1 isotype control antibody and control sham vaccinated mice that received PD-1 isotype antibody. Analysis of tumour infiltrating lymphocyte populations revealed that dual vaccination increases CD8⁺ T-cell infiltrate into these intracranial tumours with these cells showing increased cell surface expression of the activation markers CD25 and CD69.

The dipeptide carnosine was also used to treat GBM cells *in vitro*, this molecule has previously been shown to have anti-tumour activity. When carnosine was used to treat GBM cells it led to reduced mitochondrial metabolism and migration of these cells. These properties make carnosine an attractive adjunct to immunotherapy.

Overall these results provide promise for the use of ImmunoBody® vaccination with immune checkpoint blockade for the treatment of GBM. Whilst immune cells can actively access tumours systemically administered checkpoint antibodies don't cross the blood-brain-barrier freely, therefore in order for these therapies to be further developed methods for improving brain penetrance of checkpoint inhibitors needs to be explored.

ACKNOWLEDGEMENTS

The last four years have been filled with ups and downs and this thesis represents the culmination of many failed and successful experiments.

Firstly I would like to thank anyone who said that I couldn't do it or that this was not possible, you were my main driving force when times were tough.

I would like to thank my family and friends, you were always there to support me despite not having a clue what it was that I have been doing this past four years. Thank you for your patience and understanding throughout this process.

I would like to thank everyone at the John van Geest Cancer Research Centre who provided me with help and support throughout my time here. Thank you to Dr. Stephanie McArdle for giving me the opportunity to work on this project, your help and guidance has been invaluable. I would also like to thank my other supervisors Prof. Graham Pockley and Dr. Tarik Regad for providing me support and helping me develop as a scientist. I would also like to thank Steve Reeder, Anne Schneider and Cathy Johnson for keeping the centre running and providing support to all of the students during tough times. I would also like to thank Murrium Ahmad, Andy Marr, Lou Wainwright, Adam McVicar and Joe Lenton for making all of the *in vivo* work possible and looking after the welfare of experimental animals. Headcase cancer trust also deserve my thanks for financially supporting this project and making it possible.

I would also like to thank the members of the University of Portsmouth neuro-oncology lab for providing me with valuable experience and mentoring me during my short stay at the start of my PhD.

Thank you to Scancell Ltd. for generously allowing me to use their ImmunoBody® DNA vaccine platform in this project.

I would also like to thank my girlfriend for keeping me sane during tough times, you don't realise it but all of the support you have provided me throughout this process has made it all possible.

Finally I would like to dedicate this thesis to my friend Jamie who unfortunately lost his life this year, we all really miss you and you are always in our thoughts.

PUBLICATIONS

Publications published during this thesis

Pearson J.R.D. and Regad T. (2017) Targeting cellular pathways in glioblastoma multiforme. *Signal transduction and targeted therapy*. 2, e17040; doi:10.1038/sigtrans2017.40.

Al-Juboori S.I., Vadakekolathu J., Idri S., Wagner S., Zafeiris D. **Pearson J.R.**, Almshayakhchi R., Caraglia M., Desiderio V., Miles A.K., Boocock D.J., Ball G.R. and Regad T. (2019) PYK promotes HER2-positive breast cancer invasion. *J. Exp. Clin. Cancer Res.* 22; 38 (1):210. Doi: 10.1186/s13046-019-1221-0.

Conference posters

Pearson J.R.D., Durrant L.G., Brentville V.A., Pockley A.G. and McArdle S.E.B. (2018) Abstract B122: Development of a new immunotherapy treatment for glioblastoma multiforme. *Cancer Immunology Research*. Doi: 10.1158/2326-6074.CRICIMTEATIAACR18-B122.

TABLE OF CONTENTS

Copyright statement	1
Abstract.....	2
Acknowledgements.....	4
Publications.....	5
List of Figures	10
List of Tables	16
Abbreviations.....	17
Chapter 1: Introduction	21
1.1. Cancer	21
1.2. Glioblastoma multiforme.....	21
1.3. Glioblastoma multiforme therapy	23
1.4. Immunotherapy	24
1.5. The immune system in glioblastoma multiforme	28
1.6. Vaccination and the immune response	30
1.7. Human leukocyte antigen (HLA) haplotypes	32
1.8. GBM tumour immune escape	34
1.9. Immune checkpoint blockade for GBM	40
1.10. ImmunoBody® vaccination	40
1.11. Carnosine as a first line non-toxic therapeutic	44
1.12. Aims	45
Chapter 2: Materials and methods	46
2.1. Materials used.....	46
2.1.1. Cell lines	46
2.1.2. Reagents.....	47
2.1.3. Buffer recipes.....	52
2.1.4. Antibodies for Western blotting	58
2.1.5. Antibodies for immunohistochemistry	59
2.1.6. Antibodies for immunofluorescence/immunocytochemistry	60
2.1.7. Antibodies for flow cytometry.....	60
2.1.7.3. Antibodies for brain TIL staining	62
2.2. Methods.....	63
2.2.1. Cell culture	63
2.2.2. Immunohistochemistry	64
2.2.3. Western blotting	66
2.2.4. Immunocytochemistry/immunofluorescence	70
2.2.5. Flow cytometry	71

2.2.6. DNA bullet preparation.....	77
2.2.7. Immunisation and ELISpot analysis.....	80
2.2.8. Brain tumour modelling.....	86
2.2.9. Kynurenine assay	87
2.2.10. Carnosine related experiments.....	87
Chapter 3: Antigens expression profile of glioblastoma multiforme tissues and cell lines.....	89
3.1. Introduction	89
3.2. Aims and hypothesis	94
3.3. Results.....	95
3.3.1. IHC analysis of GBM tissues reveals that the immunogenic TRP-2 and WT-1 antigens are viable targets for immunotherapeutic targeting of GBM.....	95
3.3.2. TRP-2 and WT-1 expression are also commonly expressed in GBM cell lines as well as in tissues	99
3.3.3. Analysis of GBM tumour tissues reveal that these tissues have an immunosuppressive phenotype, but these tissues appear to maintain their antigen presentation capabilities ...	101
3.3.4. GBM cell lines also have an immunosuppressive phenotype much like the tissues they are derived from	105
3.3.5. Flow cytometric analyses GBM cell lines reveals expression of both immune inhibitory and immune activating proteins on the surface of these cells.....	107
3.3.6. The TRP-2 and WT-1 antigens are expressed by the murine GL261 Luc2 and B16 HHDII/DR1 Luc2 cell lines.....	113
3.4. Discussion.....	116
3.5. Conclusion.....	120
Chapter 4: Pre-clinical evaluation of the ImmunoBody® DNA vaccines	121
4.1. Introduction	121
4.1.1. Vaccination.....	121
4.1.2. Antigen presentation and the immunoproteasome.....	124
4.1.3. Immune escape and the three Es	127
4.1.4. Epitope dominance	128
4.1.5. ImmunoBody® vaccination	128
4.1.6. The humanised HHDII/DR1 C57BL/6 mouse model.....	129
4.2. Aims and hypothesis	131
4.3. Results.....	131
4.3.1. ImmunoBody® vaccination generates a strong anti-TRP-2 and WT-1 immune response in the C57BL/6 HHDII/DR1 mouse	131
4.3.2. Flow cytometric analysis of the ImmunoBody® activated immune cells reveals that ImmunoBody® vaccination generates a strong CD8 ⁺ T-cell response.....	140
4.3.3. Splenocytes from ImmunoBody® vaccinated mice recognise GBM cell lines expressing TRP-2 and WT-1 in an HLA-A2 restricted manner.....	151
4.4. Discussion.....	153

4.5. Conclusion.....	156
Chapter 5: Immune escape mechanisms employed by glioblastoma multiforme in response to immunotherapy	157
5.1. Introduction	157
5.2. Aims and hypothesis	160
5.3. Results.....	160
5.3.1. Analysis of CD119 expression on GBM cell lines.....	160
5.3.2. The effects of IFN γ on the immune profile of the SF-188 and SEBTA-027 glioblastoma multiforme cell lines as determined by flow cytometry.....	163
5.3.3. Expression of IDO in IFN γ treated GBM cell lines and measurement of IDO activity...177	
5.4. Discussion.....	181
5.5. Conclusion.....	184
Chapter 6: Pre-clinical anti-tumour assessment of the combined ImmunoBody [®] vaccines	185
6.1. Introduction	185
6.1.1. The intracranial B16 HHDII/DR1 proof of concept model	188
6.2. Aims and hypothesis	188
6.3. Results.....	189
6.3.1. Prophylactic vaccination with dual SCIB1 and WT-1 ImmunoBody [®] vaccination prolongs survival in mice bearing intracranial B16 HHDII/DR1 Luc2 tumours	189
6.3.2. Addition of checkpoint blockade into the ImmunoBody [®] vaccination strategy effects on tumour bearing animal survival	191
6.3.3. Flow cytometric analysis of brain tumour infiltrating lymphocytes from mice given therapeutic ImmunoBody [®] and anti-PD-1 treatment	195
6.4. Discussion.....	205
6.5. Conclusion.....	208
Chapter 7: Carnosine as a natural therapy for glioblastoma multiforme.....	209
7.1. Introduction	209
7.2. Aims and hypothesis	210
7.3. Results.....	210
7.3.1. Effects of carnosine on the mitochondrial activity of glioblastoma multiforme cell lines	210
7.3.2. Effects of carnosine on the migration of glioblastoma multiforme cells.....	214
7.3.3. <i>In vivo</i> effects of carnosine GL261 Luc2 bearing NOD-SCID mice.....	220
7.4. Discussion.....	222
7.5. Conclusion.....	224
Chapter 8: Discussion and future work.....	225
8.1. GBM tumours express immunogenic antigens that make them targetable with immunotherapy however they also have an immunosuppressive phenotype	226

8.2. ImmunoBody® vaccination generates a strong anti-tumour immune response and the addition of checkpoint blockade appears to help tumour infiltrating immune cells overcome intratumoural immunosuppression	228
8.3. GBM cells can respond to IFN γ in their local environment and adapt their immune-related antigen expression profile	229
8.4. Carnosine represents an attractive natural therapy for GBM	231
8.5. Issues with brain tumour immunotherapy	232
8.6. Improving future immune therapy for glioblastoma multiforme.....	234
8.7. Improving immune cell transit into the brain of vaccinated mice.....	236
8.8. Incorporation of immunotherapy into standard therapy	238
8.9. Concluding remarks	240
References	241
Appendices.....	266

LIST OF FIGURES

Figure 1. A diagram of how the immune checkpoints PD-1/PD-L1 and CTLA-4 dampen the immune response. PD-L1 expressed on tumour cells binds to PD-1 on T-cells resulting in the death of the PD-1 expressing T-cells. CTLA-4 on T-cells outcompetes CD28 when binding to B7 molecules preventing the activation of the T-cell, the CTLA-4 binding to the B7 molecules can also transendocytose the B7 molecules and lead to their degradation. Adapted from (Reardon, Freeman et al. 2014)	26
Figure 2. A schematic representation of the structure of MHC class I and II molecules. Alpha subunits are represented by green shading whilst the beta sub-units and beta 2 m molecules are shaded yellow. Adapted from (Janeway, Capra et al. 2001).	33
Figure 3. A schematic representation of the SCIB1 ImmunoBody® plasmid with the gp100 and TRP-2 peptide sequences detailed, and their insertion sites outlined. Diagram provided in a correspondence from Scancell Ltd.	43
Figure 4. ImageJ identification of protein lanes on Western blot membrane image followed by intensity peaks for each band.	69
Figure 5. Gating strategy employed when examining the cell surface antigen expression of GBM cell lines.....	72
Figure 6. Gating strategy employed when examining the cell surface and intracellular antigen expression profiles of vaccinated splenocytes.	74
Figure 7. Gating strategy employed when examining the cell surface and intracellular antigen expression profiles of brain tumour infiltrating lymphocytes.	76
Figure 8. Plasmid map of the SCIB1 ImmunoBody® plasmid.....	78
Figure 9. Plasmid map of the WT1 ImmunoBody® plasmid.....	78
Figure 10. Vaccination schedule used for testing the immune response to ImmunoBody® vaccination and for prophylactic experiments.	81
Figure 11. Vaccination schedule used for the therapeutic treatment of intracranial B16HHDII/DR1 Luc2 tumours.	83
Figure 12. Diagrams of adenine and guanine bases with the atoms methylated by temozolomide highlighted.	91
Figure 13. Methylation of guanine by the methyl diazonium ion. The methyl group is represented by the pink CH3 highlighted on the figure.	93
Figure 14. TRP-2, WT-1, gp100, HAGE and MGMT expression as observed in tissue microarray staining. A) A graphical representation of target antigen expression as observed in tissue microarray staining. B) Numerical representation of positive staining results. Percentages show the number of cases that stained positively, irrespective of the strength of the staining.....	96
Figure 15. Examples of pathologist's WT-1 IHC scoring A) 3 (deemed as strong staining) B) 2 (deemed as moderate staining) C) 1 (deemed as weak staining) D) 0 (no staining). Scale bar = 100 µm.	98
Figure 16. Examples of pathologist's TRP-2 IHC scoring A) 3 (deemed as strong staining) B) 2 (deemed as moderate staining) C) 1 (deemed as weak staining) D) 0 (no staining). Scale bar = 100 µm.	98
Figure 17. TRP-2, HAGE, WT-1, MGMT and gp100 expression in GBM cell lines as determined by Western blotting, 20 µg of protein was loaded per lane as described in chapter 2 A) TRP-2 expression as detected by a TRP-2 specific antibody B) HAGE expression as detected by a HAGE specific antibody, PCI-13 is a head and neck cancer cell line that is known to be positive for HAGE expression and as a result was used as a positive control (this lysate was obtained ready prepared for use) C) WT-1 expression as detected by a WT-1 specific antibody D) MGMT expression as detected by a MGMT specific antibody E) gp100 expression as detected by a gp100 specific antibody. All membranes were also probed with an anti-vinculin antibody that acted as a loading control due to its abundant expression.	100
Figure 18. PD-L1, HLA-G, HLA-E and HLA-A, B, C expression as observed in tissue microarray staining. A) A graphical representation of the percentage of cases the stained positive for each	

antigen B) Numerical representation of the staining results. Percentages show the number of cases that stained positively, irrespective of the strength of the staining.	102
Figure 19. Example of pathologist's HLA-E IHC scoring. A) 3 (deemed as strong staining) B) 2 (deemed as moderate staining) C) 1 (deemed as weak staining) D) 0 (no staining). Scale bar = 100 μ m.	104
Figure 20. Example of pathologist's HLA-A,B,C IHC scoring. A) 3 (deemed as strong staining) B) 2 (deemed as moderate staining) C) 1 (deemed as weak staining) D) 0 (no staining). Scale bar = 100 μ m.	104
Figure 21. HLA-G, PD-L1, HLA-E and HLA-A, B, C expression in GBM cell lines as determined by Western blotting, 20 μ g of protein was loaded per lane as described in chapter 2 A) HLA-G expression as detected by a HLA-G specific antibody B) PD-L1 expression as detected by a PD-L1 specific antibody C) HLA-E expression as detected by a HLA-E specific antibody D) MHC class I expression as detected by a HLA-A, B, C pan-specific antibody. All membranes were also probed with an anti-vinculin antibody that acted as a loading control due to its abundant expression. ...	106
Figure 22. Flow cytometric surface staining histograms of HLA-A2 the green peaks represent unstained cells whereas the red peaks represent cells stained with HLA-A2 APC. A) SEBTA-025 B) SEBTA-027 C) SF188 D) UP-007 E) UP-019.	108
Figure 23. SEBTA-025 flow cytometry surface staining, the green peaks represent unstained cells whereas the red peaks represent stained cells. Each antigen is labelled on the X axis of each histogram. The table in the right-hand corner details the percentage of cells positive for each antigen. Further detailed histograms for each cell line can be seen in appendix 1.	110
Figure 24. Representative images of immunofluorescence staining of the GL261Luc2 cell line. A) Positive TRP-2 staining as detected by an anti-mouse/human TRP-2 antibody, 100% of cells stained were positive for TRP-2 B) Positive WT-1 staining as detected by an anti-mouse/human WT-1 antibody, 100% of cells stained were positive for WT-1 C) No primary antibody control. Nuclei are counterstained blue with DAPI and positive antigen staining is represented by green fluorescence. Scale bar = 50 μ m.	114
Figure 25. Representative images of Immunocytochemical staining of the B16HHDII/DRI/Luc2 cell line. A) Positive TRP-2 staining as detected by an anti-mouse/human TRP-2 antibody, staining is apparent on the surface of cells B) Positive WT-1 staining as detected by an anti-mouse/human WT-1 antibody, staining can be seen localised in small cytoplasmic areas this is due to WT-1 being a transcription factor. Black arrows highlight some areas of positive staining C) No primary antibody control. Nuclei are stained blue/light purple and positive antigen staining is represented by brown colouration. Scale bar = 150 μ m.	115
Figure 26. A diagram of the transgenic HHDII MHC class I molecule. The transmembrane and α_3 domain are of murine origin whereas the α_1 and α_2 domains are of human origin with the human β_2M being covalently linked to the α_1 domain.	130
Figure 27. The vaccination schedule utilised to study the immunogenicity of the ImmunoBody [®] vaccine. The top left area of the figure details the days that mice were dosed, with vaccines administered at weekly intervals. Mice were split into three groups; one receiving SCIB1 (TRP-2) ImmunoBody [®] , one receiving WT-1 ImmunoBody [®] and one receiving both SCIB1 (TRP-2) and WT-1 ImmunoBody [®]	132
Figure 28. IFN γ ELISpot results from splenocytes from SCIB1 ImmunoBody [®] vaccinated mice. N= 9-3, *= P \leq 0.05 as defined by a two-way ANOVA followed by Tukey' s post hoc test. The three letter annotations after the peptide correspond to the first three amino acids of the peptide used to stimulate the splenocytes, the full sequences of these peptides are detailed in the methods (chapter 2).	134
Figure 29. IFN γ ELISpot results from splenocytes from WT-1 ImmunoBody [®] vaccinated mice. N= 9-3, *= P \leq 0.05, ***= P \leq 0.001 as defined by a two-way ANOVA followed by Tukey' s post hoc test. The three letter annotations after the peptide correspond to the first three amino acids of the peptide used to stimulate the splenocytes, the full sequences of these peptides are detailed in the methods (chapter 2).	134

Figure 30. IFN γ ELISpot results from splenocytes from SCIB1 and WT-1 ImmunoBody[®] vaccinated mice compared with mice vaccinated with both SCIB1 and WT-1 ImmunoBody[®] simultaneously. N= 9, ns= not significant as deemed by a two-way ANOVA followed by Tukey's post hoc test. The three letter annotations after the peptide correspond to the first three amino acids of the peptide used to stimulate the splenocytes, the full sequences of these peptides are detailed in the methods (chapter 2).136

Figure 31. IFN γ ELISpot results from splenocytes from SCIB1 ImmunoBody[®] vaccinated mice compared with mice vaccinated with both SCIB1 and WT-1 ImmunoBody[®] simultaneously. A) Splenocytes were treated with the SVYDFVWL TRP-2 peptide sequence diluted in 10-fold increments from 1 $\mu\text{g}/\text{mL}$ - 0.0000001 $\mu\text{g}/\text{mL}$. B) Data was normalised and transformed, and non-linear fit comparisons were made, these analyses revealed that there was no significant difference between the EC50 of SCIB1 and dual vaccinated mice.....138

Figure 32. IFN γ ELISpot results from splenocytes from WT-1 ImmunoBody[®] vaccinated mice compared with mice vaccinated with both SCIB1 and WT-1 ImmunoBody[®] simultaneously. A) Splenocytes were treated with the ALLPAVPSL WT-1 peptide sequence diluted in 10-fold increments from 1 $\mu\text{g}/\text{mL}$ - 0.0000001 $\mu\text{g}/\text{mL}$. B) Data was normalised and transformed, and non-linear fit comparisons were made, these analyses revealed that there was no significant difference between the EC50 of WT-1 and dual vaccinated mice.139

Figure 33. A representative set of flow cytometry plots of splenocytes isolated from vaccinated mice after peptide stimulation. These plots are from a mouse that received dual vaccination. The gating strategy can be seen in the methods sections (Chapter 2). All these plots are from CD3 positive live cells. A) Histogram of the CD8⁺ CD107⁺ cells. B) Histogram of the CD4⁺ CD107⁺ cells. C) Histogram of the CD8⁺ TNF α ⁺ cells. D) Histogram of the CD4⁺ TNF α ⁺ cells. E) Histogram of the CD8⁺ Ki67⁺ cells. F) Histogram of the CD4⁺ Ki67⁺ cells. G) Histogram of the CD8⁺ IL-2⁺ cells. H) Histogram of the CD4⁺ IL-2⁺ cells. I) Histogram of the CD8⁺ IFN γ ⁺ cells. J) Histogram of the CD4⁺ IFN γ ⁺ cells. K) Histogram of the CD8⁺ Granzyme B⁺ cells. L) Histogram of the CD4⁺ Granzyme B⁺ cells. Plots M-O show scatter plots of the CD8⁺ cells stained with TNF α (on the x axis) and IFN γ (on the y axis). Double positive cells are in the top right quadrant. M) Splenocytes receiving no peptide stimulation. N) Splenocytes receiving class I peptide stimulation. O) Splenocytes receiving class I and class II peptide stimulation. Plots P-R show scatter plots of the CD4⁺ cells stained with TNF α (on the x axis) and IFN γ (on the y axis). Double positive cells are in the top right quadrant. P) Splenocytes receiving no peptide stimulation. Q) Splenocytes receiving class I peptide stimulation. R) Splenocytes receiving class I and class II peptide stimulation. For plots A-L the blue peak represents splenocytes stimulated with both class I and II peptides, the green peak represents splenocytes stimulated with class I peptides only and the red peak represents splenocytes that received no peptide stimulation. The gate used to determine the percentage of positive cells is shown on each histogram and the percentage of positive cells gated is shown next to the histogram.142

Figure 34. Flow cytometric analysis of CD3+ CD8+ splenocytes from SCIB1 ImmunoBody[®] vaccinated mice that were either unstimulated (no peptide) or stimulated with TRP-2 class I (SVYDFVWL) peptide. A) % CD107⁺ CD8 T cells. B) % TNF α ⁺ CD8 T cells. C) % Ki67⁺ CD8 T cells. D) % IFN γ ⁺ CD8 T cells. E) % Granzyme B⁺ CD8 T cells. F) % TNF α ⁺ and IFN γ ⁺ CD8 T cells. N = 4, * = $p \leq 0.05$ as deemed by a paired T-test.....144

Figure 35. Flow cytometric analysis of CD3+ CD8+ splenocytes from WT-1 ImmunoBody[®] vaccinated mice that were either unstimulated (no peptide), stimulated with WT-1 class I (ALLPAVPSL) peptide or stimulated with both class I (ALLPAVPSL) and class II (VRDLNALLPAVPSLG) peptides. A) % CD107⁺ CD8 T cells. B) % TNF α ⁺ CD8 T cells. C) % Ki67⁺ CD8 T cells. D) % IFN γ ⁺ CD8 T cells. E) % Granzyme B⁺ CD8 T cells. F) % TNF α ⁺ and IFN γ ⁺ CD8 T cells. N = 7, all results were deemed non-significant by a one-way ANOVA followed by Tukey's post-hoc test.....146

Figure 36. Flow cytometric analysis of CD3+ CD8+ splenocytes from dual SCIB1 and WT-1 ImmunoBody[®] vaccinated mice that were either unstimulated (no peptide), stimulated with TRP-2 and WT-1 class I peptides or stimulated with both class I (TRP-2 and WT-1) and WT-1 class II peptides. A) % CD107⁺ CD8 T cells. B) % TNF α ⁺ CD8 T cells. C) % Ki67⁺ CD8 T cells. D) % IFN γ ⁺ CD8 T

cells. E) % Granzyme B ⁺ CD8 T cells. F) % TNFα ⁺ and IFNγ ⁺ CD8 T cells. N = 7, * = P ≤ 0.05 as deemed by a one-way ANOVA followed by Tukey's post-hoc test.	148
Figure 37. Flow cytometric analysis of CD3 ⁺ CD8 ⁺ splenocytes from naive mice that were either unstimulated (no peptide), stimulated with TRP-2 and WT-1 class I peptides or stimulated with both class I and WT-1 class II peptides. A) % CD107 ⁺ CD8 T cells. B) % TNFα ⁺ CD8 T cells. C) % Ki67 ⁺ CD8 T cells. D) % IFNγ ⁺ CD8 T cells. E) % Granzyme B ⁺ CD8 T cells. F) % TNFα ⁺ and IFNγ ⁺ CD8 T cells. N = 7, all results are non-significant as deemed by a one-way ANOVA followed by Tukey's post-hoc test.	150
Figure 38. IFNγ ELISpot results from splenocytes from SCIB1 and WT-1 ImmunoBody [®] vaccinated mice compared with mice vaccinated with both SCIB1 and WT-1 ImmunoBody [®] simultaneously when exposed to the human GBM cell lines SF-188 and SEBTA-027. When splenocytes were co-cultured with the SEBTA-027 cell line they produced a number of spots above the maximum detectable limit, as a result these results were counted as 600 (the maximum number the machine can count). N= 9, ****= P ≤ 0.0001, ns= not significant as deemed by a two-way ANOVA followed by Tukey's post hoc test.....	152
Figure 39. A schematic representation of tryptophan catabolism and the enzymes involved. IDO= indoleamine 2,3-dioxygenase, TDO= tryptophan 2,3-dioxygenase, KMO= kynurenine 3-monooxygenase, KYNU= kynureninase, QPRT= Quinolinic phosphoribosyltransferase.	159
Figure 40. Representative flow cytometry histograms of CD119 staining of A) SEBTA-027 B) SF-188 cells, the red peak represents stained cells and the green peak represents unstained cells.....	162
Figure 41. Representative flow cytometry histograms of IFNγ and control untreated live SF-188 cells. The red peak represents 24hr control cells, the green peak represents 48hr control cells, the blue peak represents 72hr control cells, the purple peak represents cells treated with IFNγ for 24 hours, the orange peak represents cells treated with IFNγ for 48 hours and the light blue peak represents cells treated with IFNγ for 72 hours. The gate is shown on each plot and the % of cells gated and the median fluorescence intensity (X-med) are shown alongside each plot. A) MICA/B B) FasL C) CD80 D) HLA-E E) HLA-G F) PD-L1 G) CD40 H) HLA-A,B,C I) CD86 staining.	166
Figure 42. Percentage of cells positive for cell surface expression of A) HLA-E B) HLA-G C) CD40 after 24,48 and 72 hours exposure to IFN γ . ****= P ≥0.0001, ***= P ≤0.001, **= P ≤0.01, *= P ≤0.05 relative to control as deemed by a one-way ANOVA followed by Tukey's ad-hoc test. N= 9-3. The control group is composed of control cells that had normal carnosine free GBM media on them for 24, 48 and 72 hours, these controls were grouped as the time difference was not deemed to have a significant effect on antigen expression.	167
Figure 43. Median fluorescence intensity results for IFNγ treated SF-188 cells A) PD-L1 B) HLA-E C) HLA-G D) HLA-A, B, C E) CD40. ****= P ≥0.0001, *= P ≤0.05 relative to control as deemed by a one-way ANOVA followed by Tukey's ad-hoc test. N= 9-3. The control group is composed of control cells that had normal media on them for 24, 48 and 72 hours. The increase in MFI indicates an increase in the number of molecules present on the cell surface.	169
Figure 44. Percentage of cells positive for cell surface expression of A) HLA-E B) HLA-G C) CD40 after 24, 48 and 72 hours growth in normal 'control' media that lacked IFNγ. There is no significant difference between any of the conditions as deemed by a one-way ANOVA followed by Tukey's ad-hoc test. N= 3.....	171
Figure 45. Median fluorescence intensity results for SF-188 cells grown in normal media for 24, 48 and 72 hours A) PD-L1 B) HLA-E C) HLA-G D) HLA-A, B, C E) CD40. There is no significant difference between any of the conditions as deemed by a one-way ANOVA followed by Tukey's ad-hoc test. N= 3.....	172
Figure 46. Percentage of SEBTA-027 cells positive for cell surface expression of A) HLA-A B) PD-L1 C) CD86 after 72 hours exposure to IFNγ, *= P ≤0.05 relative to control as deemed by a paired T-test. N= 3.....	174
Figure 47. Median fluorescence intensity results for SEBTA-027 cells positive for cell surface expression of A) HLA-A, B, C B) PD-L1 after 72 hours exposure to IFNγ, **= P ≤0.01 relative to control as deemed by a paired T-test. N= 3.....	176

Figure 48. The effects of IFN γ exposure on the expression of IDO in SF-188 and SEBTA-027 cell lines as measured by Western blotting. A) Representative blot for IFN γ treated SF-188 cells. B) Quantification of IFN γ treated SF-188 blots using ImageJ software to determine the IDO expression relative to the vinculin loading control. C) Representative blot for IFN γ treated SEBTA-027 cells. D) Quantification of IFN γ treated SEBTA-027 blots using ImageJ software to determine the IDO expression relative to the vinculin loading control. N=3 ****= P \geq 0.0001, ***= P \leq 0.001, **= P \leq 0.01, *= P \leq 0.05 as deemed by a two-way ANOVA followed by Tukey's ad-hoc test.178

Figure 49. Kynurenine concentration in A) SF-188 cell culture media and B) SEBTA-027 cell culture media after 24, 48 and 72 hours in normal control media (black circles) and IFN γ containing media (black squares). N= 3 ****= P \leq 0.0001, ***= P \leq 0.001, **= P \leq 0.01 as deemed by two way ANOVA followed by Sidak's multiple comparisons test.180

Figure 50. Kaplan-Meier survival analysis of mice prophylactically vaccinated with SCIB1 and WT-1 ImmunoBody[®] vaccination compared to unvaccinated mice. The green line represents the sham vaccinated control group, and the red line represents dually vaccinated mice. Control group n=7, treatment group n=8, ** = P \leq 0.01 as determined by the log rank test.190

Figure 51. Kaplan-Meier survival analysis of intracranial B16 bearing HHDII/DR1 mice treated with dual SCIB1 and WT-1 ImmunoBody[®] vaccination either in combination with anti-PD-1 or PD-1 isotype control and untreated mice. N= 10. * = P \leq 0.05 as determined by the log rank test. The green line represents dually vaccinated mice that received anti-PD-1 antibody therapy, the blue line represents dually vaccinated mice that received isotype control antibody and the orange line represents the sham vaccinated control group.192

Figure 52. Some examples of the cerebellar spread of intracranially implanted tumours observed in the therapeutic study; cerebellar tumours are highlighted by the red arrows, the white arrow represents the site of cell injection. Mice 14-16 are from the dual ImmunoBody[®] + anti-PD-1 group and mouse 27 is from the untreated control group.....194

Figure 53. Number of CD3, CD8⁺ positive TILs obtained from intracranial B16HHDII/DR1 tumours. Group 1= Dual vaccination + PD-1 isotype control, Group 2= Dual vaccination + anti-PD1, Group 3= Untreated controls. N= 10.196

Figure 54. Percentage of A) CD3,CD4 and B) CD3,CD8 positive cells obtained from B16HHDII/DR1 brain tumour TILs. Group 1= Dual vaccination + PD-1 isotype control, Group 2= Dual vaccination + anti-PD1, Group 3= Untreated controls. N= 5-10. * = P \leq 0.05 as deemed by one way ANOVA followed by Tukey's ad hoc test.....198

Figure 55. Flow cytometric analysis of CD3,CD8 positive cells obtained from B16HHDII/DR1 brain tumour TILs. A) CD62L and CD44 double positive cells (memory cells) B) CD69 positive cells C) PD-1 positive cells D) CD25 positive cells. Group 1= Dual vaccination + PD-1 isotype control, Group 2= Dual vaccination + anti-PD1, Group 3= Untreated controls. N = 5-10. ** = P \leq 0.01 as deemed by one way ANOVA followed by Tukey's ad hoc test.200

Figure 56. Flow cytometric analysis of CD3,CD4 positive cells obtained from B16HHDII/DR1 brain tumour TILs. A) CD62L and CD44 double positive cells (memory cells) B) CD69 positive cells C) PD-1 positive cells D) CD25 positive cells. Group 1= Dual vaccination + PD-1 isotype control, Group 2= Dual vaccination + anti-PD1, Group 3= Untreated controls. N = 5-10.....202

Figure 57. Flow cytometric analysis of regulatory T-cells obtained from B16HHDII/DR1 brain tumour TILs. A) Percentage of CD4 regulatory T cells B) Percentage of CD8 regulatory T cells. Group 1= Dual vaccination + PD-1 isotype control, Group 2= Dual vaccination + anti-PD1, Group 3= Untreated controls. N = 5-10.204

Figure 58. MTT dose response curves for human GBM cells treated with carnosine. The EC50 for each cell line is displayed in the table below the dose response curves, with the value shown representing the mM concentration. Carnosine was applied to cells for 24 hours prior to performing the MTT assay. N=3.....211

Figure 59. The MTT dose response curve for the murine GBM cell line GL261 treated with carnosine. The EC50 value is shown below the dose response curve, with the number being shown

representing the mM concentration. Carnosine was applied to cells for 24 hours prior to performing the MTT assay. N= 3.....	213
Figure 60. Microscope images of SF-188 scratch closure A) 0h control B) 48h Ctrl C) 0h EC75 D) 48h EC75. Scale bar = 400 μ m.....	215
Figure 61. Scratch assay results from SF-188 cells with and without carnosine. Control cells were grown in normal media and carnosine treated cells were given the EC75 dosage as calculated by the MTT dose response curves. N = 3 **** = P \leq 0.0001 as deemed by a paired T-test.	215
Figure 62. Microscope images of SEBTA-027 scratch closure A) 0h control B) 48h Ctrl C) 0h EC75 D) 48h EC75. Scale bar = 400 μ m.....	217
Figure 63. Scratch assay results from SEBTA-027 cells with and without carnosine. Control cells were grown in normal media and carnosine treated cells were given the EC75 dosage as calculated by the MTT dose response curves. N = 3 **** = P \leq 0.0001 as deemed by a paired T-test.	217
Figure 64. Microscope images of GL261 Luc2 scratch closure A) 0h control B) 48h Ctrl C) 0h EC75 D) 48h EC75. Scale bar = 400 μ m.	219
Figure 65. Scratch assay results from GL261 Luc 2 cells with and without carnosine. Control cells were grown in normal media and carnosine treated cells were given the EC75 dosage as calculated by the MTT dose response curves. N = 3 **** = P \leq 0.0001 as deemed by a paired T-test.	219
Figure 66. A) Tumour surface area measurements of GL261 Luc2 tumours taken from carnosine and PBS treated mice. B) Weights of tumours excised 16 days after carnosine treatment. C) In vivo bioluminescent images taken on day 16 post carnosine therapy, the left 4 mice are control mice and the 5 on the right are carnosine treated. D) Close up of an in vivo image of a carnosine treated tumour, the red arrow highlights an area of reduced tumour growth at the site of injection. Red indicates high luciferase activity (indicative of greater tumour size), and blue represents areas of less luminescence.	221

LIST OF TABLES

Table 1. Details of the human cell lines used for this study.	47
Table 2. Details of the murine cell lines used for this study.	47
Table 3. Details of the reagents used and the supplier of each reagent	52
Table 4. Recipes for the buffers used. The buffer name is emboldened and the ingredients are listed below.	58
Table 5. Antibodies used for Western blotting	59
Table 6. Antibodies used for immunostaining	60
Table 7. Antibodies used for Immunocytochemistry and Immunofluorescence	60
Table 8. Details of the antibodies used for flow cytometry	61
Table 9. Details of the antibodies used for flow cytometry	62
Table 10. Details of the antibodies used for flow cytometry	63
Table 11. Positive control tissues used for IHC optimisation.....	65
Table 12. Preparation of BSA standards for the BSA protein assay.....	67
Table 13. Peptides used for in vitro stimulation of splenocytes and their respective SYFPEITHI scores (SYFPEITHI).....	85
Table 14. Pathologist's IHC scoring of GBM TMA tissue staining intensity. Examples of staining can be seen in figures 15 and 16.	99
Table 15. Pathologist's IHC scoring of GBM TMA tissue staining intensity. Examples of staining can be seen below.	103
Table 16. Flow cytometric surface staining results for the SEBTA-025, SEBTA-027, SF-188, UP-007 and UP-019 cell lines. The percentage of live cells stained as well as the median fluorescence intensity is detailed for each antigen. The gating strategy utilised is outlined in chapter 2.	111
Table 17. A brief summary of antigens of interest expressed in the GBM cell lines studied. These results are the collated western blot and flow cytometry data obtained for each cell line, revealing the overall antigen expression for each cell line.	112
Table 18. A list of the peptides used to stimulate splenocytes ex vivo. In silico analysis was performed using SYFPEITHI, a data base that provides predicted MHC binding scores. The higher the score the stronger the binding of the peptide with the HLA molecule, and therefore the more likely this peptide is to be presented via MHC molecules.	133

ABBREVIATIONS

2-HG	2-Hydroxyglutarate
5-FU	Fluorouracil
AA	Amino acids
ACT	Adoptive cell transfer
AhRs	Aryl hydrocarbon receptor
AIC	5-aminoimidazole-4-carboxamide
AKT	Protein kinase B
APC	Antigen-presenting cells
ATRX	Alpha thalassaemia mental retardation
BBB	Blood brain barrier
beta2m	Beta2 microglobulin
bFGF	Basic fibroblast growth factor
CAR	Chimeric antigen receptor
CAIX	Carbonic anhydrase 9
CCL5	C-C motif chemokine ligand 5
CCL22	C-C motif chemokine ligand 22
CDRs	Complementarity determining regions
CMV	Cytomegalovirus
CMVIL10	Cytomegalovirus encoded interleukin-10
CNDP1	Carnosine dipeptidase 1
Cnx43	Connexin 43
CPP	Cell-penetrating peptide
CTL	Cytotoxic T lymphocytes
CTLA-4	Cytotoxic T-lymphocyte-associated antigen 4
CTRL	Control
DC	Dendritic cells
DNA	Deoxyribonucleic acid
EGF	Epidermal growth factor
EGFR	Epidermal growth factor receptor
EGFRvIII	Epidermal growth factor receptor variant III
ELISA	Enzyme-linked immunosorbent assay
EMT	Epithelial-mesenchymal transition
FasL	Fas ligand
Fc	Fragment crystallisable region
FcyR	Fragment crystallisable region gamma receptor
FCS	Fetal calf serum
FDA	Food and Drug Administration
FGF	Fibroblast growth factor
FITC	Fluorescein isothiocyanate
GABRA1	Gamma-aminobutyric acid type A receptor subunit alpha-1
Gal-1	Galectin-1
GBM	Glioblastoma multiforme
GM-CSF	Granulocyte macrophage-colony stimulating factor
gp100	Premelanosome protein
HAGE	Helicase antigen

hCMV	Human cytomegalovirus
Her2	Receptor tyrosine-protein kinase erbB-2
HIF	Hypoxia-inducible factor
HLA	Human Leucocyte Antigen
HSPG	Heparan sulfate
ICAM-1	Intracellular adhesion molecule-1
ICS	Intracellular cytokine staining
IDO	Indoleamine 2,3-dioxygenase
IDH	Isocitrate dehydrogenase
IFN	Interferon
IFNBR	Interferon beta receptor
IFNGR	Interferon gamma receptor
Ig	Immunoglobulin
IHC	Immunohistochemistry
IL	Interleukin
ILT-2	Leukocyte immunoglobulin-like receptor subfamily B member 1
IL13R α 2	Interleukin-13 receptor subunit alpha-2
KLH	Keyhole limpet hemocyanin
LFA-1	Lymphocyte function-associated antigen 1
LKB1	Liver kinase B1
LMP2	Low-molecular mass protein-2
LMP7	Low-molecular mass protein-7
M1	Classically activated macrophages
M2	Alternatively activated macrophages
mAbs	Monoclonal antibodies
MAdCAM-1	Mucosal addressin cell adhesion molecule 1
MAPK	Mitogen-activated protein kinase
MDSCs	Myeloid-derived suppressor cell
MECL-1	Low molecular mass protein 10
MGMT	Methylguanine-DNA methyltransferase
MHC	Major histocompatibility complex
MIF	Macrophage migration inhibitory factor
MMP	Matrix metalloproteinase
mRNA	Messenger ribonucleic acid
MTT	3-(4,5-dimethylthiazol-2-yl)-2,5-diphenyltetrazolium bromide
MTIC	3-methyl-(1H-imidazol-1-yl)imidazole-4-carboxamide
mTOR	Mammalian target of rapamycin
NADPH	Nicotinamide adenine dinucleotide phosphate
NEFL	Neurofilament light polypeptide
NF	Neurofibromatosis
NF- κ B	Nuclear factor kappa-light-chain-enhancer of activated B cells
NK	Natural killer cells
NKG2A	NK cell inhibitory receptor
NKG2C	NK cell activating receptor
NKG2D	NK cell activating receptor
NKX2-2	Homeobox protein Nkx-2.2

NY-ESO-1	New York esophageal squamous cell carcinoma 1
OLIG2	Oligodendrocyte transcription factor
OS	Overall survival
PAI-1	Plasminogen activator inhibitor 1
PAMPs	Pathogen-associated molecular patterns
PAP	Prostatic acid phosphatase
PBMC	Peripheral blood mononuclear cells
PDGF	Platelet derived growth factor
PD-1	Programmed cell death 1
PD-L1	Programmed cell death ligand 1
PD-L2	Programmed cell death ligand 2
PDGFRA	Platelet derived growth factor receptor A
PGE2	Prostaglandin E2
PI3K	Phosphoinositide 3-kinase
PIAS3	E3 SUMO-protein ligase PIAS3
PPPP	DL-thre-phenyl-2-hexadecanoylamino-3-pyrrolidino-1-propanol
PTEN	Phosphatase and tensin homolog
RB	Retinoblastoma
RNA	Ribonucleic acid
ROS	Reactive oxygen species
RNS	Reactive nitrogen species
RT	Radiotherapy
RTK	Receptor tyrosine kinase
ScFvs	Single chain variable fragments
SDS-PAGE	Sodium dodecyl sulphate-polyacrylamide gel electrophoresis
SEB	Staphylococcal enterotoxin B
SLC12A5	Potassium-chloride transporter member 5
STAT3	Signal transducer and activator of transcription 3
SYT1	Synaptotagmin-1
TNC	Tenascin C
T-regs	Regulatory T-cells
TAA	Tumour-associated antigens
TAM	Tumour-associated macrophages
TAP	Transporter associated with antigen processing
TCR	T cell receptor
TDO	Tryptophan 2,3-dioxygenase
TERT	Telomerase reverse transcriptase
TGFβ	Transforming growth factor b
Th	T helper lymphocytes
TIL	Tumour infiltrating lymphocytes
TLR	Toll like receptor
TME	Tumour micro-environment
TMZ	Temozolomide
TNF	Tumour necrosis factor
TNFR	Tumour necrosis factor receptor
TP53	Tumour protein 53

TRP-2	Tyrosinase-related protein-2
TSA	Tumour-specific antigens
VCAM	Vascular cell adhesion molecule
VEGF	Vascular endothelial growth factor
WT	Wild type
WT-1	Wilms' tumour 1
YKL40	Chitinase-3-like protein 1

CHAPTER 1: INTRODUCTION

1.1. Cancer

Cancer is characterised by several hallmarks; these are the sustaining of proliferative signalling, evasion of growth suppression, resistance of cell death which enables replicative immortality, induction of angiogenesis and activation of invasion and metastasis. There are also several other hallmarks that have been identified as being indicative of cancer these are: genome instability and mutation, tumour promoting inflammation, reprogramming of energy metabolism and evasion of immune destruction (Hanahan, Weinberg 2011). This uncontrolled cellular growth can be problematic, especially if these cells are expanding in a major organ such as the brain.

1.2. Glioblastoma multiforme

Glioblastoma multiforme (GBM, WHO grade 4) is the most commonly occurring malignant central nervous system tumour accounting for 47.1 % of all malignant CNS tumours. It is more common in older adults, with incidence increasing with age. Glioblastoma was found to be 1.58 times more common in men than women. Only around 5 % of patients survive five years post diagnosis (Ostrom, Gittleman et al. 2017). Glioblastoma multiforme are mainly primary and occur *de novo* however secondary glioblastoma multiforme can also arise from lower grade gliomas (Bleeker, Molenaar et al. 2012). Glioblastoma histopathology reveals GBM tumours are highly cellular comprised of poorly differentiated and pleomorphic astrocytic cells with nuclear atypia and high mitotic activity. Vascular proliferation is also evident, and necrosis is also observed in some sections of the tumour (Young, Jamshidi et al. 2015).

Glioblastoma multiforme has been divided into four main subtypes, the classical, mesenchymal, proneural and neural subtypes. These subtypes are divided by their gene expression profiles and occur at slightly differing rates with roughly 32 % of cases being proneuronal, 14 % neural, 22 % classical and 32 % mesenchymal (Verhaak, Hoadley et al. 2010). The classical subtype is characterised by chromosome 7 loss and *Epidermal growth factor receptor (EGFR)* amplification. Homozygous 9p21.3 deletion is also associated with the classical subclass. The mesenchymal subtype is characterised by focal hemizygous deletion of a region at 17q11.2 containing the *neurofibromatosis 1 (NF1)* gene. This subtype also expresses the mesenchymal markers *Chitinase-3-like protein 1 (YKL40)* and *Hepatocyte growth factor receptor (MET)*. Several genes in the tumour necrosis factor super family and nuclear factor kappa-light-chain-enhancer of activated B cells (NF- κ B) pathways are also highly expressed in this subtype. The proneural class is defined by amplification of *Platelet derived growth factor receptor A (PDGFRA)* and point mutations in

isocitrate dehydrogenase 1 (IDH1). Tumour protein 53 (*TP53*) mutations and loss of heterozygosity are frequently observed in this subtype. High expression of *homeobox protein Nkx-2.2 (NKX2-2)* and *oligodendrocyte transcription factor 2 (OLIG2)* are also typical of this subtype. The neural subtype is characterised by the expression of neuron markers such as *Neurofilament light polypeptide (NEFL)*, *Gamma-aminobutyric acid receptor subunit alpha-1 (GABRA1)*, *synaptotagmin 1 (SYT1)* and *potassium-chloride transporter member 5 (SLC12A5)* (Verhaak, Hoadley et al. 2010).

Referring to Hanahan and Weinberg's hallmarks of cancer (Hanahan, Weinberg 2011) GBM tumours have a wide array of alterations in gene expression that contribute to their malignant phenotype. Activating mutations have been observed in around 70 % of the receptor tyrosine kinases (RTKs), inactivating mutations of the *phosphate and tensin homolog (PTEN)* gene are also observed in 36 % of cases preventing the inhibition of proliferation. Mutations in the p53 and RB pathways also contribute to the sustained proliferative signalling observed in GBM tumours. With regards to evading growth suppression; loss of function mutations are seen in several tumour suppressor genes such as *NF2*, *LKB1*, *RB* and *TP53*. Metastasis is rarely seen in GBM; however, invasion is a hallmark of this type of cancer. The protein connexin 43 (*cnx43/GJA1*) is a key component of the gap junctions formed between cells; GBM cells have been shown to downregulate this protein reducing their adherence and as a result increasing their invasiveness (Verhaak, Hoadley et al. 2010). Pro-inflammatory proteins have also been shown to contribute to the invasiveness of GBM cells. These tumours are often hypoxic, and this hypoxia also contributes to the pro-inflammatory environment. Epithelial-to-mesenchymal transition (EMT) can also contribute to these tumours' invasiveness with down regulation of the junction protein E-cadherin, enabling cell invasion. These cells can then subsequently undergo epigenetic changes enabling them to develop a mesenchymal (stem-cell like) phenotype. The *telomerase reverse transcriptase (TERT)* gene has been found to be mutated in 51 % of GBMs, this gene encodes the telomerase protein which lengthens the telomeres, immortalising cells. The gene alpha thalassaemia mental retardation (*ATRX*) is responsible for the deposition of histones at the telomeres, mutations in this gene have also been seen in GBM and this is linked to telomere lengthening. Due to the hypoxic nature of GBM tumours vascular endothelial growth factor (VEGF) is often upregulated, inducing increased angiogenesis. Mutations in several of the intracellular signalling proteins such as PI3K, AKT and mTOR prevent apoptosis and autophagy. GBM tumours employ many mechanisms to avoid immune destruction such as expression of immune inhibitory checkpoint proteins and recruitment of immunosuppressive myeloid derived suppressor cells (MDSCs). The isocitrate dehydrogenase (*IDH*) gene codes for three IDH enzymes, these enzymes are responsible for the production of nicotinamide adenine dinucleotide phosphate (NADPH) via oxidative carboxylation of isocitrate. *IDH1* and *IDH2* are the only two *IDH* genes found to be mutated in GBM, these mutations decrease IDH activity leading to

increased production of 2-hydroxyglutarate (2-HG) from NADPH, decreasing NADPH levels. 2-HG inhibits α -ketoglutarate-dependent dioxygenases, resulting in further epigenetic changes (Noroxe, Poulsen et al. 2017).

1.3. Glioblastoma multiforme therapy

The current course of treatment involves surgical reduction of the tumour (where possible) followed by concomitant radiotherapy and temozolomide chemotherapy. Despite aggressive multimodal therapy the median survival for patients on this treatment regime is 14.6 months (Stupp, Mason et al. 2005).

The corticosteroid dexamethasone is given preoperatively to help reduce peritumoural swelling. Surgery can be performed in a variety of ways; craniotomy is the preferred surgical method; these can be performed as asleep-awake craniotomies where the patient is still conscious. This is particularly useful for tumours located within areas of the brain associated with certain functions (e.g. speech or hearing), this allows for monitoring of the patient's faculties whilst resection takes place (Holland 2000). The asleep-awake craniotomy is associated with increased extent of resection and reduced neurologic deficits. An asleep craniotomy may also be performed with the patient being completely unconscious. Intraoperative electrical stimulation can also be used to map brain function during awake surgery. Another method for resecting GBM tumours is stereotactic ablation; this involves the use of a stereotactic frame to insert an optic cable into the tumour; low powered laser light can then be used to destroy tumour tissue (laser-induced thermal therapy) (Bigner, Friedman et al. 2016). Glioblastoma multiforme is highly resistant to therapy and due to the tumours' highly infiltrative and diffuse nature recurrence is frequently observed. The diffuse nature of these tumours makes complete surgical resection difficult to achieve (Holland 2000).

Temozolomide (TMZ) is a pro-drug that can be administered orally. The drug is stable at acidic pH but breaks down at a pH of 7 and above (Zhang, J., Stevens, and Bradshaw 2012). TMZ is absorbed and rapidly broken down to monomethyl triazene 5-(3-methyltriazene-1-yl)-imidazole-4-carboxamide (MTIC). This MTIC then reacts with water to produce 5-aminoimidazole-4-carboxamide (AIC) and the active component methyl diazonium. This methyl diazonium cation methylates DNA at 3 positions; the *N7* position of guanine, the *N3* position of adenine and the *O6* position of guanine. The methylation at the *O6* position of guanine is responsible for the cytotoxic effects of TMZ on cancer cells. The temozolomide pro-drug is preferentially processed in brain tumours due to their higher pH. When left unchecked *O6* methyl guanine mismatches with thymine during replication, this triggers DNA mismatch repair (MMR). This results in excision of the thymine base. After several rounds of futile MMR, DNA double strand breaks occur resulting in cell cycle arrest and eventual apoptosis. Unfortunately, the lethal *O6* guanine adducts induced by TMZ may

be repaired by an enzyme known as methylguanine-DNA methyltransferase (MGMT). The methyl group on the guanine is transferred to a cysteine residue within the active site of MGMT in a single step suicide reaction (Zhang, J., Stevens, and Bradshaw 2012). Not only is the protein MGMT also involved in resistance to TMZ but several micro RNAs are implicated in acquired resistance to TMZ chemotherapy (Ujifuku, Mitsutake et al. 2010).

Bevacizumab and tumour treating fields are the only other Federal Drug Administration (FDA) approved treatments available for GBM patients. In 2009 the humanised anti-vascular endothelial growth factor (VEGF) IgG antibody bevacizumab was approved for GBM therapy (Cohen, Shen et al. 2009). Unfortunately, it was found that bevacizumab had little benefit for patient survival when used in newly diagnosed patients with standard of care therapy (Gilbert, Dignam et al. 2014). However, bevacizumab may provide an alternative to corticosteroids for reduction of cerebral oedema. This is of particular interest for immunotherapeutic approaches since the corticosteroids commonly used in GBM; such as dexamethasone are highly immunosuppressive. Tumour treating fields are administered via a device known as Optune and these were approved by the FDA in 2011. This involves users wearing scalp electrodes that apply alternating electric fields that affect mitosis of tumour cells and this method of treatment has been shown to improve progression free survival and overall survival of patients, however this method of treatment is still far from curative (Hottinger, Pacheco et al. 2016, Mittal, Klinger et al. 2018).

1.4. Immunotherapy

In the early 19th century William B. Coley unwittingly utilised the immune systems of patients to cause cancer remission by treating them with erysipelas (an infection caused by *Streptococcus* bacteria), this treatment involved the injection of these bacteria into patients tumours locally activating the immune system (Coley 1891).

Immunotherapy is the utilisation of the body's own defences to target and attack tumours within the body, breaking the 'tolerance' that tumours have developed. This involves engaging the immune system and alerting it to the presence of tumours within the body. Immunotherapy can take many forms, there are two main branches of immunotherapy; passive immunotherapy and active immunotherapy.

Immunotherapy as a mode of cancer therapy has become very popular due to its tumour specificity and reduced side effects (when compared to chemotherapy and radiotherapy). Immunotherapeutic treatments for cancer have gained traction with several therapies being

approved for use and well over 2,000 clinical trials currently ongoing involve immunotherapeutic treatments.

Sipuleucel-T was the first FDA approved therapeutic cancer vaccine, an active form of immunotherapy. Sipuleucel-T is used to treat metastatic castration-resistant prostate cancer, it works by targeting the prostate acid phosphatase (PAP) antigen expressed by prostate cancer cells. To generate the vaccine autologous peripheral blood mononuclear cells (PBMC) from the patient are stimulated with a PAP-GM-CSF fusion protein comprised of the prostate cancer specific antigen prostatic acid phosphatase (PAP) and the immune stimulating granulocyte macrophage-colony stimulating factor (GM-CSF). These *ex vivo* stimulated cells are then infused into the patient where activated immune cells target the PAP expressing prostate cancer cells (Cheever, Higano 2011).

A plethora of therapeutic antibodies have also been approved in the cancer setting (Postow, Callahan et al. 2015). The most relevant antibodies in the immunotherapy setting are the checkpoint blockade antibodies that target cytotoxic T-lymphocyte-associated protein 4 (CTLA-4), programmed death receptor 1 (PD-1) and programmed death ligand 1 (PD-L1).

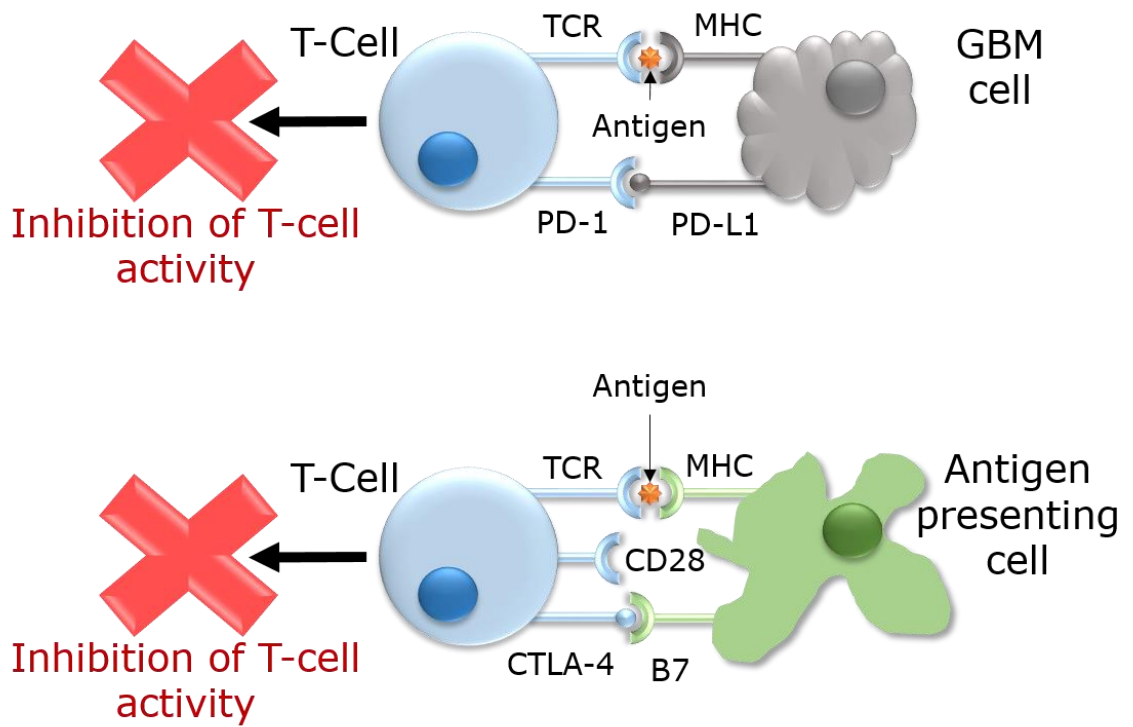


Figure 1. A diagram of how the immune checkpoints PD-1/PD-L1 and CTLA-4 dampen the immune response. PD-L1 expressed on tumour cells binds to PD-1 on T-cells resulting in the death of the PD-1 expressing T-cells. CTLA-4 on T-cells outcompetes CD28 when binding to B7 molecules preventing the activation of the T-cell, the CTLA-4 binding to the B7 molecules can also transendocytose the B7 molecules and lead to their degradation. Adapted from (Reardon, Freeman et al. 2014)

PD-1 is a member of the CD28 family and it shares over 20 % homology with CTLA-4. CTLA-4 is expressed exclusively on T-cells however PD-1 is expressed on B cells and myeloid cells as well as T-cells. PD-1 is expressed on activated T-cells and binds to its ligands PD-L1 (B7-H1) and PD-L2 (B7-DC). PD-L1 is classically expressed on immune cells and specific tissues such as β cells in the pancreas and the placenta, however cancers have been shown to co-opt the PD-L1 antigen to evade the anti-tumour immune response. PD-L2 is expressed on activated macrophages and dendritic cells; tumours also utilise PD-L2 to evade immune detection (Okazaki, Honjo 2006). PD-L2 expression is far less common in tumours compared to PD-L1 (Chen, D. S., Irving et al. 2012). PD-L1 expression has been well documented in the GBM setting with expression of PD-L1 being found in 25-88 % of GBM cases (Vlahovic, Fecci et al. 2015, Berghoff, Kiesel et al. 2015a). PD-L1 expression in GBM has been examined as a prognostic factor; Nduom et al. (2016) revealed that expression of PD-1 and PD-L1 were found to be predictors of negative patient outcome (Nduom, Wei et al. 2016). Interestingly it was also found that PD-L1 expression by neurons close to tumours conveyed a better prognosis in GBM patients. It was found that when PD-L1 wasn't expressed in surrounding neurons the tumour expressed high levels of PD-L1. This research highlights an active interaction between the tumour and its surrounding tissues however the mechanisms by which the PD-L1 expression in surrounding neurons induces/increases glioma cell death is still not fully understood (Liu, Y., Carlsson et al. 2013). Currently there are five FDA approved antibodies that target the PD-1/PD-L1 axis; Nivolumab and Pembrolizumab inhibit PD-1 whereas Atezolizumab, Avelumab and Durvalumab target PD-L1. Whilst there are several approved PD-1/PD-L1 inhibitors many more are being clinically trialled. Unfortunately these antibodies have not been approved for use in the GBM setting, however these antibodies are being tested in over 40 clinical trials for GBM (either alone or in combination with other therapies) (clinicaltrials.gov - PubMed - NCBI).

To generate activation of T-cells the T-Cell Receptor (TCR) needs to engage antigenic peptide presented on a major histocompatibility complex (MHC) molecule. After this TCR engagement a secondary signal also occurs from T-cell CD28 binding to the ligands B7-1 (CD80) and B7-2 (CD86) on the surface of antigen presenting cells. Cytotoxic T-lymphocyte-associated protein 4 (CTLA-4/CD152) binds to both B7-1 and B7-2 with much higher affinity than CD28, outcompeting it. The binding of CTLA-4 to the B7 ligands results in the inhibition of T-cell proliferation (Leach, Krummel et al. 1996). CTLA-4 not only outcompetes CD28 for ligation with CD80/CD86 it can also occupy CD80/86 preventing CD28 on neighbouring cells from interacting with CD80/86 (Walker, Sansom 2015). The binding of CTLA-4 to CD80/86 has also been shown to lead to the transfer of CD80 and CD86 to CTLA-4 expressing cells, these CTLA-4 expressing cells then degrade these CD80 and CD86 molecules. This results in decreased immune cell activity and stunts the immune cell activation capabilities of dendritic cells (Qureshi, Zheng et al. 2011). Ipilimumab is the only FDA approved anti-

CTLA-4 antibody and much like the PD-1 and PD-L1 checkpoint inhibitors CTLA-4 use has not received approval for GBM therapy. Whilst Ipilimumab has not been approved for GBM therapy there are currently 10 ongoing clinical trials examining its efficacy in this setting (either alone or in combination with other therapies). Early stage clinical trials using combinatorial Ipilimumab and the anti-VEGF antibody Bevacizumab have shown that this regime is well tolerated in patients. 31 % of the 20 patients studied had a partial response to this combined therapy and 31 % had stable disease with the remaining 38 % showing disease progression. Some adverse immune effects such as pulmonary embolism and arthritis were observed however these were controlled with the use of corticosteroids (Carter, Shaw et al. 2016).

Trastuzumab (Herceptin) is an antibody that targets the epidermal growth factor HER2 and its use has been approved for Her2 positive breast cancer. Trastuzumab is a humanised monoclonal antibody that binds the extracellular domain of HER2. This results in a reduction of HER2 signalling resulting in apoptosis of Her2 expressing cells. Trastuzumab may also induce an anti-tumour immune response, this is thought to be due to NK immune cells binding to the Fc region of the Trastuzumab via their Fc receptors stimulating NK cell lysis of Her2 expressing tumours (Nahta, Esteva 2006). The Her2 antigen is found to be expressed in GBM tissues and the Trastuzumab antibody is found to induce death of GBM cells, however this antibody is yet to be approved for use in the treatment of GBM (Mineo, Bordron et al. 2004). Whilst *in vitro* activity was demonstrated Trastuzumab never underwent clinical trials for GBM as a monotherapy.

Kymriah (Tisagenlecleucel) and Yescarta (Axicabtagene Ciloleucel) are chimeric antigen receptor (CAR)-T-cell therapies that have been approved for use in leukaemia. Both therapies are CD19-specific meaning that they target B-cell lymphomas and leukaemias (Zheng, Kros et al. 2018). CAR T-cells are genetically engineered T-cells that are engineered so that they have an antigen specific domain fused with an intracellular signalling domain, this enables these cells to specifically target cells and activate the T-cell. Some interesting pre-clinical data is being amassed for the use of CAR T-cells in the GBM setting however the use of CAR T-cells in the clinic is still in its relative infancy with primarily phase I/II clinical trials ongoing (Bagley, Desai et al. 2018). In the GBM setting CAR T-cells have been engineered to target the truncated EGFRviii receptor (O'Rourke, Nasrallah et al. 2017), the stem cell marker CD133 (Zhu, X., Prasad et al. 2015) and the GBM associated antigen IL13R α 2 (Brown, C. E., Alizadeh et al. 2016) to name a few.

1.5. The immune system in glioblastoma multiforme

The brain has been traditionally thought of as being an immunoprivileged organ, however there is mounting evidence of an interaction between the brain and the immune system. An early indicator

of the effects of the peripherally activated immune system at targeting antigens within the brain was evidenced in skin graft experiments performed on rabbits (MEDAWAR 1948). When heterotypic skin grafts are implanted directly into the brain, they do not elicit an immune response, however when these skin grafts are engrafted on a raw area of the skin the cerebral grafts were rejected due to an immune response (MEDAWAR 1948). Regression of brain tumours has also been linked to perisurgical bacterial infection, it was hypothesised that bacteria acted as an immune adjuvant that boosted the anti-tumour response as evidenced by increased granulocyte and lymphocyte infiltration (Bowles, Perkins 1999). Prins et al. (2008) revealed that antigen specific CD8+ T-cells penetrated the brain parenchyma and penetrated tumours within the brains of a pre-clinical mouse model of GBM (Prins, Shu et al. 2008). Immunohistochemical analysis of glioblastoma multiforme tumours taken from patients has also revealed evidence of immune cell infiltration and this immune cell infiltrate can be a predictor of clinical outcome, with high CD4+ and low CD8+ tumour infiltration being correlated with poorer prognosis (Han, Zhang et al. 2014). Glioblastoma patients have also been shown to have circulating CD8+ T-cells specific for GBM cells indicating that there is an active interaction between the immune system and GBM tumours located within the brain (Tang, Flomenberg et al. 2005). The recent discovery of a brain specific lymphatic system has also helped to highlight the fact that there is an active interaction between the brain and the immune system (Louveau, Smirnov et al. 2015, Aspelund, Antila et al. 2015). Studies have found that implantation of allografts near the ventricles or within the subarachnoid space were rejected without prior peripheral exposure, indicating that these meningeal spaces containing cerebrospinal fluid have increased immune cell infiltration (Louveau, Plog et al. 2017). Under normal conditions immune cells are present within the meningeal compartment, the endothelial cells surrounding the cerebrospinal fluid filled areas is more permissive to immune cell crossing than the blood brain barrier. Tracers injected into the brain parenchyma and the subarachnoid spaces were both seen to drain to the cervical lymph nodes within the neck. Immune cells injected into the subarachnoid spaces were also seen to drain to these cervical lymph nodes. The data for immune cells injected into the parenchyma is far more varied with some studies witnessing drainage to the cervical lymph nodes and others failing to observe this phenomenon. These findings indicate that antigens located within the brain can be drained into the cervical lymph nodes and these can in turn educate extracranial immune cells. It may also be possible that intracranial immune cells drain to these lymph nodes and lead to further immune cell education/activation (Louveau, Plog et al. 2017). Whilst the brain is not immunoprivileged it is however a unique immune environment.

1.6. Vaccination and the immune response

Numerous approaches have been used to generate an immune response, one of the most frequent methods is to inject an antigenic peptide specific for the bacteria/virus/cancer, and this antigen is then up-taken and processed by the immune system generating antigen specific immune cells and a peptide-specific immune response. There are several classes of antigens utilised for targeting cancers: Cancer-testis antigens, these are expressed in germ cells but are also aberrantly expressed in tumour cells, differentiation antigens of melanocyte lineage, mutational antigens, overexpressed self-antigens and viral antigens (such as human cytomegalovirus antigens) (Jager, Gnjatic et al. 2000).

To develop a peptide vaccine specific immunodominant epitopes need to be selected that provide protection against the disease of interest. The epitopes chosen should induce both effector T- and/or B-cell responses as well as T-helper cell responses. This ensures efficient protection against the chosen epitopes and helps develop memory cell responses (Li, W., Joshi et al. 2014). CD8 cytotoxic T-cell epitopes are very specific and a single amino acid change within the epitope can render it non-immunogenic. Traditional vaccines are usually used in a protective manner, preventing future infection. In the cancer settings peptide vaccines are usually therapeutic, acting upon established disease. In the cancer setting, peptides longer than the standard 9-11 amino acid epitope size are used. These large peptides usually contain both MHC class 1 (CD8) and MHC class 2 (CD4) epitopes. These larger peptides are usually processed by the immunoproteasome and presented via MHC I and MHC II molecules by antigen presenting cells. These longer peptides have been shown to induce a stronger immune response than shorter 9-11 amino acid long peptides. This was thought to be due to CD4 T-cell help. This theory was proven using MHCII knockout mice, where these mice failed to elicit a strong anti-peptide CD8 T-cell response when vaccinated with a long peptide (Li, W., Joshi et al. 2014). A key factor to consider is the method of delivery and use of potential adjuvant, in some cases these two things can be combined. Adjuvants are used to boost the immunogenicity of peptide vaccinations and increase the efficacy of the vaccine, this can be achieved in a variety of ways. Some adjuvants may work to modify the cytokine network enhancing immune cell activation. Some adjuvants work by increasing the uptake of peptide by antigen presenting cells, allowing the peptide to remain in its native state and be processed as desired (Cox, Coulter 1997, Khong, Overwijk 2016).

B cells can also contribute to the vaccine induced immune response by present antigens to CD8 and CD4 T-cells enhancing the anti-tumour immune response (Yuen, Demissie et al. 2016). Depending upon the signals B cells receive they can become effector B cells or antibody secreting plasma cells. Tumour infiltrating B cells can secrete antibodies that induce antibody-dependent cell-mediated toxicity or activation of the complement system resulting in the death of tumour cells. Activated B

cells can present antigen to T-cells and they secrete costimulatory cytokines that help maintain T cell activation. Regulatory B cells may also be present within the tumour infiltrating B cell population, these cells may promote tumour growth by secreting immunosuppressive cytokines such as IL-10 and TGF- β (Guo, F. F., Cui 2019). In a pre-clinical brain tumour model the recruitment of B cells to brain tumours was found to be necessary for the anti-tumour immune effects of Ad-TK+AdFLT3I gene therapy. When B-cells were blocked with an anti-CD20 antibody, or B cell deficient mice were treated with this Ad-TK+AdFLT3I gene therapy it was less efficacious than mice with functioning B cells (Candolfi, Curtin et al. 2011). Interestingly a DNA vaccine targeting the cancer associated antigen HER-2/neu was found to be efficacious in mice lacking B cells. B cell deficient mice were shown to reject HER-2 expressing tumours just as well as mice who still had an intact B cell compartment indicating that in the case of HER-2 expressing tumours, the T-cell compartment is necessary for anti-tumour immunity and the subsequent tumour rejection (Lindencrona, Preiss et al. 2004). As mentioned previously B cells can also contribute to tumour immune escape, anti-tumour CD8 T-cell cytotoxicity was shown to be improved in B cell knockout mice (Inoue, Leitner et al. 2006). Murine studies have revealed that the presence of B cells limits the repertoire of CD4 T cells, resulting in a lesser anti-tumour immune response. Immunoglobulins secreted by plasma cells have been shown to act as a carrier for immunosuppressive TGF- β highlighting the immunosuppressive potential of B cells. B-cells have been shown to act as antigen presenting cells when they are activated by CD40, these CD40 activated B cells can lead to the expansion of antigen specific CD4 and CD8 T cells (Fremd, Schuetz et al. 2013). Increased B cell infiltrate in GBM tumours has been shown to predict a significant survival advantage (Li, B., Severson et al. 2016). B cells much like many of the other immune cell types can act in both in a pro-tumourigenic and anti-tumourigenic manner. Antibodies secreted by plasma cells can induce antibody-dependent cell-mediated cytotoxicity (ADCC) resulting in antibody mediated tumour cell death. Antigen specific antibodies bind to antigens expressed on tumour cells, and the Fc regions on these antibodies are recognised by Fc receptors on effector cells. This crosslinking results in activation of immune effector cells resulting in tumour cell death (Iannello, Ahmad 2005). Whilst antibodies can contribute to immune cell killing of cancer cells, these immunoglobulins can form immune complexes, these complexes can support tumour growth and their presence is associated with increased tumour burden. These immune complexes have also been shown to interact with immune suppressive TGF- β , reducing the anti-tumour response within the tumour microenvironment (Tan, Coussens 2007).

1.7. Human leukocyte antigen (HLA) haplotypes

MHC antigen presentation is dependent upon the HLA haplotypes expressed by the patient. The HLA complexes are grouped into three main classes: MHC class 1, 2 and 3. MHC class I is comprised of HLA-A, HLA-B, HLA-C, HLA-E, HLA-F and HLA-G. MHC class II is comprised of HLA-DP, HLA-DR, HLA-DQ, HLA-DO and HLA-DM (Maenaka, Jones 1999). Less is known about the MHC class III complexes and they will not be detailed here since the interest is focussed on the MHC class I and II genes. Structurally MHC class I and II genes differ. MHC class I consists of two heterodimeric polypeptide chains linked non-covalently. The beta 2 microglobulin (β_2M) is also non-covalently linked to the alpha 3 chain which contains a transmembrane domain. The alpha 1 and 2 domains form a peptide binding groove that can hold peptides 8-10 amino acids long for presentation to T-cells. MHC class II is also a heterodimer formed with one alpha and one beta polypeptide chains. The alpha 1 and beta 1 domains form a peptide binding groove that can present peptides 15-24 amino acids long to T-cells. The alpha 3 region on the MHC class I receptor binds to CD8 on cytotoxic T-cells leading to presentation of the bound peptides to the TCR of these types of cells (Maenaka, Jones 1999). CD4 on helper T-cells binds to the beta 2 domain on MHC class II molecules, this domain is structurally analogous to the CD8 binding domain on the alpha 3 domain on MHC class I. This binding of CD4 to the MHC class II allows bound peptides to be presented to the TCRs on these CD4 positive cells (Konig, Huang et al. 1992).

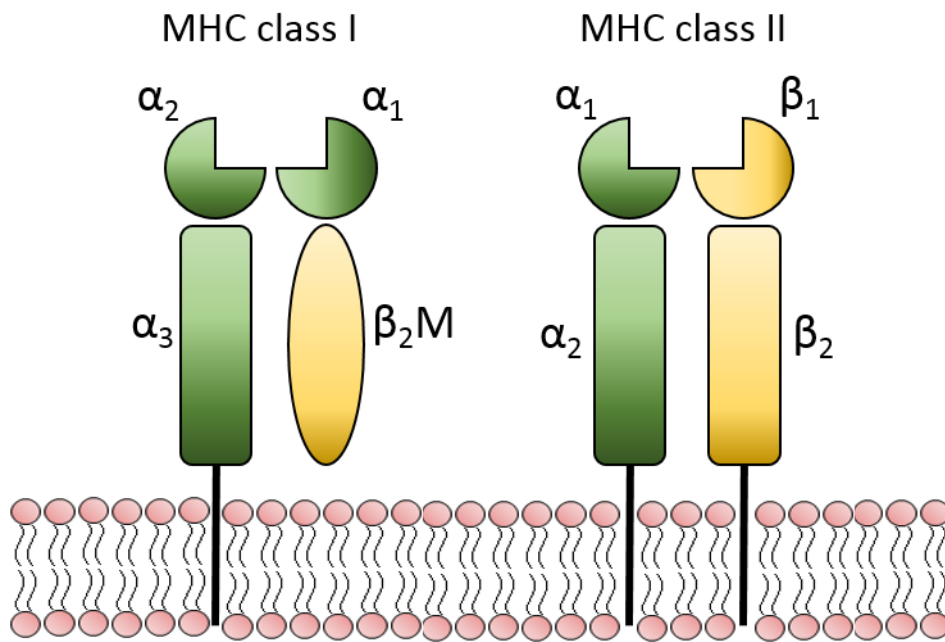


Figure 2. A schematic representation of the structure of MHC class I and II molecules. Alpha subunits are represented by green shading whilst the beta sub-units and beta 2 m molecules are shaded yellow. Adapted from (Janeway, Capra et al. 2001).

Each MHC molecule binds a different range of peptides, therefore possessing several genes for each MHC class is advantageous; enabling an individual to present a broad range of peptides. Most humans are heterozygous at MHC loci, the combination of genes at this MHC loci is known as the MHC/HLA haplotype. MHC alleles are codominant so both haplotypes are expressed within cells, this makes the antigen presenting capabilities of cells highly diverse. Each MHC variant is unique, and these differences lead to differing peptide-binding grooves on the MHC molecules making the peptide binding properties of MHC molecules unique. Antigen recognition of antigens by T-cells is dependent upon the presence of specific MHC molecules present on the surface of antigen presenting cells. The MHC molecule is also necessary for specific TCR engagement; when the same peptide is presented by different MHC molecules T-cells will distinguish between the two MHC receptors, despite the same peptide being presented. This reveals the importance of the MHC molecule in not only dictating peptide binding but also T-cell recognition of the peptide (Janeway, Capra et al. 2001).

1.8. GBM tumour immune escape

GBM tumours are known to be poorly immunogenic, this is mainly due to their highly immunosuppressive nature; with tumours employing a wide array of immune inhibitory escape mechanisms. Programmed death ligand 1 (PD-L1) is an immune inhibitory check point ligand that binds to its cognate receptor programmed death 1 (PD-1), the binding of PD-1 on activated T-cells to PD-L1 leads to apoptosis of T-cells, preventing immune response directed towards the PD-L1 expressing cells (Reardon, Freeman et al. 2014). GBM tumours have been shown to express PD-L1 with as many as 88 % of patients expressing this immunosuppressive marker (Berghoff, Kiesel et al. 2015b). As expected, patients expressing high levels of PD-L1 have also been shown to have a worse overall survival (Xue, S., Song et al. 2017). Due to the high levels of PD-L1 expression within these tumours the use of antibodies that block the PD-1/PD-L1 interaction have been tested to try and treat GBM, unfortunately GBM patients take the immunosuppressive anti-inflammatory drug dexamethasone. Dexamethasone is taken to control cerebral oedema in these patients however at the dosages taken it can dampen the response to immune checkpoint blockade (McGrath, Therkelsen et al. 2019). Regulatory T-cells (T-regs) are a subset of immune cell that act to dampen the immune response and prevent auto-immunity. These regulatory T-cells are immunoinhibitory and as a result their recruitment to the tumour microenvironment is undesirable for an efficient anti-tumour immune response. Unfortunately, in the case of GBM these tumours secrete soluble factors which increase the presence and expansion of regulatory T-cells. Increased levels of T-regs are found within GBM tumours when compared with circulating peripheral blood mononuclear cells. This increased recruitment of T-regs to the tumours was shown to be due to secretion of the

chemokine CCL22 by the tumours (Crane, Ahn et al. 2012). Glioblastoma multiforme tumours have also been shown to secrete numerous other immunosuppressive cytokines, one such example being transforming growth factor beta (TGF- β). TGF- β has been shown to be secreted by GBM tumours and its secretion has been shown to reduce T-cell infiltration in high grade gliomas (Lohr, Ratliff et al. 2011, Bodmer, Strommer et al. 1989). TGF- β interacts with a plethora of other growth factors in the GBM setting, such as basal fibroblast growth factor (bFGF), epidermal growth factor (EGF), platelet derived growth factor (PDGF) and plasmin activator inhibitor-1 (PAI-1). TGF- β 1 leads to increased collagen synthesis by GBM cells. PAI-1 expression by GBM cell lines can be reversed using an anti TGF- β blocking antibody. GBM cells unlike other cancer cell lines release TGF- β in its bioactive form (Platten, Wick et al. 2001). This TGF- β has been shown to lead to increased matrix metalloproteinase 2 and 9 (MMP2 and MMP9) activity on the surface of GBM cells. This in turn results in increased cell motility and invasion of surrounding brain (Platten, Wick et al. 2001). MMP9 interacts with intracellular adhesion molecule-1 (ICAM-1) resulting in its cleavage resulting in a tumour cell resistance to natural killer cell mediated cytotoxicity (Fiore, Fusco et al. 2002).

Interleukin-10 (IL-10) is an immunoinhibitory cytokine that inhibits synthesis of other cytokines, reducing the immune response. IL-10 mRNA was found to be highly expressed in recurrent and high-grade gliomas (Huettnner, Paulus et al. 1995). Further research revealed that IL-10 not only has immunosuppressive effects but it also increases proliferation and migration of glioblastoma multiforme cell lines in culture. This IL-10 was shown to be produced by cells of microglia/macrophage origin (Wagner, Czub et al. 1999). Not only do tumour associated macrophages produce IL-10 they have also been shown to have immunoinhibitory effects by becoming M2-type macrophages. There are two main types of macrophage, the classically activated M1 pro-inflammatory macrophage and the alternatively activated M2-type macrophages which exert anti-immune effects. Glioblastoma multiforme tumour mass is largely composed of these M2 macrophages which promote growth of tumour cells (Kennedy, Showers et al. 2013). Human cytomegalovirus (hCMV) is a herpes virus that persistently infects 50-90 % of the adult human population. Immunohistochemical analysis of GBM tumours revealed that 100 % of GBM tumours expressed the hCMV encoded protein IE1-72; these results were further corroborated by polymerase chain reaction (PCR) of GBM tissues (Cobbs, Harkins et al. 2002). Another study by Lucas *et al.* (2011) found that 51 % of GBM tumours studied express the pp65 CMV protein and only 16 % expressed the IE1 protein (Lucas, Bao et al. 2011). Human cytomegalovirus has been shown to secrete IL-10, enabling persistent viral infection, seeing that GBM tissue appears to be commonly infected with CMV, and this attenuation of the immune response prevents eradication of the tumour along with the virus. CMV IL-10 was shown to lead to the differentiation of CD14+ monocytes to macrophages, which was shown to support hCMV infection. Dendritic cell maturation

and life span is also affected by CMV IL-10, with *in vitro* studies revealing that the dendritic cells have delayed maturation and less longevity. Monocytic dendritic cells exposed to CMV IL-10 can reach maturation, however their cytokine production is impaired in a non-reversible manner. CMV IL-10 was shown to result in a decrease in antiviral IgG, this results in less efficient control of virus spreading and as a result more aggressive tumour growth (Chang, Barry 2010).

Immune cell populations have been shown to contribute to glioma pathology as well as regression. The presence of tumour infiltrating lymphocytes (TILs) correlates with glioma grade but this increase in TILs is also correlated to preferential prognosis (Han, Zhang et al. 2014). Lymphocytes entering the central nervous system/tumour compartment have been shown to down regulate costimulatory CD28 and CD62L ligands. Elevated regulatory T-cell presence in tumours has been correlated with shorter recurrence free survival. CD8+ T cell infiltration into GBM tumours has been correlated with survival. Radiotherapy has been shown to increase cytotoxic T-cell infiltrate and deplete regulatory T-cells providing a good adjunct to immunotherapy. Microglia and macrophages that transport to glioma tumours are altered into the protumorigenic M2 phenotype, promoting immune suppression and tumour cell suppression. These tumour associated microglia/macrophages have been shown to comprise up to 30 % of GBM tumour bulk. These microglia/macrophages express high levels of PD-L1 contributing to the local immunosuppressive phenotype. M1 macrophages induce anti-tumorigenic immune responses by leading to a decrease in regulatory T cells and an increase in CD8+ T cells. Soluble factors produced by GBM cells induce CCL22 secretion by M2 macrophages/microglia resulting in T Reg and MDSC cell recruitment to the tumour (D. Caponegro, Tetsuo Miyauchi et al. 2018).

VEGF secretion can inhibit the maturation and function of dendritic cells. Extracellular matrix components are found at high levels in the glioma tumour micro-environment. The presence of these extracellular matrix components leads to a retention of growth factors such as FGF and VEGF, which promotes tumour progression (Brown, N. F., Carter et al. 2018). These factors increase angiogenesis increasing the tumour vasculature resulting in upregulation of the macromolecules periostin and tenascin C (TNC). TNC blocks the migration of T cells across blood vessels preventing them penetrating the parenchyma. Periostin has also been shown to recruit circulating M2 macrophages into the tumour. GBM cells have been shown to down regulate MHC expression, proteins essential for antigen presentation. The presence of the immunosuppressive cytokines IL-10 and TGF- β are thought to cause the down regulation of MHC molecules in the tumour micro environment (Brown, N. F., Carter et al. 2018). TNF- α is responsible of dendritic cell maturation within the brain, it can also stimulate the growth of T-cells. TNF- α can have both pro-tumourigenic and anti-tumourigenic effects in the GBM setting. Exposure of GBM cells to TNF- α leads to increased

neovascularisation via the upregulation of pro angiogenic cytokines such as IL-8 and VEGF (Zhu, V. F., Yang et al. 2012).

IL-1 β is a pro-inflammatory cytokine that has been shown to be upregulated in the U373 glioblastoma multiforme cell line and radiation has been shown to lead to upregulation of IL-1 β in GBM tumours (Kore, Abraham 2014). IL-1 β leads to increased intracellular signalling through mitogen-activated protein kinase (MAPK) and c-Jun N-terminal kinase 2 (JNK2) resulting in increased GBM cell proliferation and invasion. IL-1 β exposure also leads to increased VEGF secretion which as mentioned previously contributes to the immune evasion of GBM (Yeung, McDonald et al. 2013).

Intracellular adhesion molecule 1 (ICAM-1/CD54) is key for regulating the cellular microenvironment and mediating cell-cell interactions. ICAM-1 is commonly upregulated in the GBM setting with GBM tumours being shown to express higher levels of ICAM-1 when compared to normal brain when studied immunohistochemically (Gingras, Roussel et al. 1995). ICAM-1 is a ligand for lymphocyte function-associated antigen 1 (LFA-1/CD11a/CD18) this results in increased myeloid cell migration into the tumours and increased numbers of macrophages enhancing immune suppression within the tumours (Piao, Henry et al. 2017).

Expression of galectin-1 (Gal-1) by glioblastoma cells has been shown to promote proliferation and migration of these cells, not only does this Gal-1 expression promote migration and proliferation it also leads to the death of T-cells when they are co-cultured with Gal-1 expressing cells, further highlighting the ability of GBM to evade immune attack (Kovacs-Solyom, Blasko et al. 2010). Macrophage migration inhibitory factor (MIF) expression in GBM has been shown to be linked to immune escape. This antigen was found to be expressed in GBM tumours, and when MIF is knocked down in GBM tumour cells they become more susceptible to natural killer (NK) cell mediated killing (Mittelbronn, Platten et al. 2011).

HLA-G is a non-classical MHC class I molecule that plays a role in tolerance; it is often expressed on trophoblasts to prevent immune reactions to the developing foetus. HLA-G is also expressed in adult thymic epithelial cells, nail matrix and cornea. It is rarely expressed elsewhere in the body; however, GBM cells have been shown to express this protein (Wastowski, Simoes et al. 2013). HLA-G also has a soluble form that has been found in plasma, cerebrospinal fluid and sperm. High levels of HLA-G have also been correlated with cytomegalovirus, a virus commonly found present in GBM tumour tissues. HLA-G has several receptors, these are the inhibitory receptors ILT-2, ILT-4 and the non-inhibitory receptors CD8, CD160 and KIR2DL4. ILT-2 and ILT-4 are expressed on immune cells, they recognise MHC class I molecules via their $\alpha 3$ and $\beta 2m$ domains however they bind preferentially to HLA-G. Binding of soluble HLA-G to CD8 on T cells results in Fas-FasL mediated

CD8⁺ T cell apoptosis. HLA-G binding to ILT-2 inhibits NK cell cytotoxicity by inhibiting polarisation of lytic granules and the microtubule-organising centre at the contact zone (Carosella, Rouas-Freiss et al. 2015). HLA-E is another non-classical MHC class I molecule; it is a ligand for both NKG2A and NKG2C expressed on NK, CD8 $\alpha\beta$ and $\gamma\delta$ T cells. HLA-E can either lead to immune cell activation by binding with C-type lectin-like receptor NKG2C and it can also lead to immune cell inhibition by binding to C-type lectin-like receptor NKG2A. HLA-E has been shown to be expressed in glioblastoma tumour tissues and cell lines. HLA-E much like HLA-G is thought to play a role in maternal tolerance of a foetus (Wischhusen, Friese et al. 2005). GBM has been shown to express FasL (CD95L), this ligand binds to Fas (CD95/APO-1) on T-cells leading to their apoptosis. GBM tissue staining revealed that this expression of FasL by GBM cells induced cell death of CD3 T-cells expressing Fas (Didenko, Ngo et al. 2002).

Stat3 is a cytoplasmic transcription factor that is activated by upstream events such as growth factor and cytokine signalling. When Stat3 is activated it is phosphorylated and persistent Stat3 phosphorylation is seen in numerous cancers including GBM. Stat3 phosphorylation has been found to varying degrees in GBM and the amount of Stat3 phosphorylation has been directly correlated to brain tumour grade with GBM (grade IV) showing the highest level of Stat3 phosphorylation (Birner, Toumangelova-Uzeir et al. 2010). Stat3 regulatory proteins have also been shown to be downregulated in GBM patients. One such example is protein inhibitor of Stat3 (PIAS3), and this protein was only detected in 11 % of GBM samples compared to 100 % control non-neoplastic brain samples from epileptic patients. IL-6 is a key activator of Stat3, IL-6 and its receptor are often upregulated in GBM tumours further highlighting the importance of Stat3 activation in GBM tumour malignancy. Knockdown of Stat3 in GBM cell lines results in slower *in vitro* and *in vivo* growth (Luwor, Stylli et al. 2013).

Indoleamine 2, 3-dioxygenase (IDO) is an enzyme involved in the catabolism of the amino acid tryptophan into immune-regulatory kynurenines. IDO much like many other immune inhibitory proteins is involved in prevention of maternal foetal rejection. Activation of several receptors leads to downstream signalling events that induce IDO expression. Toll like receptors (TLRs), tumour necrosis factor receptor superfamily members (TNFRs), interferon gamma receptors (IFNGR), interferon beta receptors (IFNBR), transforming growth factor beta receptors (TGFBRs) and aryl hydrocarbon receptors (AhRs) have all been shown to induce IDO expression upon activation. The depletion of tryptophan by IDO has been shown to inhibit immune cells and prevent dendritic cell maturation (Mbongue, Nicholas et al. 2015). IDO has been identified as a significant immunosuppressive factor in glioblastoma multiforme. IDO is upregulated in recurrent GBMs, with Mitsuka et al. (2013) finding that 100 % of patients studied expressed IDO upon second surgery (Mitsuka, Kawataki et al. 2013).

Research has also shown that GBM promotes T-cell death via CD70 and ganglioside expression (Chahlavi, Rayman et al. 2005). Activated T-cells were shown to be more susceptible to GBM-cell induced death. CD70 expressed by GBM binds to CD27 a TNFR family member that modulates apoptosis upon binding of CD70. Blockade of CD70 on GBM cell lines partially protected T cells from apoptosis. The contribution of gangliosides to T cell death was also studied using DL-thre-phenyl-2-hexadecanoylamino-3-pyrrolidino-1-propanol (PPPP) an inhibitor of glucosylceramide synthesis. PPPP was proven to induce a reduction in ganglioside expression when PPPP cells were assessed by HPLC. This reduction in gangliosides resulted in reduced T-cell apoptosis by GBM cell lines (Chahlavi, Rayman et al. 2005).

Unfortunately, standard therapies have also been shown to increase glioblastoma multiforme immunosuppression. *In vitro* studies have revealed that GBM cell lines exposed to doxorubicin and radiation therapy release the immunosuppressive cytokine prostaglandin E2 (PGE2). Cells exposed to TMZ were also shown to suppress the proliferation of T-cells via the release of PGE2 (Authier, Farrand et al. 2015). Furthermore, the current treatment strategies have also been shown to hamper immunotherapeutic approaches. Steroids are often given to patients to counteract cerebral oedema, dexamethasone is frequently used in this context. Dexamethasone has been shown to result in upregulation of the immunosuppressive checkpoint CTLA-4 on T-cells, reducing their anti-tumour activity. Dexamethasone was also shown to reduce the proliferation of T-cells (Giles, Hutchinson et al. 2018). To alleviate the potential deleterious effects of dexamethasone alternative treatments need to be considered. One such alternative for the relief of oedema is the previously mentioned FDA approved anti-VEGF antibody Bevacizumab.

Tumours establish a somewhat immunoprivileged environment via their altered physiology and co-opting of stromal cells. The brain is a unique organ with an extracellular matrix composed of proteoglycans, glycosaminoglycans and glycoproteins. In the brain tumour microenvironment significant increases in heparan sulphate proteoglycans (HSPG) have been observed. These HSPGs can trap growth factors such as FGF and VEGF in the tumour microenvironment. As mentioned previously this VEGF secretion leads to upregulation of TNC and periostin promoting cancer cell survival and increased trapping of T-cells within blood vessels preventing their penetration of the tumour bulk (Quail, Joyce 2017). Hypoxia is one of the hallmarks of GBM tumours, this hypoxia potentiates the immune suppression exerted by these tumours. Hypoxia can lead to increased secretion of angiogenic factors such as VEGF by tumour cells, which as mentioned previously generates an immunosuppressive microenvironment. Another factor that enables GBMs to suppress the immune system and evade immune surveillance is their high heterogeneity as indicated in their name 'multiforme'. The presence of stem-like/cancer initiating GBM cells has

been shown to contribute to the immunosuppressive nature of GBM (Wei, Barr et al. 2010, Wu, Wei et al. 2010).

1.9. Immune checkpoint blockade for GBM

As mentioned previously tumours upregulate immune inhibitory checkpoints such as PD-L1. Research has found a plethora of immune inhibitory proteins that can be targeted to boost the resident anti-tumour immune response. Many of these immune checkpoints are being targeted in the cancer setting with several checkpoint blockade antibodies being approved for therapy and many more being tested in clinical trials. Ipilimumab (anti-CTLA4) and Pembrolizumab (anti-PD-1) have been approved for the treatment of melanoma and renal cell carcinoma. Pembrolizumab has also been approved for non-small cell lung cancer and Hodgkin lymphoma. These checkpoint blockade modalities are gaining traction in the field of cancer therapy. Checkpoint blockade has been tested in the GBM setting and researchers have tried to identify molecular patterns linked with immune checkpoint blockade responsiveness. In recurrent GBM non-response to anti-PD-1 therapy was linked to PTEN mutations, whereas mutations in the MAPK pathway were linked with a response to anti-PD-1 therapy. These PTEN mutations were linked with immunosuppressive gene signatures meaning that despite PD-1 blockade the immune system is still being suppressed via other mechanisms within the tumour microenvironment (Zhao, Chen et al. 2019). When used in a neoadjuvant manner (prior to surgical resection) PD-1 therapy was not linked to an increase infiltration of immune cells and no significant changes in T-cell function were observed when compared to the immune microenvironment prior to treatment. When comparing neoadjuvant Pembrolizumab with adjuvant Pembrolizumab therapy in the GBM setting it was found that neoadjuvant therapy was linked to an increase in IFN- γ related genes and a repression of cell cycle gene expression in tumour cells. These findings seem to suggest that pembrolizumab checkpoint blockade is more efficacious in the neoadjuvant setting as opposed to the adjuvant setting (Ito, Nakashima et al. 2019). What is even more exciting about these immune checkpoint blockade therapies is that they can also be combined with other treatment modalities, most interestingly is the potential of combining checkpoint blockade with active immunotherapy with the purpose of boosting the anti-tumour immune response generated by vaccination.

1.10. ImmunoBody® vaccination

As previously mentioned immunotherapy has been tested in the GBM setting however there appear to be several challenges involved in treating these types of tumours with immunotherapy

and several clinical trials have fallen at the last hurdle, as a result of these failures there is a great need to find novel ways of generating an active immune response in GBM patients.

ImmunoBody[®] (Scancell) is a DNA plasmid vaccine that encodes a human IgG1 antibody with CD8+ and CD4+ T-cell epitopes engrafted into the complementarity determining regions (CDRs) of the antibody. This method of vaccinations generates an immune response via direct presentation (transfection of the antigen presenting cells (APCs)) and by cross presentation (transfection of non-APCs resulting in secretion of the IgG1 protein and its uptake by APCs (Pudney, Metheringham et al. 2010). The ImmunoBody[®] vector generates a 100-fold higher avidity response than an identical peptide vaccination (Brentville, Metheringham et al. 2012).

SCIB1 is an ImmunoBody[®] vaccine that encodes three immunogenic epitopes, two for the melanoma antigen gp100 (glycoprotein 100/PMEL/melanocyte protein) and one for the antigen TRP-2 (tyrosine-related protein 2/dopachrome tautomerase (DCT)/dopachrome delta-isomerase) (Xue, W., Brentville, Symonds, Cook, Yagita, Metheringham, and Durrant 2016). These two antigens are abundant in the melanoma setting. SCIB1 encodes a CD8+ T-cell 9-mer epitope for TRP-2 and a 16-mer and 18-mer gp100 sequences containing both CD4+ and CD8+ T-cell epitopes (See *Figure 3*). Pre-clinical results with a TRP-2 directed ImmunoBody[®] have shown that this mode of vaccination generates a high avidity T-cell response that resulted in a significant decrease in B16F10 murine melanoma tumour size (Metheringham, Pudney et al. 2009, Pudney, Metheringham et al. 2010). These promising pre-clinical results have led to the initiation of ImmunoBody[®] clinical trials in the melanoma setting. Phase I results showed that SCIB1 ImmunoBody[®] vaccination was well tolerated with no adverse events seen in patients. Even more impressive was that 23/25 patients showed a detectable immune response and one patient's tumour lesions were seen to decrease in size (Patel, Poulam M., Durrant et al. 2014, Patel, P. M., Ottensmeier et al. 2018). The promising early results for SCIB1 have led to some pre-clinical work looking at combining SCIB1 vaccination with anti-PD-1 checkpoint blockade. SCIB1 and anti-PD-1 were used in combination to treat B16F1-DR4 melanoma tumours in transgenic HLA-DR4 mice. This combination was shown to increase survival and reduce tumour volume. Even when mice were challenged with a high number of tumour cells the combined SCIB1 anti-PD-1 therapy still led to improved survival in these animals when compared to SCIB1 or anti-PD-1 monotherapy (Xue, W., Brentville, Symonds, Cook, Yagita, Metheringham, and Durrant 2016). The ImmunoBody[®] plasmid can be engineered to target cancer related antigens other than TRP-2 and gp100; SCIB2 is an ImmunoBody[®] plasmid that has epitopes for New York oesophageal squamous cell carcinoma 1 (NY-ESO-1) engrafted into its complementarity determining regions (CDRs) as opposed to TRP-2 and gp100. Combining PD-1 blockade with SCIB2 ImmunoBody[®] vaccination was shown to result in 100 % long term survival in mice harbouring NY-ESO-1 expressing B16 tumours (Xue, W., Metheringham et al. 2016). The

advantage of ImmunoBody[®] vaccination is that it generates high avidity T-cell responses which have been shown to be enough for eradication of antigen expressing tumours. Another advantage of the ImmunoBody[®] plasmid is that it can easily be engineered to target other tumour specific epitopes and this method of vaccination does not require administration of an adjuvant to generate a strong anti-tumour response.

Epitope inserted into H1 & L3 site - gp100₁₇₃₋₁₉₀ (GTGRAMLGHTHTMEVTYH)
 H2 site - TRP2₁₈₀₋₁₈₈ (SVYDFFVWL)
 H3 & L1 site - gp100₄₄₋₅₉ (WNRQLYPEWTEAQRDL)

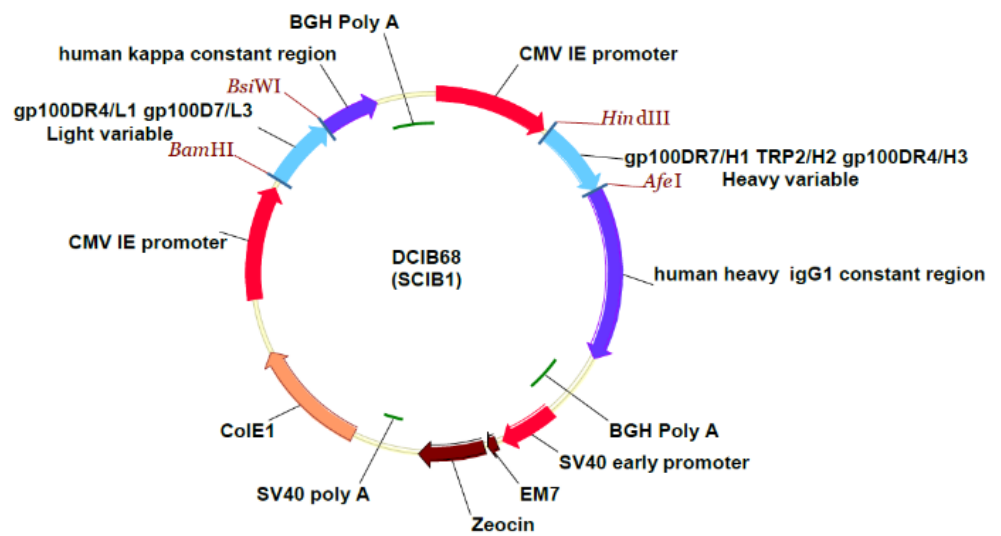


Figure 3. A schematic representation of the SCIB1 ImmunoBody[®] plasmid with the gp100 and TRP-2 peptide sequences detailed, and their insertion sites outlined. Diagram provided in a correspondence from Scancell Ltd.

1.11. Carnosine as a first line non-toxic therapeutic

In order to treat GBM a multitude of treatment modalities will most likely need to be combined. Previous research has found that single therapies are not as effective as combinatorial therapies (Stupp, Mason et al. 2005). Whilst combining therapeutic modalities can help improve patient survival one key factor to consider is the increased potential for deleterious side effects, for example the combination of anti-PD-1 and anti-CTLA-4 immune checkpoint blockade has been linked to increased incidences of adverse immune events in the melanoma setting (Hassel, Heinzerling et al. 2017). As a result combining standard therapy with treatments that have little to no side effects represents an exciting avenue for GBM therapy. In GBM the use of a ketogenic diet (low carbohydrate high fat) has been explored in combination with the current standard therapy (TMZ and radiotherapy (RT)). Early studies using a ketogenic diet in combination with standard therapy have revealed that this method of treating GBM holds promise and indicate that altering metabolism may hold the key to tackling GBM (Champ, Palmer et al. 2014, Zuccoli, Marcello et al. 2010).

Carnosine is a dipeptide composed of the amino acids beta alanine and L-histidine. Carnosine is abundant within the brain and skeletal muscle. Carnosine is a relatively enigmatic compound which has been shown to have many functions in numerous settings. It has been suggested that carnosine can act as a free radical scavenger, metal ion chelator, neurotransmitter, immunomodulatory, anti-oxidant and pH buffer to name a few (Hipkiss, Preston et al. 1998). Carnosine has been shown to have anti-tumour effects in numerous cancers, however the mechanism by which carnosine affects tumour cells has not been fully elucidated, and carnosine has been shown to induce various changes within tumour cells. Previous research has shown that carnosine can inhibit human GBM cell growth (Oppermann, Dietterle et al. 2018). The activity of carnosine has been examined in numerous cancers and the proposed mechanism of action seems to be varied depending on the cancer studied.

In the cancer setting carnosine has been shown to reduce the acidification of growth media when HeLa cervical cancer cells were grown under hypoxia *in vitro*. This reduced acidification was attributed to a reduction in the amount of carbonic anhydrase IX (CAIX) enzyme activity within these cells, and carnosine was shown to directly interact with CAIX tumours (Ditte, Ditte et al. 2014). Carnosine was also shown to lead to increased HIF-1 α expression in HeLa cells cultured under hypoxic conditions. *In vivo* carnosine treatment led to a lower rate of tumour growth in a HeLa xenograft model with a reduction in the size of carnosine treated tumours even observed. The carnosine treated tumours were also shown to express higher levels of HIF-1 α compared to control tumours (Ditte, Ditte et al. 2014). The reduction of extracellular acidification has been explored as potential treatment strategy for cancer and as a result the pH buffering effects of carnosine represent an attractive therapeutic modality. Combination of carnosine with the chemotherapeutic

agent 5-fluorouracil (5-FU) has also shown therapeutic potential against HT29 colon cancer cells *in vitro*. Carnosine did not directly induce apoptosis of 5-FU resistant HT29 cells, but it did however reduce the proliferation of these cells. Carnosine was shown to increase the sensitivity of these cells by reducing HIF-1 α expression and its downstream targets (Iovine, Guardia et al. 2016). These results contradict those findings found using HeLa cervical cancer cells highlighting the enigmatic nature of the carnosine dipeptide. Carnosine also seemed to be cytotoxic for the human renal carcinoma cell line Caki-2, leading to increased activity of the apoptotic protein caspase-3. Computer modelling revealed that carnosine binds to a specific drug binding pocket on caspase-3 (Pandurangan, Mistry et al. 2016). Carnosine appeared not to induce apoptosis or necrosis of the gastric cancer cell line SGC-7901 however it did appear to have an anti-proliferative effect. Further analyses revealed that carnosine treatment reduced the basal oxygen consumption rate and extra cellular acidification rate of SGC-7901 cells indicating that carnosine has the potential to inhibit glycolysis by these cells (Shen, Yang et al. 2014). Carnosine is broken down by the enzyme carnosinase, interestingly it has been found by proteomic analysis that the carnosinase 1 precursor (CNDP1) protein is down-regulated in GBM patient plasma compared to healthy control plasma (Gautam, Nair et al. 2012). These findings point to an anti-cancer effect of carnosine, if not by inducing cell death it affects the proliferation of cancer cells. Either effect would be greatly beneficial for the treatment of GBM, due to the relatively rapid growth of GBM tumours and their highly invasive nature. This holds promise for the use of carnosine as a therapeutic agent in the GBM setting.

1.12. Aims

The aim of this thesis is to examine the antigen expression profile of human GBM tumours and human and murine cell lines with the aim of identifying targetable immunogenic antigens and potential antigens that can be targeted immunotherapeutically. Once targetable antigens have been identified ImmunoBody[®] vaccination will be utilised to target the identified tumour associated antigens. The effect of IFN γ on the immune profile of GBM cell lines will also be studied as active immunotherapy generates IFN γ release from immune cells. Once the efficacy of ImmunoBody[®] vaccination has been demonstrated, PD-1/PD-L1 blockade will be incorporated into the vaccination strategy to boost the anti-tumour immune response in a proof of concept pre-clinical *in vivo* model of GBM using antigen expressing tumour cells implanted in the brains of humanised mice. As an adjunct to these immunotherapeutic studies the effects of carnosine on GBM cell lines will be studied.

CHAPTER 2: MATERIALS AND METHODS

2.1. Materials used

2.1.1. Cell lines

Name	Description	Age (Years)	Sex	Culture medium	Supplier
SEBTA-022	GBM left parietal lobe	67	Male	DMEM + GlutaMAX (Gibco) + 10% FCS	A generous gift from the Portsmouth neuro-oncology group
SEBTA-025	GBM right frontal lobe	24	Male	DMEM + GlutaMAX (Gibco) + 10% FCS	A generous gift from the Portsmouth neuro-oncology group
SEBTA-027	Recurrent GBM right parieto-occipital region	59	Female	DMEM + GlutaMAX (Gibco) + 10% FCS	A generous gift from the Portsmouth neuro-oncology group
UP-007	GBM	71	Male	DMEM + GlutaMAX (Gibco) + 10% FCS	A generous gift from the Portsmouth neuro-oncology group
UP-019	GBM	68	Female	DMEM + GlutaMAX (Gibco) + 10% FCS	A generous gift from the Portsmouth neuro-oncology group
UP-029	GBM	66	Male	DMEM + GlutaMAX (Gibco) + 10% FCS	A generous gift from the Portsmouth neuro-oncology group
SF-188	GBM	8	Male	DMEM + GlutaMAX	A generous gift from the

				(Gibco) + 10% FCS	Portsmouth neuro- oncology group
IN-699	GBM	15	Male	DMEM + GlutaMAX (Gibco) + 10% FCS	A generous gift from the Portsmouth neuro- oncology group

Table 1. Details of the human cell lines used for this study.

Name	Description	Origin	Modifications	Culture medium	Supplier
B16 HHDII/DR1 Luc2	Murine melanoma	Naturally occurring tumour taken from the C57BL/6 mouse	Transfected with the luciferase gene and the chimeric HLA- A2/DR1 receptors HHDII/DR1	RPMI 1640 + 1% L- glutamine + 10% FCS + 550 µg/mL Zeocin + 300 µg/mL Hygromycin + 500 µg/mL G418	A generous gift from Scancell Ltd.
GL261 Luc2	Murine glioblastoma	Induced via intracranial injection of methylcholanthrene into a C57BL/6 mouse	Transfected with the luciferase gene	DMEM (Lonza) + 10% FCS + 100 µg/mL G418	A generous gift from the Barrow Neurological Institute

Table 2. Details of the murine cell lines used for this study.

2.1.2. Reagents

Reagent	Supplier
0.22 µm syringe filter	Sartorius
1.0 µm gold microcarriers	BioRad

1M Tris-HCl	Invitrogen
2-mercaptoethanol	Sigma
4% Paraformaldehyde in PBS	Santa Cruz
40 µm nylon strainer	Greiner bio-one
Agar	Bioline
Agarose	Bioline
Ammonium persulphate (APS)	Geneflow
Ampicillin	Sigma
Anhydrous ethanol	Sigma
Anti PD-1 for in vivo	BioXCell
Avidin D solution	Vector labs
Bicinchoninic acid	Sigma
Biotin solution	Vector labs
Bovine serum albumin (BSA)	Merck Millipore
Brefeldin A	BioLegend
Bromophenol blue	Arcos Organics
Calcium chloride	Sigma
Carnosine	Sigma
Cell culture flasks for GBM cells	Greiner bio-one
Cell culture flasks for murine tissue culture	Sarstedt
Clarity western ECL substrate	BioRad
Collagenase type 1 from clostridium histolyticum	Sigma
Conical flasks	Pyrex
Copper (II) sulphate	Sigma
DAPI Vectashield mounting media	Vector labs
Dimethyl sulfoxide (DMSO)	Insight biotechnology
DMEM	Lonza
DMEM+ GLUTAMAX	Gibco

DNA ladder 1 Kb plus	Promega
DNase	Sigma
Double distilled water	Barnstead, Nanopure Diamond
DPX mounting media	Sigma
Dulbecco's phosphate buffered saline	Lonza
EDTA 0.5M	Ambion
Eppendorf tubes	Starsedt
Ethanol	Fisher scientific
Ethyl alcohol absolute	VWR
Ethyldiamine tetraacetic acid (EDTA)	Sigma
FACS tubes	Tyco healthcare group
Falcon tubes	Sarstedt
FCS	Fisher Scientific
Filter paper	Schleicher-Schuell
Flow check beads	Beckman Coulter
Flow set beads	Beckman Coulter
Fungizone (amphotericin B)	Promega
Genetecin (G418)	Sigma
Glacial acetic acid	Fisher scientific
Glass coverslips	SLS
Glass microscope slides	SLS
Glycerol	Sigma
Glycine	Sigma
Goat serum	Sigma
HALT protease and phosphatase inhibitor cocktail	ThermoFisher
HEPES	Lonza
Hydrochloric acid	Fisher scientific
Hydrogen peroxide	Sigma
Hygromycin	Merck Millipore

Isopropanol	Sigma
Isoton sheath fluid	Beckman Coulter
LB broth	Sigma
LB broth low salt (Luria)	Sigma
LB broth with agar	Sigma
L-Carnosine	Sigma
L-glutamine	Lonza
L-shaped spreader	Sigma
Marvel skimmed milk powder	Marvel
Mayer's Haematoxylin	Sigma
Methanol	Fisher scientific
Mitomycin C	Sigma
Monensin	Biolegend
MTT reagent	Sigma
Murine IFN γ elispot kit	Mabtech
OneComp eBeads compensation beads	Thermo Fisher
PD-1 isotype control	BioXCell
P-dimethylaminobenzaldehyde	Sigma
Penicillin/Streptomycin	Lonza
Peptides	GenScript
PerFix-nc kit	Beckman Coulter
Petri dishes	Sarstedt
Phosphate buffered saline (PBS) tablets	Oxoid
Pipette tips	Greiner bio-one/Sarstedt
Polyvinyl pyrrolidone (PVP)	Sigma
Protogel (30% acylamide)	GeneFlow
PVDF blotting membrane	GE healthcare
QIAGEN QUA-filter plasmid midi kit	QIAGEN
Recombinant human IFN γ	Peptidech

RPMI 1640	Lonza
Scalpels	SLS
SCIB1 ImmunoBody® plasmid	Scancell Ltd.
Serological pipettes	Sarstedt
Sodium chloride	Calbiochem
Sodium citrate trisodium salt dihydrate	Sigma
Sodium dodecyl sulphate (SDS)	Sigma
Sodium pyruvate	Lonza
Solution 18	ChemoMetec
Spermidine	Sigma
Staphylococcal enterotoxin B (SEB)	Sigma
Streptavidin alkaline phosphate conjugate substrate kit	BioRad
Sucrose	Sigma
SYBR® safe DNA gel stain	Invitrogen
Syringes	Becton Dickenson
Tefzel tubing	BioRad
TEMED	GeneFlow
Tetraethylammonium bromide (TEAB) 25 mM	Sigma
Tissue culture plates	Sarstedt
Trichloro-acetic acid (TCA)	Sigma
Triton X-100	Sigma
Trizma base	Sigma
Trypan blue solution 0.4%	Sigma
TrypLE Express	Gibco
Trypsin/versine	Lonza
TWEEN20	Sigma
Vectastain Elite ABC HRP kit	Vector labs
WT-1 ImmunoBody® plasmid	Scancell Ltd.

Xylene	Fisher scientific
Zeocin	Invitrogen

Table 3. Details of the reagents used and the supplier of each reagent

2.1.3. Buffer recipes

0.025 mg/mL PVP
8.75 μ L 20 mg/mL PVP
7 mL anhydrous ethanol
0.1% triton X100 in PBS
10 μ L triton X100
10 mL dH ₂ O
0.5% BSA in PBS
0.5 g BSA
100 mL PBS
0.5 M spermidine
14.525 g calcium chloride
100 ml dH ₂ O
0.05 M spermidine
50 μ L 0.5 M spermidine
450 μ L nuclease free water
1 M Calcium chloride
11.098 g calcium chloride
100 ml dH ₂ O
1M Sodium chloride
0.5844 g sodium chloride
10 mL dH ₂ O

1M Tris pH 6.8
12.114 g trizma base
90 mL dH ₂ O
Adjust pH to 6.8 using hydrochloric acid then top up to 100 mL with dH ₂ O
1.5 M Tris pH 8.8
18.171 g trizma base
90 mL dH ₂ O
Adjust pH to 8.8 using hydrochloric acid then top up to 100 mL with dH ₂ O
1x PBS
10 PBS tablets
1000 mL dH ₂ O
1x Running buffer
100 mL 10x Running buffer
900 mL dH ₂ O
1x Transfer buffer
100 mL 10x Transfer buffer
900 mL dH ₂ O
3% hydrogen peroxide in methanol
10 mL 30 % hydrogen peroxide
90 mL ethanol
5 % Stacking gel (x1 gel)
4.1 mL dH ₂ O
1 mL 30 % acylamide mix
750 µL 1M Tris pH 6.8

60 µL 10 % APS
60 µL 10 % SDS
6 µL TEMED
5x SDS-PAGE loading buffer
1 mL glycerol
1g SDS
3.125 1M Tris-HCl pH 8.0
2.5 mL beta mercaptoethanol
1 mL 0.5% bromophenol blue
1.375 dH ₂ O
10 % APS
10 mL dH ₂ O
1 g APS
10% Resolving gel (x1 gel)
4 mL dH ₂ O
3.3 mL 30 % acylamide mix
2.5 mL 1.5M Tris pH 8.8
100 µL 10 % APS
100 µL 10 % SDS
4 µL TEMED
10 % sodium deoxycholate
0.3 g sodium deoxycholate
3 mL dH ₂ O
10 % SDS

10 mL dH ₂ O
1 g SDS
10 % Triton X100
600 µL Triton X100
5.4 mL dH ₂ O
10x Running buffer
30.3 g trizma base
144 g glycine
10 g SDS
1000 mL dH ₂ O
10 x TBS
24.2 g trizma base
80 g sodium chloride
800 mL dH ₂ O
Adjust pH to 7.6 using hydrochloric acid then top up to 1000 mL with dH ₂ O
10x Transfer buffer
30.3 g trizma base
144 g glycine
1000 mL dH ₂ O
20 mg/mL PVP
10 mg PVP powder
500 µL anhydrous ethanol
100 mM EDTA
0.2922 g EDTA

10 mL dH ₂ O
Complete T-cell media
50 mL FCS (10 %)
5 mL penicillin and streptomycin (1 %)
5 mL L-glutamine (200 mM)
10 mL HEPES (200 mM)
0.5 mL fungizone (0.1 %)
1 mL 1 M beta mercaptoethanol (2 mM)
428.5 mL RPMI 1640
Ehrlich's reagent
200 mg P-dimethylaminobenzaldehyde
10 mL glacial acetic acid
LB broth Luria low salt
30.5 g LB broth low salt powder
1000 mL dH ₂ O
Autoclave at 151 °C for 15 minutes
LB broth with agar
40 g LB broth with agar powder
1000 mL dH ₂ O
Autoclave at 151 °C for 15 minutes
5 mg/mL MTT reagent
250 mg MTT
50 mL DPBS
PBST

0.5 mL TWEEN 20
1000 mL PBS
RIPA buffer
2.5 mL 1M Tris-HCl pH 8.0
7.5 mL 1 M sodium chloride
0.5 mL 10 % SDS
2.5 mL sodium deoxycholate
5 mL 10 % Triton X100
0.5 mL 100 mM EDTA
31.5 mL dH ₂ O
Sodium citrate pH 6.0
2.94 g sodium citrate trisodium salt dihydrate
800 mL dH ₂ O adjust pH to 6.0 using hydrochloric acid then top up to 1000 mL with dH ₂ O
0.5 mL TWEEN 20
TBST
100 mL 10 x TBS
900 mL dH ₂ O
1 mL TWEEN 20
TE buffer
1 mL 1M tris pH 8.0
200 µL 0.5 M EDTA pH 8.0
99.8 mL dH ₂ O
Tris-EDTA pH 9.0
1.21 g Trizma base

0.37 g EDTA
900 mL dH ₂ O adjust pH to 9.0 using hydrochloric acid or sodium hydroxide then top up to 1000 mL with dH ₂ O
0.5 mL TWEEN 20

Table 4. Recipes for the buffers used. The buffer name is emboldened and the ingredients are listed below.

2.1.4. Antibodies for Western blotting

Antibody	Dilution	Manufacturer
Mouse anti-human HLA-A, B, C	1:1000	Abcam
Mouse anti-human HLA-E	1:1000	Abcam
Mouse anti-human HLA-G	1:1000	Abcam
Rabbit anti-human PD-L1	1:1000	Cell Signalling
Rabbit anti-human MGMT	1:1000	Abcam
Rabbit anti-mouse/human TRP-2	1:1000	Abcam
Rabbit anti-human/mouse WT-1	1:500	Abcam
Rabbit anti-human/mouse gp100	1:500	Abcam

Rabbit anti-human HAGE	1:250	Sigma
Rabbit anti human/mouse Vinculin	1:10000	Abcam
Mouse anti human IDO	1:250	Abcam
HRP conjugated goat anti-rabbit	1:1000	Cell Signalling
HRP conjugated horse anti-mouse	1:1000	Cell Signalling

Table 5. Antibodies used for Western blotting

2.1.5. Antibodies for immunohistochemistry

Antibody	Dilution	Manufacturer	Antigen retrieval buffer used
Mouse anti-human HLA-A, B, C	1:500	Abcam	Sodium citrate pH 6.0
Mouse anti-human HLA-E	1:500	Abcam	Sodium citrate pH 6.0
Mouse anti-human HLA-G	1:25	Abcam	TRIS-EDTA pH 9.0
Rabbit anti-human PD-L1	1:50	Cell Signalling	Sodium citrate pH 6.0
Rabbit anti-human MGMT	1:500	Abcam	Sodium citrate pH 6.0

Rabbit anti-mouse/human TRP-2	1:500	Abcam	TRIS-EDTA pH 9.0
Mouse anti-human WT-1	1:50	Dako	Sodium citrate pH 6.0
Rabbit anti-human/mouse gp100	1:50	Abcam	Sodium citrate pH 6.0
Rabbit anti-human HAGE	1:100	Sigma	Sodium citrate pH 6.0

Table 6. Antibodies used for immunostaining

2.1.6. Antibodies for immunofluorescence/immunocytochemistry

Antibody	Dilution	Manufacturer
Rabbit anti-mouse/human TRP-2	1:150	Abcam
Rabbit anti-human/mouse WT-1	1:50	Abcam
Donkey anti-rabbit Alexa Fluor® 488	1:500	Abcam

Table 7. Antibodies used for Immunocytochemistry and Immunofluorescence

2.1.7. Antibodies for flow cytometry

2.1.7.1 Antibodies for cell surface staining of human cells

Antibody	Clone	Fluorophore	Supplier
Anti-human HLA-A, B, C	W6/32	APC/Cy7	BioLegend

Anti-human HLA-E	3D12	PerCP/Cy5.5	BioLegend
Anti-human HLA-G	87G	PE/Cy7	BioLegend
Anti-human HLA-A2	BB7.2	APC	BioLegend
Anti-human CD80	2D10	PE/Dazzle™ 594	BioLegend
CD86	IT2.2	Pacific blue™	BioLegend
Anti-human FasL	NOK-1	PE	BioLegend
Anti-human MICA/B	6D4	Alexa Fluor® 488	BioLegend
Anti-human PD-L1	29E.2A3	APC	BioLegend
Anti-human CD40	53C	Alexa Fluor® 700	BioLegend
Anti-human CD119	GIR-208	PE	BioLegend
LIVE/DEAD™ fixable violet	N/A	N/A	ThermoFisher
FcR blocking reagent	N/A	N/A	Miltenyi Biotec

Table 8. Details of the antibodies used for flow cytometry

2.1.7.2. Antibodies for intracellular murine splenocyte staining

Antibody	Clone	Fluorophore	Supplier
Anti-mouse CD107a	MEL-14	FITC	BioLegend

Anti-mouse TNFα	MP6-XT22	PE	BioLegend
Anti-mouse Ki67	SolA15	PE-eFluor 610	eBioscience
Anti-mouse IL-2	JES6-5H4	PerCP/Cy5.5	BioLegend
Anti-mouse IFNγ	XMG1.2	Pe/Cy7	BioLegend
Anti-mouse/human Granzyme B	QA16A02	APC	BioLegend
Anti-mouse CD4	GK1.5	Alexa Fluor [®] 700	BioLegend
Anti-mouse CD8a	53-6.7	APC/Cy7	BioLegend
Anti-mouse CD3	17A2	Brilliant violet 421 [™]	BioLegend
LIVE/DEAD[™] fixable violet	N/A	N/A	ThermoFisher
Hamster anti-mouse CD28 (for stimulation)	N/A	N/A	Becton Dickinson
Rat anti-mouse CD49d (for stimulation)	N/A	N/A	Becton Dickinson
Anti-CD16/32 (FcR blocking reagent)	N/A	N/A	BioLegend

Table 9. Details of the antibodies used for flow cytometry

2.1.7.3. Antibodies for brain TIL staining

Antibody	Clone	Fluorophore	Supplier
Anti-mouse CD69	H1.2F3	PE/Dazzle [™]	BioLegend
Anti-mouse FoxP3	MF-14	Pacific blue [™]	BioLegend
Anti-mouse CD62L	MEL-14	Alexa fluor [®] 488	BioLegend

Anti-mouse CD25	3C7	PerCP/Cy5.5	BioLegend
Anti-mouse CD3	17A2	PE	BioLegend
Anti-mouse PD-1	29F.1A12	APC/Cy7	BioLegend
Anti-mouse/human CD44	IM7	Alexa Fluor®700	BioLegend
Anti-mouse CD4	RM4-5	PE/Cy7	BioLegend
Anti-mouse CD8a	53-6.7	APC	BioLegend
LIVE/DEAD™ fixable violet	N/A	N/A	ThermoFisher
Anti-CD16/32 (FcR blocking reagent)	N/A	N/A	BioLegend

Table 10. Details of the antibodies used for flow cytometry

2.2. Methods

2.2.1. Cell culture

2.2.1.1 Human cell culture

All glioblastoma multiforme cell lines were cultured in GBM cell media (detailed in *Table 1*). Once cells had reached 80-90% confluency they were washed once with DPBS. Once washed a thin coating of TrypLE express was added to the cells. Cells were then left under TrypLE express at room temperature and checked at regular intervals using a light microscope. Once cells were visibly detached and floating complete media containing FCS was added to neutralise the TrypLE express. The volume of media added depended upon the size of flask used, for a T25 flask 5 mL of media was added for a T75 flask 10 mL of media was added and for a T175 flask 20 mL of media was added. The media was gently pipetted up and down the cell culture surface to rinse the cells off and then the media was transferred to a Falcon tube. The cells were then pelleted by centrifugation at 12,000 RPM for 5 minutes. Once complete media was removed from the pellet and the pellet was re-suspended in fresh culture media. Fresh tissue culture flasks had the desired amount of GBM media added to them and then the desired amount of cell suspension was added to each flask. Tissue culture flasks were then placed in a humidified incubator at 37 °C with 5% CO₂ (Sanyo).

2.2.1.2. Murine cell culture

The B16 HHDII/DR1 Luc cell line and the GL261 Luc2 cell lines were cultured in the appropriate media detailed above. Once cells had reached 80-90% confluency they were washed once with DPBS. Once washed a thin coating of trypsin/versine was added to the cells. Cells were then left under trypsin/versine in a 37 °C humidified tissue culture incubator (Sanyo) and checked at regular intervals using a light microscope. Once cells were visibly detached and floating complete media containing FCS was added to neutralise the trypsin/versine. The volume of media added depended upon the size of flask used, for a T25 flask 5 mL of media was added for a T75 flask 10 mL of media was added and for a T175 flask 20 mL of media was added. The media was gently pipetted up and down the cell culture surface to rinse the cells off and then the media was transferred to a Falcon tube. The cells were then pelleted by centrifugation at 12,000 RPM for 5 minutes, once complete media was removed from the pellet and the pellet was re-suspended in fresh culture media. Fresh tissue culture flasks had the desired amount of GBM media added to them and then the desired amount of cell suspension was added to each flask. Tissue culture flasks were then placed in a humidified incubator at 37 °C with 5% CO₂ (Sanyo).

2.2.1.3. IFN γ treatment of GBM cell lines

Human GBM cells were cultured in a T75 flask, once cells had reached 80% confluency all of the media was removed and replaced with the appropriate culture media containing 100 ng/mL IFN γ . Cells were then left for either 24, 48 or 72 hours, at which point they were detached using TrypLE express and then either analysed using western blotting or flow cytometry.

2.2.1.4. Carnosine treatment of cell lines

GBM cells were cultured in a T75 flask, once cells had reached 80% confluency all of the media was removed and replaced with carnosine containing media of varying concentrations. The carnosine was prepared by dissolving L-carnosine in the appropriate culture media and then this solution sterile filtered using a 0.22 μ M syringe filter. Carnosine was then added to cells for 24 hours and once completed cells were detached and prepared for analysis.

2.2.2. Immunohistochemistry

2.2.2.1. Immunohistochemistry

Antibody staining conditions were optimised using the appropriate positive control tissues detailed in the table below. The antibody manufacturers' antigen retrieval conditions and antibody concentrations were utilised, as well as slightly higher and lower concentrations of antibodies. In

all cases the antibody suppliers' antigen retrieval method was suitable for the antibodies used, this is detailed in the table below.

Antibody	Positive control tissue used for optimisation	Supplier	Antigen retrieval method
Mouse anti-human HLA-A, B, C	Tonsil and spleen	US Biomax	Sodium citrate pH 6.0
Mouse anti-human HLA-E	Tonsil	US Biomax	Sodium citrate pH 6.0
Mouse anti-human HLA-G	Spleen	US Biomax	TRIS-EDTA pH 9.0
Rabbit anti-human PD-L1	Tonsil and placenta	US Biomax	Sodium citrate pH 6.0
Rabbit anti-human MGMT	Spleen	US Biomax	Sodium citrate pH 6.0
Rabbit anti-mouse/human TRP-2	Melanoma	US Biomax	TRIS-EDTA pH 9.0
Rabbit anti-mouse/human WT-1	Embryonic kidney	Cell Marque	Sodium citrate pH 6.0
Rabbit anti-human/mouse gp100	Melanoma	US Biomax	Sodium citrate pH 6.0
Rabbit anti-human HAGE	Testis	US Biomax	Sodium citrate pH 6.0

Table 11. Positive control tissues used for IHC optimisation

Once conditions were optimised FFPE GBM tissue microarrays (US Biomax) were stained using the same antigen retrieval methods and antibody concentrations that were deemed as appropriate during optimisation (detailed in *Table 11*). Prior to commencing immunohistochemical staining sections were baked for 30 minutes at 60 °C in a dry oven then they were dewaxed by two

consecutive immersions in xylene and then the sections were re-hydrated by immersion in graded ethanol (100%, 100%, 90% then 70%). Slides were then briefly immersed in dH₂O for 2 minutes before endogenous peroxidase activity was blocked using 3% hydrogen peroxide in methanol. Slides were then rinsed in dH₂O for 3 minutes. After rinsing slides were immediately immersed in 100 °C antigen retrieval buffer (Tris-EDTA pH 9.0 or sodium citrate pH 6.0) for 20 minutes. The slides were then left to cool in the antigen retrieval buffer for 20 minutes on the bench top. Once slides had cooled they were washed in TBST (0.1% TWEEN20) for 5 minutes. Sections were then blocked with 2.5% normal horse serum (Vectastain Elite ABC HRP kit, Vector labs) for 10 minutes at room temperature. Blocking buffer was then removed and avidin D solution (Vector labs) was applied to sections for 15 minutes. Slides were then washed in TBST for 2 minutes. Biotin (Vector labs) solution was then applied to sections for 15 minutes. After 15 minutes the biotin was removed, and primary antibody was applied to the sections for 1 hour at room temperature. Slides were then washed twice in TBST for 10 minutes. Pan-specific biotinylated secondary antibody (Vectastain Elite ABC HRP kit, Vector labs) was then applied to sections for 10 minutes at room temperature, slides were then washed twice in TBST for 10 minutes. Next ABC reagent (Vectastain Elite ABC HRP kit, Vector labs) was applied to the sections for 5 minutes, slides were then washed twice in TBST for 10 minutes. DAB reagent was then added to sections for 3 minutes at room temperature, slides were then washed in dH₂O for 2 minutes and counterstained with Mayer's hematoxylin (Sigma). Sections were then run through consecutive immersion in 70%, 90%, 100%, 1000% ethanol and then finally twice in xylene. Coverslips were then mounted with DPX mountant. Slides were imaged using a Leica Ariol (Leica) or Hamatsu NanoZoomer microscope (Hamatsu).

2.2.3. Western blotting

2.2.3.1. Preparation of cellular lysates

A confluent T75 flask of cells were trypsinised and pelleted, then 700 µL of radioimmunoprecipitation assay (RIPA) buffer was added (with HALT protease inhibitor), cells were then vigorously vortexed then placed on ice every 10 minutes for a 30-minute period. Cells were then centrifuged to separate cellular debris from lysate.

2.2.3.2. Bicinchoninic acid (BCA) assay

2 mg/mL of BSA was prepared by dissolving BSA in RIPA buffer, this 2 mg/mL BSA stock solution was then used to prepare a BSA standard curve as below.

Final BSA concentration (µg/mL)	Volume of BSA (µL)	Volume of RIPA buffer (µL)
--	---------------------------	-----------------------------------

2000	300 of 2 mg/mL BSA	0
1500	375 of 2 mg/mL BSA	125
1000	325 of 2 mg/mL BSA	325
750	175 of 1500 µg/mL BSA	175
500	325 of 1000 µg/mL BSA	325
250	325 of 500 µg/mL BSA	325
125	325 of 250 µg/mL BSA	325
25	100 of 125 µg/mL BSA	400
0	0	400

Table 12. Preparation of BSA standards for the BSA protein assay

The cellular lysates of unknown protein concentration were diluted 1 in 4 in RIPA buffer and then thoroughly vortexed. Once the samples and standards were prepared 25 µL of standards and samples were added in triplicate to a flat-bottomed 96 well plate. Once all samples and standards were plated working reagent was prepared by diluting copper II sulphate solution 1 in 50 in bicinchoninic acid solution. 200 µL of working solution was added to each well containing standards and samples. The plate was then covered with foil and left to incubate at 37 °C for 30 minutes. After incubation the plate was read with absorbance set to 570 nm in a plate reader (Tecan). When analysing data background (0 µg/mL BSA) was subtracted from all measurements and then protein concentrations of the unknown samples were then calculated using the standard curve.

2.2.3.3. Western blotting

A 5% stacking gel with 10% resolving gel was made and 20-30 µg of protein was loaded into the gel. The gel was run at 100 V and once complete proteins were transferred to a PVDF membrane at 100 V for 90 minutes in cooled transfer buffer. Once transfer was completed membranes were blocked in 5% (w/v) milk solution in TBST. Membranes were then washed 5 times for 5 minutes in TBST. Once membranes were washed they were incubated in primary antibody diluted in 5% (w/v) milk solution in TBST overnight at 4°C. After incubation in primary antibody membranes were washed 5 times for 5 minutes in TBST. After washing, the membranes were incubated in HRP conjugated secondary antibody and anti-ladder secondary diluted in 5% (w/v) milk solution in TBST. Membranes were placed in secondary antibody diluted in 5% (w/v) milk in TBST for 1 hour at room temperature. After incubation in secondary antibody membranes were washed 5 times for 5 minutes in TBST. After washing membranes were coated with ECL developing solution

and imaged using the Syngene G:Box station (Syngene).

2.2.3.4. Western blot quantification using ImageJ

Once blots had been imaged ImageJ software was used to analyse the intensity of the bands on the blots. Each lane was determined and then the intensity peaks were obtained for bands within that lane (see *Figure 4*).

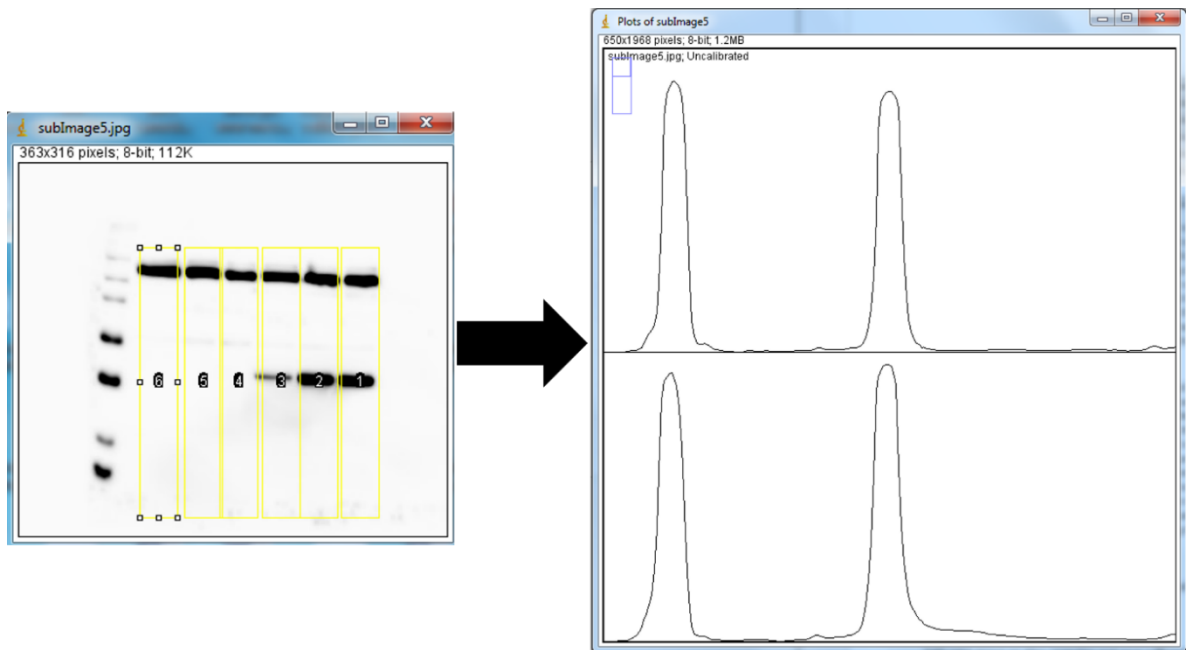


Figure 4. ImageJ identification of protein lanes on Western blot membrane image followed by intensity peaks for each band.

Once the area under the intensity peak was discovered the protein expression was determined using the following equation: Intensity of protein of interest / Intensity of loading control. This generates a relative intensity compared to the loading control for each lane.

2.2.4. Immunocytochemistry/immunofluorescence

2.2.4.1. Immunocytochemistry

Cells were grown on glass coverslips and once sufficiently confluent cells were stained. Cells were first fixed in 4% paraformaldehyde in PBS (Santa Cruz) for 1 hour at room temperature. Cells were then washed three times with PBS. Cells were then permeabilised with 0.1% Triton X-100 in PBS for 5 minutes at room temperature. Cells were then washed three times with PBS. Cells were then blocked using 2.5% horse serum (Vectastain Elite ABC HRP kit, Vector labs) for 10 minutes at room temperature. Serum was then removed, and cells were incubated with avidin D solution (Vector labs) for 15 minutes at room temperature. Cells were then washed in PBS for 2 minutes. Biotin solution (Vector labs) was then added to cells for 15 minutes at room temperature. Cells were then incubated in the appropriate primary antibodies (see *table....*) diluted in 2.5% horse serum overnight at 4°C. Cells were washed three times in PBS, cells were then incubated in pan-specific biotinylated secondary anti-mouse/rabbit IgG antibody (Vectastain Elite ABC HRP kit, Vector labs) for 10 minutes at room temperature. Cells were then washed three times in PBS. Cells were incubated in ABC kit streptavidin complex (Vector lab) for 5 minutes at room temperature. Cells were washed three times in PBS. Cells were incubated in DAB solution (Vector labs) for 3 minutes. Cells were washed in dH₂O for 2 minutes. Cells were then counterstained with Mayer's Hematoxylin (Sigma). Cells were then washed under tap water for 5 minutes. The cells on the coverslips were then mounted to slides using DPX mounting media (Sigma). Cells were then imaged microscopically (Zeiss).

2.2.4.2. Immunofluorescence

Cells were grown on glass coverslips and once sufficiently confluent cells were stained. Cells were first fixed in 4% paraformaldehyde in PBS (Santa Cruz) for 1 hour at room temperature. Cells were then washed three times with PBS. Cells were then permeabilised with 0.1% Triton X-100 in PBS for 5 minutes at room temperature. Cells were then washed three times with PBS. Cells were then blocked with 0.5% BSA in PBS for 30 minutes at room temperature. Cells were then incubated in primary antibody diluted in 0.5% BSA in PBS overnight at 4°C (see *Table 5.*). Cells were then washed three times with PBS. Cells were then incubated in donkey anti-rabbit IgG Alexa Fluor® 488 diluted in 0.5% BSA in PBS for 1 hour at room temperature in the dark. Cells were then washed three times

with PBS. The cells on the coverslips were then mounted to slides using vectashield hardset DAPI mounting medium (Vector labs). Cells were then imaged using a fluorescence microscope (Zeiss).

2.2.5. Flow cytometry

2.2.5.1. Cell surface flow cytometry

A confluent flask of cells was trypsinised and then 1 million cells were placed in a polystyrene flow cytometry tube, cells were washed with 2 mL of PBS (phosphate buffered saline), cells were spun at 300g for 5 minutes and the supernatant was poured off. Cells were re-suspended in 50 μ L of FCS and then FCR block was added and tubes were mixed immediately and incubated for 15 minutes at 4 °C. The appropriate antibodies diluted in PBS were then added to each tube at the manufacturers recommended concentration. Tubes were then incubated for 30 minutes at 4 °C in the dark. After antibody staining cells were washed with 2 mL of PBS, the cells were spun at 300g for 5 minutes and the supernatant poured off. The cells were then re-suspended in 350 μ L of isoton and analysed on a Gallios flow cytometer (Beckman Coulter) and data analysis was performed using Kaluza software (Beckman Coulter).

2.2.5.2. Gating strategy for cell surface staining

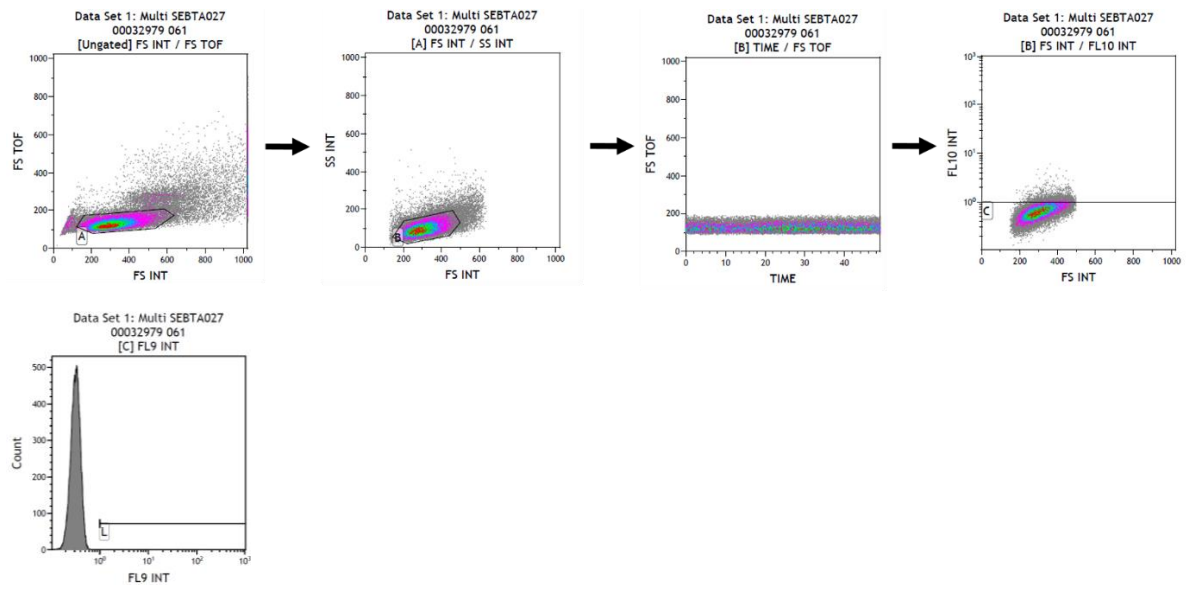


Figure 5. Gating strategy employed when examining the cell surface antigen expression of GBM cell lines.

Firstly singlets were gated out, once the singlets were gated events with low side scatter and forward scatter were excluded as these were deemed to be cellular debris. Next the forward scatter time of flight and time were plotted to see if there were any breaks in the flow, if any breaks were seen these were gated out (in the above example there is no break in the flow), finally FL10 (LIVE/DEAD) was plotted against forward scatter and any events positive on FL10 were gated out of the analysis as these are dead cells. These live cells were then analysed for antigen staining and gates were set to exclude unstained populations.

2.2.5.3. Flow cytometry staining of vaccinated splenocytes

1 million splenocytes in 50 μ L of T-cell media were plated in a flat bottomed 96 well plate. 50 μ L of T-cell media containing either no peptide, 4 μ g/mL of class I peptide or 4 μ g/mL of class I peptide and 40 μ g/mL of class II peptide was then added to the wells containing splenocytes (these concentrations are 4 times the final concentration, however further additions to the plate result in the final concentrations being 1 μ g/mL of class I peptide and 10 μ g/mL of class II peptide). Next 50 μ L of T-cell media containing co-stimulatory anti-CD28 and anti-CD49d (final concentration 1 μ g/mL for both). Cells were then incubated for 1 hour at 37 °C in a tissue culture incubator (Sanyo). After incubation 50 μ L of Brefeldin A and monensin diluted 1 in 250 in T-cell media (final dilution 1 in 1000) was added to each well, wells were then pipette mixed and 3 μ L of anti-CD107a was added to each well and the plate was incubated for 5 hours at 37 °C in a tissue culture incubator (Sanyo). After incubation cells were transferred to a FACS tube and the tube was centrifuged at 300 G for 5 minutes, the supernatant was removed and the cell pellet was re-suspended in 50 μ L of FCS, 1 μ L of FcR blocking reagent was then added and tubes were mixed immediately and incubated for 15 minutes at 4 °C. The appropriate cell surface antibodies (CD107a, CD4, CD8, CD3 and LIVE/DEAD) diluted in PBS were then added to each tube at the manufacturers recommended concentration. Tubes were then incubated for 30 minutes at 4 °C in the dark. 25 μ L of fixative agent R1 (Beckman Coulter PerFix-nc kit) was then added to each tube and mixed then tubes were incubated for 15 minutes at 4 °C in the dark. 300 μ L of permeabilising reagent R2 (Beckman Coulter PerFix-nc kit) containing the required concentration of intracellular antibody (TNF α , Ki67, IL-2, IFN γ and Granzyme B) was added to each tube and mixed immediately, the tubes were then incubated for 30 minutes at 4 °C in the dark. 2mL of 1 x reagent R3 (Beckman Coulter PerFix-nc kit) was added per tube and the tubes were then centrifuged at 500 G for 5 minutes. The resulting cell pellets were then re-suspended in 250 μ L of reagent R3 and then run on a Gallios flow cytometer (Beckman Coulter), data was then analysed using Kaluza software (Beckman Coulter).

2.2.5.4. Gating strategy for intracellular staining of vaccinated splenocytes

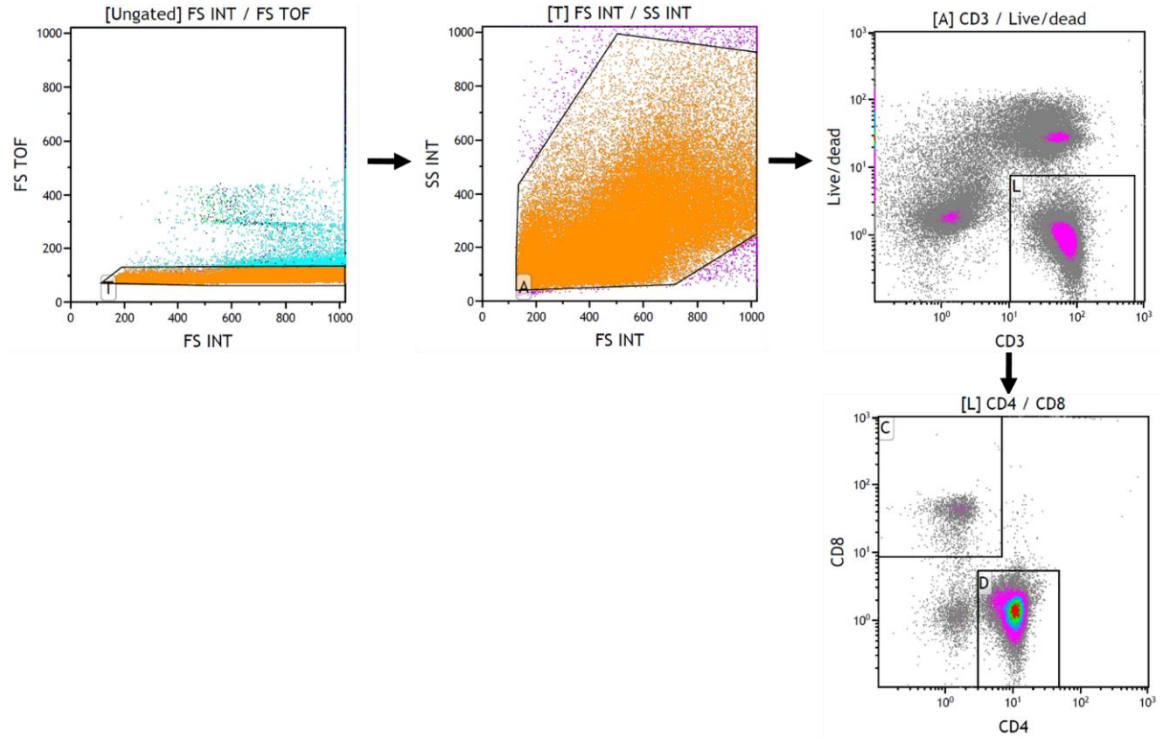


Figure 6. Gating strategy employed when examining the cell surface and intracellular antigen expression profiles of vaccinated splenocytes.

Firstly singlets were gated out, once the singlets were gated events with low side scatter and forward scatter were excluded as these were deemed to be cellular debris. Next Live CD3 cells were isolated from the splenocyte population using gate L (*Figure 6*), the CD3 cells were then separated into CD4 (Gate D) and CD8 (Gate C) positive cells and then these two populations were further analysed.

2.2.5.5. Flow cytometry staining of brain TILs

A FACS tube containing 1 million cells was centrifuged at 300 G for 5 minutes, the supernatant was removed and the cell pellet was re-suspended in 50 μ L of FCS, 1 μ L of FcR blocking reagent was then added and tubes were mixed immediately and incubated for 15 minutes at 4 °C. The appropriate cell surface antibodies (CD62L, CD3, CD69, CD25, CD4, CD8a, CD44, PD-1 and LIVE/DEAD) diluted in PBS were then added to each tube at the manufacturers recommended concentration. Tubes were then incubated for 30 minutes at 4 °C in the dark. 25 μ L of fixative agent R1 (Beckman Coulter PerFix-nc kit) was then added to each tube and mixed then tubes were incubated for 15 minutes at 4 °C in the dark. 300 μ L of permeabilising reagent R2 (Beckman Coulter PerFix-nc kit) containing the required concentration of intracellular antibody (FOXP3) was added to each tube and mixed immediately, the tubes were then incubated for 30 minutes at 4 °C in the dark. 2mL of 1 x reagent R3 (Beckman Coulter PerFix-nc kit) was added per tube and the tubes were then centrifuged at 500 G for 5 minutes. The resulting cell pellets were then re-suspended in 250 μ L of reagent R3 and then run on a Gallios flow cytometer (Beckman Coulter), data was then analysed using Kaluza software (Beckman Coulter).

2.2.5.6. Gating strategy for brain TILs

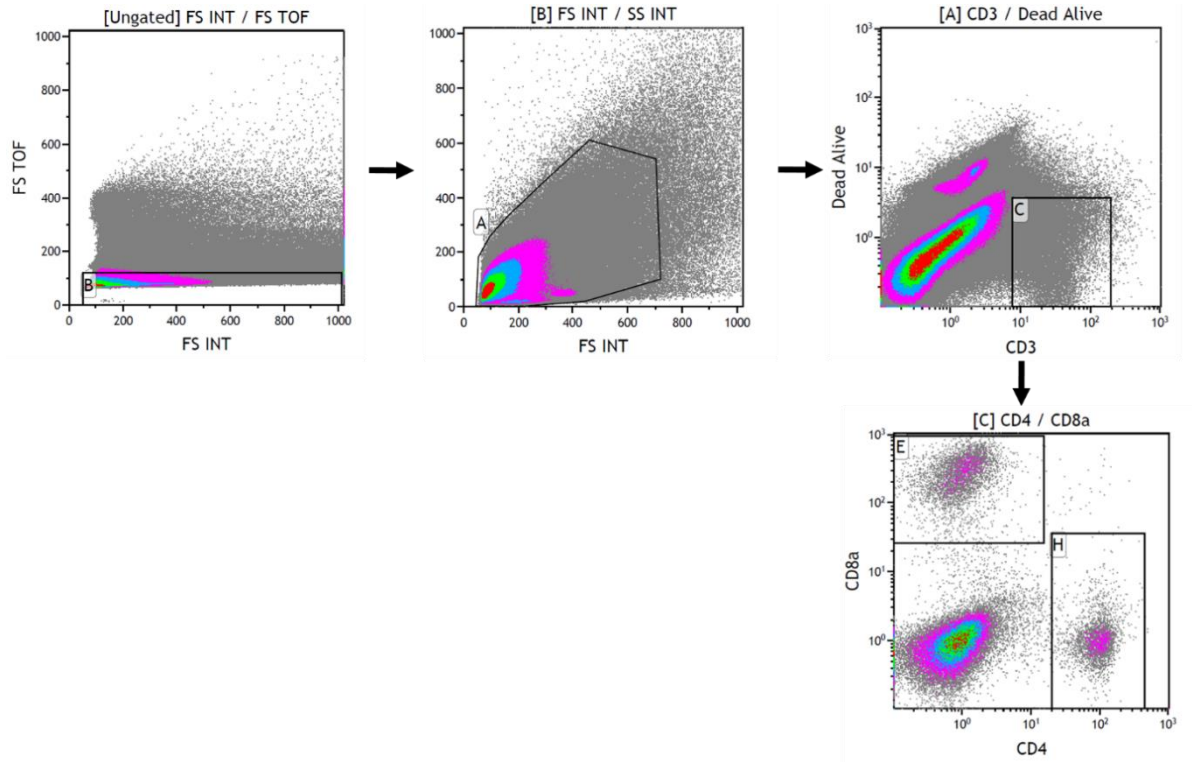


Figure 7. Gating strategy employed when examining the cell surface and intracellular antigen expression profiles of brain tumour infiltrating lymphocytes.

Firstly singlets were gated out, once the singlets were gated events with low side scatter and forward scatter were excluded as these were deemed to be cellular debris. Next Live CD3 cells were isolated from the population using gate C, the CD3 cells were then separated into CD4 (Gate H) and CD8 (Gate E) positive cells and then these two populations were further analysed.

2.2.6. DNA bullet preparation

2.2.6.1. Bulking up of ImmunoBody® plasmid using XL1-blue E. coli

Purified ImmunoBody® plasmid was transformed into XL-1 blue E. coli via heat shock. XL-1 cells were slowly thawed on ice, once thawed 100 µL of bacteria were transferred to a 1.5 mL Eppendorf tube, 1000 ng of plasmid was added to the bacteria and the mixture was left on ice for 30 minutes. The tube was then placed in a 42 °C water bath (SLS) for 3 minutes and then placed on ice for 5 minutes. 400 µL of antibiotic free low salt Laurie broth was then added to the tube and the tube was incubated at 37 °C with shaking at 200 RPM for 1 hour. Laurie agar plates containing 35 µg/mL of zeocin were then prepared. After 1 hour of incubation 250 µL of the bacteria solution was then placed on the zeocin containing agar plate and spread using an L-shaped spreader. The plate was incubated for 16 hours in a 37 °C oven. After incubation colonies had formed on the plate, a single colony was then taken off the plate and transferred into a 50 mL universal tube containing 30 mL of low salt Laurie broth containing 35 µg/mL of zeocin, this tube was then incubated at 37 °C with shaking at 200 RPM for 1 hour. This 30 mL was then transferred to a conical flask containing 70 mL low salt Laurie broth containing 35 µg/mL of zeocin. This conical flask was then incubated at 37 °C with shaking at 200 RPM overnight. After incubation the plasmids were extracted from the bacterial using a QIAfilter plasmid midi kit.

2.2.6.2. ImmunoBody® plasmids utilised

Below in *Figure 8* and *Figure 9* are the plasmid maps for the ImmunoBody® DNA vaccines used in this study. Above each map are the details of the peptide epitopes inserted into the CDRs of the encoded antibodies.

Epitope inserted into H1 & L3 site - gp100₁₇₃₋₁₉₀ (GTGRAMLGTHTMEVTVYH)
 H2 site - TRP2₁₈₀₋₁₈₈ (SVYDFFVWL)
 H3 & L1 site - gp100₄₄₋₅₉ (WNRQLYPEWTEAQRLD)

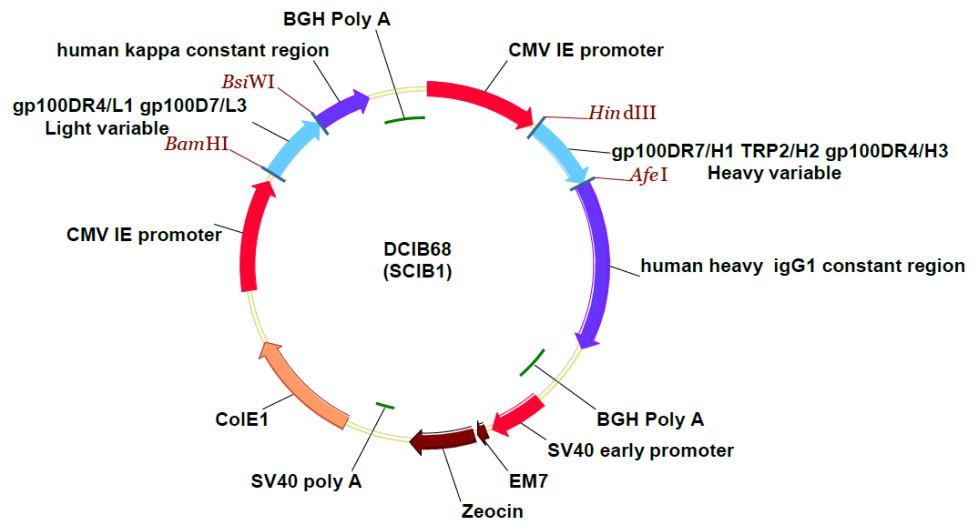


Figure 8. Plasmid map of the SCIB1 ImmunoBody® plasmid.

Epitope inserted into H2 site- Human WT1 5-19 (VRDLNALLPAVPSLG)
 (Accession number: P19544)

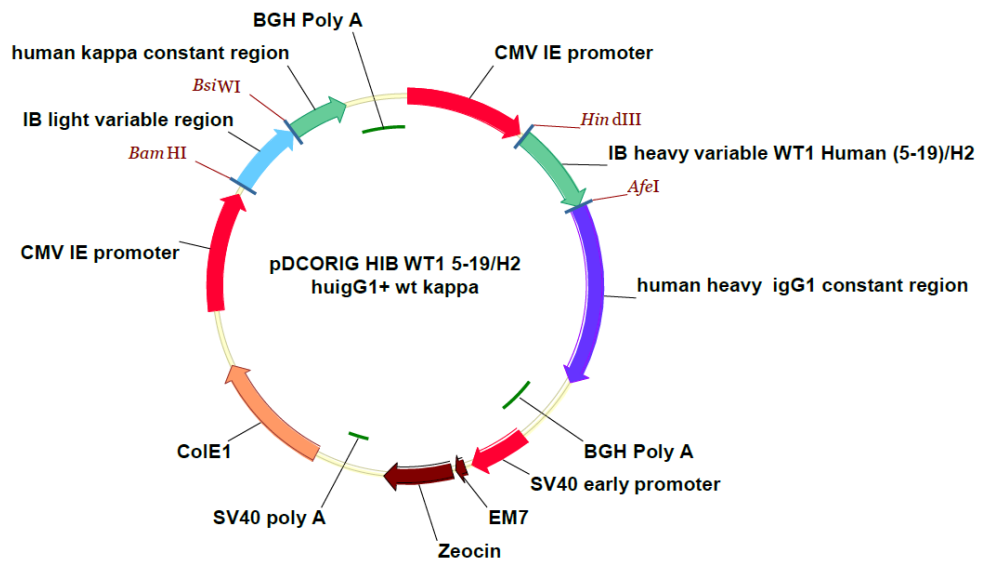


Figure 9. Plasmid map of the WT1 ImmunoBody® plasmid.

2.2.6.3. Plasmid extraction from transformed bacteria

The plasmid was extracted from the transformed bacteria using the QIAGEN QIAfilter plasmid midi kit following the manufacturer's protocol. After growth the bacteria was transferred to 50 mL flacon tubes, these tubes were then spun at 6000 G for 15 minutes at 4 °C to pellet the bacteria. The media was poured off the pellet and then the pellet was re-suspended in 4 mL of buffer P1 from the QIAfilter kit (QIAGEN). Once the pellet was resuspended 4 mL of buffer P2 (QIAGEN) was added and the mixture was incubated for 5 minutes at room temperature. 4 mL of chilled buffer P3 (QIAGEN) was then added to the mixture and then this mixture was then transferred to a QIAfilter syringe (QIAGEN) and the mixture was left to stand for 10 minutes at room temperature. Whilst this mixture was incubating a QIAGEN tip was prepared by allowing 4 mL of buffer QBT (QIAGEN) to run through the tip. Once the QIAfilter syringe had stood for 10 minutes a plunger was inserted and the mixture was then syringed into the QIAGEN tip where it was allowed to through. Once the solution had passed through the tip the tip was washed by allowing 10 mL of buffer QC (QIAGEN) to flow through the QIAGEN tip, this was then repeated once the solution had flowed through. The QIAGEN tip was then suspended over a 50 mL tube where the DNA was eluted using 5 mL of buffer QF (QIAGEN) pre-heated to 65 °C. The flow through then had 3.5 mL of room temperature isopropanol added to it, this precipitates the DNA. The DNA containing tube was then spun at 6000 G for 15 minutes at 4 °C, the supernatant was then decanted and then the DNA pellet was re-suspended in 700 µL of room temperature 70 % ethanol and transferred to a 1.5 mL Eppendorf tube. The tube was then centrifuged at 15000 G for 10 minutes at room temperature. The ethanol was then removed and the DNA pellet was allowed to air dry. Once dry the DNA pellet was dissolved in 50 µL of TE buffer. Once the DNA was dissolved the DNA concentration was measured using a NanoDrop spectrophotometer (Thermo Fisher).

2.2.6.4. Preparation of DNA bullets

16.6 – 20 mg of gold nanoparticles were weighed out and placed in a 1.5 mL Eppendorf tube. 500 µL of anhydrous ethanol was added to the gold particles and the tube was centrifuged at 13000 RPM for 1 minute at room temperature. The ethanol was removed via pipette and then 200 µL of 0.05M spermidine was added to the gold pellet. The mixture was then sonicated and vortexed and then 36 µg of ImmunoBody® plasmid was added to the mixture and this was mixed by brief sonication and gentle vortexing. Whilst the mixture was vortexing 1M calcium chloride was added in a drop wise manner, the resulting mixture was then left to stand on the bench top for 10 minutes. Tefzel tubing (BioRad) was then inserted into a DNA bullet preparation station (BioRad) and nitrogen was blown through the tube to remove any dust that there may be within the tube. After the tube containing the gold and the plasmid had finished incubating it was centrifuged at 13000

RPM for 1 minute at room temperature. The supernatant was then discarded and the pellet was re-suspended in 1 mL of anhydrous ethanol by gentle sonication and vortexing, the tube was then centrifuged at 13000 RPM for 1 minute at room temperature and the supernatant removed, this process was then repeated once more. The pellet was then re-suspended in 2 mL of 0.025 mg/mL PVP and transferred into a 15 mL falcon tube. A syringe was then attached to the Tefzel tubing and it was placed in the gold solution containing falcon tube, the syringe was then used to draw the solution up into the plastic tubing whilst the tube was simultaneously being gently sonicated. The tube containing the solution was then placed back into the tubing station (with the air turned off) with the syringe still attached. The tubing was allowed to stand for 5 minutes and then the attached syringe was used to draw the liquid out of the tubing, the syringe was then removed and nitrogen gas was slowly flown through the tubing for 15 minutes to dry out. Once dry the tubing was cut using a bullet cutter (BioRad) and bullets were test fired.

2.2.7. Immunisation and ELISpot analysis

2.2.7.1. *Immunisation schedule*

When studying the splenocytes from vaccinated mice they were vaccinated as shown in *Figure 10* at the start of the study the mice were given a priming dose of ImmunoBody® followed by a boost a week later then a further boost a week after that. Splenocytes were then removed and analysed 21 days after the initial priming boost. In the prophylactic treatment regime, mice were given the same prime, boost, boost regime followed by tumour implantation on day 21.

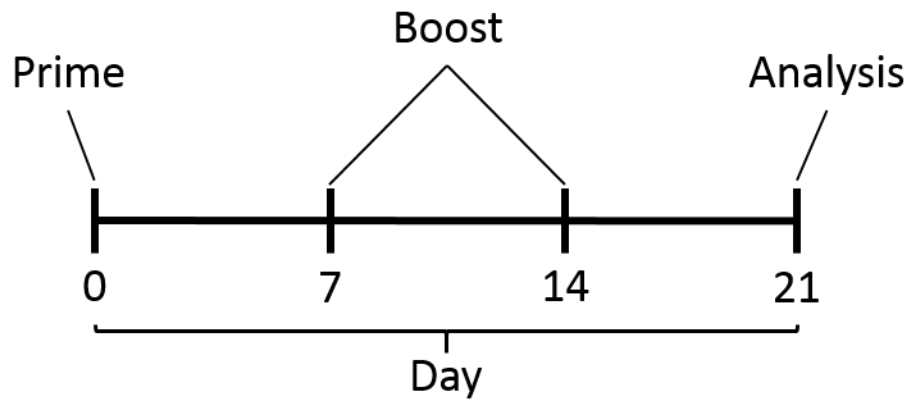


Figure 10. Vaccination schedule used for testing the immune response to ImmunoBody® vaccination and for prophylactic experiments.

When analysing the use of ImmunoBody® to treat established tumours the vaccination schedule from *Figure 11* was utilised. Due to the rapid growth of the tumours the vaccination schedule was shortened so mice received vaccination with anti-PD-1 antibody or PD-1 isotype control (both given in a 250 µg dose intra peritoneally) on days 3, 7 and 10.

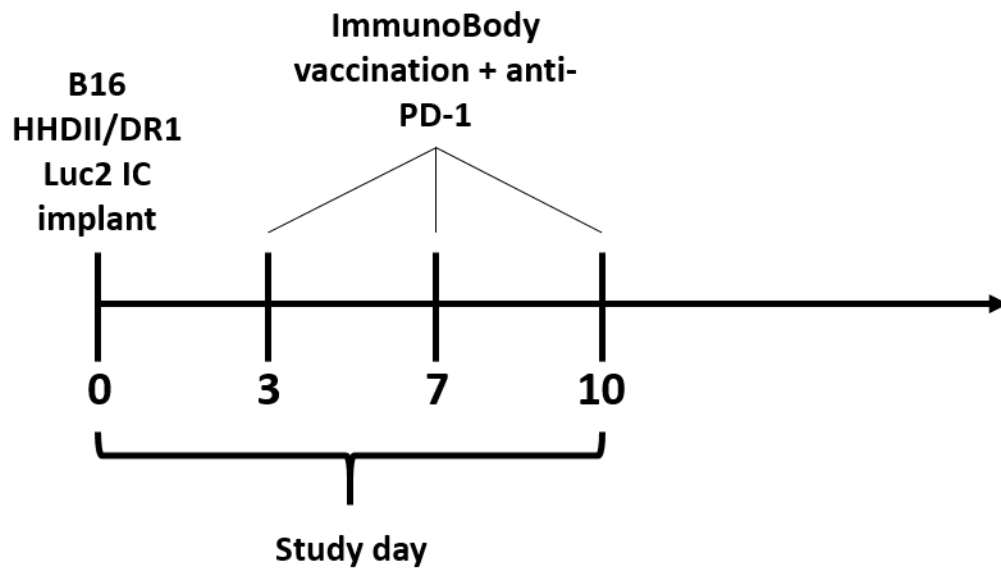


Figure 11. Vaccination schedule used for the therapeutic treatment of intracranial B16HHDII/DR1 Luc2 tumours.

Once tumour bearing mice experienced bodyweight loss or displayed symptoms of malaise they were humanely culled.

2.2.7.2. Processing of murine splenocytes

Mice were culled via cervical dislocation and their spleens removed and placed into complete T-cell media. The spleen was then placed into a petri dish containing 10 mL of T-cell media, 10 mL of T-cell media was then drawn up into a 20 mL syringe with a 21 G needle attached. Forceps were used to gently hold the spleen and the needle was used to puncture the capsule at each end of the spleen, the needle was then inserted into the spleen and the syringe was used to gently flush the 10 mL of T-cell media through the spleen, once all of the media was passed through the spleen the needle was removed and the capsule was agitated with forceps to remove any remaining splenocytes. The resulting solution was then transferred to a 30 mL universal tube and the debris was allowed to settle for 5 minutes, at which point the cell suspension was decanted into a fresh universal tube. The cells were then centrifuged at 1000 RPM for 10 minutes and the supernatant removed. The cell pellet was then re-suspended in 10 mL of T-cell media. Once re-suspended 5 μ L of this solution was taken and diluted in 45 μ L of T-cell media, 2.5 μ L of Solution 18 was added to this cell suspension and then 10 μ L was transferred to a NucleoCounter slide and counted using a NucleoCounter NC250 (Chemometec).

2.2.7.3. ELISpot analysis

ELISpot plates (Merck Millipore) were coated the day before spleens were processed, this was done by adding 50 μ L/well of 70% ethanol to the plates for 2 minutes. After incubation plates were washed 5 times with 200 μ L/well of sterile distilled water. After washing anti-mouse IFN γ capture antibody (Mabtech) was diluted 1 in 100 in sterile PBS and then 50 μ L/well was added to the plates and left overnight at 4 $^{\circ}$ C. Once incubation with capture antibody was complete it was flicked off the plate and then plates were washed 4 times with 200 μ L/well of sterile PBS, once complete 100 μ L/well of complete T-cell media was added to plates and then plates were incubated for a minimum of 30 minutes at room temperature, after incubation the media was flicked off the plates. Once the splenocytes were ready they were diluted to a concentration of 5 million cells per mL and then 100 μ L (500000 cells)/well was added to the plates as required. Next 100 μ L/well of peptides (see *Table 13*. For details) were then added to the plates at the required concentration (1 μ g/mL final concentration for class I peptide and 10 μ g/mL final concentration for class II peptides), if cells were used to stimulate splenocytes 100 μ L/well of T-cell media containing 50000 cells (500000 cells/mL) was added to the splenocytes. Plates were then left to incubate for 40 hours at 37 $^{\circ}$ C in a humidified 5 % CO $_2$ tissue culture incubator. After incubation the cells were flicked off the plates

and then plates were washed 5 times with 200 μ L/well of PBST. Once washes were complete 50 μ L/well of biotinylated detection antibody (Mabtech) diluted 1 in 1000 PBS was added to the plates and left to incubate at room temperature for 2-4 hours. After incubation plates were then washed 5 times with 200 μ L/well of PBST and then 50 μ L/well of streptavidin alkaline phosphatase (Mabtech) diluted 1 in 1000 PBS was added to the plates and left to incubate at room temperature for 1-2 hours. After incubation plates were washed 6 times with 200 μ L/well of PBST. Development solution was then prepared using the BioRad streptavidin alkaline phosphatase conjugate substrate kit, this was done by combining 4.8 mL of distilled water, 200 μ L of development buffer (BioRad), 50 μ L of reagent A (BioRad) and 50 μ L of reagent B (BioRad) per plate. This development buffer was mixed well and then 50 μ L/well was added as required. Plates were then incubated until purple spots began to develop (seen in the SEB positive control wells), once spots started to develop the reaction was stopped by running the plates under tap water. Once plates were fully developed and dry they were read using the ELISpot plate reader (ImmunoSpot).

Peptide	Sequence	Human HLA-specificity	SYFPEITHI score
WT-1	ALLPAVPSL	A2	33
WT-1	DLNALLPAV	A2	27
WT-1	VRDLNALLPAVPSLG	DR1	31
TRP-2	SVYDFFVWL	A2	21
gp100	AMLGHTMEV	A2	26
gp100	GTGRAMLGHTMEVT	DR1	24
gp100	QLYPEWTEA	A2	19
gp100	NRQLYPEWTEAQLD	DR1	14

Table 13. Peptides used for *in vitro* stimulation of splenocytes and their respective SYFPEITHI scores (SYFPEITHI).

2.2.7.4. ELISpot peptide titration

For ELISpot peptide titration the protocol is exactly the same as above however when peptides were added the WT-1 class I (ALLPAVPSL) and the TRP-2 (SVYDFFVWL) class I peptides were added at 9 different concentrations; 1, 0.1, 0.01, 0.01, 0.001, 0.0001, 0.00001, 0.000001 and 0 μ g/mL.

2.2.8. Brain tumour modelling

2.2.8.1. Intracranial tumour implantation

All animal work was carried out under a Home Office approved project licence. Intracranial implantation of B16HHDII/DR1 Luc2 cells was performed by injecting 5×10^3 cells in 3 μ L PBS into anaesthetized C57BL/6 HHDII/DR1 mice. Cells were injected using a Hamilton syringe, the needle was positioned 2 mm to the left of the bregma, the needle was then inserted to a depth of 3.5 mm and then left in place for 60 seconds. After 60 seconds the needle was withdrawn to depth of 3mm and then cells were injected at a rate of 1.5 μ L per 60 seconds. After implantation the needle was left in place for 60 seconds and then withdrawn at a rate of 0.1mm every 2 seconds until clear of the brain. Once craniotomy was completed the wound was closed and mice were monitored at regular intervals. Mice that developed symptoms indicative of brain tumours or had severe body weight loss were humanely euthanized by cervical dislocation.

2.2.8.2. Imaging of intracranial brain tumours

When mice required imaging they were given a 150mg/kg intraperitoneal dose of XenolightRediJect D-luciferin (Perkin Elmer), mice were then left for fifteen minutes and then they were anaesthetised ready for imaging. Once mice were unconscious they were placed inside an IVIS (Perkin Elmer) *in vivo* imager where bioluminescence measurements were taken and analysed using the IVIS software (Perkin Elmer)

2.2.8.3. Brain tumour processing for flow cytometric analysis

Once mice were euthanized their brains were extracted and placed into T-cell media, the brain was transferred into a petri dish and the tumour containing areas were excised from the rest of the brain. The excised tumours were then put into a new petri dish containing 10 mL of T-cell media and minced using a scalpel. The resulting cell suspension was transferred into a 50 mL Falcon tube and DNase and collagenase I were added to give a final concentration of 50 μ g/mL DNase and 0.1 U/mL of collagenase I. The falcon tube was then placed into a 37 °C orbital incubator at 200 RPM for 30 minutes, after 30 minutes the tube was removed and the suspension was passed through a 40 μ M cell strainer, any remaining lumps were mashed through using a syringe plunger. The cell strainer was then washed with 10mL of T-cell media. The resulting cell suspension was then spun at 300 G for 5 minutes, the supernatant removed and the pellet was re-suspended in 5 mL of T-cell media. Cells were then counted using the NucleoCounter NC250 (Chemometec). 1 million cells was then transferred to a polystyrene FACS tube for staining.

2.2.9. Kynurenine assay

2.2.9.1. Colorimetric kynurenine assay

Cells were treated with 100 ng/mL IFN γ for 24, 48 or 72 hours, for each time point there were also untreated control cells that were left under normal media for 24, 48 and 72 hours. After treatment media was collected from the cells. Kynurenine standards were made using L-Kynurenine ranging from 0-200 μ M kynurenine in GBM culture media. Once prepared 300 μ L of media and 300 μ L of kynurenine standard was mixed with 150 μ L 30 % trichloroacetic acid to precipitate protein out of the mixture. Tubes were then vortexed and then centrifuged at 8000 g for 5 minutes at 4 °C. After centrifugation 75 μ L of the standards and media from cells were added to a 96 well flat-bottomed plate in triplicate. The media was mixed with 75 μ L of Ehrlich's reagent (20 mg/mL p-dimethylaminobenzaldehyde in glacial acetic acid). The plate was incubated for 15 minutes at room temperature and then it was read at 492 nm in a plate reader (Tecan). Background readings from media alone were subtracted from all wells and then the concentration of the unknown samples was calculated using the standard curve. This process was repeated across 3 different passages.

2.2.10. Carnosine related experiments

2.2.10.1. MTT assay of carnosine treated cells

Cells were seeded onto a 96 well tissue culture plate alongside wells containing cells there were three control wells containing culture medium alone. Cells were left overnight in a 37 °C humidified 5% CO $_2$ tissue culture incubator (Sanyo) to attach. Once cells were attached all of the culture media was removed and replaced with 200 μ L/well carnosine containing media ranging from a concentration of 0-130 mM going up in 10 mM increments. After 24 hours of carnosine treatment 20 μ L/well of 5 mg/mL MTT reagent assay was added to each well and then the plate was left at 37 °C for 2-4 hours. Once incubation was complete all media was removed from the cells and 100 μ L/well of DMSO was added to dissolve formazan crystals, the plate was then left on a plate shaker for 10 minutes. Absorbance was then measured at 570 nm using a Tecan plate reader (Tecan). The values for the blank wells containing no cells was subtracted from all readings.

2.2.10.2. IncuCyte scratch assay of carnosine treated cells

Cells were seeded on a 96 well plate and once they reached 100 % confluency a scratch was made through the monolayer of cells using the IncuCyte wound maker (Essen bioscience). Once scratches has been made all media was removed and the cells were given a gentle wash with sterile D-PBS, after washing carnosine containing media was then placed on the cells and the cells were placed in

an IncuCyte live cell analysis incubator. The analyser then took images every two hours using the 10 x objective for a period of 110 hours.

2.2.10.3. Subcutaneous implantation of GL261 LUC2 cells in NOD-SCID mice and subsequent carnosine treatment

2500000 GL261 Luc2 cells in 100 μ L PBS were implanted subcutaneously in the flank of NOD-SCID mice. Once palpable tumours 4-6 mm² had developed a single dose of 1 M carnosine in PBS (20 μ L) was injected directly into the tumours. Tumours were then monitored twice weekly using callipers, and mice were imaged once a week using an IVIS in vivo imager (PerkinElmer).

CHAPTER 3: ANTIGENS EXPRESSION PROFILE OF GLIOBLASTOMA MULTIFORME TISSUES AND CELL LINES

3.1. Introduction

The current 'gold standard' treatment for GBM is surgical resection followed by radiotherapy and temozolomide (TMZ) chemotherapy. This therapeutic regime has been the standard for over 10 years and very little progress has been made in terms of therapeutic developments for GBM. The median survival for patients after undergoing standard therapy is still just under 15 months (Stupp, Mason et al. 2005). In some cases, GBM patients may express an enzyme called O-6-methylguanine-DNA methyltransferase (MGMT), this enzyme conveys a resistance to TMZ chemotherapy, and MGMT promoter methylation has been shown to be a prognostic factor for patients receiving standard therapy (Dunn, J., Baborie et al. 2009). The dismally poor survival of GBM patients highlights the need for novel therapeutic approaches for treating this disease. Immunotherapy represents an attractive treatment, specifically active immunotherapy induced by vaccination. This method of immunotherapy is highly attractive due to its tumour specificity and the ability of immune cells to target tumours located within the brain (Prins, Shu et al. 2008). Previous studies have utilised vaccination as a method for treating GBM; early clinical trials have been promising however no treatments thus far have progressed past phase III clinical trial (Swartz, Shen et al. 2018). Whilst GBM is poorly immunogenic it has been shown to express several tumour antigens that enable immune recognition of these tumours. As previously mentioned in *chapter 1*, the cells of the skin and the brain are derived from the same neuroectodermal tissues. As a result GBM shares many of the same antigens as melanoma skin tumours. Previous research has found that GBMs express the melanoma associated antigens gp100, TRP-2, MAGE-A1, MAGE-A3 and MAGE-A11 (Saikali, Avril et al. 2007, Guo, L., Sang et al. 2013). GBM tumours have also been shown to express several other immunogenic antigens such as EGFRvIII and IL-13R α 2 (Saikali, Avril et al. 2007). Assessment of patient derived glioblastoma cell lines has also revealed expression of a plethora of other immunogenic cancer testis –antigens (Akiyama, Komiyama et al. 2014). These studies reveal varying levels of expression of these antigens and differing methods have been used to study the expression of these cancer related antigens.

As well as expressing immunogenic antigens these tumours also express numerous antigens that interact with immune cells and dampen the anti-tumour immune response. The immune evasive profile of glioblastoma multiforme is well documented (Jackson, Ruzevick et al. 2011, Reardon, Freeman et al. 2014). GBM tumours have been shown to express the immunosuppressive checkpoint ligand PD-L1, and the expression of PD-L1 has been linked to loss of phosphatase and tensin homolog (PTEN) (Parsa, Waldron et al. 2007). The expression of PD-L1 is not ubiquitous

across all glioblastoma multiforme cases, however PD-L1 is an interferon gamma inducible gene, meaning that tumour reactive immune cells secreting IFN γ near the tumour can lead to induction of PD-L1 expression. HLA-E is a ligand for the NKG2A immune inhibitory receptor expressed by NK and T-cells, previous research has found that GBM (grade IV) tumours express the HLA-E antigen to a significantly higher level than lower grade brain tumours (Mittelbronn, Simon et al. 2007). HLA-G is another non-classical MHC molecule that interacts with CD8 $^+$ and CD4 $^+$ T-cells to prevent immune activation and enable GBM cells to avoid immune detection (Wiendl, Mitsdoerffer et al. 2002). HLA-G also has a soluble form that has been detected in the cancer setting with cancer patients being found to have higher levels of soluble HLA-G in their plasma. HLA-G interacts with NK and T-cells via LILRB1, LILRB2 and KIR2DL4 receptors (Sheu, Shih 2010). Tumours are also believed to down regulate MHC-I and MHC-II molecules on their surface to evade immune recognition, this phenomenon has been shown in the glioblastoma setting, with invasive GBM cells downregulating these antigens (Zagzag, Salnikow et al. 2005).

Temozolomide is an oral alkylating agent used as a chemotherapeutic in the GBM setting. TMZ is a pro-drug that is hydrolysed at physiological pH, generating the active metabolite MTIC, this is then hydrolysed to AIC and a methyldiazonium ion. The methyldiazonium ion then methylates DNA at several residues. The N 3 position of adenine, the N 3 position of guanine, the N 7 position of guanine and the O 6 position of guanine are methylated by TMZ's methyldiazonium ion (see *Figure 13*) (Kaina, Christmann et al. 2007, Lee 2016).

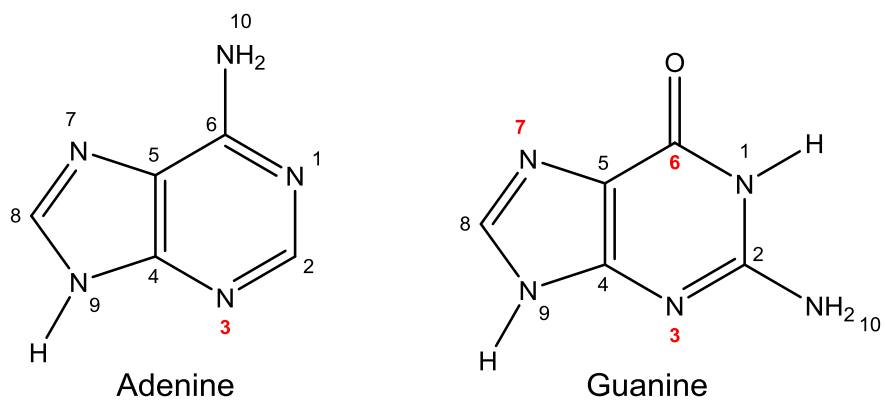


Figure 12. Diagrams of adenine and guanine bases with the atoms methylated by temozolomide highlighted.

Whilst TMZ therapy generates numerous methyl adducts on adenine and guanine, the adduct on the O⁶ position of guanine is essential for its anti-tumour activity. The N³ adducts on guanine and adenine are short lived and readily hydrolysed, the N⁷ methylguanine adduct is longer lasting, but still relatively transient and the O⁶ methylguanine adduct is much longer lasting. The methylation of guanine by the methyldiazonium ion (see *Figure 13*) leads to a series of downstream events that triggers apoptosis (Kaina, Christmann et al. 2007, Lee 2016).

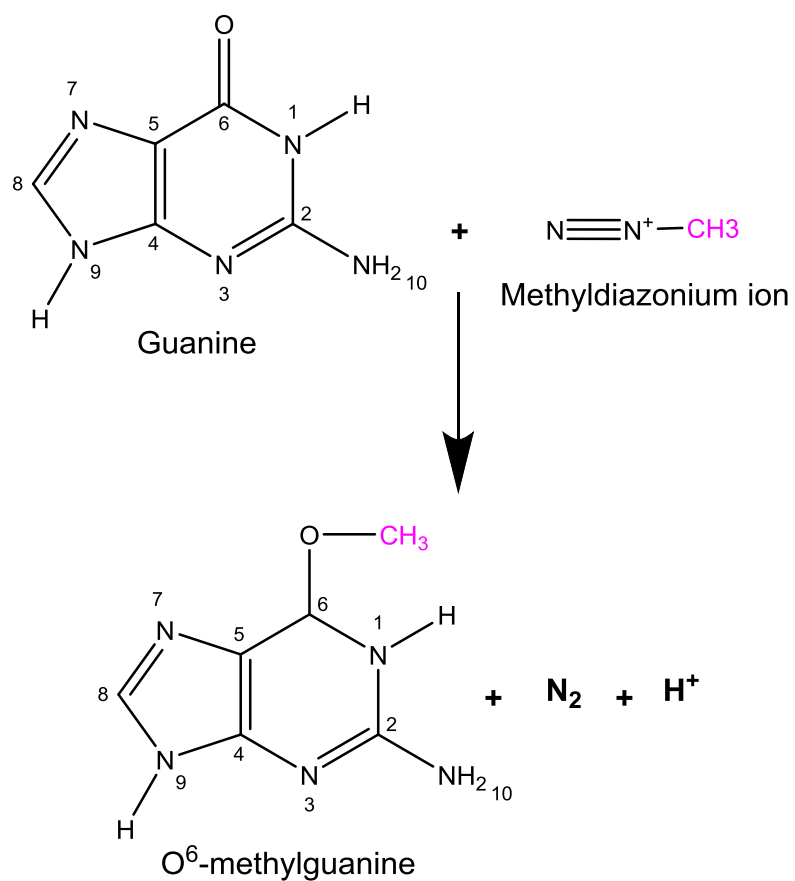


Figure 13. Methylation of guanine by the methyl diazonium ion. The methyl group is represented by the pink CH₃ highlighted on the figure.

The O⁶ methylguanine adduct results in mispairing during DNA replication, it results in GC to AT point mutations after two rounds of DNA replication. O⁶ methylguanine requires mismatch repair to induce apoptosis. During DNA synthesis O⁶ methylguanine mis-pairs with thymine, activating mismatch repair causing MutS α (a heterodimer formed of MSH2 and 6) to bind to the adduct, MutL α (a heterodimer formed of PMS2 and MLH1) is then recruited along with exonuclease 1 leading to excision of the thymine base, however this is futile as thymine is re-paired with the O⁶ methylguanine present in the DNA. After multiple DNA replications, this futile reinsertion of thymine creates long strands of single stranded DNA resulting in double strand breaks of the DNA and subsequent cell death (Roos, Kaina 2013).

The responsiveness of GBM to temozolomide chemotherapy is dependent upon expression of a key protein: O⁶-methylguanine-DNA methyltransferase, this protein conveys a resistance to alkylating temozolomide chemotherapy by removing lethal adducts from the DNA, preventing apoptosis of tumour cells. MGMT repairs O⁶ methylguanine adducts by transferring the methyl group from the guanine to a cysteine residue within the MGMT active site, inactivating the MGMT enzyme, resulting in the degradation of MGMT. The level of MGMT within cells is the rate limiting factor regarding DNA repair (Zhang, J., Stevens, and Bradshaw 2012). MGMT functions to protect normal cells from DNA damage, however in the cancer setting some tumours may express this protein making them difficult to treat with chemotherapy.

The expression of MGMT has been shown to be a key prognostic indicator in GBM temozolomide therapy responsiveness. Methylation of the MGMT promoter has been linked to improved overall survival in GBM patients treated with alkylating agents. This promoter methylation was shown to be advantageous even in cases where alkylating agents were not utilised for therapy (Zhang, K., Wang et al. 2013). The presence of MGMT within these GBM tumours makes them resistant to standard therapy making immunotherapy an attractive alternative.

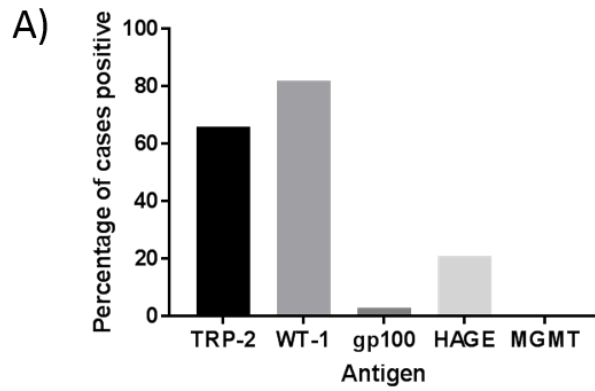
3.2. Aims and hypothesis

The aim of this chapter was to examine the expression of various proteins in GBM tissues and cell lines. The emphasis will be on discovering immunogenic targets for targeting with vaccination. The immune profile of these tumours will be assessed with the aim of incorporating combinatorial checkpoint blockade therapy with the vaccine-based therapy. These analyses will enable the development of an immunotherapeutic strategy to target these tumours, taking immune evasion strategies into account. Once target antigens have been identified in human GBMs their expression will also be examined in murine cell lines that could potentially be used for *in vivo* modelling of the disease.

3.3. Results

3.3.1. IHC analysis of GBM tissues reveals that the immunogenic TRP-2 and WT-1 antigens are viable targets for immunotherapeutic targeting of GBM

In order to target GBMs immunotherapeutically suitable GBM specific immunogenic antigens need to be discovered. These antigens need to be present in a large portion of tissues studied and they need to be known to be immunogenic. Immunohistochemistry was used to study tissue expression of several immunogenic tumour antigens in GBM tissues. Immunohistochemical staining of commercially available tissue microarrays revealed that GBM tumours express the immunogenic antigens TRP-2 and WT-1. The expression levels of these antigens vary, and their expression is not ubiquitous across all tumours. Despite expression not being ubiquitous many tumours express at least one of these antigens. Amongst the antigens tested WT-1 was the most expressed with 82% of the cores staining positively followed by TRP2 (66%) and HAGE (21%). The antigen gp100 was only expressed by one case. Images of staining can be seen in Appendix 1.



B)

	Antigen				
	TRP-2	WT-1	gp100	HAGE	MGMT
Positive staining	22 (66 %)	27 (82 %)	1 (3 %)	7 (21%)	0 (0%)
No staining	11 (33 %)	6 (18 %)	32 (99 %)	26 (79 %)	33 (100%)

Figure 14. TRP-2, WT-1, gp100, HAGE and MGMT expression as observed in tissue microarray staining. A) A graphical representation of target antigen expression as observed in tissue microarray staining. B) Numerical representation of positive staining results. Percentages show the number of cases that stained positively, irrespective of the strength of the staining.

Stained sections were then given a staining score by a pathologist with a score between 0 and 3 given to the tissue. 0 represents no staining, 1 represents mild staining, 2 represents moderate staining and 3 represents strong staining, these results are represented below in *Table 14* with examples of the pathologist's scoring being given in *Figures 15* and *16*. Whilst looking at the intensity of the staining WT-1 represents the antigen that is most strongly expressed in the 33 GBM cases studied, with TRP-2 being the second most intensely expressed. Even more importantly it was found that 20 (61%) of the GBM cases stained express both the TRP-2 and WT-1 antigens.

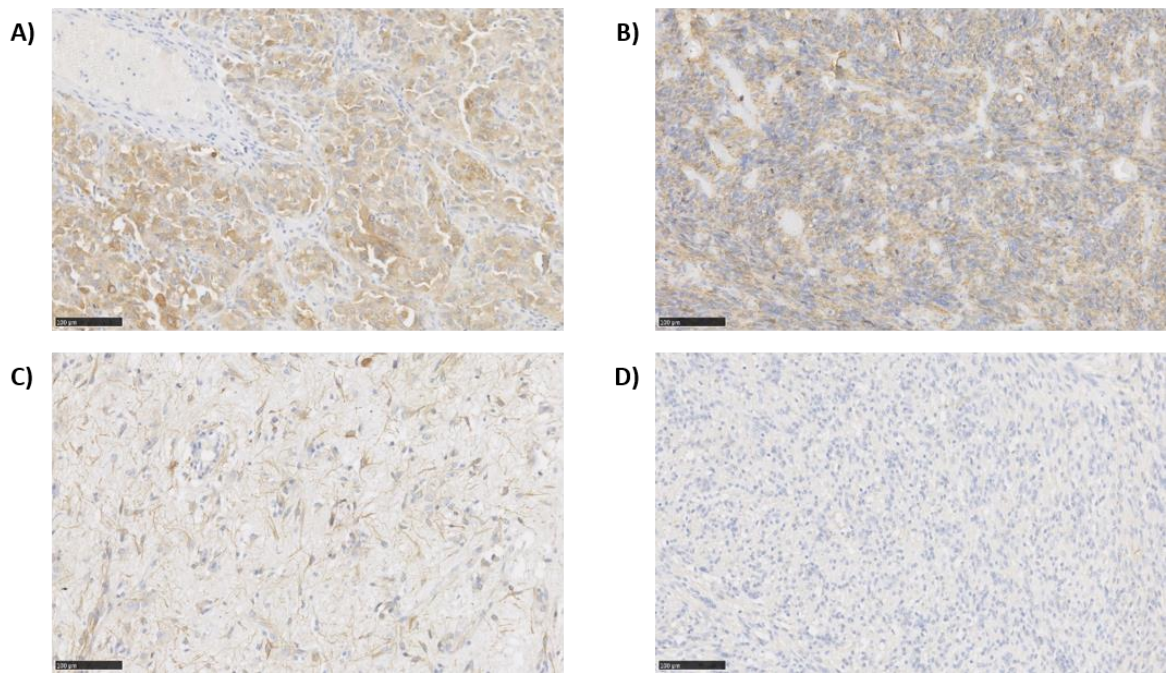


Figure 15. Examples of pathologist's WT-1 IHC scoring A) 3 (deemed as strong staining) B) 2 (deemed as moderate staining) C) 1 (deemed as weak staining) D) 0 (no staining). Scale bar = 100 µm.

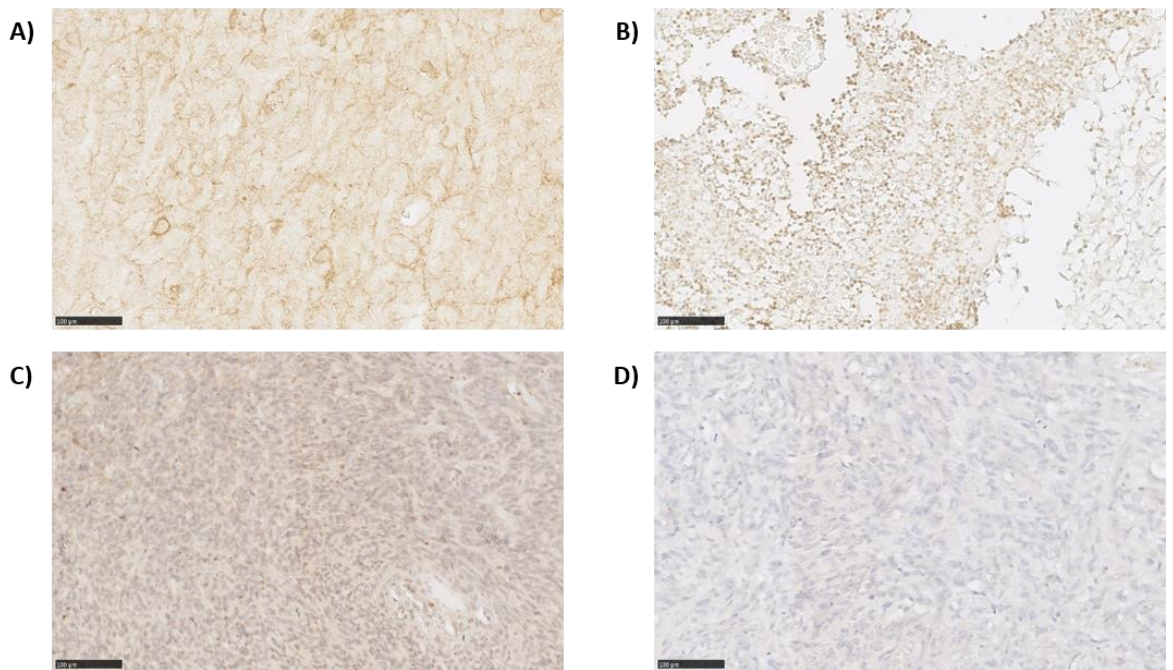


Figure 16. Examples of pathologist's TRP-2 IHC scoring A) 3 (deemed as strong staining) B) 2 (deemed as moderate staining) C) 1 (deemed as weak staining) D) 0 (no staining). Scale bar = 100 µm.

IHC staining score	Antigen				
	TRP-2	WT-1	gp100	HAGE	MGMT
3	1 (3 %)	10 (30 %)	0 (0 %)	0 (0 %)	0 (0 %)
2	4 (12 %)	11 (34 %)	0 (0 %)	0 (0 %)	0 (0 %)
1	17 (52 %)	6 (18 %)	1 (3 %)	7 (21 %)	0 (0 %)
0	11 (33 %)	6 (18 %)	32 (99 %)	26 (79 %)	33 (100 %)

Table 14. Pathologist's IHC scoring of GBM TMA tissue staining intensity. Examples of staining can be seen in figures 15 and 16.

3.3.2. TRP-2 and WT-1 expression are also commonly expressed in GBM cell lines as well as in tissues

As well as studying GBM tumour tissues it was also decided to analyse the antigen expression profile of patient derived GBM cell lines. This helps to identify cell lines that can be used for *in vitro* analyses of the immune response generated by vaccination. These analyses also helped to reveal how much the cell lines utilised are representative of the tissue phenotype. Western blotting was used to study the antigen expression profile of these cell lines as it was a quick and easy method to analyse multiple cell lines side by side. Western blotting analyses revealed that all the cell lines studied expressed high level of TRP-2, but only two out of eight expressed WT-1 and most had very low level of HAGE protein; these results differ from the GBM tissue phenotype (see previous section). The SEBTA027 and SF188 cell lines were found to both express WT-1 and TRP-2 with very low levels of the gp100 protein. MGMT is a prognostic indicator in GBM associated with a poorer response to temozolomide chemotherapy and as a result poorer survival. Five of the eight cell lines probed expressed the MGMT protein. The benefit of utilising immunotherapy is that this natural chemotherapy resistance provided by MGMT expression can be overcome (*Figure 17*).

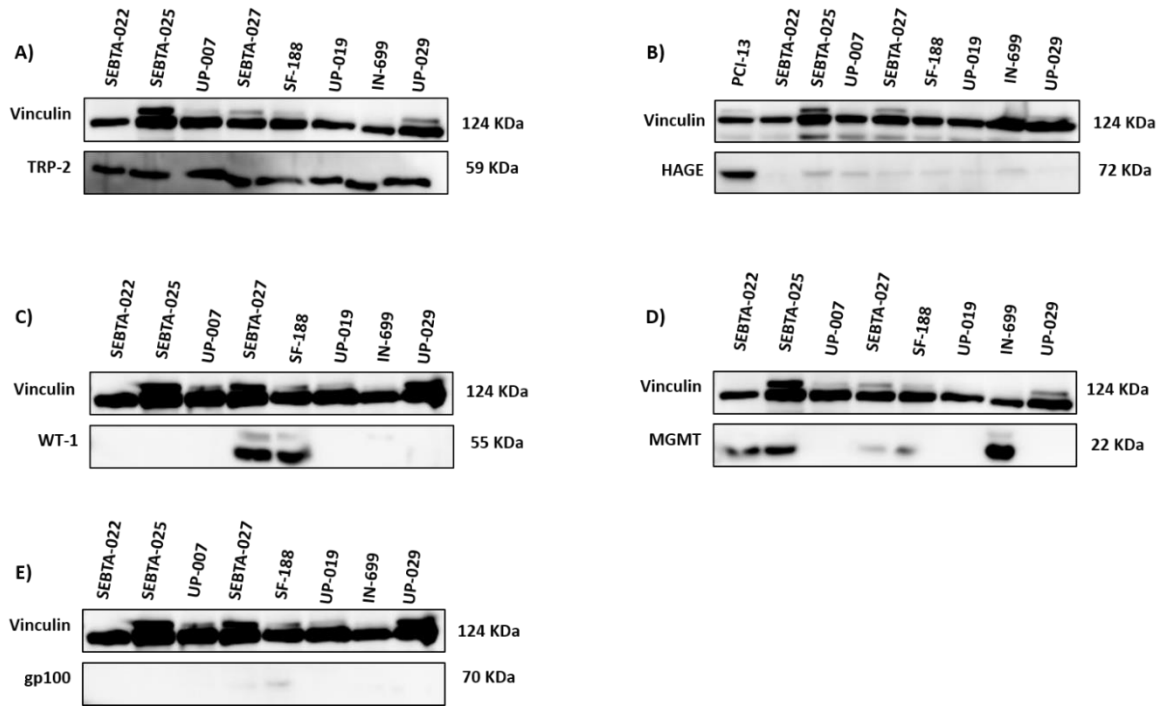
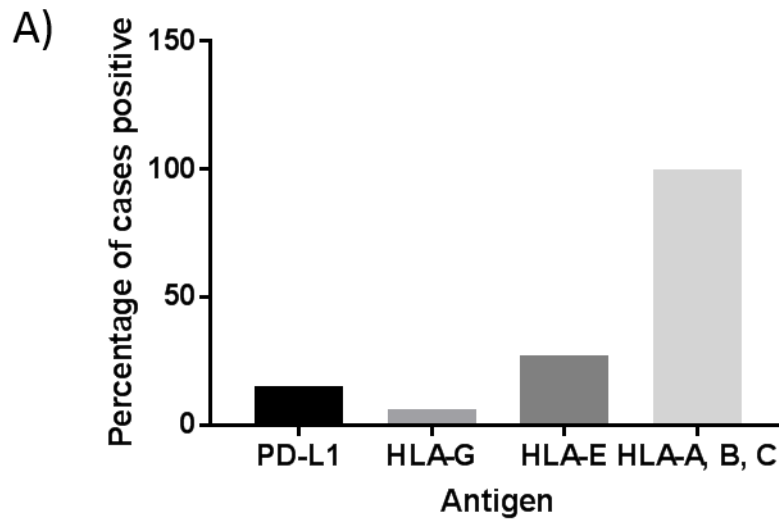


Figure 17. TRP-2, HAGE, WT-1, MGMT and gp100 expression in GBM cell lines as determined by Western blotting, 20 μ g of protein was loaded per lane as described in chapter 2 A) TRP-2 expression as detected by a TRP-2 specific antibody B) HAGE expression as detected by a HAGE specific antibody, PCI-13 is a head and neck cancer cell line that is known to be positive for HAGE expression and as a result was used as a positive control (this lysate was obtained ready prepared for use) C) WT-1 expression as detected by a WT-1 specific antibody D) MGMT expression as detected by a MGMT specific antibody E) gp100 expression as detected by a gp100 specific antibody. All membranes were also probed with an anti-vinculin antibody that acted as a loading control due to its abundant expression.

3.3.3. Analysis of GBM tumour tissues reveal that these tissues have an immunosuppressive phenotype, but these tissues appear to maintain their antigen presentation capabilities

Whilst discovering antigens for targeting immunotherapeutically was of high importance it was also necessary to study the immune landscape of GBM tumours. These tumours are renowned for being immunosuppressive and therefore this needs to be considered when targeting these cancers with immunotherapy. It was decided to stain TMAs all from the same tissue block with antibodies against several immune suppressive ligands and the pan-MHC class I antibody HLA-A, B, C. The results are shown below in *Figure 18* and *Table 15*.



B)

	Antigen			
	PD-L1	HLA-G	HLA-E	HLA-A, B, C
Positive staining	5 (15 %)	2 (6 %)	9 (27%)	33 (100 %)
No staining	28 (85 %)	31 (94 %)	24 (73 %)	0 (0 %)

Figure 18. PD-L1, HLA-G, HLA-E and HLA-A, B, C expression as observed in tissue microarray staining. A) A graphical representation of the percentage of cases the stained positive for each antigen B) Numerical representation of the staining results. Percentages show the number of cases that stained positively, irrespective of the strength of the staining.

All the brain tumour tissues apart from one studied expressed HLA-A, B, C indicating that almost all the tumours studied express MHC class I molecules and can present immunogenic antigens, making this type of cancer targetable with immunotherapeutic approaches. In accordance with the literature these tumours also express the immunosuppressive ligands PD-L1, HLA-E and HLA-G. Only a small proportion of tumours express these antigens (15% PD-L1, 6% HLA-G and 27% HLA-E) so immunotherapy is a viable therapeutic avenue. Images of staining can be seen in Appendix 1. It is however important to note that the genes encoding these proteins are interferon gamma responsive, as a result it is of importance to take this into account. The expression of these proteins after interferon gamma exposure will be explored in a later chapter.

Stained sections were then given a staining score by a pathologist with a score between 0 and 3 given to the tissue. 0 represents no staining, 1 represents mild staining, 2 represents moderate staining and 3 represents strong staining, these results are represented below in *Table 15* with examples of pathologist's scoring being shown in *Figures 19* and *20*. Whilst looking at the intensity of the staining it can be seen that the HLA-A, B, C staining was intense in most of the cases stained, the immunosuppressive ligands PD-L1, HLA-E and HLA-G are much less intensely stained, this may be due to the expression of these molecules primarily on a small subset of 'stem-like' cancer cells, a phenomenon previously shown to occur (Wolpert, Roth et al. 2012, Silver, Sinyuk et al. 2016).

IHC staining score	Antigen			
	PD-L1	HLA-G	HLA-E	HLA-A, B, C
3	0 (0 %)	0 (0 %)	1 (3 %)	29 (88 %)
2	0 (0 %)	0 (0 %)	4 (12 %)	3 (9 %)
1	5 (15 %)	2 (6 %)	4 (12 %)	1 (3 %)
0	28 (85 %)	31 (94 %)	24 (73 %)	0 (0 %)

Table 15. Pathologist's IHC scoring of GBM TMA tissue staining intensity. Examples of staining can be seen below.

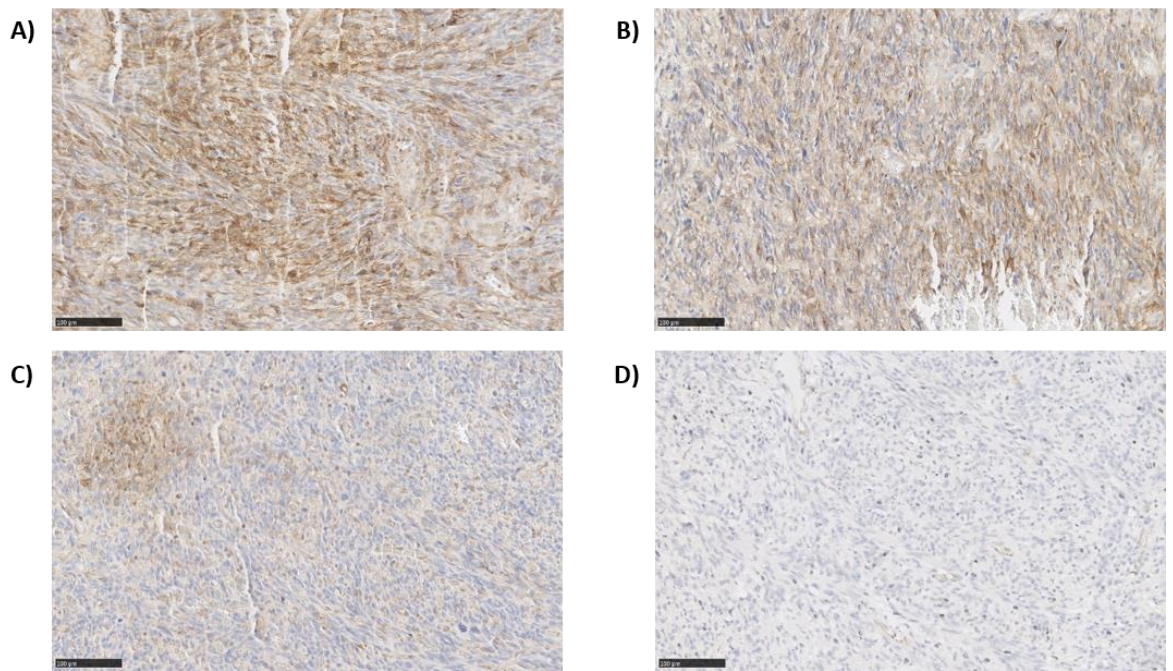


Figure 19. Example of pathologist's HLA-E IHC scoring. A) 3 (deemed as strong staining) B) 2 (deemed as moderate staining) C) 1 (deemed as weak staining) D) 0 (no staining). Scale bar = 100 μ m.

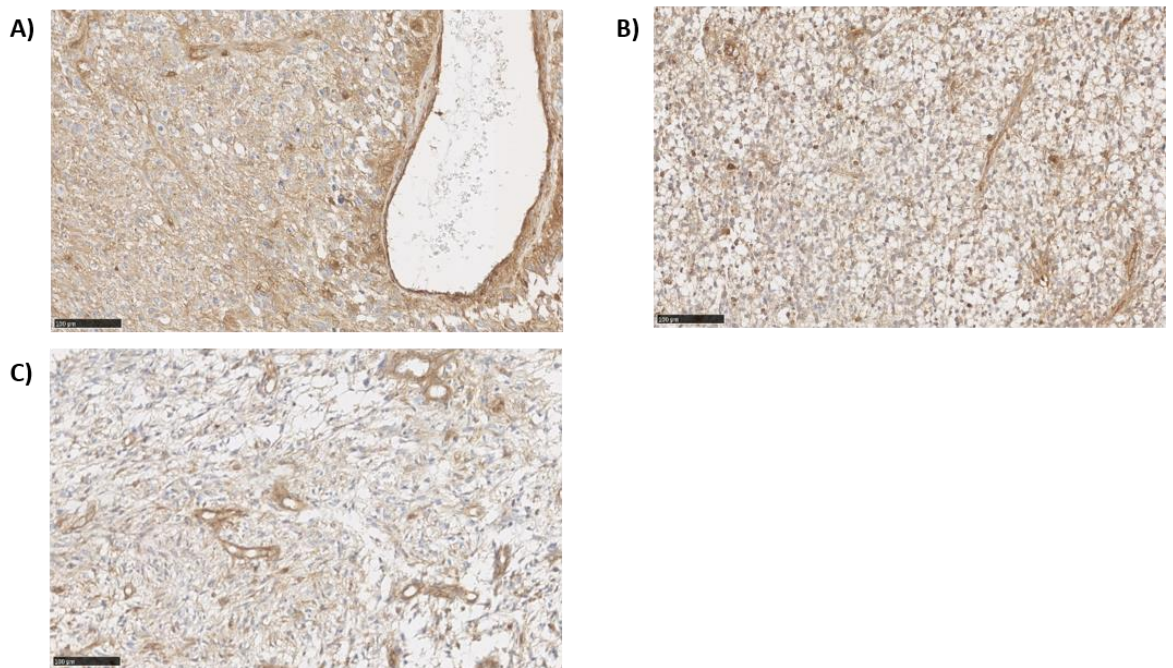


Figure 20. Example of pathologist's HLA-A,B,C IHC scoring. A) 3 (deemed as strong staining) B) 2 (deemed as moderate staining) C) 1 (deemed as weak staining) D) 0 (no staining). Scale bar = 100 μ m.

3.3.4. GBM cell lines also have an immunosuppressive phenotype much like the tissues they are derived from

Western blotting was used to study the antigen expression profile of GBM patient derived cell lines this was performed to see if these cell lines were representative of the tumour tissues. Western blotting analyses of cell lines reveals expression of PD-L1, HLA-E and HLA-G. These proteins enable these tumours to escape immune surveillance and as a result their targeting needs to be considered when utilising immunotherapy to treat GBM. Much like tumour tissues tumour cell lines appear to express high levels of HLA-A, B, C, indicating that they express MHC class I and are capable of presenting class I peptides to CD8⁺ T-cells. The location of these proteins within the cellular architecture is key for their immune dampening effects. Expression of PD-L1, HLA-E and HLA-G on the cell surface hampers the activity of immune cells that make direct contact with the tumour cells. In order to fully elucidate the cellular location of these proteins flow cytometric surface staining was performed.

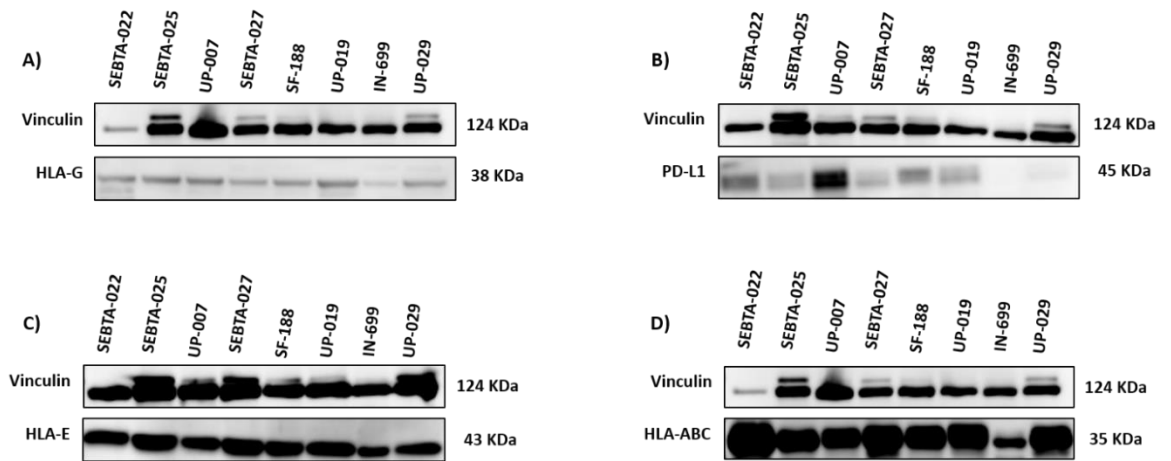


Figure 21. HLA-G, PD-L1, HLA-E and HLA-A, B, C expression in GBM cell lines as determined by Western blotting, 20 μ g of protein was loaded per lane as described in chapter 2 A) HLA-G expression as detected by a HLA-G specific antibody B) PD-L1 expression as detected by a PD-L1 specific antibody C) HLA-E expression as detected by a HLA-E specific antibody D) MHC class I expression as detected by a HLA-A, B, C pan-specific antibody. All membranes were also probed with an anti-vinculin antibody that acted as a loading control due to its abundant expression.

3.4.5. Flow cytometric analyses GBM cell lines reveals expression of both immune inhibitory and immune activating proteins on the surface of these cells

Western blotting revealed that all the cell lines studied expressed MHC class I (HLA-A, B, C) however the specific HLA haplotype was unknown. HLA-A2 is the most common haplotype in the Caucasian population and many vaccines target HLA-A2 specific peptides in the Western world due to its prevalence, making vaccination applicable to a large proportion of patients. Flow cytometry was used to study the cell surface expression of the HLA-A2 protein on GBM cell lines. Flow cytometric surface staining reveals that four out of five of the cell lines studied express the HLA-A2 antigen on their surface (see *Figure 22*). This is of importance because the ImmunoBody® vaccination utilised in this study encodes peptides specific for the HLA-A2 haplotype.

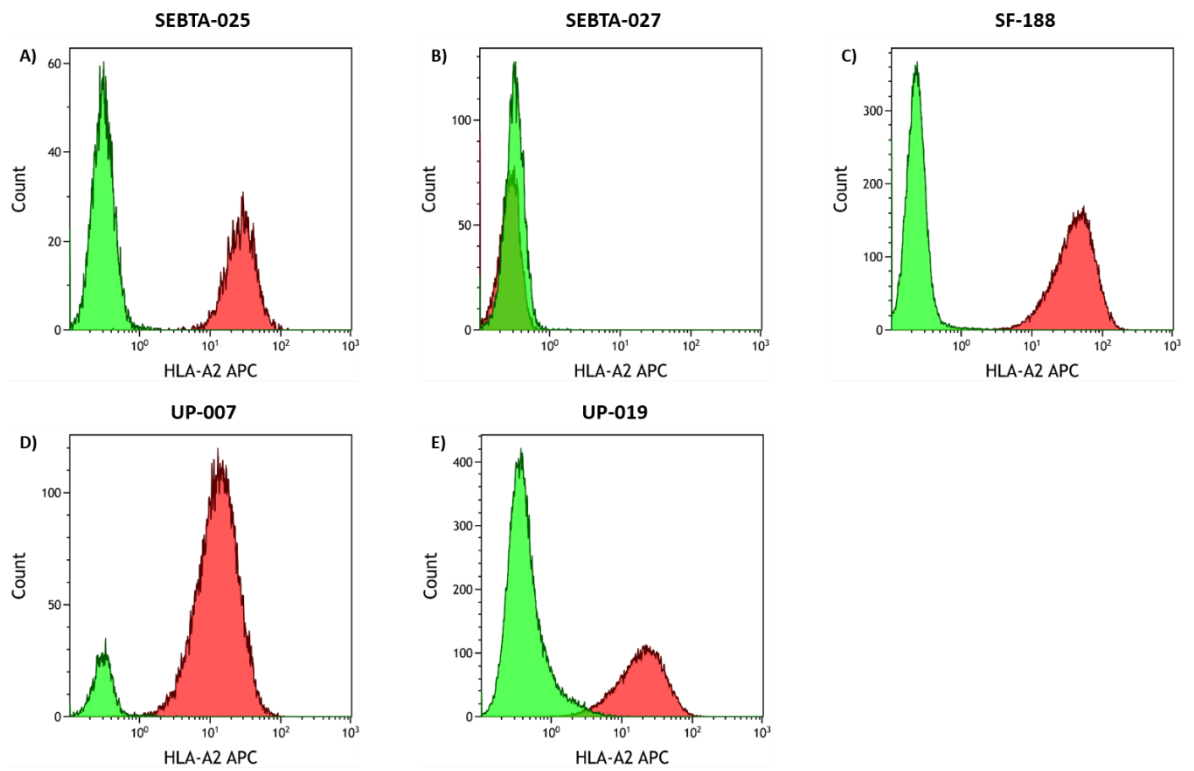


Figure 22. Flow cytometric surface staining histograms of HLA-A2 the green peaks represent unstained cells whereas the red peaks represent cells stained with HLA-A2 APC. A) SEBTA-025 B) SEBTA-027 C) SF188 D) UP-007 E) UP-019.

Cell surface staining was also performed for the immune stimulating ligands CD40, CD80, CD86, MICA/B and HLA-A, B, C. The immunosuppressive ligands HLA-E, HLA-G and FasL were also stained for. These analyses help further characterise the immune phenotype of GBM cell lines and since surface staining was used it revealed the location of many of these immune system interacting proteins. A representative set of histograms for the SEBTA-025 cell line are shown below in *Figure 23*. The histograms for each cell line studied are in appendix 2. The data for all the cell lines is tabulated in *Table 16*.

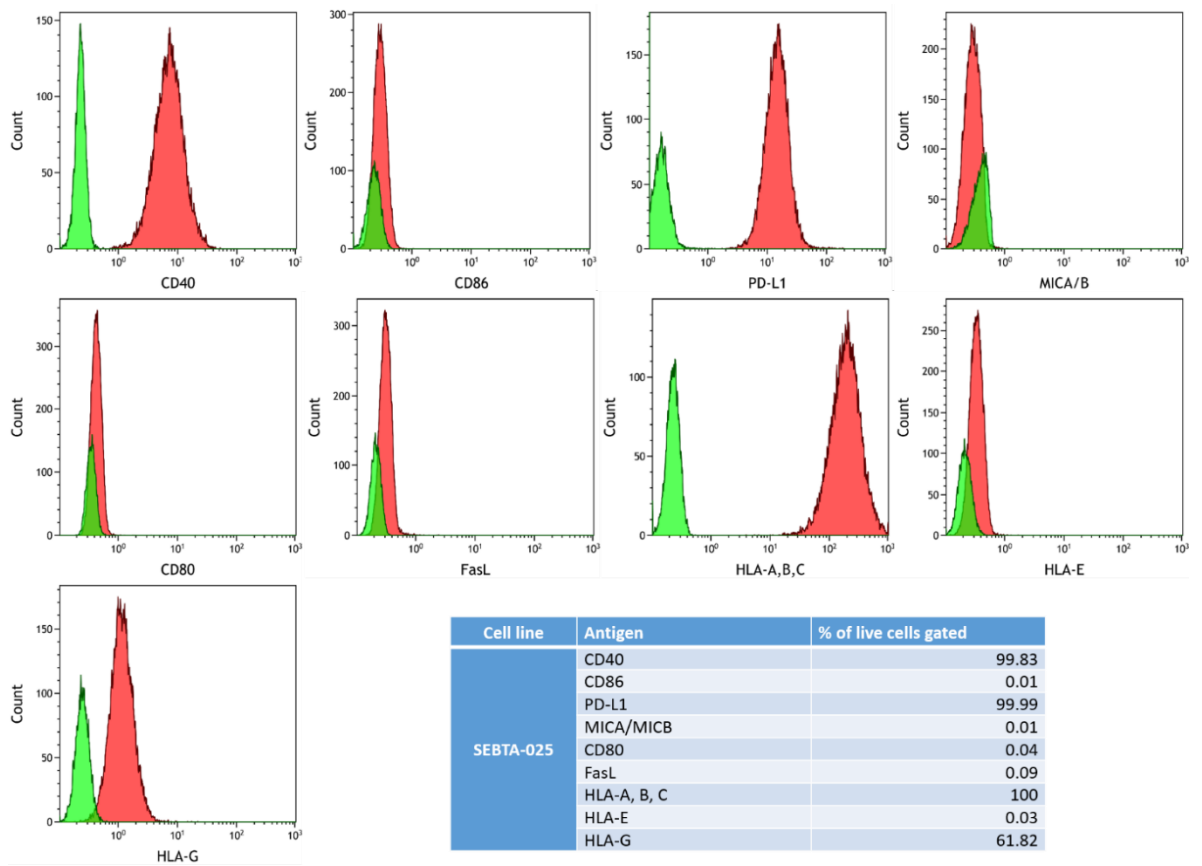


Figure 23. SEBTA-025 flow cytometry surface staining, the green peaks represent unstained cells whereas the red peaks represent stained cells. Each antigen is labelled on the X axis of each histogram. The table in the right-hand corner details the percentage of cells positive for each antigen. Further detailed histograms for each cell line can be seen in appendix 1.

	Antigen																	
	CD40		CD86		PD-L1		MICA/B		CD80		FasL		HLA-A, B, C		HLA-E		HLA-G	
	% positive	MFI	% positive	MFI	% positive	MFI	% positive	MFI	% positive	MFI	% positive	MFI	% positive	MFI	% positive	MFI	% positive	MFI
SEBTA-025	99.83	7.21	0.01	1.06	99.99	14.75	0.01	1.09	0.04	1.27	0.09	1.19	100	193.58	0.03	1.12	61.82	1.41
SEBTA-027	99.7	5.76	0	0	100	11.53	80.51	1.66	0.04	1.49	0	0	100	150.61	0.01	1.20	54.08	1.38
SF-188	98.87	4.70	0	0	99.96	11.01	8.89	1.15	0	0	0	0	99.98	126.38	0.03	1.18	29.2	1.29
UP-007	68.4	1.72	0	0	99.96	10.45	0.01	1.05	0	0	0	0	99.98	31.05	0.03	5.22	1.69	1.18
UP-019	78.02	1.87	0	0	99.78	4.94	1.54	1.10	0.01	1.12	0	0	100	37.32	0	0	4.86	1.12

Table 16. Flow cytometric surface staining results for the SEBTA-025, SEBTA-027, SF-188, UP-007 and UP-019 cell lines. The percentage of live cells stained as well as the median fluorescence intensity is detailed for each antigen. The gating strategy utilised is outlined in chapter 2.

These analyses reveal that GBM cell lines express several immune activating and immune inhibitory molecules on their surface, in order to target these cell lines immunotherapeutically the balance must be shifted towards the immune activating pathways as opposed to the immune inhibitory pathways, this can be done via checkpoint blockade, a concept that will be further explored later within this thesis. PD-L1 expression appears to be a common feature of GBM cell lines with all of the cell lines studied exhibiting expression of PD-L1. All the cell lines also appear to express immune stimulating CD40 on their surface as well as MHC class I, these are highly desirable features for immunotherapeutic targeting of GBM.

Table 17 below provides a brief summary of the antigens of interest expressed by the cell lines studied. Due to the prevalence of the WT-1 and TRP-2 antigens in GBM tumour tissues and cell lines these antigens will be targeted immunotherapeutically. In order to vaccinate against these antigens, the ImmunoBody® DNA vaccine will be utilised. The ImmunoBody® encodes peptides specific for the HLA class I antigen HLA-A2, therefore the expression of HLA-A2 was probed. The SF-188 and SEBTA-027 cell lines are of great interest for further study due to both cell lines expressing WT-1 and TRP-2. The key difference between these two cell lines is their HLA-A2 expression, with SF-188 expressing this antigen and SEBTA-027 displaying no HLA-A2 expression. This differing HLA-A2 expression will allow for HLA-A2 specificity of the ImmunoBody® generated immune response.

	TRP-2	gp100	WT-1	HAGE	HLA-A, B, C	HLA-A2	PD-L1
SEBTA-025	✓	✗	✗	✓	✓	✓	✓
SEBTA-027	✓	✓	✓	✓	✓	✗	✓
SF-188	✓	✓	✓	✓	✓	✓	✓
UP-007	✓	✗	✗	✓	✓	✓	✓
UP-019	✓	✗	✗	✓	✓	✓	✓
UP-029	✓	✗	✗	✗	✓	✗	✗

Table 17. A brief summary of antigens of interest expressed in the GBM cell lines studied. These results are the collated western blot and flow cytometry data obtained for each cell line, revealing the overall antigen expression for each cell line.

3.3.6. The TRP-2 and WT-1 antigens are expressed by the murine GL261 Luc2 and B16 HHDII/DR1 Luc2 cell lines

In order to try and model GBM pre-clinically it would be beneficial to utilise murine cell lines that express the antigens of interest that are present in human GBMs. Due to the previous tissue and cell line analysis the TRP-2 and WT-1 antigens were chosen as GBM specific targets for ImmunoBody® vaccine therapy. It was decided to examine the expression of TRP-2 and WT-1 in the GL261 Luc2 murine GBM cell line and the B16 HHDII/DR1 Luc2 humanised murine melanoma cell line using immunofluorescence and immunocytochemistry. The results of these analyses are detailed in *Figures 24 and 25*.

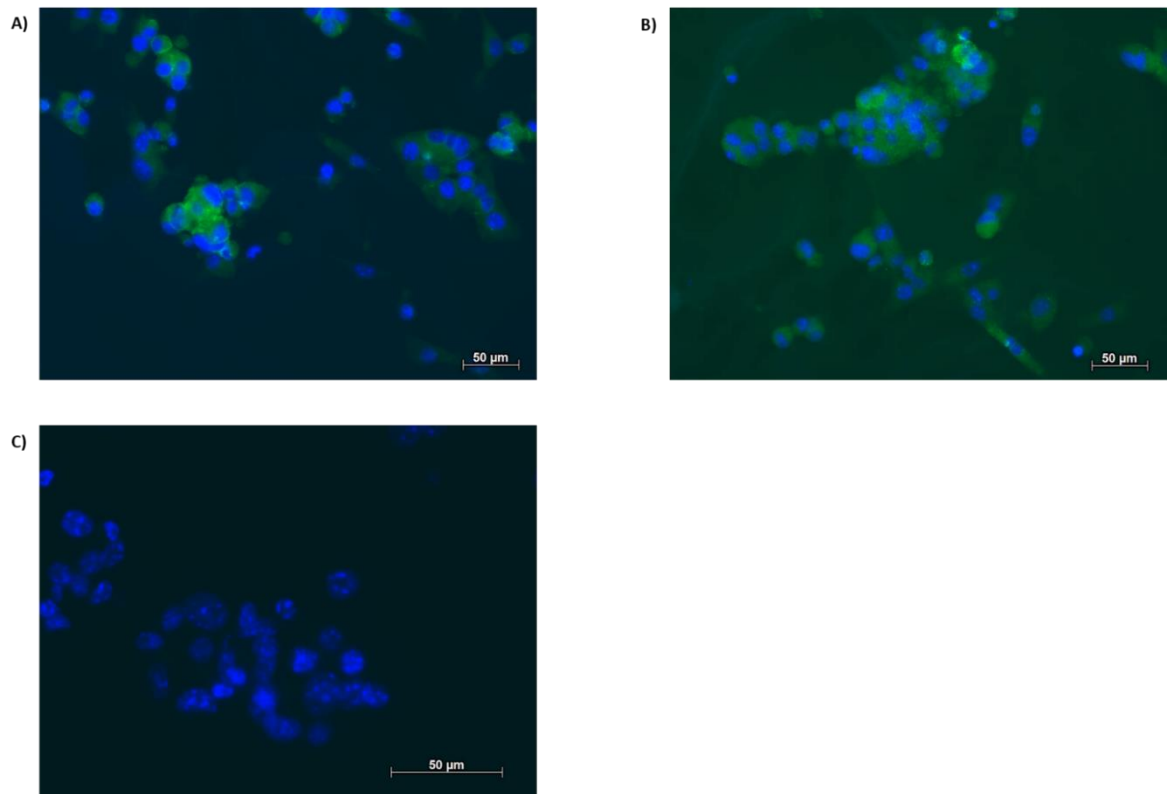


Figure 24. Representative images of immunofluorescence staining of the GL261Luc2 cell line. A) Positive TRP-2 staining as detected by an anti-mouse/human TRP-2 antibody, 100% of cells stained were positive for TRP-2 B) Positive WT-1 staining as detected by an anti-mouse/human WT-1 antibody, 100% of cells stained were positive for WT-1 C) No primary antibody control. Nuclei are counterstained blue with DAPI and positive antigen staining is represented by green fluorescence. Scale bar = 50 μm .

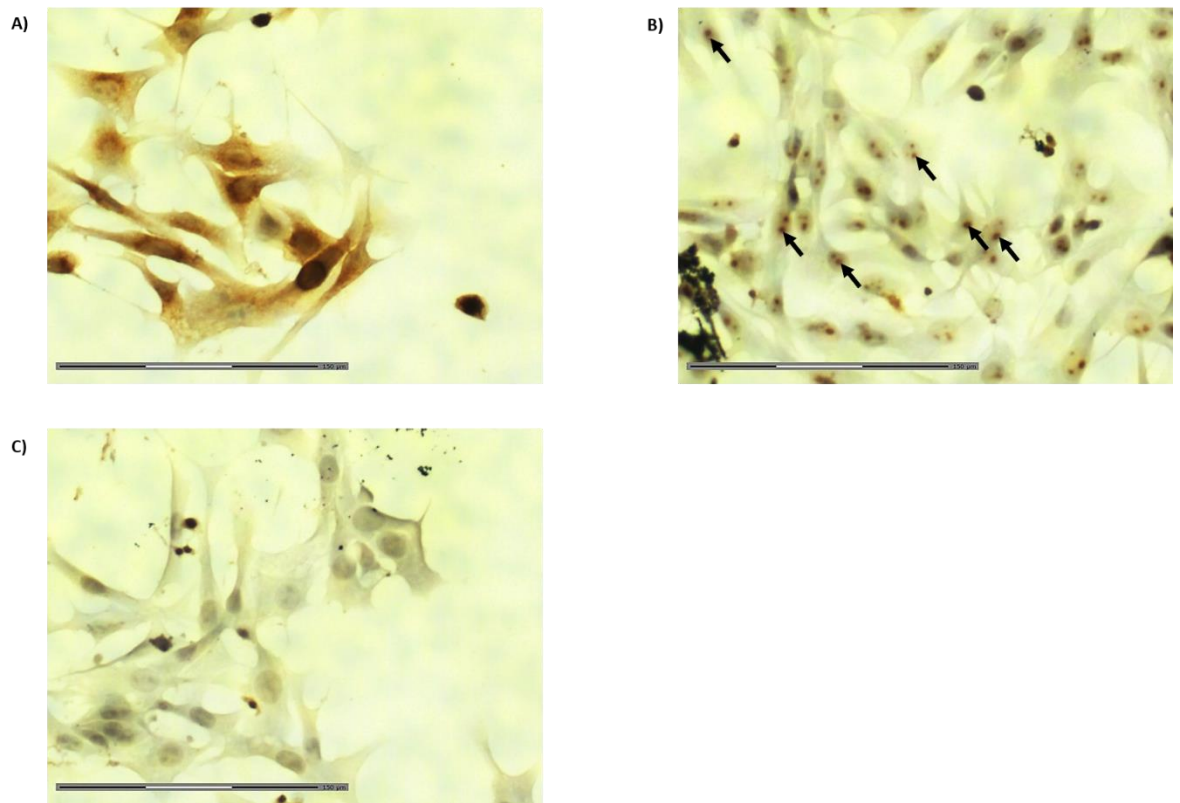


Figure 25. Representative images of Immunocytochemical staining of the B16HHDII/DRI/Luc2 cell line. A) Positive TRP-2 staining as detected by an anti-mouse/human TRP-2 antibody, staining is apparent on the surface of cells B) Positive WT-1 staining as detected by an anti-mouse/human WT-1 antibody, staining can be seen localised in small cytoplasmic areas this is due to WT-1 being a transcription factor. Black arrows highlight some areas of positive staining C) No primary antibody control. Nuclei are stained blue/light purple and positive antigen staining is represented by brown colouration. Scale bar = 150 μm .

The B16HHDD/DR1 Luc cell line expresses the TRP-2 and WT-1 antigens as reported in the literature. The GL261 Luc2 cell line also expressed the TRP-2 and WT-1 antigens. As a result, these cell lines will be used in *in vitro* models to assess potential TRP-2 and WT-1 directed immunotherapy.

3.4. Discussion

Glioblastoma multiforme has a dismal prognosis and as a result novel therapies are required with the hope of improving patient survival whether at first instance of GBM or after recurrence. Immunotherapy provides an exciting novel avenue for treating many types of cancer, including GBM due to its tumour specificity, and reduced bystander effects as compared to chemotherapy and radiotherapy. In order to target GBM tumours with immunotherapy immunogenic targets needed to be identified. The original goal of this project was to target the HAGE (DDX43) antigen in the GBM setting. Whilst HAGE expression was detected at low levels in many of the cell lines studied it was not detected in GBM tissue staining. The HAGE expression observed in the cell lines may be due to changes induced by the culture of the cells, a phenomenon known to occur *in vitro* (Pallini, Casalbore et al. 2000).

The analyses revealed that TRP-2 was expressed in GBM tissues and cells lines. TRP-2 (Tyrosinase-related protein 2) is a protein frequently expressed in the melanin producing cells within the skin, as a result it is a protein commonly found in melanoma tumours. Cells within the brain and the skin are derived from the same progenitors during embryogenesis; the neuroectoderm. Because of this shared lineage tumours of the skin and brain often express similar antigens. In the melanoma setting TRP-2 has been found to be a viable immunogenic target. In the B16 murine melanoma model an 8 amino acid long sequence within TRP-2 was found to be essential for the rejection of B16 tumours in C57BL/6 mice (Bloom, Perry-Lalley et al. 1997). In human beings' expansion of melanoma infiltrating lymphocytes has revealed that these lymphocytes react to the TRP-2 protein. Adoptive transfer of these tumour infiltrating lymphocytes with the cytokine IL-2 resulted in clinical responses within patients. Immunogenic peptide sequences within the TRP-2 antigen have been discovered and are being utilised in immunotherapeutic approaches. For this study a peptide specific for the HLA-A2 MHC-I haplotype will be studied, HLA-A2 being the most prevalently expressed family of MHC class I molecule within the Caucasian population, with 46% of American melanoma patients expressing HLA-A2. The sequence corresponding to amino acids 180-188 of TRP-2 is specific for HLA-A2 and has previously been shown to induce TRP-2 reactive lymphocytes (Parkhurst, Fitzgerald et al. 1998). More importantly this peptide sequence is ubiquitous to all isoforms of the TRP-2 protein and HLA-A2 positive GBM cell lines have been shown to present this peptide, resulting in the recognition of the MR7 cell line (a TRP-2 180-188 specific T-cell) (Liu, G., Khong et al. 2003). In the GBM setting TRP-2 was shown to be expressed by most of these tumours

and 100 % of patient derived cell lines studied making this antigen a viable target for immunotherapy. Moreover, cytotoxic T-cell targeting of TRP-2 expressing GBM cells rendered them more sensitive to chemotherapy suggesting a possible synergy between vaccination and chemotherapy (Liu, G., Akasaki et al. 2005). Importantly, however, after TRP-2 specific targeting patients whose tumour recurred expressed significantly lower levels of TRP-2 due to the eradication of TRP-2 high expressing cells, emphasising the need to target multiple antigens. Interestingly however, was the fact that the cells derived from the recurrent tumours were more sensitive to TMZ chemotherapy than cells derived from the primary tumour. In order to confirm these findings, researchers transfected GBM cells with TRP-2 and treated them with TMZ. These *in vitro* studies showed that the TRP-2-transfected cells were indeed more resistant to TMZ chemotherapy than their un-transfected counterparts. The increased TRP2 levels after transfection did not, however, alter the levels of chemotherapy resistance proteins such as MGMT and breast cancer resistance protein-1 (BCRP-1) (Liu, G., Akasaki et al. 2005) indicating that the newly acquired chemo sensitivity was not due to a reduced level in these proteins. In search of an additional GBM target gp100, another melanoma associated antigen commonly expressed in melanin producing cells was assessed and low levels was detected within GBM cell lines and tissues. Analysis of cytotoxic T-cells within melanoma patients' peripheral blood cells and tumour infiltrating lymphocytes revealed the presence of gp100 reactive cells (Eisenberg, Machlenkin et al. 2010). Previous studies have found much like TRP-2, gp100 is also expressed in GBM due to the shared neuroectodermal lineage (Saikali, Avril et al. 2007, Liu, G., Ying et al. 2004). What is even more important is that cytotoxic T-cells recognise the gp100 protein when it is expressed by GBM cells (Liu, G., Ying et al. 2004). However, gp100 was only detected in two GBM cell lines at a low level and therefore for the purpose of this study it was deemed necessary to identify an additional target with a more widespread and pronounced expression within the cell lines studied.

WT-1 is a zinc finger transcription factor involved in development of the mammalian kidney during embryogenesis. This WT-1 expression is lost upon birth (Fanni, Fanos et al. 2011). Previous research has revealed high levels of WT-1 expression in GBM tumours and cell lines (Nakahara, Okamoto et al. 2004, Menssen, Bertelmann et al. 2000). Due to the observed expression of WT-1 within glioblastoma multiforme tumours its use as an immunotherapeutic target has previously been studied in clinical trials. WT-1 peptide pulsed dendritic cells have been administered to patients with recurrent GBM, these patients notoriously have a very poor prognosis and as a result novel therapeutics are desperately required. This early trial revealed that WT-1 pulsed dendritic cells generated WT-1 reactive T cells in patients, 5/7 of the patients treated with WT-1 pulsed dendritic cell vaccination exhibited stable disease (Sakai, Shimodaira et al. 2015). WT-1 peptide vaccination has also been explored as a therapeutic avenue in the GBM setting. Not only does WT-1 represent

an immunogenic target it also appears to have a functional role in the tumorigenicity of GBM cells. Indeed, WT-1 knock-down using WT-1 shRNA has been shown to reduce the proliferation of the U251MG cell lines *in vitro*, as well as *in vivo* when injected into mice (Clark, Ware et al. 2010). Similar *in vitro* and *in vivo* findings have been found with the U87MG GBM cell line, where WT-1 knockdown showed a reduced cell proliferation and tumour formation (Kijima, Hosen et al. 2014). These characteristics make WT-1 an even more attractive therapeutic target due to its role in GBM tumour growth.

Murine B16 and GL261 cell lines both express the TRP-2 and WT-1 antigens, sharing the same trend seen in human brain tumours (GL261) expressing many of the same antigens as melanoma tumours (B16) due to their shared developmental lineage. This is of great use for future *in vivo* modelling of GBM.

Unfortunately, whilst immunogenic targets were discovered the immune inhibitory nature of GBM was also revealed. PD-L1 expression was prevalent in patient derived GBM cell lines. This antigen has previously been shown to be expressed in GBM tumours and the tissue and cell line analysed in this chapter confirmed these findings. The expression of PD-L1 by GBM tumour cell lines has been shown to be dependent upon AKT activation. Mutation or loss of the tumour suppressor PTEN has been shown to result in an increased expression of PD-L1 by GBM cell lines (Parsa, Waldron et al. 2007). Knockdown of PD-L1 in the U87MG cell line prevented formation of GBM tumours in a xenograft model using immunocompromised Balb/c nude mice whereas normal U87MG cells successfully formed tumours. Overexpression of PD-L1 was also shown to increase GBM cell migration *in vitro* (Qiu, Hu et al. 2018). The flow cytometry analyses revealed that this PD-L1 is expressed on the surface of the cell lines studied, meaning that it can exert its immune inhibitory effects when these cells encounter activated PD-1 expressing T-cells. However, this cell-surface expression also allows for the PD-L1 to be targeted via therapeutic blocking antibodies, allowing the immune inhibitory effect to be nullified.

HLA-E was evident in Western blotting however this was not detected on the surface of the GBM cell lines studied. HLA-G just like HLA-E has a secreted soluble form (sHLA-G) which is stored in intracellular vesicles. This would explain the presence of this protein within the cellular lysates obtained from cells that are negative for cell surface staining of HLA-G. HLA-E and HLA-G are immune inhibitory proteins that bind to inhibitory receptors on the surface of NK cells. It is therefore possible that the HLA-E expressed by GBM cells is the soluble form as opposed to the cell surface form as was found for melanoma, colorectal, lung, kidney, ovary, breast, prostate and thyroid cancer cell lines *in vitro* (Allard, Oger et al. 2011). Melanoma patients have been shown to have higher levels of sHLA-E in their sera compared to healthy controls (Allard, Oger et al. 2011). In future it would be of great interest to measure levels of sHLA-E within the sera or CSF of GBM

patients in order to confirm this hypothesis. Glioblastoma multiforme stem-like cells have been shown to express HLA-E on their surface to escape immune surveillance by NK cells, this was confirmed by knockdown of HLA-E. GBM stem-like cells with HLA-E gene silencing were more susceptible to NK cell mediated lysis (Wolpert, Roth et al. 2012). HLA-G expression is limited throughout normal tissues and it acts to protect cells from NK cell mediated lysis, however tumour cells have been shown to co-opt this HLA-G expression as an immune evasion strategy. GBM cell lines have also been previously shown to express HLA-G and expression of HLA-G has been shown to reduce tumour cell lysis by PBMCs, even more interestingly is the small number of HLA-G-expressing cells to inhibit the immune cell lysis of an entire population of cells i.e. even when only 10% of cells express HLA-G, lysis of HLA-G negative cells was inhibited (Wiendl, Mitsdoerffer et al. 2002).

The expression of Fas L was also probed, because previous research has shown that GBM tumours can express the Fas ligand (FasL). This ligand binds to the Fas receptor on T-cells which then results in caspase activation and apoptosis of T-cells enabling GBM tumour cells to escape immune surveillance (Didenko, Ngo et al. 2002). Fortunately, the cell lines studied here did not appear to express the Fas ligand meaning that they are incapable of inducing apoptosis of Fas expressing T cells.

HLA-A, B, C represents the classical MHC class I molecules, those molecules responsible for presentation of class I peptides to cytotoxic CD8 T-cells. Many tumours downregulate MHC class I molecules in order to avoid immune surveillance by cytotoxic T-cells, this phenomenon has been witnessed in the GBM setting. Invasive GBM cells have been shown in both the *in vitro* and *in vivo* settings to down regulate MHC class I expression allowing them to spread the tumour whilst evading immune regulation, GBM cell invasion is well documented and is the major cause of tumour recurrence (Zagzag, Salnikow et al. 2005). The mice used in this study express the chimeric HLA-A2 molecule and therefore potential target cells for the assessment of vaccine induced T-cell response will need to be HLA-A2 positive. In addition to this HLA-A2 is the most common HLA haplotype in the Western world. As a result, the HLA-A2 expression was studied in all of the cell lines available, this revealed that the majority of these cells lines expressed HLA-A2, with only SEBTA-027 and UP-029 being negative for HLA-A2 expression.

CD40 expression was also discovered on the surface of all the cell lines studied, this is a phenomenon observed in many cancers (Tong, Stone 2003a). CD40 binds to its ligand CD40L; activated CD4⁺ T-helper cells have been shown to express the CD40L ligand on their surface. The interaction between CD40 on antigen presenting cells and CD40L on these CD4⁺ T-cells has been shown to improve antigen presentation by APCs thus improving CD8 cytotoxic T-cell priming (Schoenberger, Toes et al. 1998). Interestingly the activation of B-cells by CD40 enables them to

present cancer associated peptides via MHC class II to T-cells enabling the generation of antigen specific T-cells (Lapointe, Bellemare-Pelletier et al. 2003). It would be of great interest to see if exposing the CD40 positive GBM cells to B-cells would alter their antigen presentation and result in improved T-cell recognition of GBM cell lines. Ligation of CD40 on tumour cells has been shown to have anti-cancer effects and the use of CD40L therapy has been studied in a plethora of cancer types and numerous clinical trials using CD40L are ongoing (Tong, Stone 2003b). Interestingly CD40L therapy has not been studied in the GBM setting and there are currently no active clinical trials. It may be of interest to examine the potential of this type of therapy in the GBM setting.

MICA and MICB (MHC class I chain-related protein A and B) are ligands of NKG2D, a receptor expressed on NK and CD8⁺ T-cells. The NKG2D ligands are not widely expressed in normal tissues, however their expression has been evidenced in cancer marking a potential cancer target. GBMs have previously been shown to express MICA (Spear, Wu et al. 2013). The binding of NKG2D to its ligands has been shown to be involved in tumour immunosurveillance, the expression on MHC class I prevents NK-cell mediated cytolytic activity, in the GBM setting MICA and MICB are expressed however these tumours also appear to have MHC class I expression which acts to dampen NK cell mediated lysis (Friese, Platten et al. 2003).

Preliminary analyses of GBM tissues reveal that these tumours express immunogenic antigens that are targetable, however these tumours seem to also express several immunosuppressive antigens in their native environment a result that will need to be taken into consideration when assessing the vaccine *in vivo*. These results provide promising targets; however the second set of findings make it difficult to target these tumours with activated immune cells. As a result, checkpoint blockade will have to be incorporated into future immunotherapeutic approaches.

3.5. Conclusion

TRP-2 and WT-1 proteins are viable targets for GBM immunotherapy due to their presence within the majority of the GBM tumours studied in this thesis and their absence from normal brain tissues. Unfortunately, flow cytometric and Western blotting analyses revealed that despite expressing targetable antigens these tumours are highly immunosuppressive. Because of the expression of several immunosuppressive proteins future immunotherapeutic targeting of these tumours will need to take immunosuppression into account, this may be done by blocking some of these immunosuppressive checkpoints whilst targeting the antigens expressed via active immunotherapy (a concept that will be explored later in this thesis). The expression of MGMT renders patients' resistant to temozolomide chemotherapy. Western blotting analyses of the GBM cell lines revealed that five out of the eight cell lines studied express the MGMT protein. This indicates a high proportion of temozolomide resistance, as a result it is of great interest to discover novel methods for targeting these tumours, and this is where immunotherapy comes into play.

CHAPTER 4: PRE-CLINICAL EVALUATION OF THE IMMUNOBODY® DNA VACCINES

4.1. Introduction

4.1.1. Vaccination

Vaccination has been a key discovery in the history of medicine, traditionally vaccination was used to protect against infection however it has also been explored in a therapeutic context. The earliest documented case of therapeutic vaccination for cancer is the work published by William B. Coley in the late 19th century. Coley used injection of bacteria into patient tumours to induce a localised immune response (Coley 1891). Whilst Coley utilised bacteria to induce an immune response to tumours there are numerous other anti-tumour vaccination methods. Cancer immunotherapy was Science magazine's breakthrough of the year in 2013 (Couzin-Frankel 2013) and numerous immunotherapeutic approaches are being approved and currently being trialled in the cancer setting. Currently there are no approved immunotherapeutic treatments for glioblastoma multiforme available however there are numerous immunotherapeutic treatments currently being trialled (clinicaltrials.gov - PubMed - NCBI).

The purpose of a vaccination is to eliminate pathogens/cancer cells utilising the body's own immune system. This involves "educating" cells within the immune system to recognise, kill and remove these pathogens/deleterious cells. In the context of cancer cells, antigens recognised by the immune system are not necessarily foreign in nature, the immune system also appears to recognise cells overexpressing certain antigens, which is often the case in cancer. Tumour antigens can broadly be grouped into tumour-associated antigens (TAAs) and tumour specific antigens (TSAs). Tumour specific antigens are antigens that are exclusive to tumour cells, quite often these may be mutated, or truncated forms of native antigens normally expressed within the body, one such example is the EGFRvIII antigen, which is a truncated version of the epidermal growth factor receptor with deletion of exons 2-7 of the corresponding gene. Another type of 'tumour specific' antigens are the cancer testis antigens. These are antigens which are expressed by tumour cells and the testes; the reason why these antigens are considered tumour specific is that the testes are an immune privileged site, essentially making antigens they express invisible to the immune system and therefore to the immune system these antigens appear to be exclusive to cancer cells due to their 'foreign' nature. Tumour associated antigens are antigens expressed normally within the body, however they are usually more abundant in tumour cells, this elicits an immune reaction due to the abnormal expression levels. The presence of these antigens provides us with a means to target these tumours and turn the immune system onto them (Reardon, Freeman et al. 2014).

Tumours can be targeted by identifying the antigens they express and targeting these antigens. The most straightforward way to home the immune system onto tumour cells is to vaccinate patients with their own tumour cells. The preparation methods of the tumour cells can be varied, and the reasoning behind using autologous tumour cells is that they should contain all the patient's tumour antigens. With regards to preparation prior to vaccination the tumour cells may be irradiated, lysed or even genetically modified. This prevents the tumorigenicity of these cells whilst allowing their antigens to stimulate the immune system (de Gruijl, van den Eertwegh et al. 2008). Irradiated tumour cells given in conjunction with an immune adjuvant have been shown in animal models to protect from subsequent tumour challenge, the administration of this vaccination in colorectal cancer resulted in improved disease-free survival, however further analysis of this vaccination method highlighted the importance of standardising the vaccination preparation procedure. This was highlighted by the variability of the quality of the vaccinations produced at different experimental sites (de Gruijl, van den Eertwegh et al. 2008).

Dendritic cells like macrophages are professional antigen presenting cells, whose function is to clear the body of dead cells/debris/proteins, "digest" these into smaller peptide fragments that are then presented via MHC molecules to other immune cells, thereby kick starting the immune response (Guermonprez, Valladeau et al. 2002). Utilising dendritic cells as a method of vaccination is another avenue for therapy. Dendritic cells can be obtained from the patient's body; this is done by extracting PBMCs from the patient via leukapheresis. PBMCs are then treated with cytokines resulting in their differentiation into dendritic cells and then these cells are expanded *in vitro*. These patient derived dendritic cells can then either be pulsed with autologous tumour cell lysate or a peptide/multiple peptides. These dendritic cells can then be matured and re-introduced into the patient with the goal of priming the immune cells within the body to recognise tumour antigens and generate an anti-tumour immune response. DCVax[®]L is one such example of this type of therapy utilised in the glioblastoma multiforme setting (Polyzoidis, Ashkan 2014). This vaccine is generated by using patient monocyte-derived DCs and pulsing them with autologous tumour lysate. This method of vaccine therapy has undergone numerous clinical trials and early Phase I/II trials were promising with 33% of patients surviving for over 4 years, and 27% surviving more than 6 years. As a result of these promising early results DCVax[®]L progressed into Phase III trial (Hdeib, Sloan 2015). Preliminary results from the phase III study of DCVax[®]L for GBM have revealed that the median overall survival of the intent-to-treat population was 23.1 months from surgery vs the 15 months achieved via standard therapy. Upon recurrence all patients could receive DCVax[®]L and as a result 90% of patients enrolled received DCVax[®]L vaccinations. Only 7% of patients within the study experienced serious adverse side effects. It would be of great interest to see how DCVax[®]L affects survival once the data has been unblinded, but these early results are promising (Liau,

Ashkan et al. 2018). ICT-107 is another example of a dendritic cell vaccine being tested in GBM (Wen, Reardon et al. 2019). ICT-107 uses patients' monocyte-derived DCs pulsed with six synthetic GBM associated peptides (MAGE-1, HER-2, AIM-2, TRP-2, gp100 and IL13-R α 2) before being re-administered into patients. In a Phase II study comparing ICT-107 with unpulsed dendritic cells it was found that overall survival of ICT-107 treated patients two months longer than control patients given unpulsed dendritic cells (Wen, Reardon et al. 2019). Unfortunately, due to funding constraints Phase III study of ICT-107 has been halted. These methods of generating vaccinations are extremely expensive and the methods for generating these vaccines highly invasive with patients needing to undergo leukapheresis sessions. These vaccines also require time to develop so there may be a latency period between surgery and receipt of dendritic cell vaccination (Mastelic-Gavillet, Balint et al. 2019).

The immune system can also be simply educated via injection of immunogenic cancer-specific peptide sequences that home immune cells onto tumours. This method of vaccination is less invasive and far more rapid than dendritic cell vaccination making it an attractive method for generating an immune response. Often these peptides will need to be given in conjunction with immune boosting adjuvants. One such example of a peptide vaccination for the treatment of GBM is Rindopepimut (Swartz, Li et al. 2014). Rindopepimut is a 14 amino acid long peptide sequence specific for the previously mentioned GBM antigen EGFRviii conjugated to keyhole limpet hemocyanin; an immunogenic carrier protein. Keyhole limpet hemocyanin is a highly immunogenic protein that can activate dendritic cells via its interaction with the mannose receptor resulting in increased cytokine release and upregulation of costimulatory molecules (Presicce, Taddeo et al. 2008). Due to pre-clinical successes Rindopepimut was moved into the clinic for early trials, in a Phase II trial combining Rindopepimut vaccination with the immune adjuvant GM-CSF, low toxicity was observed. EGFRviii positive patients were treated with Rindopepimut; the overall survival for treated patients was 26 months compared to 15.2 months for matched controls. In patients whose tumours recurred 82% had complete loss of EGFRviii expression and of those still expressing EGFRviii less than 1% of cells within the tumour expressed the protein. Rindopepimut was advanced to Phase III in newly diagnosed patients whose tumours expressed EGFRviii. Patients were given Rindopepimut with GM-CSF along with standard therapy (TMZ+RT), in this phase II trial the overall survival of patients was 24.6 months compared to the 15.2 months of matched controls (Swartz, Li et al. 2014). In a further Phase III trial utilising Rindopepimut in combination with TMZ for the treatment of EGFRviii positive *de novo* GBM post-surgical resection and completion of standard radiation. The control group received just keyhole limpet hemocyanin along with TMZ. Comparison of the control and treatment groups revealed that there was no increase in overall survival, as a result Rindopepimut's usage has not been approved for use in GBM (Weller, Butowski et al. 2017).

4.1.2. Antigen presentation and the immunoproteasome

All internal proteins and misfolded proteins are eventually ubiquitinated and sent for “recycling”. This natural degradation process is performed by a complex of enzymes called proteasomes at the end of which process peptides are produced and presented via MHC class I molecules (expressed by all nucleated cells in the body) to CD8⁺ T-cells. The 26S proteasome is responsible for degrading polyubiquitylated proteins. The 26S complex is made up of the 20S proteasome and two 19S regulator complexes. The 20S protease unit is composed of alpha and beta subunits that form a barrel shaped complex is the catalytic core comprised of seven beta subunits, three of which are responsible for its hydrolytic activity (Basler, Kirk et al. 2013). The 19S regulator units are composed of 6 ATPase subunits and 9-10 non-ATPase subunits; these attach to the outer alpha rings of the 20S core. Defective proteins known as defective ribosomal products are synthesised by cells, due to their defects they are ubiquitylated and degraded by the proteasome, resulting in the production of antigenic peptides. Protein synthesis is key for the generation of MHC class I peptides however many proteins need to be hydrolysed to yield MHC class I epitopes. Interferon gamma has been shown to enhance antigen presentation via MHC upregulation. Interferon gamma also leads to replacement of the β 1, β 2 and β 5 hydrolytic subunits of the 20S core with LMP2, LMP7 and MECL-1 leading to formation of the ‘immunoproteasome’: a proteasome that is more efficient at generating immunogenic peptides than the standard proteasome. IFN γ also leads to regulation of the proteasome activator complex PA28 (comprised of the α and β PA28 subunits). This complex binds to the α rings on the 20S complex enhancing its proteolytic activity. This leads to increased protein break down and as a result a generation of more potentially immunogenic peptide sequences due to the increased rate of proteolysis and production of immunoproteasome specific peptides (Kloetzel, Ossendorp 2004). Once immunogenic peptides are generated, they are shuttled to the endoplasmic reticulum by TAP (Transporter associated with antigen presentation). These peptides are then trimmed by aminopeptidases enabling their binding to MHC class I. These MHC class I peptide (now 8-11 amino-acids long) complexes are then shuttled to the cell surface where they are presented to CD8⁺ T-cells (Wearsch, Cresswell 2008).

MHC class II is only expressed by antigen presenting cells, thymic epithelial cells, some endothelial cells and B cells (Roche, Furuta 2015). The majority of peptides bound to MHC class II are derived from the processing of proteins that have been internalised from within the microenvironment. These MHC class II molecules present peptides of 11-20 amino-acid long to CD4⁺ T-helper cells. The presentation of peptides to CD4⁺ T-cells results in their differentiation into the differing T-helper cell subsets, the type of cell presenting these class II peptides, along with differing costimulatory

signals result in the generation of differing cell subsets. Once MHC class II molecules are produced within cells, they bind to a protein known as the invariant chain, this invariant chain is involved in the shuttling of the MHC class II molecules to the endosomal-lysosomal antigen processing compartments. MHC class II bound to the invariant chain is shuttled to the endosomal-lysosomal processing compartment where it is exposed to antigenic peptides. The invariant chain prevents the binding of peptides to the MHC class II molecule, so the invariant chain is proteolytically degraded freeing up the MHC molecule for peptide binding (Cresswell 1996). After peptide binding to the MHC class II molecule the MHC peptide complex is transported to the plasma membrane for recognition by CD4⁺ T-cells. Antigens are obtained from various sources; antigen presenting cells can take up extracellular proteins via a process known as micropinocytosis (Lim, Gleeson 2011). Dendritic cells are the most potent antigen presenting cells within the immune system being at the centre of innate and adaptive immune responses. Immature dendritic cells have a high level of basal macropinocytosis, and this is believed to be the major route of antigen acquisition used by these. B cells on the other hand have little to no macropinocytic activity and they uptake antigenic material via receptor mediated endocytosis (Roche, Furuta 2015). As dendritic cells mature their rate of macropinocytic activity decreases. APCs and B cells have several cell surface receptors that enable binding and uptake of antigenic material. These are receptors such as the B cell receptors, complement receptors and the Fcγ receptors (FcγR) specific for IgG. FcγRs are present on both immature and mature dendritic cells enabling these cells to uptake immune complexes and process them for antigen presentation. Once antigenic material is bound to these receptors they are internalised and shuttled to the antigen-processing compartments by clathrin-mediated endocytosis (Roche, Furuta 2015). This receptor mediated method of antigen processing is far more efficient at priming CD4⁺ T-cells than micropinocytosis, roughly one thousand times more efficient (Rock, Benacerraf et al. 1984). Antigens can also be taken up via phagocytosis, uptake of apoptotic cells via this method enables antigen presenting cells to present self-peptides resulting in the generation of peripheral tolerance. Mature dendritic cells are still capable of performing phagocytosis. Antigenic cargo is internalised by phagosomes, these are relatively non-proteolytic so these phagosomes fuse with lysosomes generating phagolysosomes. The phagolysosome breaks down the antigenic cargo contained, and it contains the complete MHC class II peptide-loading machinery allowing for peptide loading and presentation. The phagolysosome is tightly regulated in order to prevent the breakdown of potentially antigenic peptide sequences. MHC class II peptides can also be obtained by autophagy. Autophagosomes engulf cytosolic macromolecules and organelles which fuse with lysosomes to form autophagolysosomes resulting in breakdown of peptides and presentation via MHC class II. In immature dendritic cells large amounts of MHC class II are present, upon activation of dendritic cells there is a change in MHC class II expression and cellular localisation. In immature dendritic cells MHC class II is present on the plasma membrane

and within intracellular endosomes and lysosomes, MHC class II is primarily on the plasma membrane of mature dendritic cells (Roche, Furuta 2015).

The Fc gamma receptor FcγR is an important regulator of immune responses due to its ability to bind to IgG antibodies. The immune response is a fine balance between immune activation and inhibition, modulated by cytokine action, cell signalling and cell-cell contact. When pro-inflammatory signals dominate pathogens are eliminated. When there is a lack of positive stimulation anti-inflammatory mechanisms down regulate immune activation. The FcγRs are key regulators of a balanced immune system setting thresholds for immune cell activation by simultaneous stimulation of activating and inhibitory pathways. FcγRs have roles in antigen presentation and immune-complex mediated maturation of dendritic cells, as a result FcγRs can regulate dendritic cell activity and control whether an immunogenic or tolerogenic response is initiated after peptide recognition. FcγRs bind to IgG antibodies via their Fc fragment. FcγRs on dendritic cells are essential for endocytosis and/or phagocytosis of antibody-antigen immune complexes and the resultant processing and presentation of antigenic peptides on MHC molecules, regulating the activity of dendritic cells. Immune complexes are strong activators of dendritic cells and they have been shown to prime a stronger immune response than antigen alone. Immune complex internalisation via the FcγRs has been shown to result in priming of both CD8⁺ and CD4⁺ T-cell responses (Nimmerjahn, Ravetch 2008).

Cross priming is key for the generation of a robust immune response. This is the process by which dendritic cells present tumour antigens to T-cells providing the necessary co-stimulatory signals required for immune cell activation that are lacking when the tumours present antigens on their surface. As previously mentioned, dendritic cells are the most potent antigen presenting cells of the immune system. Dendritic cells process and present antigens via both MHC class I and class II molecules enabling them to activate both CD8⁺ and CD4⁺ T-cells using the methods mentioned above. Dendritic cells can endocytose cellular debris enabling uptake and presentation of tumour antigens. These dendritic cells can then travel to lymph nodes where they present the antigens they have taken up to T-cells. Intratumoural dendritic cells can also present antigens to T-cells located within tumours along with co-stimulatory signals that result in T-cell activation (Sanchez-Paulete, Teijeira et al. 2017). For dendritic cells to induce T-cell maturation they need to present peptides on MHC molecules to naive T-cells; these peptides bind to the T-cell receptor (TCR) on the surface of the T-cell forming an immunological synapse. The strength of this synapse contributes to the level of T-cell activation. Costimulatory molecules also function to enhance the T-cell response, with engagement of CD28 on T-cells to B7 molecules expressed on dendritic cells resulting in a 100-fold increase in TCR signalling; this occurs via the increased recruitment of downstream kinases.

Cytokines released by activated T-cells into the microenvironment contribute to T-cell proliferation expanding these antigen specific T-cells (Lanzavecchia, Sallusto 2001).

4.1.3. Immune escape and the three Es

It is now well known that there are active interactions between tumours and the immune system, even in the GBM setting despite its perceived 'immune privileged' state. In the case of advanced late stage cancers such as grade IV glioblastoma multiforme these tumours have developed methods for escaping basal immune surveillance resulting in their increased growth and aggressiveness (Mittelbronn, Platten et al. 2011). In the cancer setting there are several stages leading to the immune escape of tumours, these are known as the three Es: elimination, equilibrium and escape. During the elimination phase tumour cells are actively targeted by the immune system and as a result there is eradication of tumour cells. This hypothesis is supported by data showing that the presence of tumour infiltrating lymphocytes within tumours are a positive prognostic factor. Despite the presence of a healthy immune system people still develop cancer, this suggests that there is an active response by cancer cells that enables some cells to evade the immune response and this eventually leads to the development of a tumour. After elimination of tumour cells by the immune system any cells that have survived immune surveillance are held in equilibrium by the immune system where the tumour cells can survive but they do not expand to produce an aggressive tumour mass. Many of these tumour cells may be eradicated, but new immune escape variants develop due to the highly adaptive nature of tumour cells. After continuous immune pressure, populations of immune-resistant tumour cells that have developed mechanisms to escape the immune system eventually start to grow, leading to the development of cancer (Dunn, G. P., Old et al. 2004). In the active immunotherapy setting tumours can also adapt to overcome the immune pressures put upon them, this has been seen in the GBM setting with patients immunised with Rindopepimut (a vaccine targeting the EGFRviii peptide expressed by GBM tumours). Patients vaccinated with Rindopepimut developed EGFRviii immune responses and slightly improved survival, however tumours eventually recurred, and the tumours that recurred no longer expressed the EGFRviii antigen. This is an indication that an immune escape variant has developed, with all EGFRviii expressing tumour cells being eradicated improving patient survival, equilibrium phase followed. Unfortunately by the emergence of a cell which managed to survive without the need of EGFRviii protein this immune escape variant was then free to expand resulting in the tumour recurrence (Sampson, Heimberger et al. 2010). In order to prevent such an immune escape multiple antigens need to be targeted. Not only can antigen-escape variants develop, cancer cells displaying an immune suppressive phenotype can expand and prevent immune responses

within the tumour mass. As a result, combinatorial therapies may be utilised to overcome development of a potentially more aggressive cancer.

4.1.4. Epitope dominance

The risk of targeting multiple antigens is the phenomenon of epitope dominance (Kedl, Kappler et al. 2003). Immunodominance can result in a selective immune response towards one antigen over the other one. The immunodominance of one epitope may prevent the development of responses to other antigenic antigens expressed by tumour cells. The ability of an antigen to become immunodominant appears to be due to its capability of generating a rapid response when compared to other antigens, therefore dominance is given to the antigen that seems to induce the first response. Research has shown that when a combination of five immunodominant epitopes are presented as a mixed antigen only two of the epitopes generate a dominant immune response, revealing that a hierarchy emerges when numerous dominant epitopes are encountered (Sandberg, Grufman et al. 1998). New hierarchies can also develop when an immunodominant antigen is lost by immune selection. As tumours progress, they acquire more mutations which can lead to the expression of an increased repertoire of immunogenic antigens. It has been found that a response to an antigen already present on a tumour will prevent responses to newly developed immunogenic antigens even if the new antigens that have developed generate a stronger response. This indicates that there is an innate priority to the first response (Schreiber, Wu et al. 2002). Tumours have been shown to evade immune regulation via loss of a single HLA molecule. This allows tumours to escape cytolysis by immunodominant CD8⁺ T-cells due to the immunodominant epitope not being presented. Uptake of antigenic material from these HLA-deficient immune-escape variants by dendritic cells still allows for presentation of antigenic material by the dendritic cells to the CD8⁺ T-cells maintaining this immunodominant phenotype, preventing T-cells from responding to new antigens the cancer has developed. One way to overcome immunodominance is to administer subdominant epitopes prior to immunodominant epitopes this will allow for the induction of new immunodominant CD8⁺ T-cell subtypes specific for previously weakly antigenic epitopes (Chen, W., McCluskey 2006).

4.1.5. ImmunoBody[®] vaccination

The ImmunoBody[®] vaccination (Scancell Ltd.) is a DNA plasmid vaccination that codes an IgG1 antibody that contains peptide targets of interest engrafted into the complementarity determining

regions (CDRs) (Metheringham, Pudney et al. 2009, Durrant, Parsons et al. 2001). The plasmid is administered and then the DNA is transcribed into mRNA and the resultant mRNA is then translated into the IgG1 protein. The IgG1 acts as a carrier for the immunogenic peptides of interest. IgG1 is ideal due to its long half-life and the ability of antigen presenting cells to interact with the IgG via the Fc region of the antibody. ImmunoBody® can work by two distinct methods: direct presentation and cross presentation. Direct presentation is when antigen presenting cells are transfected with the ImmunoBody® plasmid. These cells then process the DNA resulting in production of the encoded IgG. The immunoproteasome then breaks down the resultant IgG resulting in loading of the immunogenic peptides onto MHC class I and class II molecules where they are then presented to T-cells. Cross presentation is when 'bystander' cells are transfected. These cells then process the DNA leading to production of the encoded IgG. This IgG is then secreted by these cells where it is then taken up by antigen presenting cells via the Fc region of the IgG. Removal of the Fc region from the IgG results in a one thousand-fold reduction of T-cell activation, revealing that this cross presentation is vital for boosting the immune response (Metheringham, Pudney et al. 2009, Durrant, Parsons et al. 2001). The ImmunoBody® vaccine can be administered using intramuscular electroporation in humans, and pre-clinical experiments have administered the plasmid biolistically using a gene gun that utilises helium gas to shoot plasmid coated gold nanoparticles into the skin of test animals. Due to its preclinical efficacy a TRP-2/gp100 directed ImmunoBody® vaccination known as SCIB1 is being trialled in melanoma patients. In Phase I/II trial SCIB1 vaccination induced T-cell responses in 88% of patients treated, seven out of fifteen tumour bearing patients were shown to have stable disease and 100% patients with resected tumours remained alive at the conclusion of the study (median observation time of 37 months) (Patel, P. M., Ottensmeier et al. 2018).

4.1.6. The humanised HHDII/DR1 C57BL/6 mouse model

The HHDII/DR1 mouse is a transgenic mouse that allows for the study of human HLA-A2.1 and HLA-DR1 restricted peptide immune responses. This mouse strain was generated from a parental C57BL/6 mouse, the parental mice had H-2Db and β 2M knocked out (Pascolo, Bervas et al. 1997). The transgenic HHDII consists of a murine MHC class I alpha 3 chain and transmembrane domain connected to a human alpha 1 and alpha 2 chain. The human alpha 1 chain is covalently linked to a human beta 2 M subunit (see *Figure 26*) (Pascolo, Bervas et al. 1997). This transgenic HHDII mouse was then bred with a transgenic HLA-DR1 mouse to generate the HHDII/DR1 mouse. The HLA-DR1 transgenic mouse was generated via knockout of murine MHC class II ($I\text{A}\beta^{0/0}$) in C57BL/6 mice and knock in of a chimeric mouse/human HLA-DR1.

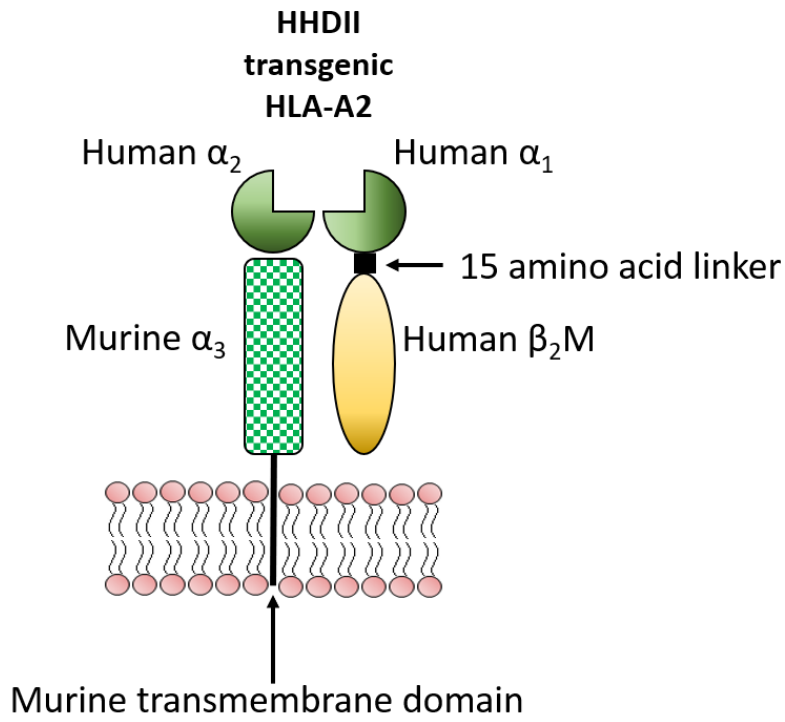


Figure 26. A diagram of the transgenic HHDII MHC class I molecule. The transmembrane and α_3 domain are of murine origin whereas the α_1 and α_2 domains are of human origin with the human β_2M being covalently linked to the α_1 domain.

This mouse model allows for the screening of candidate vaccines for use in humans without any interference from murine MHC meaning that translation from mouse to man should be more efficient.

4.2. Aims and hypothesis

After identifying suitable target antigens for therapy (as discussed in chapter 3), the next step was to target these with a therapeutic vaccine. For the reasons explained above ImmunoBody® was selected as the vaccination method for this study. To study the effects of the ImmunoBody® the humanised HHDII/DR1 mouse were used, in order for the study to indirectly assess what the human response would be like for HLA-A2 and HLA-DR1 positive individuals, providing a more translatable model for the study of immune responses. The response of immunised mice to the ImmunoBody® vaccination was measured using ELISpot and flow cytometry.

4.3. Results

4.3.1. ImmunoBody® vaccination generates a strong anti-TRP-2 and WT-1 immune response in the C57BL/6 HHDII/DR1 mouse

Mice were vaccinated as summarised in *Figure 27*, where day 0 mice were immunised with gold-coated ImmunoBody® plasmids (see methods in chapter 2.2.) using a helium air gun on the flank of the mice, followed by two booster doses administered seven days apart (on day 7 and 14 post prime). This vaccination schedule was chosen because it had previously been shown to be the most efficient at inducing a persistent peptide specific immune response (Metheringham, Pudney et al. 2009). On day twenty-one immunised (or naive) HHDII/DR1 mice were humanely culled and their spleen harvested. The splenocytes extracted from these mice were then used in an IFN γ ELISpot assay where TRP2 and/or WT1 peptides were used (see methods in chapter 2.2.). Wells containing cells only were used as controls while wells with cells receiving the super antigen staphylococcal enterotoxin B (SEB) were used as positive controls, all conditions were performed in triplicate and each experiment contained three mice per group. SEB is a bacterial antigen known to generate IFN γ release from immune cells without prior exposure.

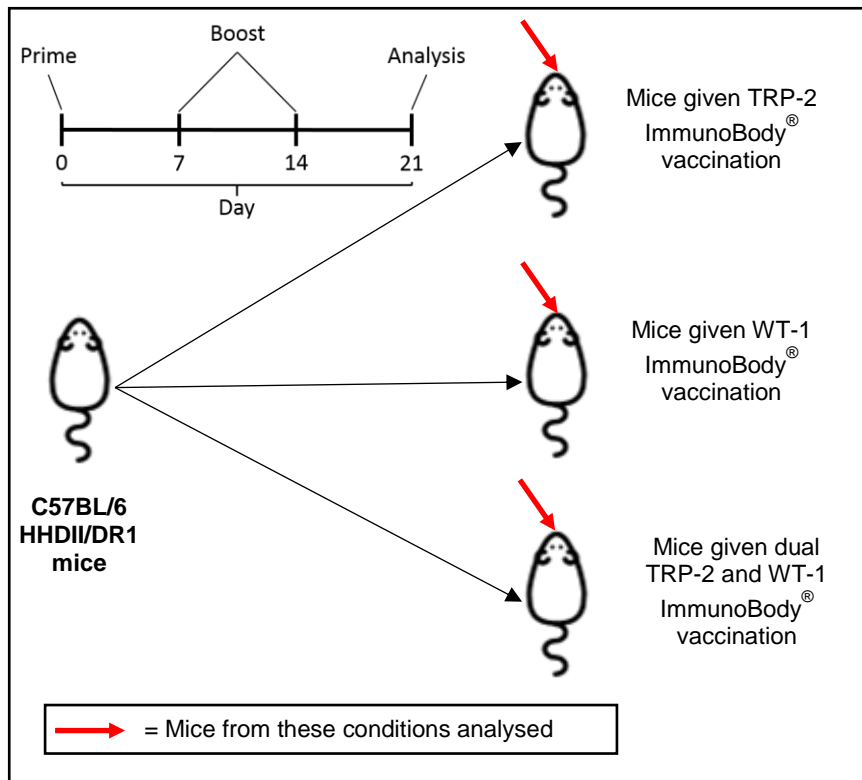


Figure 27. The vaccination schedule utilised to study the immunogenicity of the ImmunoBody[®] vaccine. The top left area of the figure details the days that mice were dosed, with vaccines administered at weekly intervals. Mice were split into three groups; one receiving SCIB1 (TRP-2) ImmunoBody[®], one receiving WT-1 ImmunoBody[®] and one receiving both SCIB1 (TRP-2) and WT-1 ImmunoBody[®].

Peptide	Sequence	Human HLA-specificity	SYFPEITHI score
WT-1	ALLPAVPSL	A2	33
WT-1	DLNALLPAV	A2	27
WT-1	VRDLNALLPAVPSLG	DR1	31
TRP-2	SVYDFFVWL	A2	21
gp100	AMLGHTMEV	A2	26
gp100	GTGRAMLGHTMEVT	DR1	24
gp100	QLYPEWTEA	A2	19
gp100	NRQLYPEWTEAQRD	DR1	14

Table 18. A list of the peptides used to stimulate splenocytes *ex vivo*. *In silico* analysis was performed using SYFPEITHI, a data base that provides predicted MHC binding scores. The higher the score the stronger the binding of the peptide with the HLA molecule, and therefore the more likely this peptide is to be presented via MHC molecules.

Mice immunised with either SCIB1 or WT1-ImmunoBody® generated vaccine and peptide specific-responses with the exception of gp100 where no significant gp100 specific immune response could be detected after the co-culture of splenocytes derived from SCIB1 vaccinated with gp100 peptides (see Figure 28). However, since tumour tissues analysed previously appeared not to express the gp100 protein this will not impact on the efficacy of the proposed vaccine combination.

The WT-1 ImmunoBody® generated a strong response to the full 15mer class II sequence encoded within the ImmunoBody® construct. Two of the HLA-A2 specific sequences within the 15mer peptide were also used to stimulate the splenocytes from WT-1 ImmunoBody® vaccinated mice. The two sequences used were: ALLPAVPSL and DLNALLPAV, of the two sequences ALLPAVPSL generated a strong IFN γ response from the splenocytes of WT-1 ImmunoBody® vaccinated mice (see Figure 29). The DLNALLPAV peptide sequence did generate an IFN γ response from vaccinated splenocytes however this was at a much lower level than the ALLPAVPSL sequence and the response was deemed non-significant (see Figure 29). When looking to the *in silico* SYFPEITHI HLA-A2 binding scores the ALLPAVPSL sequence has a higher binding score than the DLNALLPAV sequence which can explain the dominance of the ALLPAVPSL sequence observed.

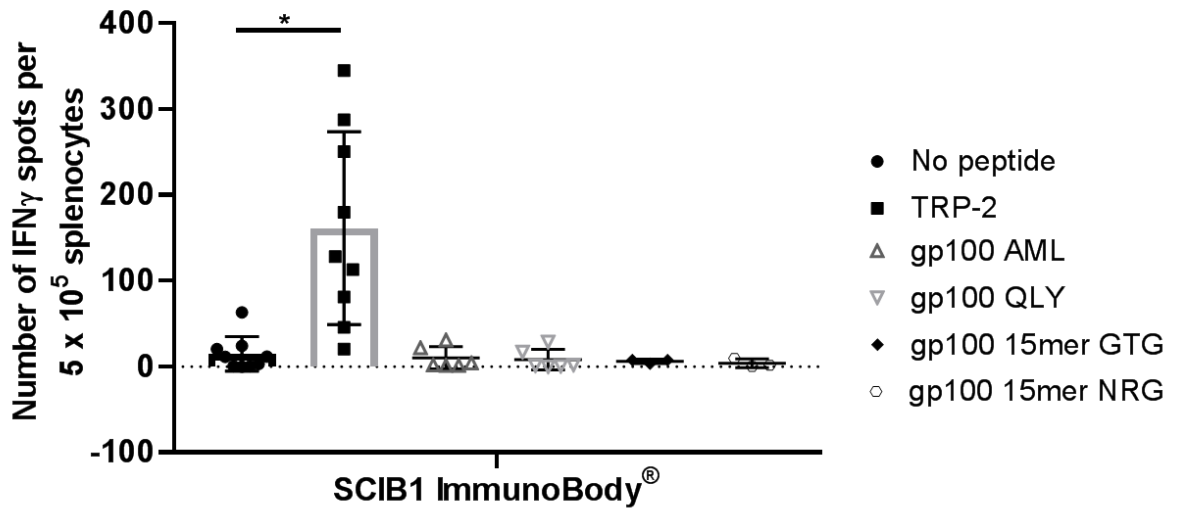


Figure 28. IFN γ ELISpot results from splenocytes from SCIB1 ImmunoBody[®] vaccinated mice. N= 9-3, *= $P \leq 0.05$ as defined by a two-way ANOVA followed by Tukey's post hoc test. The three letter annotations after the peptide correspond to the first three amino acids of the peptide used to stimulate the splenocytes, the full sequences of these peptides are detailed in the methods (chapter 2).

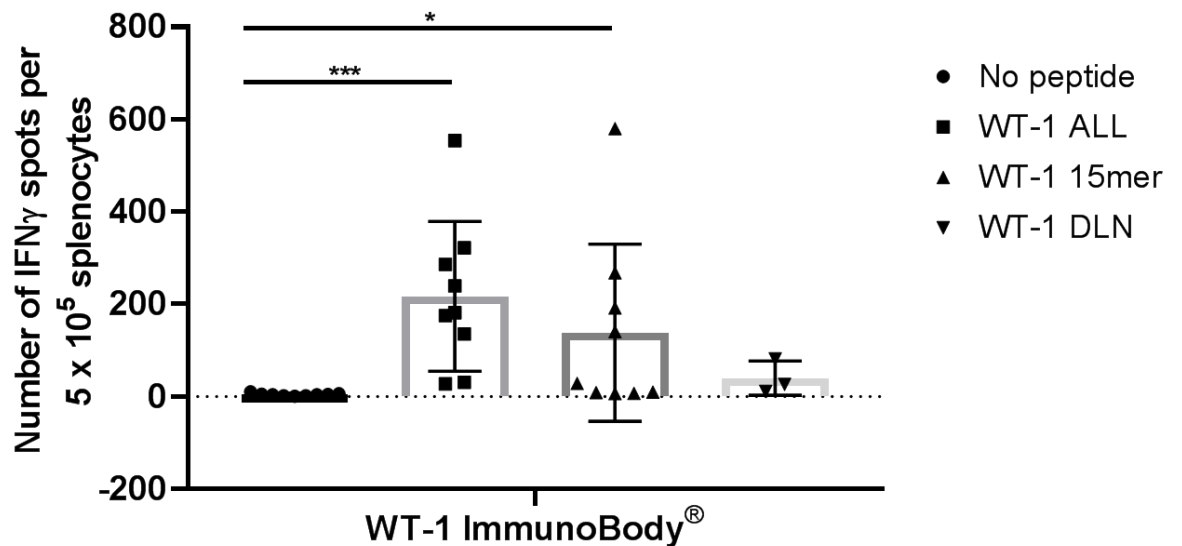


Figure 29. IFN γ ELISpot results from splenocytes from WT-1 ImmunoBody[®] vaccinated mice. N= 9-3, *= $P \leq 0.05$, ***= $P \leq 0.001$ as defined by a two-way ANOVA followed by Tukey's post hoc test. The three letter annotations after the peptide correspond to the first three amino acids of the peptide used to stimulate the splenocytes, the full sequences of these peptides are detailed in the methods (chapter 2).

The aim of this study is to use both vaccines together, the next sets of experiments compared the IFN γ responses after mice were immunised with either SCIB1, WT1-ImmunoBody® or both.

This is particularly important because it allows for a broader range of patients to be treated and it acts to eradicate as much of the heterogeneous tumour population as possible whilst overcoming the possibility of antigen escape variants developing. When the two vaccines are administered together there is a significant response to both the WT-1 and TRP-2 peptides as was the case when the two vaccines were given individually. What is even more important is that there is no significant difference in the response between the dual and both single vaccines.

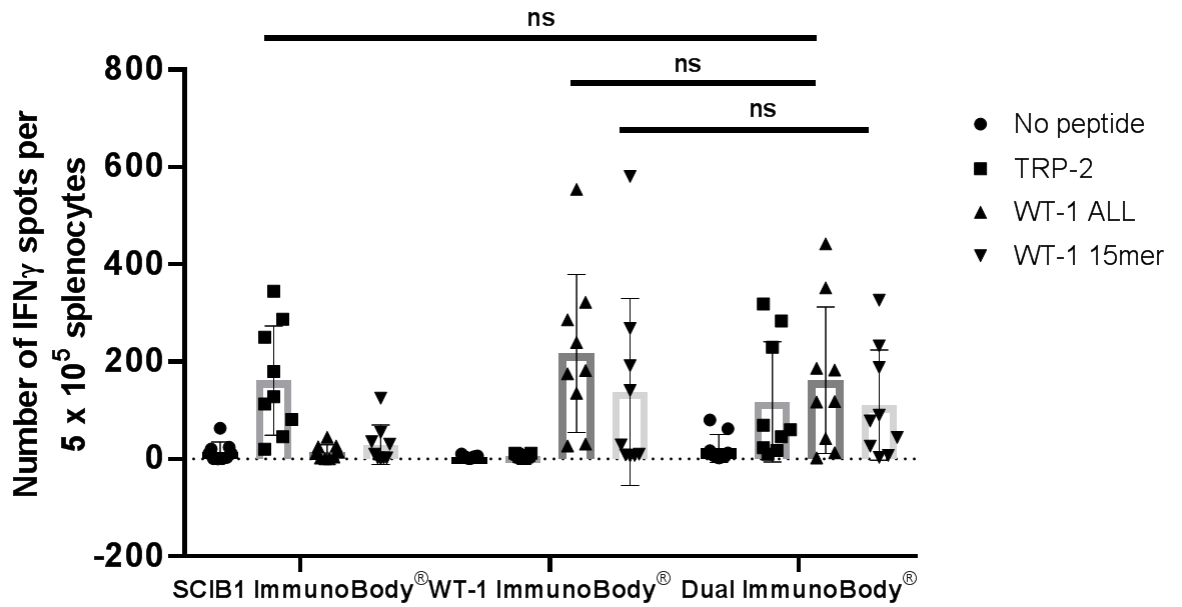


Figure 30. IFN γ ELISpot results from splenocytes from SCIB1 and WT-1 ImmunoBody[®] vaccinated mice compared with mice vaccinated with both SCIB1 and WT-1 ImmunoBody[®] simultaneously. $N=9$, $ns=$ not significant as deemed by a two-way ANOVA followed by Tukey's post hoc test. The three letter annotations after the peptide correspond to the first three amino acids of the peptide used to stimulate the splenocytes, the full sequences of these peptides are detailed in the methods (chapter 2).

Due to the frequency of the IFN γ response being equivalent in both the singly and dually vaccinated mice, it is also important to see if the avidity of these responses is equivalent. In order to do this a peptide titration of the WT-1 and TRP-2 HLA-A2 specific peptides was performed to measure the avidity of the immune response of splenocytes from singly and dually vaccinated mice.

Peptide titration revealed that when both ImmunoBody[®] vaccines were given together the avidity of the response to the TRP2 HLA-A2 specific peptide was equivalent with no significant difference being found between the two peptide dose response curves. Nonlinear regression analysis found no significant difference between the EC50 of the TRP-2 peptide for both the dually and singly vaccinated splenocytes. The WT-1 peptide titration also reveals the same results with no significant difference being found between the EC50 for both the singly and dually vaccinated splenocytes.

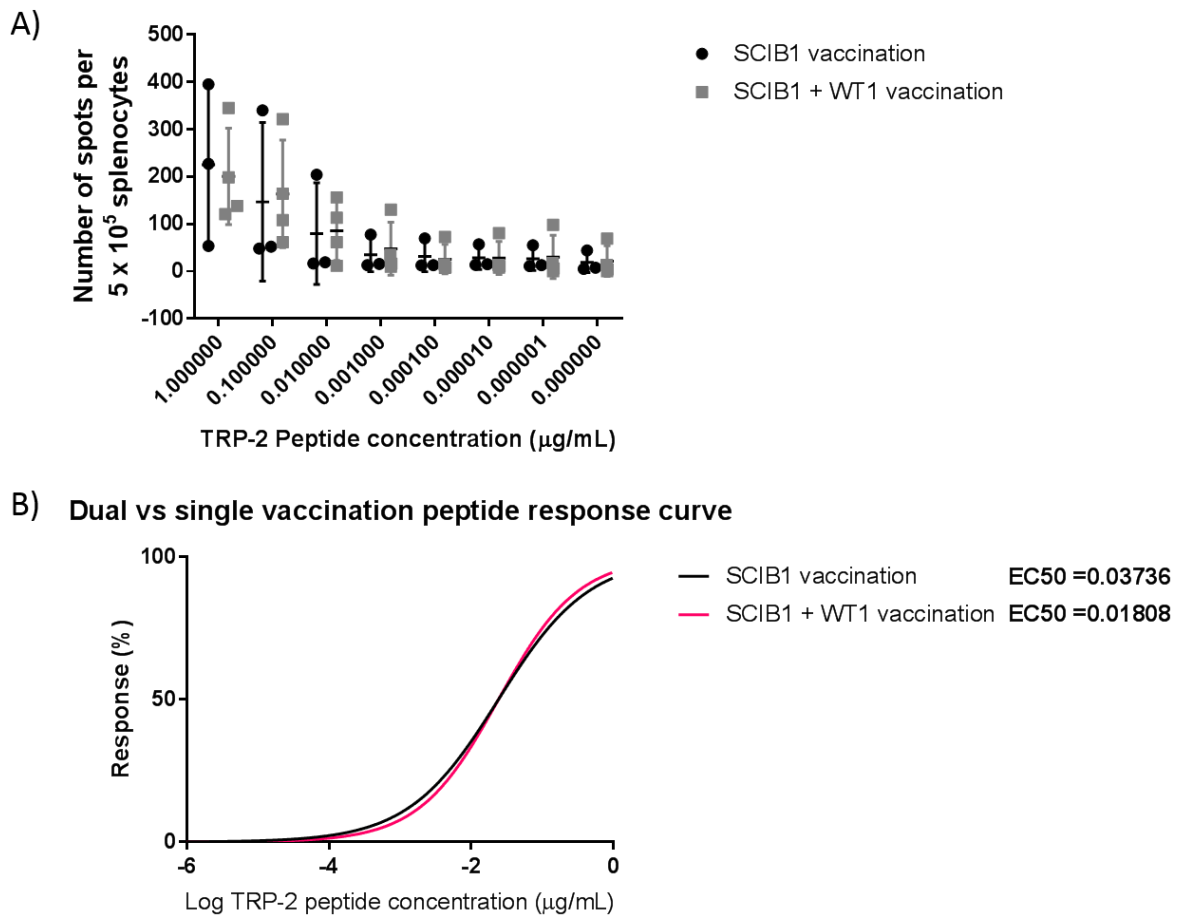


Figure 31. *IFN γ ELISpot results from splenocytes from SCIB1 ImmunoBody[®] vaccinated mice compared with mice vaccinated with both SCIB1 and WT-1 ImmunoBody[®] simultaneously. A) Splenocytes were treated with the SVYDFVWL TRP-2 peptide sequence diluted in 10-fold increments from 1 $\mu\text{g/mL}$ - 0.0000001 $\mu\text{g/mL}$. B) Data was normalised and transformed, and non-linear fit comparisons were made, these analyses revealed that there was no significant difference between the EC_{50} of SCIB1 and dual vaccinated mice.*

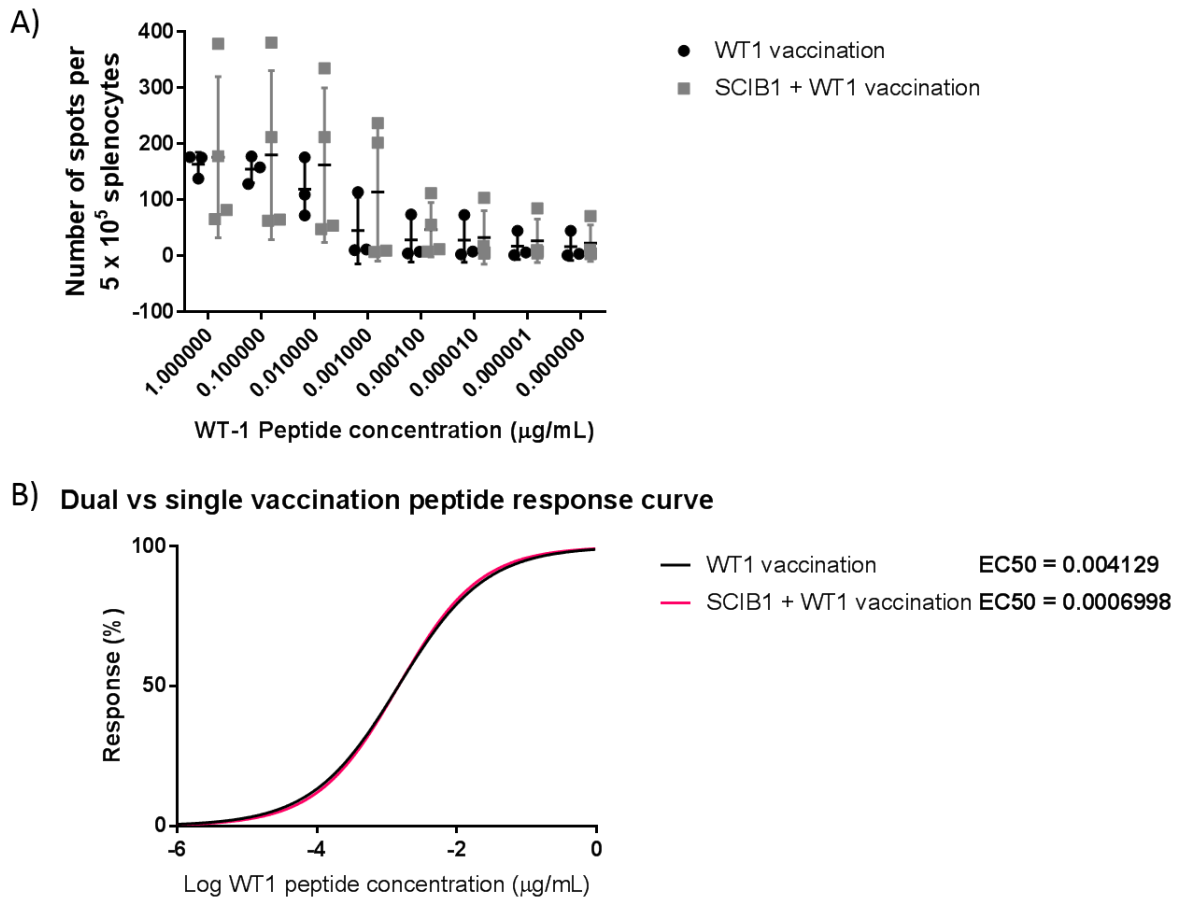
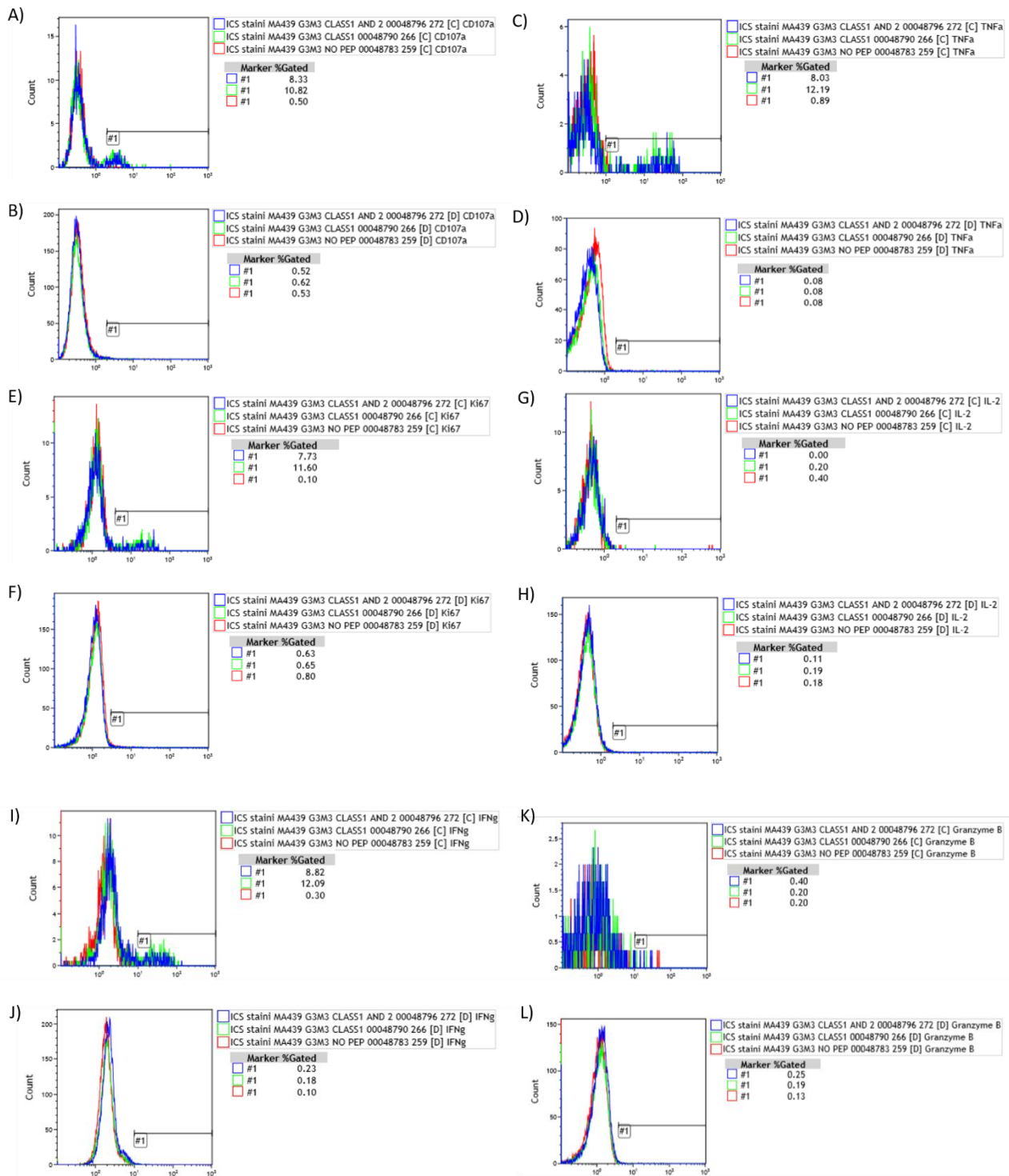


Figure 32. $IFN\gamma$ ELISpot results from splenocytes from WT-1 ImmunoBody[®] vaccinated mice compared with mice vaccinated with both SCIB1 and WT-1 ImmunoBody[®] simultaneously. A) Splenocytes were treated with the ALLPAVPSL WT-1 peptide sequence diluted in 10-fold increments from 1 $\mu\text{g/mL}$ - 0.0000001 $\mu\text{g/mL}$. B) Data was normalised and transformed, and non-linear fit comparisons were made, these analyses revealed that there was no significant difference between the EC_{50} of WT-1 and dual vaccinated mice.

4.3.2. Flow cytometric analysis of the ImmunoBody® activated immune cells reveals that ImmunoBody® vaccination generates a strong CD8⁺ T-cell response

Flow cytometry was utilised to study the lymphocytes from vaccinated animals. The splenocytes from these animals were stimulated *in vitro* and then surface staining was used to differentiate between CD3, CD4⁺ and CD3, CD8⁺ T-cell populations. Once these two populations were identified their expression of immune activating ligands and cytokines was stained for allowing for the immune response of vaccinated and unvaccinated splenocytes to immunologic peptides to be measured.



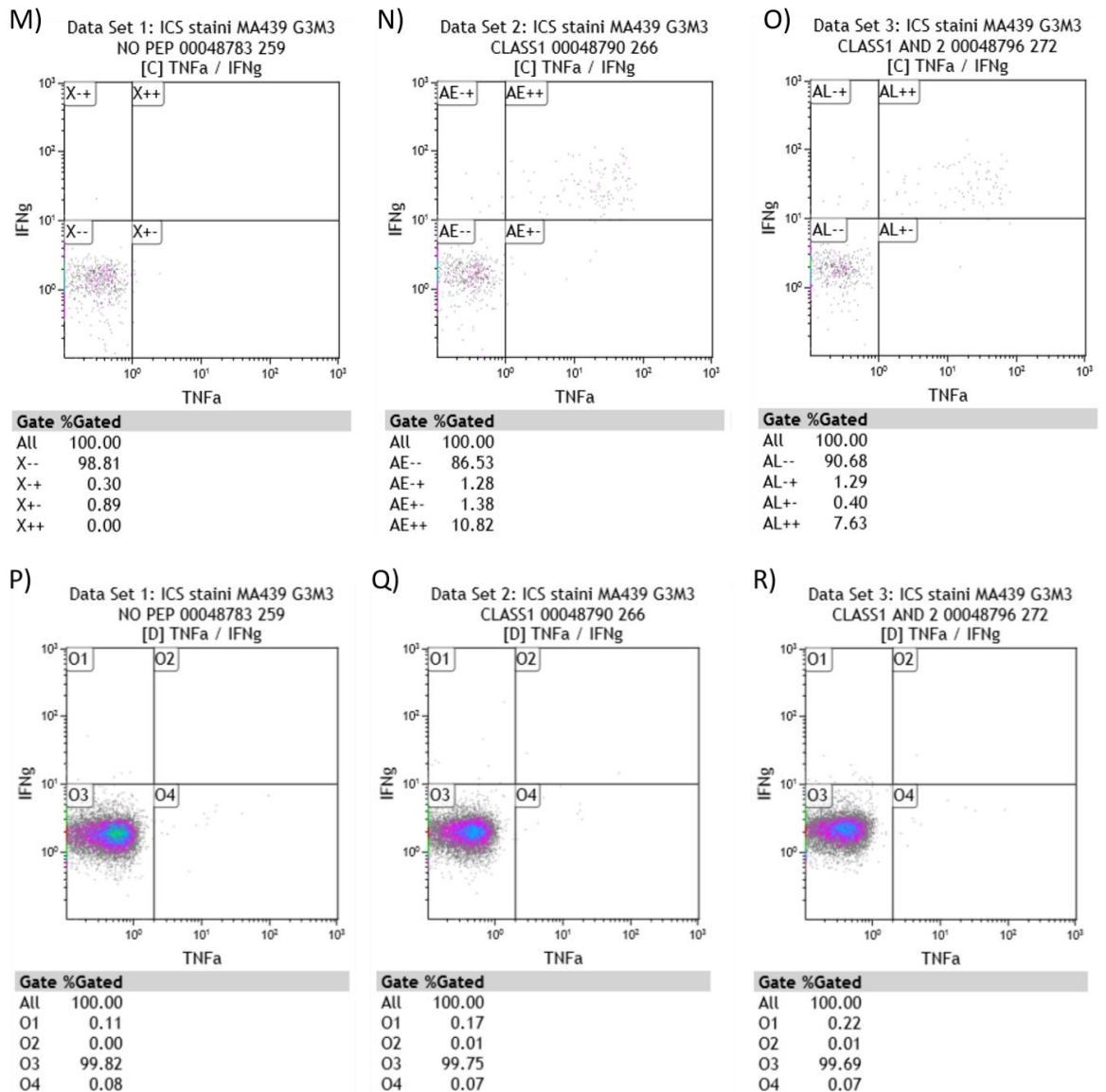


Figure 33. A representative set of flow cytometry plots of splenocytes isolated from vaccinated mice after peptide stimulation. These plots are from a mouse that received dual vaccination. The gating strategy can be seen in the methods sections (Chapter 2). All these plots are from CD3 positive live cells. A) Histogram of the CD8⁺ CD107⁺ cells. B) Histogram of the CD4⁺ CD107⁺ cells. C) Histogram of the CD8⁺ TNFα⁺ cells. D) Histogram of the CD4⁺ TNFα⁺ cells. E) Histogram of the CD8⁺ Ki67⁺ cells. F) Histogram of the CD4⁺ Ki67⁺ cells. G) Histogram of the CD8⁺ IL-2⁺ cells. H) Histogram of the CD4⁺ IL-2⁺ cells. I) Histogram of the CD8⁺ IFNγ⁺ cells. J) Histogram of the CD4⁺ IFNγ⁺ cells. K) Histogram of the CD8⁺ Granzyme B⁺ cells. L) Histogram of the CD4⁺ Granzyme B⁺ cells. Plots M-O show scatter plots of the CD8⁺ cells stained with TNFα (on the x axis) and IFNγ (on the y axis). Double positive cells are in the top right quadrant. M) Splenocytes receiving no peptide stimulation. N) Splenocytes receiving class I peptide stimulation. O) Splenocytes receiving class I and class II peptide stimulation. Plots P-R show scatter plots of the CD4⁺ cells stained with TNFα (on the x axis) and IFNγ (on the y

axis). Double positive cells are in the top right quadrant. P) Splenocytes receiving no peptide stimulation. Q) Splenocytes receiving class I peptide stimulation. R) Splenocytes receiving class I and class II peptide stimulation. For plots A-L the blue peak represents splenocytes stimulated with both class I and II peptides, the green peak represents splenocytes stimulated with class I peptides only and the red peak represents splenocytes that received no peptide stimulation. The gate used to determine the percentage of positive cells is shown on each histogram and the percentage of positive cells gated is shown next to the histogram.

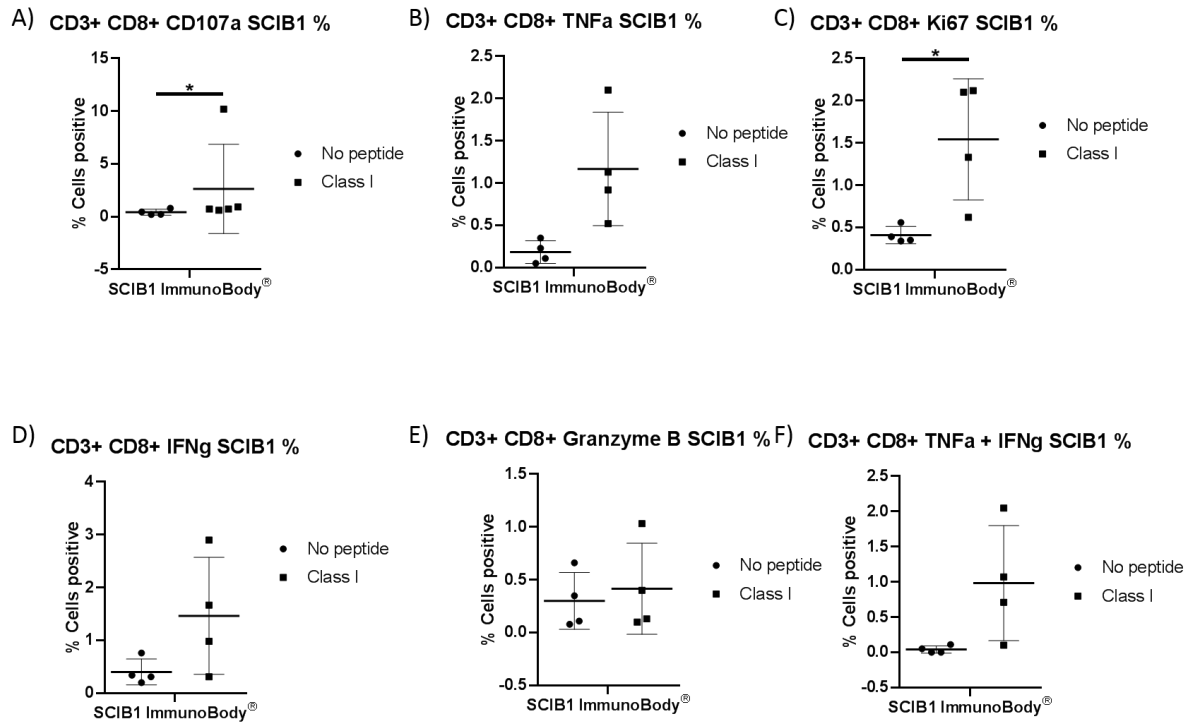


Figure 34. Flow cytometric analysis of CD3⁺ CD8⁺ splenocytes from SCIB1 ImmunoBody[®] vaccinated mice that were either unstimulated (no peptide) or stimulated with TRP-2 class I (SVYDFVWL) peptide. A) % CD107⁺ CD8 T cells. B) % TNFα⁺ CD8 T cells. C) % Ki67⁺ CD8 T cells. D) % IFNγ⁺ CD8 T cells. E) % Granzyme B⁺ CD8 T cells. F) % TNFα⁺ and IFNγ⁺ CD8 T cells. N = 4, * = p ≤ 0.05 as deemed by a paired T-test.

When studying the CD8⁺ T-cells from SCIB1 ImmunoBody[®] vaccinated mice there was a significant increase in the percentage of cells that stained positive for CD107a when these cells were stimulated with class I peptide. There is also a slight increase in the percentage of granzyme B positive cells. This increase of CD107a and granzyme B indicates an increase of the cytolytic activity of these CD8⁺ T-cells. These cells also increase their expression of the immune stimulating cytokines TNF α and IFN γ , promoting an inflammatory anti-tumour microenvironment. Finally, the increase in marker of proliferation Ki67 expressing cells also indicates that there is an antigen-specific increase in proliferation of CD8⁺ T-cells when vaccinated splenocytes are stimulated with peptide. Taken together these changes indicate that the SCIB1 ImmunoBody[®] vaccination generates a SCIB1 specific immune response from HHDII/DR1 mice and there appears to be an immunological memory directed towards the TRP-2 antigen encoded within the ImmunoBody[®] plasmid.

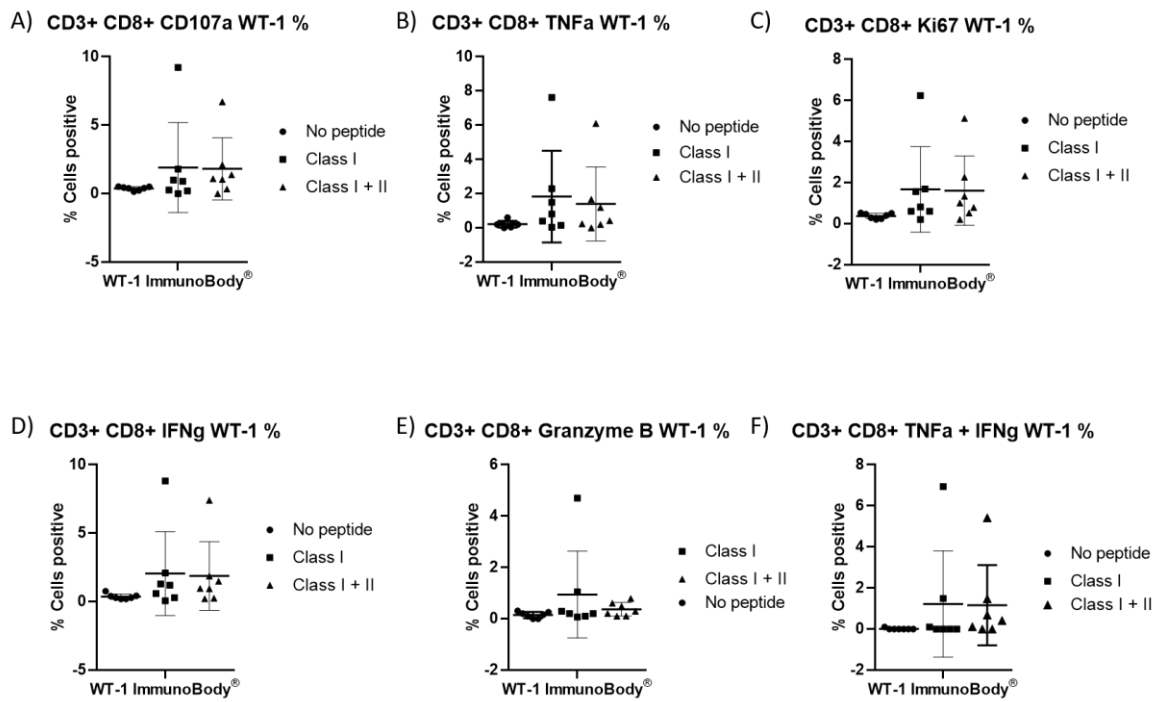


Figure 35. Flow cytometric analysis of CD3+ CD8+ splenocytes from WT-1 ImmunoBody® vaccinated mice that were either unstimulated (no peptide), stimulated with WT-1 class I (ALLPAVPSL) peptide or stimulated with both class I (ALLPAVPSL) and class II (VRDLNALLPAVPSLG) peptides. A) % CD107⁺ CD8 T cells. B) % TNFα⁺ CD8 T cells. C) % Ki67⁺ CD8 T cells. D) % IFNγ⁺ CD8 T cells. E) % Granzyme B⁺ CD8 T cells. F) % TNFα⁺ and IFNγ⁺ CD8 T cells. N = 7, all results were deemed non-significant by a one-way ANOVA followed by Tukey's post-hoc test.

When stimulated with class I peptides there is a slight increase in the percentage of CD107a, TNF α , Ki67 and IFN γ positive cytotoxic T-cells from WT-1 ImmunoBody[®] vaccinated mice when stimulated *in vitro*. These cells increase their expression of the immune stimulating cytokines TNF α and IFN γ , promoting an inflammatory anti-tumour microenvironment. Finally, the increase in Ki67 expressing cells also indicates that there is an antigen-specific increase in proliferation of CD8⁺ T-cells. This trend is also the same for splenocytes exposed to both class I and II peptides. Unfortunately, these results are non-significant, but they do indicate there is some antigen specific immune cell responses.

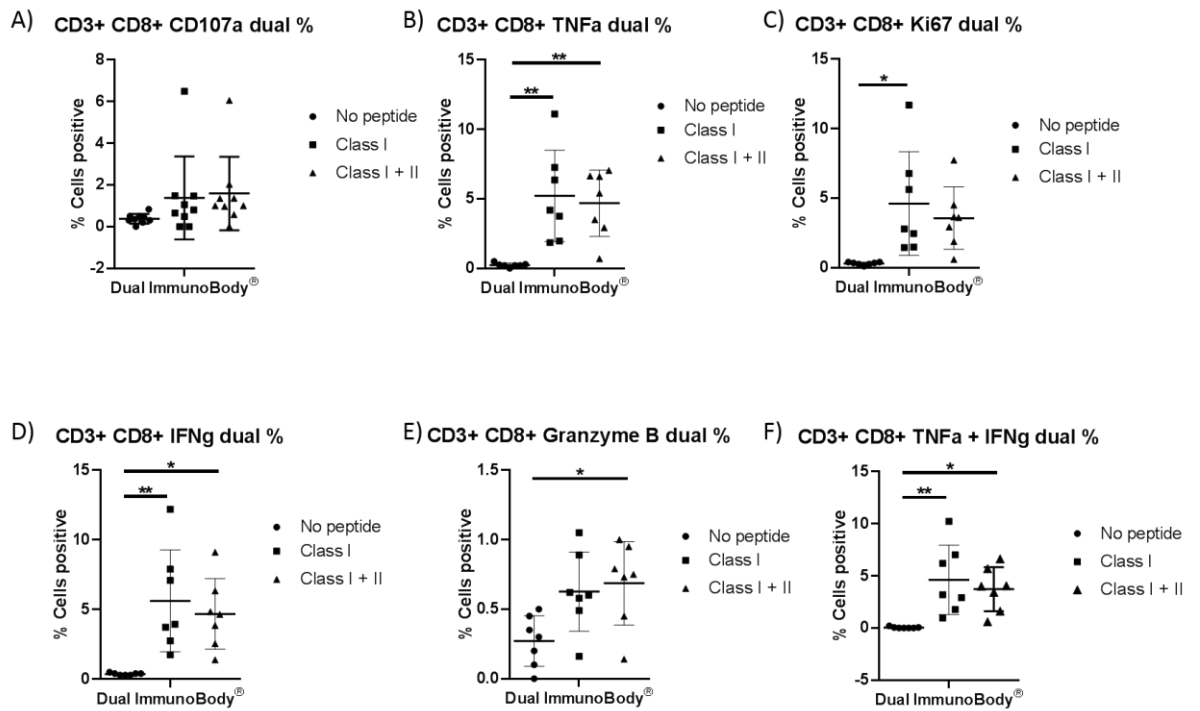


Figure 36. Flow cytometric analysis of CD3+ CD8+ splenocytes from dual SCIB1 and WT-1 ImmunoBody® vaccinated mice that were either unstimulated (no peptide), stimulated with TRP-2 and WT-1 class I peptides or stimulated with both class I (TRP-2 and WT-1) and WT-1 class II peptides. A) % CD107⁺ CD8 T cells. B) % TNF α ⁺ CD8 T cells. C) % Ki67⁺ CD8 T cells. D) % IFN γ ⁺ CD8 T cells. E) % Granzyme B⁺ CD8 T cells. F) % TNF α ⁺ and IFN γ ⁺ CD8 T cells. N = 7, * = P \leq 0.05 as deemed by a one-way ANOVA followed by Tukey's post-hoc test.

Dual vaccination with both the WT-1 and SCIB ImmunoBodies® appears to generate a stronger cytokine response to antigenic peptide stimulation than when the vaccines were administered alone. Peptide stimulation of dually vaccinated splenocytes leads to a significant increase in the percentage of TNF α and IFN γ positive CD8⁺ T-cells (as well as double positive TNF α and IFN γ cells). These responses are indicative of immune recognition of the target antigens and generation of immunological memory. The stimulation of these CD8⁺ T-cells also leads to increased proliferation of these cells (indicated by Ki67) further highlighting the presence of immune memory and an active anti-antigen immune response. There is also evidence of an increase in the percentage of granzyme B positive cells after *in vitro* stimulation. This would translate to increased lytic activity of these cells *in vivo*, indicating that these cells are capable of killing antigen expressing target cells.

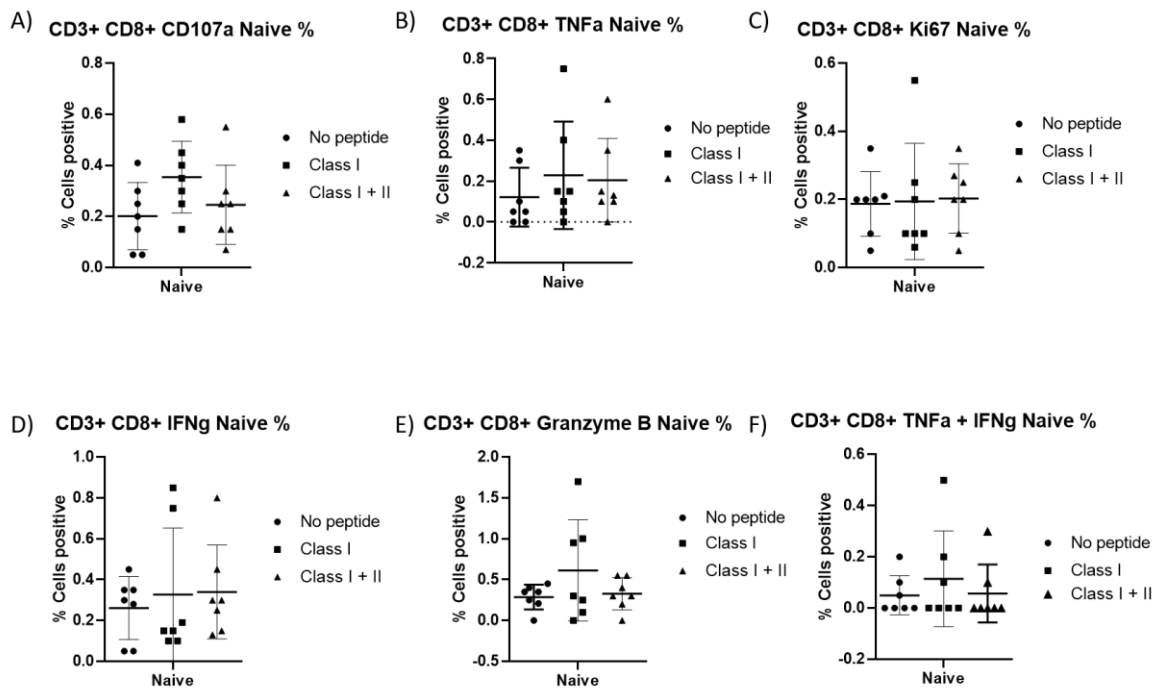


Figure 37. Flow cytometric analysis of CD3+ CD8+ splenocytes from naive mice that were either unstimulated (no peptide), stimulated with TRP-2 and WT-1 class I peptides or stimulated with both class I and WT-1 class II peptides. A) % CD107⁺ CD8 T cells. B) % TNFα⁺ CD8 T cells. C) % Ki67⁺ CD8 T cells. D) % IFNγ⁺ CD8 T cells. E) % Granzyme B⁺ CD8 T cells. F) % TNFα⁺ and IFNγ⁺ CD8 T cells. N = 7, all results are non-significant as deemed by a one-way ANOVA followed by Tukey's post-hoc test.

In order to see if the CD8⁺ T-cell responses observed were due to immunological memory generated by vaccination, naive splenocytes were extracted and stimulated *in vitro* and stained in the same manner as the splenocytes from vaccinated mice. Flow cytometric analysis revealed that there were no significant changes in the expression of any immune activating cytokines. These data confirm that the changes observed in vaccinated mice are due to immunological memory.

The CD4⁺ T-cell population was also studied in these mice and their response to class I and class II peptide stimulation was measured. The *in vitro* stimulation of these CD3⁺, CD4⁺ cells revealed that there were no changes observed in antigen expression profile of the CD4⁺ T-cell population (data not shown).

4.3.3. Splenocytes from ImmunoBody[®] vaccinated mice recognise GBM cell lines expressing TRP-2 and WT-1 in an HLA-A2 restricted manner

Data from chapter 3 revealed that the human GBM cell lines SF-188 and SEBTA-027 express the TRP-2 and WT-1 antigens. What is of even more importance is that the SF-188 cell line is HLA-A2 positive and the SEBTA-027 cell line is HLA-A2 negative. As a result, splenocytes from vaccinated mice were incubated with either SF-188 or SEBTA-027 in a 10:1 effector: target ratio and the IFN γ response was measured using ELISpot (see *Figure 38*).

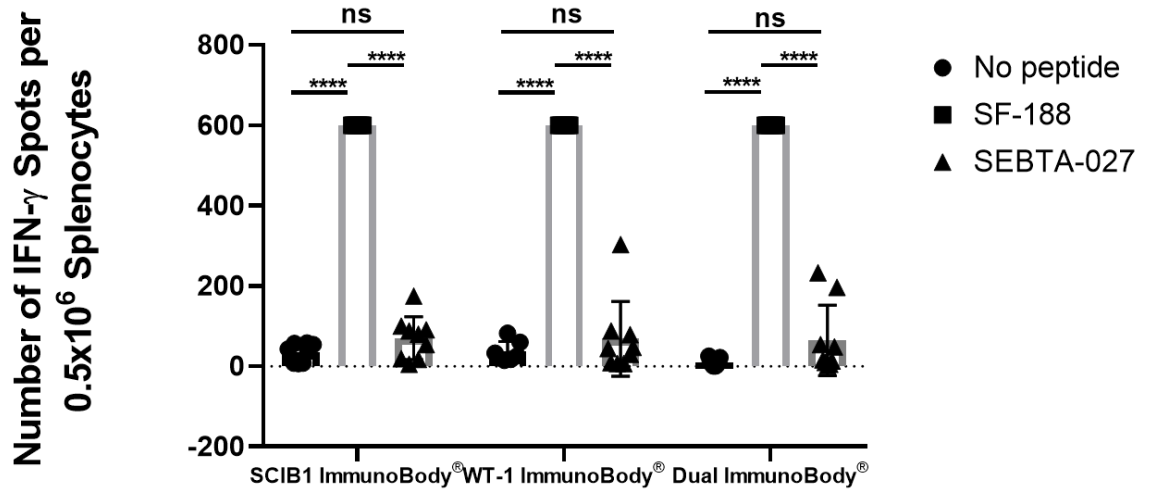


Figure 38. IFN γ ELISpot results from splenocytes from SCIB1 and WT-1 ImmunoBody[®] vaccinated mice compared with mice vaccinated with both SCIB1 and WT-1 ImmunoBody[®] simultaneously when exposed to the human GBM cell lines SF-188 and SEBTA-027. When splenocytes were co-cultured with the SEBTA-027 cell line they produced a number of spots above the maximum detectable limit, as a result these results were counted as 600 (the maximum number the machine can count). $N=9$, ****= $P \leq 0.0001$, ns= not significant as deemed by a two-way ANOVA followed by Tukey's post hoc test.

When splenocytes from SCIB1, WT-1 and dual ImmunoBody® mice are co-incubated with SF-188 cells there is a strong IFN γ response. All three vaccination conditions induce a maximal response when assessed via IFN γ ELISpot. What is even more important is that this response is significantly greater than the response to the SEBTA-027 cell line. No significant difference in response to SEBTA-027 cells is observed in any of these conditions (when compared to unstimulated no peptide splenocytes). This strong response to the SF-188 cell line when compared to the SEBTA-027 cell line helps highlight that the ImmunoBody® vaccination generates an HLA-A2 specific response. Due to the SF-188 cell line being HLA-A2 positive it should present the same peptide sequences as those encoded by the ImmunoBody® vaccines utilised, therefore it should generate a strong anti-SF-188 response due to the immunised CD8⁺ T-cells recognising the same peptides as those presented on the surface of SF-188. Since the SEBTA-027 cell line is not HLA-A2 positive it does not present the same peptide sequences as those encoded within the ImmunoBody® vaccines utilised. This is apparent with the SEBTA-027 cell line failing to generate a significantly stronger IFN γ response from vaccinated splenocytes than when these splenocytes are incubated with no peptide.

4.4. Discussion

The ImmunoBody® plasmid vaccination is an effective method for generating antigen specific responses without the need for immune adjuvants. These analyses reveal that the SCIB1 ImmunoBody® generates a strong TRP-2 directed response, unfortunately the SCIB1 ImmunoBody® failed to generate a strong response to the gp100 peptides encoded within the construct. There is a lack of response to the gp100 peptide sequences reveals that the TRP-2 epitope encoded generates an immunodominant response that appears to override the gp100 directed immune responses. The WT-1 ImmunoBody® also appeared to generate a strong WT-1 directed immune response. The future aim is to utilise both the SCIB1 and WT-1 ImmunoBody® vaccines in tandem to try and treat GBM; as a result, it was of great interest to see if there was immunodominance between these two antigens when the two vaccines are given at the same time. Fortunately, there appeared to be no immunodominance to either WT-1 or TRP-2 when both vaccines were given together, splenocytes stimulated with WT-1 and TRP-2 class I peptides generated an equivalent immune response as the singly vaccinated mice. Both the frequency and the avidity of the immune response was equivalent between both singly and dually vaccinated mice. What is also of great importance is that the splenocytes from HHDII/DR1 ImmunoBody® vaccinated mice showed a clear anti-GBM cell line response, specific for the HLA-A2 positive GBM cell line SF-188. These results provide great promise for the use of the SCIB1 and WT-1 ImmunoBody® vaccinations for HLA-A2 positive patients and this highlights the importance of the HHDII/DR1 mouse model for the research of human vaccines. Both singly and dually vaccinated mice generated a strong SF-188 response that

was equivalent between both the single and dual vaccinated groups. These preliminary results reveal that this dual vaccination combination is enough to generate GBM antigen-specific immune cell responses as a result this dual method of vaccination will be taken forward and tested in animal models of GBM.

Flow cytometric analysis reveals that ImmunoBody® vaccination results in an increase in the number of cytotoxic CD8⁺ T-cells compared to unvaccinated mice. There is also an increase in CD8⁺ T-cell proliferation when these cells are exposed to their peptide targets, indicating an antigen-specific CD8⁺ T-cell expansion and providing proof of an antigen-specific CD8⁺ T-cell response and the presence of CD8⁺ memory T-cells. There also appears to be a clear CD8⁺ antigen-specific response with an increase in the percentage of CD8 T-cells positive for the cytokines IFN γ and TNF α in ImmunoBody® vaccinated mice when stimulated with the target peptides. TNF α is a pro-inflammatory cytokine with potential anti-cancer effects. TNF α can mediate cancer cell death via a variety of mechanisms; this can either be by direct binding to cell-surface receptors, blocking of regulatory T-cell activity, attracting neutrophils and monocytes to tumour sites and switching of tumour associated macrophages to the immune stimulating M1 phenotype (Josephs, Ichim et al. 2018). IFN γ and TNF α have previously been shown to be essential for CD8 anti-tumour activity. When CD8⁺ tumour infiltrating lymphocytes are adoptively transferred into tumour bearing mice they induce tumour regression. This even occurs when non-lytic clones are transferred into tumour bearing mice. This regression was shown to be due to the secretion of IFN γ and TNF α in response to the presence of tumour. Blockade of IFN γ or TNF α with antibodies inhibits the anti-tumour effects of these CD8⁺ TILs *in vivo* (Barth, Mule et al. 1991). These results highlight the importance of these IFN γ and TNF α positive CD8⁺ T-cells in mounting an effective anti-tumour response. It is important to note that IFN γ also has a similar immune activating and dampening effect. IFN γ can itself have anti-cancer effects and as a result IFN γ itself has been used as an anti-cancer agent. IFN γ has an anti-proliferative effect on GBM cells and induces apoptosis via activation of STAT-1 and caspases. IFN γ can also lead to the up-regulation of MHC molecules on the surface of tumour cells increasing their immune recognition, however immune-inhibitory markers such as PD-L1 are also upregulated (Kane, Yang 2010). This expression of both IL-2 and IFN γ indicates an active immune response to the antigenic targets encoded within the ImmunoBody® vaccine. These flow cytometric results indicate that there is a memory response with an increase in cytokine secreting T-cells in response to antigen exposure after ImmunoBody® vaccination.

What is of great importance is the ability of the ImmunoBody® vaccination to generate both a CD8⁺ cytotoxic and a CD4⁺ helper T-cell response. This activation of both T-cell subsets is pivotal for a durable anti-tumour response. Immune responses have previously been generated in mice using GM-CSF transfected irradiated B16 melanoma cells injected into the flank, mice were then

challenged with normal B16 cells and their responses monitored (Hung, Hayashi et al. 1998). CD4 knockout mice did not appear to mount an anti-tumour response and died after a similar amount of time as mice that did not receive vaccination with B16-GM-CSF. Interestingly CD8 knockout mice managed to mount an anti-tumour response with around 40% of mice surviving long term, in comparison 70% of wild-type mice displayed long term survival following tumour challenge (Hung, Hayashi et al. 1998). These results overturn the previously held dogma that CD8⁺ T-cells are responsible for tumour rejection. Th1 and Th2 CD4⁺ T-helper cells appear to be required for tumour rejection as evidenced by the presence of IFN γ (Th1) and IL-4 (Th2) at the tumour challenge site in CD4 competent mice. These cytokines were absent in the CD4 null mice. Knockout of either IFN γ or IL-4 impaired the tumour protection granted to mice provided by the B16-GM-CSF vaccination (Hung, Hayashi et al. 1998). Th1 and Th2 cells can both initiate CTL immune responses, via cell-surface molecules or secretion of cytokines. Th cells themselves can also induce tumour cell death via the binding of Fas ligand on their surface to the Fas receptor on tumour cells. Interferon gamma release by Th1 cells has been shown to activate tumour macrophages resulting in increased super- and nitric-oxide production necessary for tumour cell killing (Knutson, Disis 2005). Th2 cells can also activate eosinophils that help to eradicate tumour cells. These findings suggest that CD4⁺ cells do not just function within the adaptive immune system, they also exert their effects on the innate immune system to boost anti-tumour immunity. Th1 cells secrete IFN γ and this activates the immunoproteasome improving antigen presentation by antigen presenting cells. This improved antigen presentation can result in the promotion of subdominant antigens improving tumour recognition and preventing the development on antigen escape variants (Knutson, Disis 2005).

Previous immunotherapeutic approaches for GBM have provided lacklustre results with many vaccine therapies failing at phase III clinical trials. As a result combinatorial immunotherapy is being heralded as the future of GBM immunotherapy. In order to fully gain the benefits from the anti-tumour immune response generated by immunotherapy several other types of therapy can be combined with active immunotherapy to boost the response. Traditionally chemotherapy has been considered immunosuppressive with leukopenia being a common side effect of temozolomide chemotherapy. It is believed however that chemotherapy induces immunogenic cell death with increased dendritic cell recruitment and expression of co-stimulatory molecules. Chemotherapy also leads to an increase in pro-inflammatory cytokine and a reduction in the number of regulatory T-cells within the tumour microenvironment. Radiotherapy can also synergise with immunotherapy by leading to up-regulation of immune co-stimulatory molecules and MHC class I molecules. However, it is important to note that there are also some negative side effects of these chemo and radiotherapeutic approaches such as increased PD-L1 expression and TGF β release by tumour cells (Derer, Spiljar et al. 2016, Zhang, M., Kleber et al. 2011) . As a result of these potential down sides

it may be necessary to investigate alternative chemotherapeutic regimes such as low dose metronomic chemotherapy when combining these therapies with immunotherapy. Anti-angiogenic therapy is one of the few approved therapies approved in GBM with the anti-VEGF antibody bevacizumab receiving FDA approval for the treatment of GBM (Cohen, Shen et al. 2009). VEGF has previously been shown to have an immunosuppressive effect with the enhancement of regulatory T-cell activity and induction of the apoptosis of cytotoxic T-cells. Since VEGF has immune inhibitory activity it would make sense to combine bevacizumab with immunotherapy, what is more bevacizumab is already approved in the GBM setting to annexing it with novel therapies makes sense when translating into the clinic. In the GBM setting Rindopepimut (EGFRviii-KLH peptide) vaccination has been combined with bevacizumab, this combination was shown to generate a longer overall survival when compared to bevacizumab alone (Reardon, Gilbert et al. 2015). Another approach is to combine numerous immunotherapeutic modalities together such as active vaccination combined with immune checkpoint blockade.

4.5. Conclusion

Dual SCIB1 and WT-1 ImmunoBody[®] vaccination generates an equivalent anti-TRP-2 and anti-WT-1 response to when the vaccines are administered singly. The targeting of numerous tumour antigens enables a large variety of cells within the heterogeneous tumour population to be targeted preventing potential tumour immune escape. Unfortunately, due to the highly immunosuppressive nature of GBM immunotherapy alone is not enough to treat and potentially cure the disease; as a result, combinatorial immunotherapy needs to be explored. Combining the dual ImmunoBody[®] vaccination with checkpoint blockade would make the most sense, this idea will be explored later within this thesis. These analyses reveal that the ImmunoBody[®] vaccination results in IFN γ release from activated splenocytes, IFN γ has many immune altering functions and as a result it is of great interest to examine what immune augmenting effects this IFN γ has on the profile of glioblastoma multiforme.

CHAPTER 5: IMMUNE ESCAPE MECHANISMS EMPLOYED BY GLIOBLASTOMA MULTIFORME IN RESPONSE TO IMMUNOTHERAPY

5.1. Introduction

Upon activation by immune therapy such as antigen specific vaccine, immune cells, specifically T-cells and NK-cells release pleiotropic cytokines such as interferon gamma (IFN γ). IFN γ exerts many effects that alter the immune system, some of these can be immune stimulatory and some can be immune inhibitory. IFN γ exerts its effects by binding to the IFN γ receptor (comprised of CD119/IFN γ R1 and IFN γ R2) activating downstream pathways such as the JAK-STAT, PI3K-AKT-mTOR and MEK-ERK pathway. These pathways affect numerous processes within cells contributing to the pleiotropic nature of IFN γ (Boehm, Klamp et al. 1997). IFN γ does not just exert its effects on immune cells it can also act upon native tissues within the body. This is due to the abundant expression of the IFN γ receptor within the human body. Tumour cells can also express the IFN γ receptor meaning that they will also be affected by an IFN γ rich environment. Interferon gamma is a central regulator of the immune response, originally thought of as an anti-viral agent; further research revealed that IFN γ exerted a host of many other effects all centred in on regulation of the immune system. As previously mentioned IFN γ activates the JAK-STAT pathway, a pathway commonly activated by cytokines. IFN γ binding to its receptor leads to its dimerization, which in turn, induces its phosphorylation and subsequently the activation of the JAKs, which then phosphorylate STAT1 α leading to the formation of STAT1 α -homodimers. These homodimers then shuttle to the nucleus where they bind to specific DNA-sequences known as gamma activated sites, initiating transcription of specific genes known as gamma responsive genes (Boehm, Klamp et al. 1997). Many immunoregulatory genes such as those encoding cell signalling chemokines and inhibitory proteins such as macrophage inhibitory protein as well as immune stimulating molecules such as the MHC molecules (McLaren, Ramji 2009).

IFN γ has been used in the clinical setting to try and treat many cancers. It has been shown to exert anti-GBM effects *in vitro* reducing adhesion and invasion of malignant glioma cells. The induction of IFN γ in the tumour microenvironment via adenoviruses expressing IFN γ was shown to improve T-cell infiltration in a murine model of GBM. This IFN γ also induced increased MHC I and MHC II expression on tumour cells (Ehtesham, Samoto et al. 2002). All these changes point towards a potential therapeutic role for IFN γ however many trials using IFN γ to treat solid tumours have provided lacklustre results (Okura, Smith et al. 2014). Recombinant IFN γ was administered into the surgical cavity of newly diagnosed high grade glioma patients. No noticeable toxicities were observed however the median survival of the IFN γ treated patients was in fact 11 weeks less than patients treated via conventional methods (41 weeks vs. 52 weeks) (Farkkila, Jaaskelainen et al.

1994). IFN γ has been shown to be upregulated in GBM tumours, leading to increased MHC I and II expression and therefore improved antigen presentation, however IFN γ also leads to an increase in PD-L1 potentially counteracting the increased antigen presentation (Zhu, V. F., Yang et al. 2012). This up-regulation of immune inhibiting factors could explain the shortcomings of IFN γ therapy in the GBM setting.

Indoleamine 2, 3-dioxygenase (IDO) is an immunoregulatory enzyme that catabolises tryptophan into numerous bioactive catabolites. It is important to note that IDO expression is also inducible by IFN γ exposure. IDO has been shown to be expressed in several tumours and this is thought to contribute to tumour immune tolerance. It is also important to note that antigen presenting cells themselves can also express IDO and this may also be a mechanism by which tumours induce immune tolerance. Macrophages and dendritic cells expressing IDO have been shown to reduce the proliferation of T-cells and tumour cells transfected with the IDO gene have also been shown to have the same effect (Munn, Mellor 2004). IDO expression in patient tumours was shown to result in decreased survival when compared to patients whose tumours had lower IDO levels (Wainwright, Balyasnikova et al. 2012). IDO expression levels seem to correlate with tumour grade, with grade 4 GBM tumours expressing much higher levels of IDO compared to lower grade gliomas (Wainwright, Balyasnikova et al. 2012). Murine models helped to reveal that tumour derived IDO as opposed to peripheral IDO results in a reduced survival and increased regulatory T-cell recruitment to the tumour sites in murine models of GBM. Not only did tumour derived IDO increase regulatory T cell recruitment but it also led to fewer CD8⁺ T-cells within the tumour infiltrating lymphocyte population (Wainwright, Balyasnikova et al. 2012).

One important immune modulating catabolite produced by IDO which, induces tryptophan degradation, is kynurenine (see *Figure 39*). This kynurenine induces naive T-cells to differentiate into regulatory T-cells and increase their activities (Mandi, Vecsei 2012). In addition, the depletion of tryptophan by IDO prevents the clonal expansion of antigen specific T-cells.

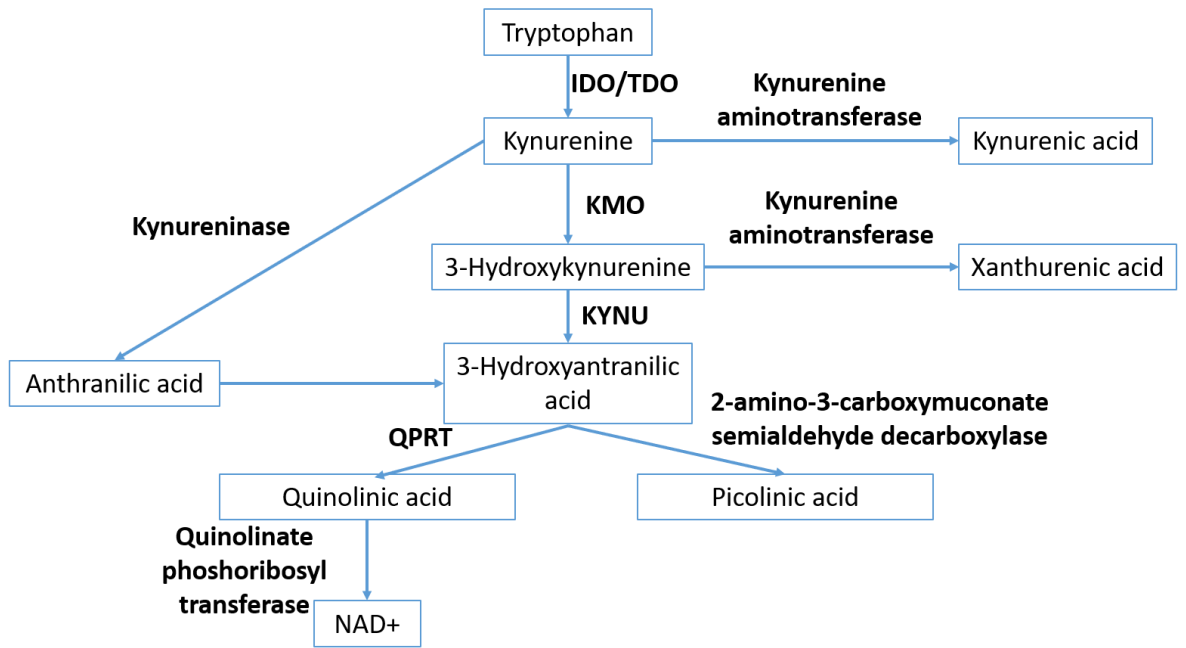


Figure 39. A schematic representation of tryptophan catabolism and the enzymes involved. IDO= indoleamine 2,3-dioxygenase, TDO= tryptophan 2,3-dioxygenase, KMO= kynurenine 3-monoxygenase, KYNU= kynureninase, QPRT= Quinolate phosphoribosyltransferase.

This is why many researchers have come up with ways to inhibit IDO, one of the most commonly used IDO inhibitors is 1-methyl-tryptophan (1MT). The use of 1MT has been examined *in vitro* (Miyazaki, Moritake et al. 2009) and in pre-clinical murine GBM models (Li, M., Bolduc et al. 2014, Hanihara, Kawataki et al. 2016). These analyses reveal that blockade of IDO with 1-MT with standard therapy conveys a survival benefit in mice harbouring GBM tumours (Li, M., Bolduc et al. 2014, Hanihara, Kawataki et al. 2016). Promising pre-clinical results have resulted in clinical trialling of IDO inhibitors in GBM patients with five clinical trials involving IDO blockade being listed on clinicaltrials.gov at the time of writing.

Not only does IFN γ induce the expression of IDO it also increased the expression of MHC class I molecules. As well as increasing classical MHC class I expression IFN γ can also lead to expression of non-classical MHCI molecules such as HLA-E and HLA-G. These non-classical MHC class I proteins have immunosuppressive activities that enable tumour immune escape by inducing resistance to NK and CTL mediated killing. Indeed, IFN γ has previously been shown to result in the up-regulation of HLA-E on acute myeloid leukaemia blasts which prevented their lysis by NK cells (Nguyen, Beziat et al. 2009). IFN γ has also been shown to increase the expression of HLA-E by GBM stem-cells and this helped protecting them from NK cell lysis (Wolpert, Roth et al. 2012). HLA-G has previously been shown to be expressed by some GBM cell lines and exposure to IFN γ enhanced further its expression which then protected GBM cells from cytolytic T-cell activity (Maier, Geraghty et al. 1999, Wiendl, Mitsdoerffer et al. 2002).

IFN γ induces expression of numerous other genes such as macrophage inhibitory protein (McLaren, Ramji 2009), PD-L1 and PD-L2 (Garcia-Diaz, Shin et al. 2019).

that can affect tumour cells and stromal cells in the microenvironment promoting a potentially immunosuppressive microenvironment. In the immunotherapy setting interferon gamma can be a 'double-edged' sword with some pro-immune and some anti-immune effects observed.

5.2. Aims and hypothesis

The two vaccines used in this study generated T-cells that were shown to produce strong IFN γ responses upon ex-vivo incubation with the vaccine-derived peptides (See chapter 4). It was therefore important to assess the effect of IFN γ on the GBM cells aimed to be used as targets against vaccine-induced T-cells.

5.3. Results

5.3.1. Analysis of CD119 expression on GBM cell lines

The aim of this chapter was to assess the effect of IFN γ on the selected GBM target cells (SEBTA-027 and SF-188, due to their expression of both TRP-2 and WT-1) and therefore it was necessary to confirm that they expressed the receptor for IFN γ (CD119). The flow cytometry analysis of the cells stained with the anti-CD119-PE conjugated antibody clearly shows that both the cell lines studied express the CD119 subunit of the IFN γ receptor. This implies that these cells can actively respond to IFN γ .

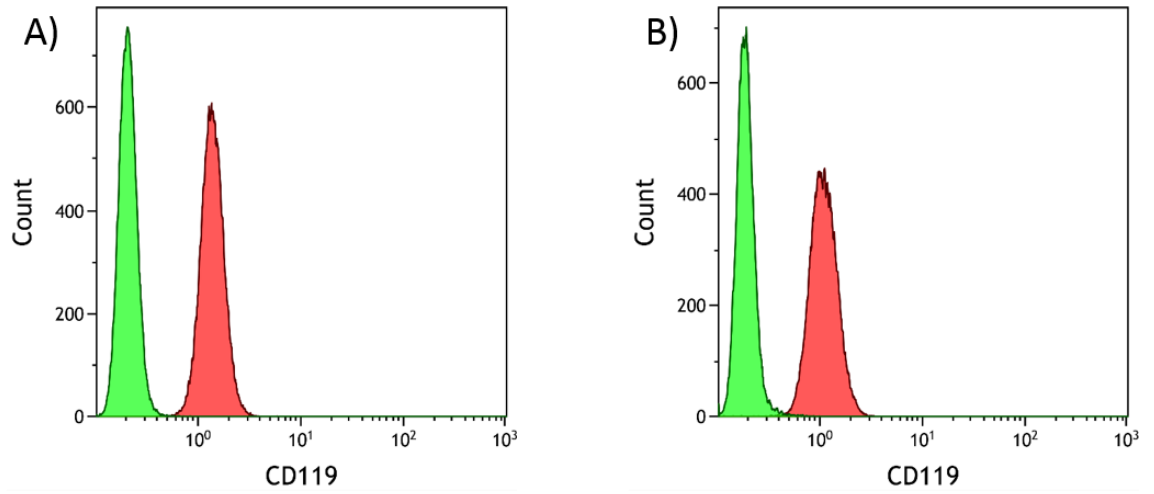
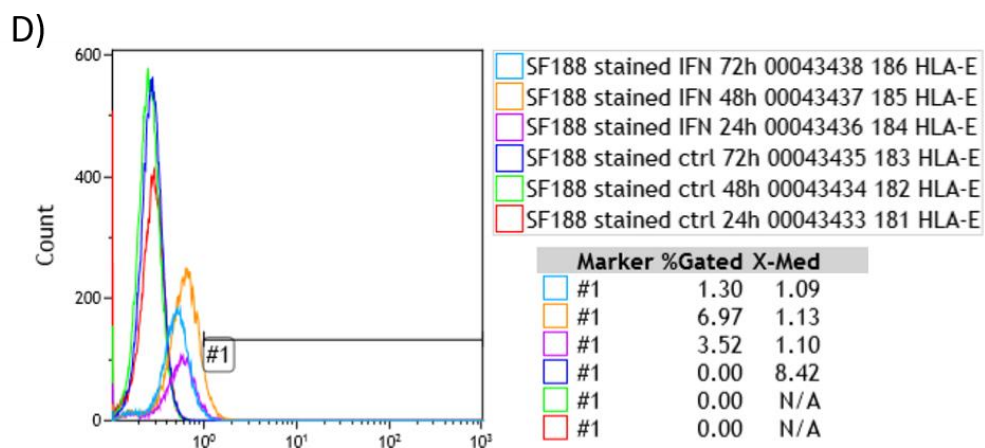
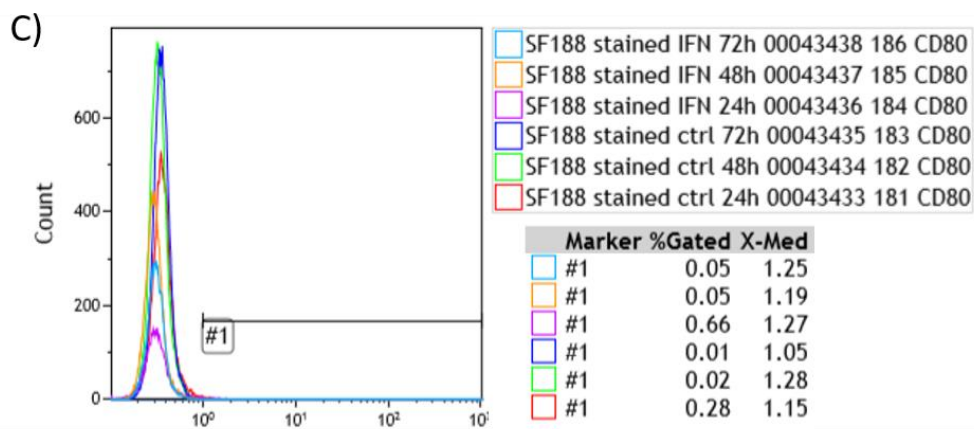
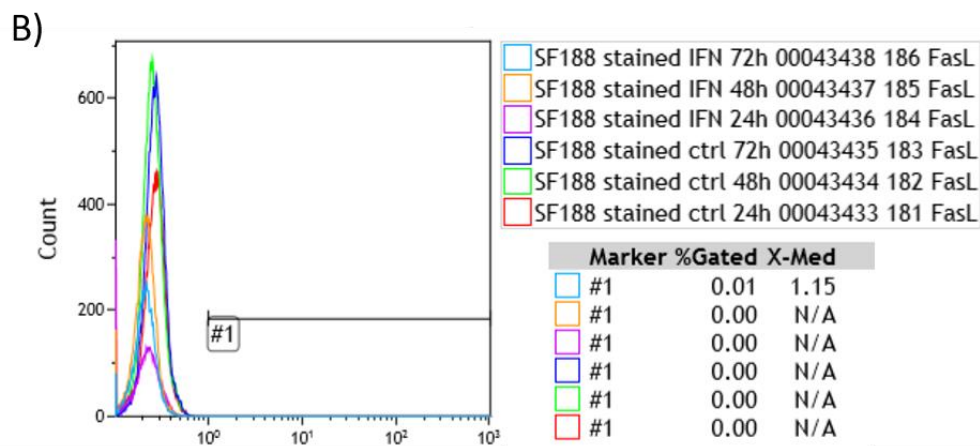
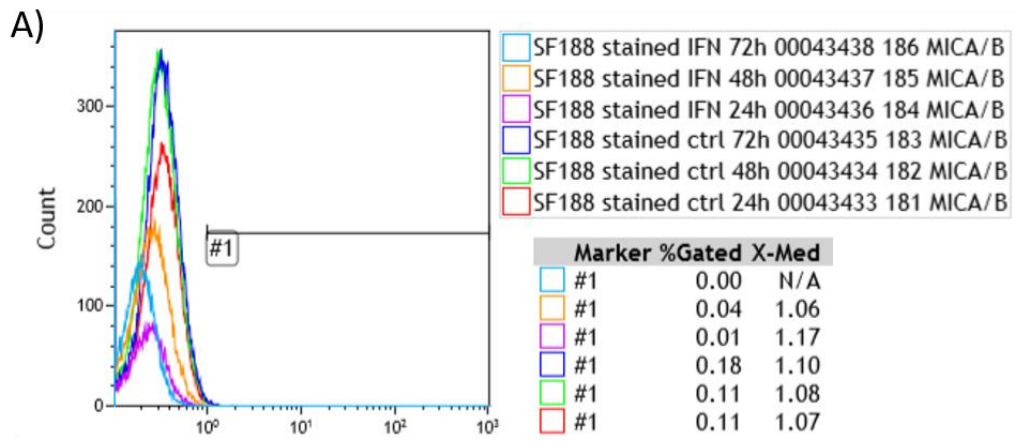
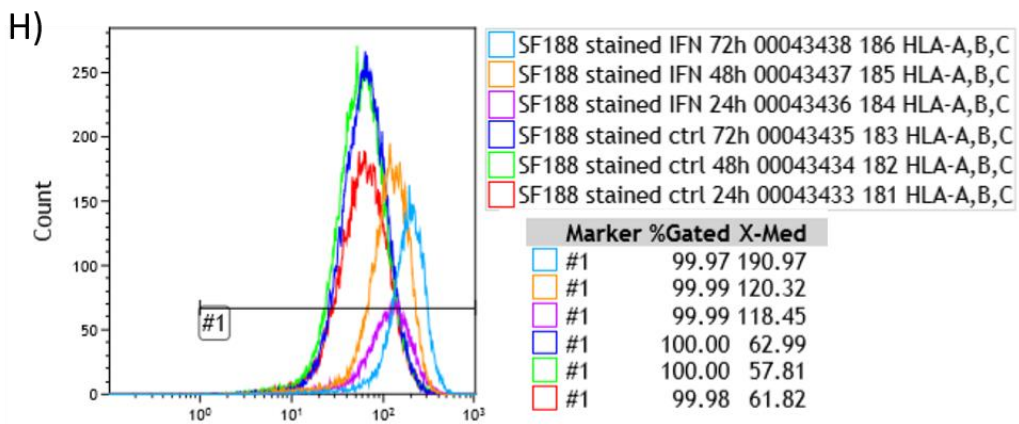
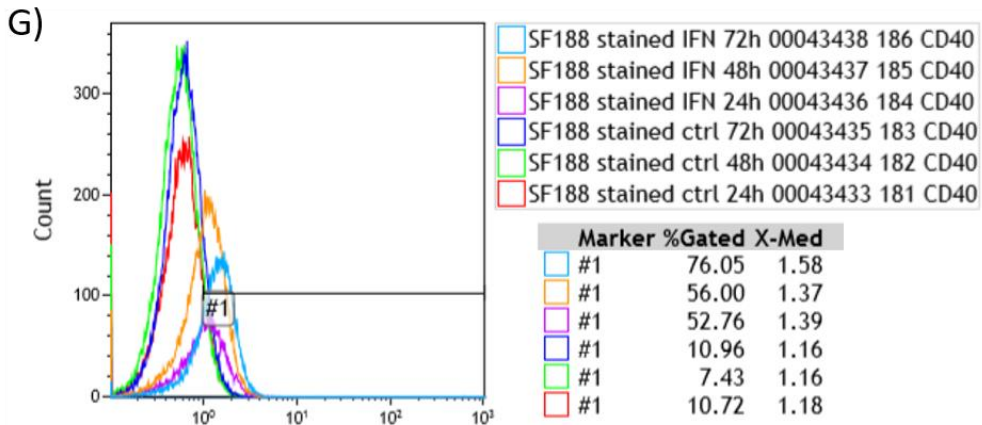
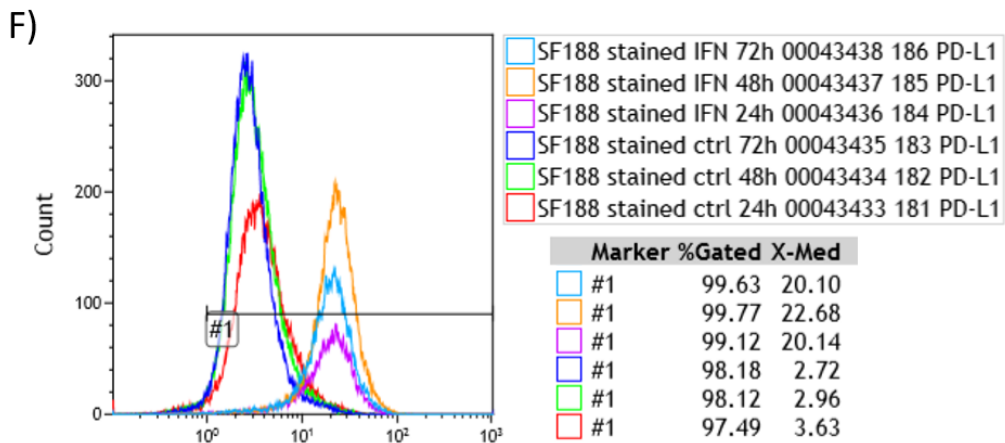
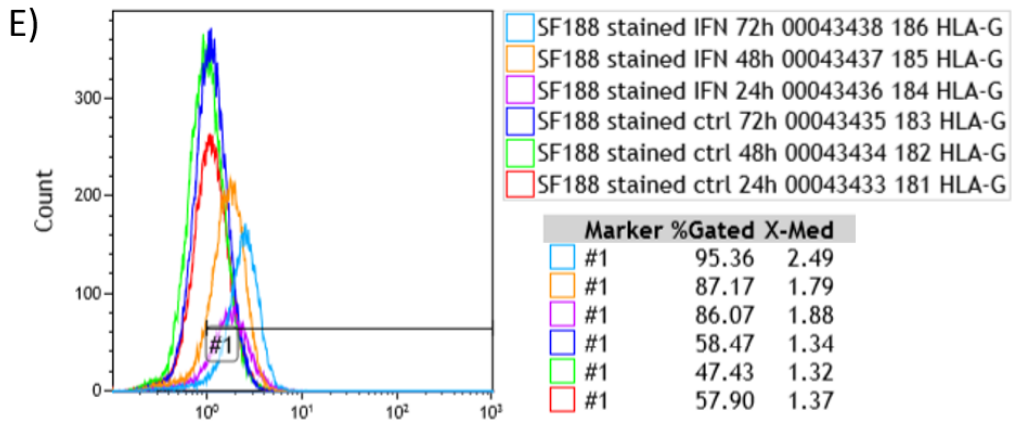


Figure 40. Representative flow cytometry histograms of CD119 staining of A) SEBTA-027 B) SF-188 cells, the red peak represents stained cells and the green peak represents unstained cells.

5.3.2. The effects of IFN γ on the immune profile of the SF-188 and SEBTA-027 glioblastoma multiforme cell lines as determined by flow cytometry

Cells were treated with IFN γ and thereafter stained for HLA-E, HLA-G, pan-MCHI, FasL, PD-L1 and the co-stimulatory molecules CD80, CD86, MICA/B and CD40. Flow cytometric analysis revealed an increase in the number of SF-188 cells that stained positive for HLA-E, HLA-G and CD40. CD40 and HLA-G which increased significantly in time-dependent manner, with increased IFN γ exposure resulting in an increase in the percentage of cells positive for these antigens (*Figure 41* and *42*). It is important to note that no change was seen in the percentage of cells that stained positive for HLA-A, B, C and PD-L1 because these cells are already 100% positive prior to IFN γ exposure.





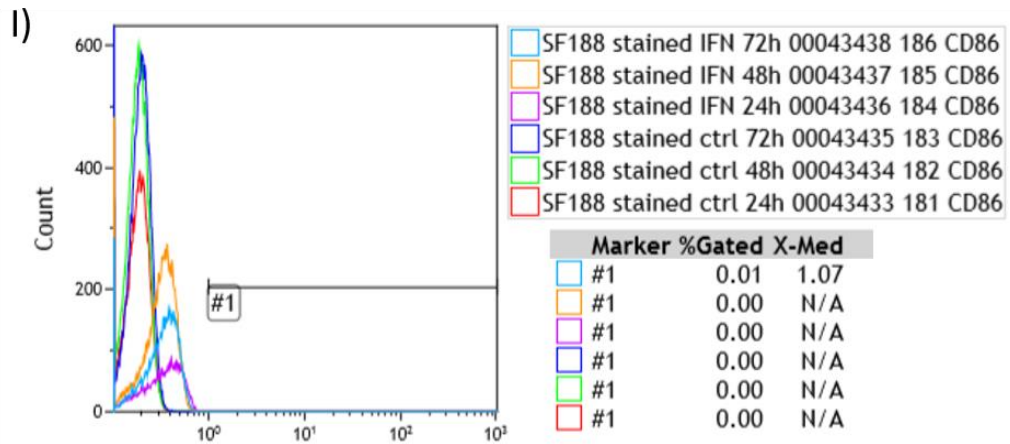


Figure 41. Representative flow cytometry histograms of IFN γ and control untreated live SF-188 cells. The red peak represents 24hr control cells, the green peak represents 48hr control cells, the blue peak represents 72hr control cells, the purple peak represents cells treated with IFN γ for 24 hours, the orange peak represents cells treated with IFN γ for 48 hours and the light blue peak represents cells treated with IFN γ for 72 hours. The gate is shown on each plot and the % of cells gated and the median fluorescence intensity (X-med) are shown alongside each plot. A) MICA/B B) FasL C) CD80 D) HLA-E E) HLA-G F) PD-L1 G) CD40 H) HLA-A,B,C I) CD86 staining.

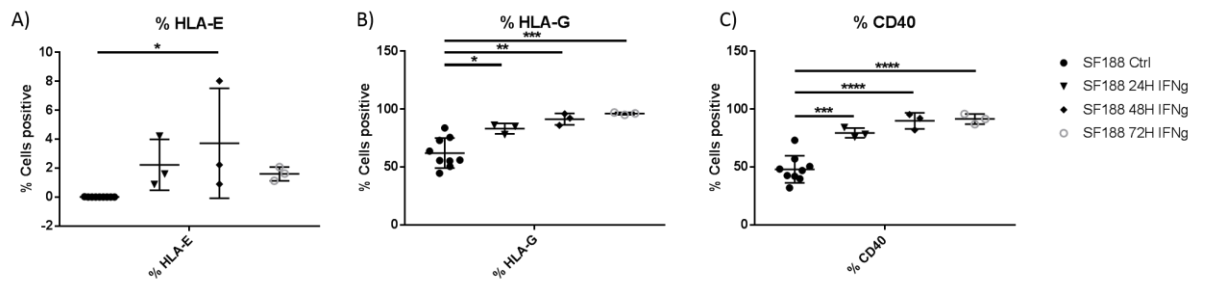


Figure 42. Percentage of cells positive for cell surface expression of A) HLA-E B) HLA-G C) CD40 after 24,48 and 72 hours exposure to IFN γ . ****= $P \geq 0.0001$, ***= $P \leq 0.001$, **= $P \leq 0.01$, *= $P \leq 0.05$ relative to control as deemed by a one-way ANOVA followed by Tukey's ad-hoc test. N= 9-3. The control group is composed of control cells that had normal carnosine free GBM media on them for 24, 48 and 72 hours, these controls were grouped as the time difference was not deemed to have a significant effect on antigen expression.

However when looking at the median fluorescence intensity for IFN γ treated SF-188 cells a clear increase in the surface expression of PD-L1, HLA-E, HLA-G, HLA-A, B, C and CD40 was detected. Similar to HLA-E/-G/and CD40 this increase was time dependant with increased exposure time to IFN γ resulting in a further increase in cell-surface expression of these antigens (*Figure 43*). IFN γ treatment did not alter the cell-surface levels of the FasL, MICA/MICB, CD86 and CD80 (data not shown). In order to verify that the changes observed after IFN γ exposure are due to IFN γ and not just an effect that naturally occurs over time the cell surface expression was observed for cells that were grown in IFN γ free-media for 24, 48 and 72 hours, the results are shown below.

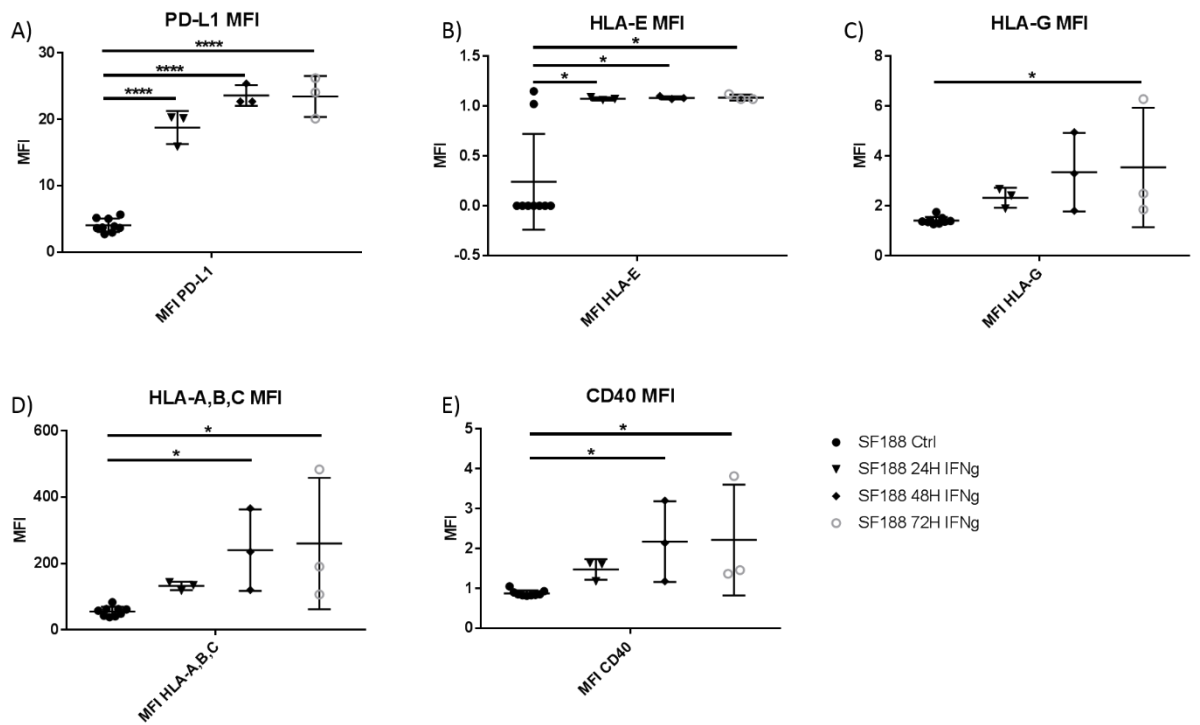


Figure 43. Median fluorescence intensity results for IFN γ treated SF-188 cells A) PD-L1 B) HLA-E C) HLA-G D) HLA-A, B, C E) CD40. ****= $P \geq 0.0001$, *= $P \leq 0.05$ relative to control as deemed by a one-way ANOVA followed by Tukey's ad-hoc test. N= 9-3. The control group is composed of control cells that had normal media on them for 24, 48 and 72 hours. The increase in MFI indicates an increase in the number of molecules present on the cell surface.

Analysis of cells cultured in normal media reveals that the changes in HLA-E, HLA-G, CD40, PD-L1 and HLA-A, B, C expression observed in IFN γ treated cells is in fact due to IFN γ and not due to temporal changes that may occur in cultured cells (see *Figures 44 and 45*).

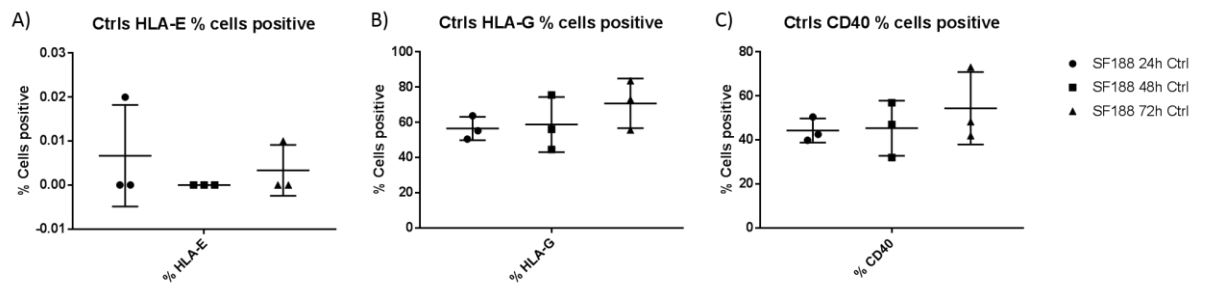


Figure 44. Percentage of cells positive for cell surface expression of A) HLA-E B) HLA-G C) CD40 after 24, 48 and 72 hours growth in normal 'control' media that lacked IFN γ . There is no significant difference between any of the conditions as deemed by a one-way ANOVA followed by Tukey's ad-hoc test. N= 3.

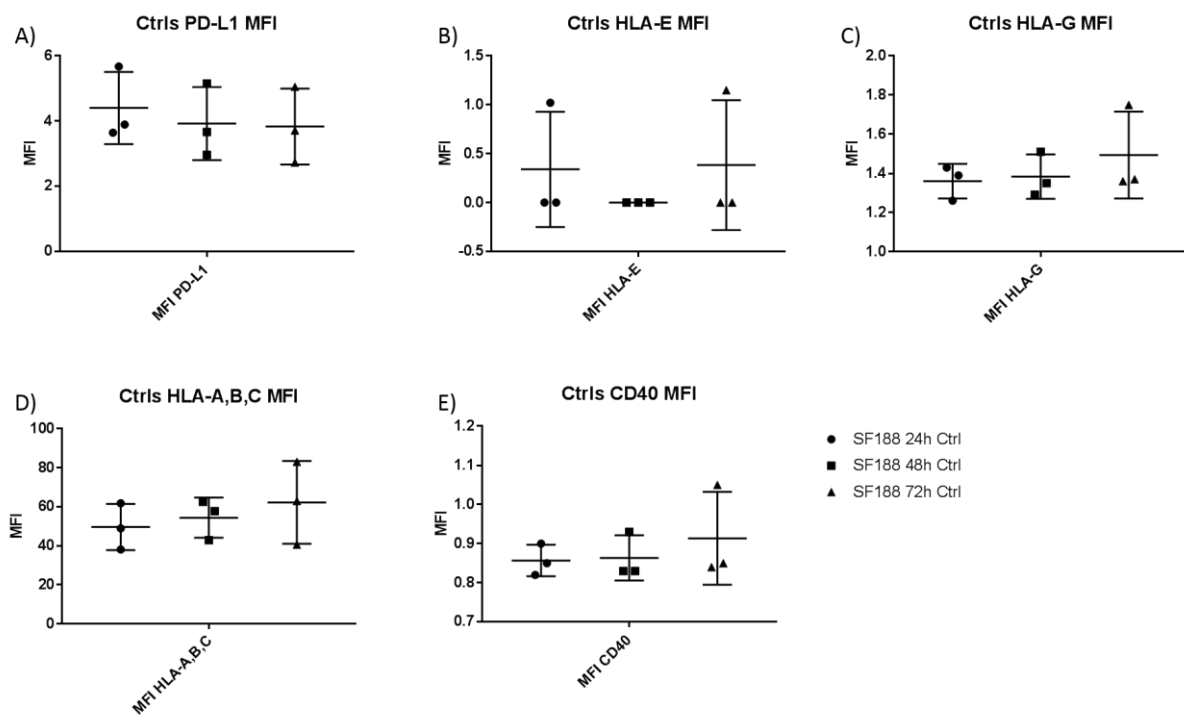


Figure 45. Median fluorescence intensity results for SF-188 cells grown in normal media for 24, 48 and 72 hours A) PD-L1 B) HLA-E C) HLA-G D) HLA-A, B, C E) CD40. There is no significant difference between any of the conditions as deemed by a one-way ANOVA followed by Tukey's ad-hoc test. N=3.

Due to the changes observed in the SF-188 cell lines it was decided to also analyse the SEBTA-027 cell line after IFN γ exposure. Seeing as the most marked changes were observed after 72 hours of IFN γ exposure it was decided to treat the SEBTA-027 cells for 72 hours, the changes observed are detailed in *Figure 46* and *Figure 47* below.

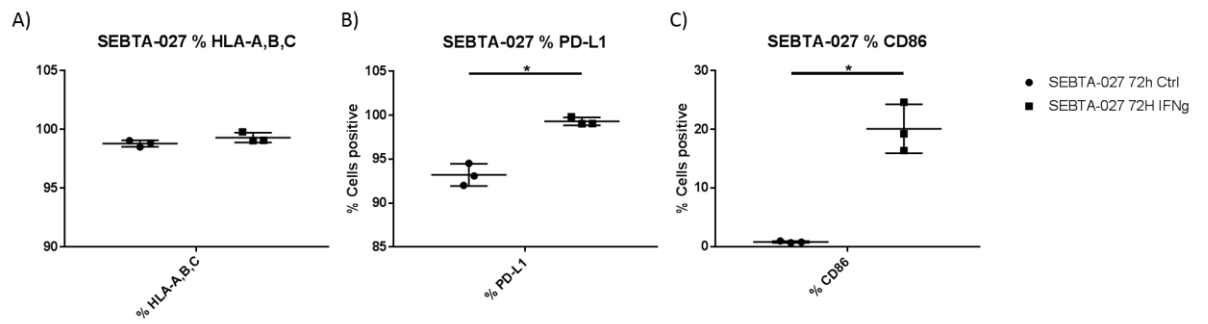


Figure 46. Percentage of SEBTA-027 cells positive for cell surface expression of A) HLA-A B) PD-L1 C) CD86 after 72 hours exposure to IFN γ , $*= P \leq 0.05$ relative to control as deemed by a paired T-test. $N= 3$.

The percentage of PD-L1 and CD86 positive SEBTA-027 cells increases after 72 hours of IFN γ exposure. As mentioned previously PD-L1 is immunosuppressive, however CD86 is a co-stimulatory molecule that is required for T-cell activation.

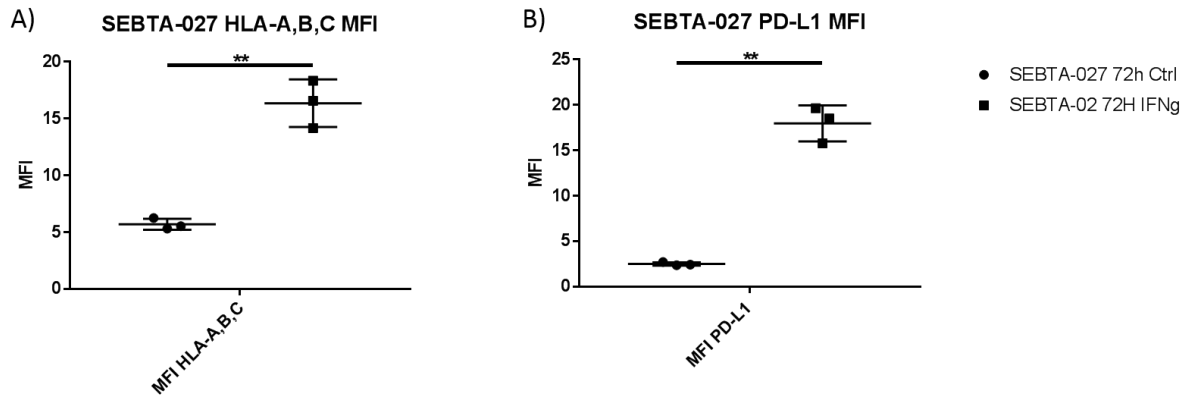


Figure 47. Median fluorescence intensity results for SEBTA-027 cells positive for cell surface expression of A) HLA-A, B, C B) PD-L1 after 72 hours exposure to IFN γ , ** = $P \leq 0.01$ relative to control as deemed by a paired T-test. N= 3.

In the SEBTA-027 cell line much like the SF-188 cell line the cell surface expression of MHC class I (HLA-A, B, C) and PD-L1 increases after IFN γ exposure. The expression of HLA-E, HLA-G and CD40 did not change in the SEBTA-027 cell line (data not shown).

These findings show that exposure of GBM cell lines to IFN γ leads to an increase in both immune stimulating (CD40, MHC class I and CD86) and immune-evasion markers (HLA-G, HLA-E and PD-L1) on the surface of these cells. The two main markers that are upregulated are MHC class I and PD-L1 in both cell lines, this is to be expected as both of these are IFN γ responsive genes.

5.3.3. Expression of IDO in IFN γ treated GBM cell lines and measurement of IDO activity

The SF-188 and SEBTA-027 cell lines were treated with interferon gamma for 24, 48 and 72 hours and the change in expression levels of IDO was measured using Western blotting. As stated previously these cell lines are being further probed due to their antigen expression profile (detailed in chapter 3) and relevance to the immunotherapeutic approach. Both cell lines revealed that treatment with IFN γ induces the expression of IDO which continues to increase with increased exposure time (See *Figure 48*).

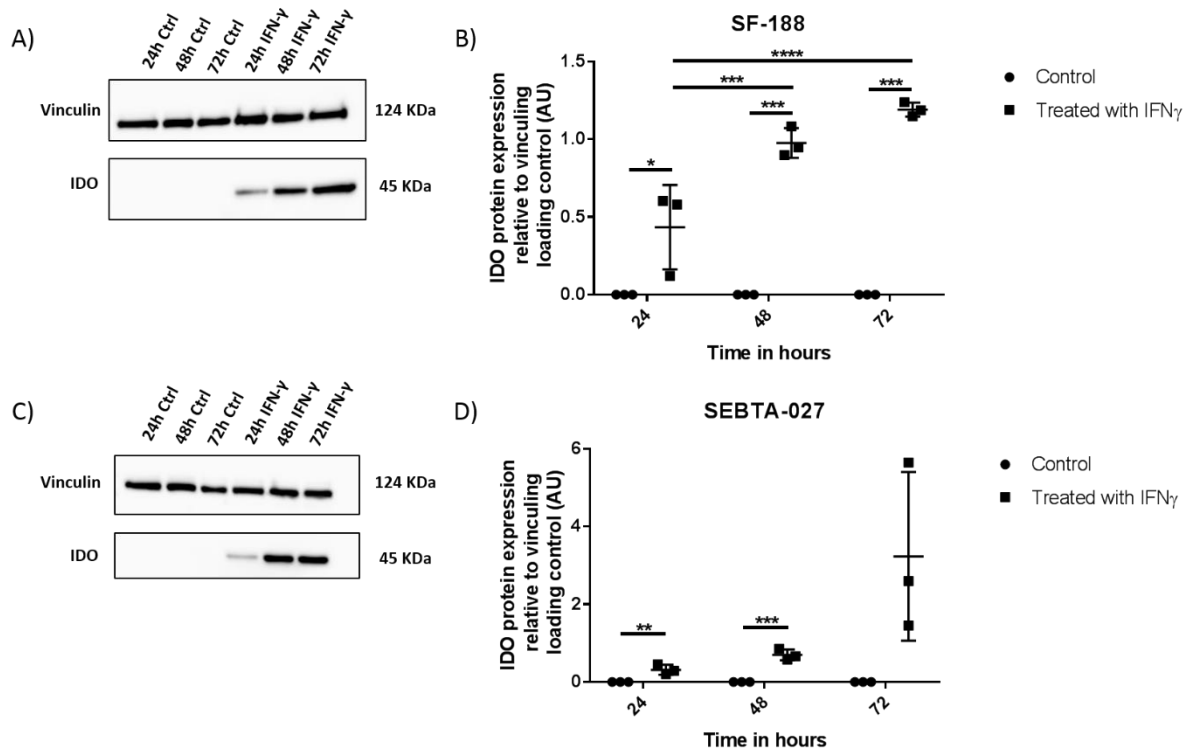


Figure 48. The effects of IFN γ exposure on the expression of IDO in SF-188 and SEBTA-027 cell lines as measured by Western blotting. A) Representative blot for IFN γ treated SF-188 cells. B) Quantification of IFN γ treated SF-188 blots using ImageJ software to determine the IDO expression relative to the vinculin loading control. C) Representative blot for IFN γ treated SEBTA-027 cells. D) Quantification of IFN γ treated SEBTA-027 blots using ImageJ software to determine the IDO expression relative to the vinculin loading control. N=3 ****= $P \geq 0.0001$, ***= $P \leq 0.001$, **= $P \leq 0.01$, *= $P \leq 0.05$ as deemed by a two-way ANOVA followed by Tukey's ad-hoc test.

The increase in IDO protein expression does not always mean that the catabolism of tryptophan into kynurenine is also increased, therefore levels of kynurenine within the culture media of the IFN γ treated SF-188 and SEBTA-027 cell lines was also measured, the results are shown in *Figure 49*.

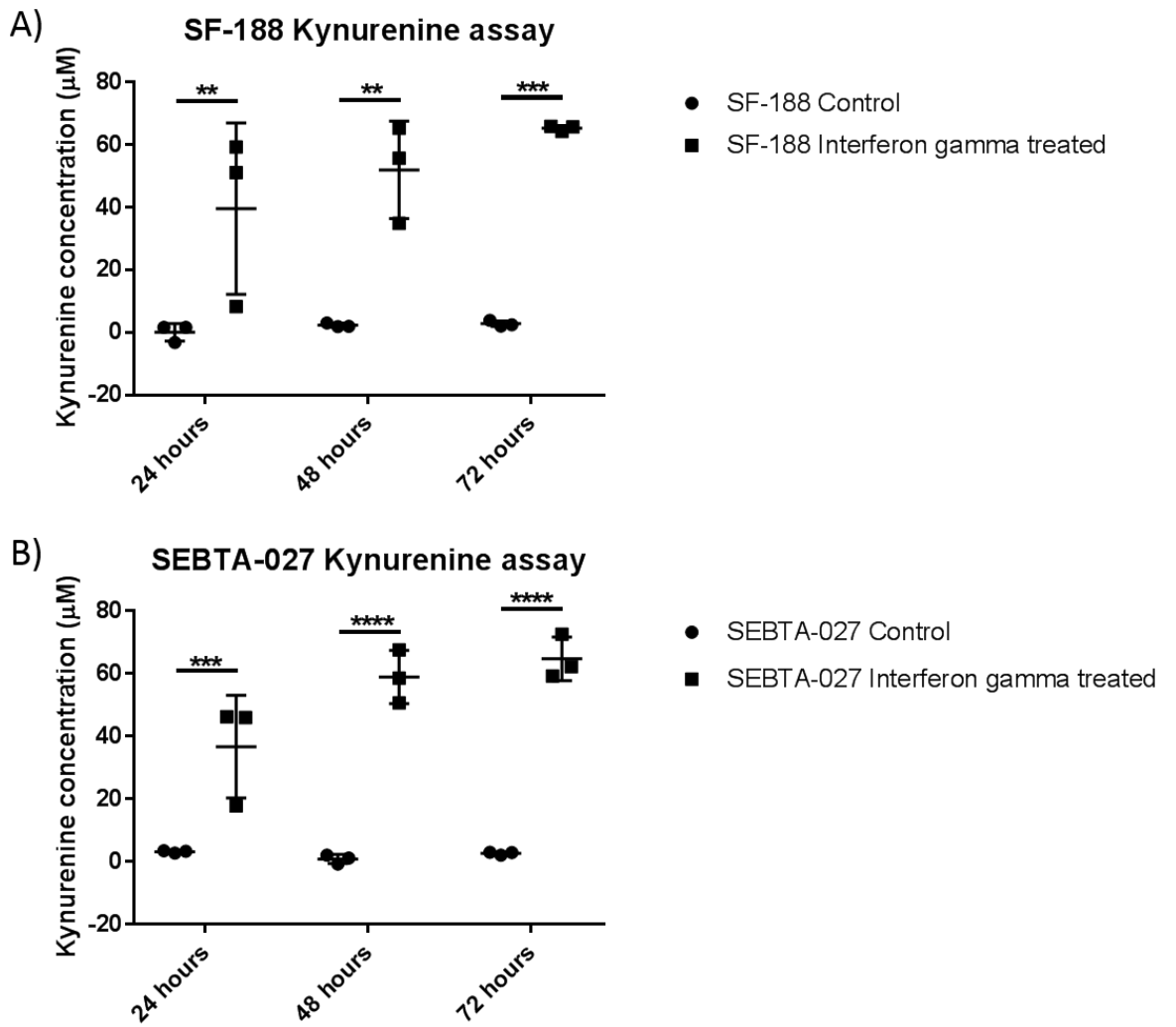


Figure 49. Kynurenine concentration in A) SF-188 cell culture media and B) SEBTA-027 cell culture media after 24, 48 and 72 hours in normal control media (black circles) and IFN γ containing media (black squares). N= 3 ****= $P \leq 0.0001$, ***= $P \leq 0.001$, **= $P \leq 0.01$ as deemed by two way ANOVA followed by Sidak's multiple comparisons test.

The increase in IDO expression observed in the GBM cell lines studied after IFN γ exposure, led to a significant increase in kynurenine production by these cells as indicated by the increased kynurenine levels observed in the cell culture media. Another important enzyme that needs to be considered is tryptophan 2,3-dioxygenase (TDO), this much less frequently occurring enzyme also contributes to the degradation of tryptophan and resultant production of kynurenine. The expression of TDO after exposure of GBM cells to IFN γ was also assessed, however TDO enzyme could not be detected in both treated and untreated cells (data not shown). All of these results taken together strongly link IFN γ exposure to enhanced immune escape, although it should be noted that there also seem to be some pro-immune functions enhanced by IFN γ exposure, such as the increased expression of MHC class I (HLA-A, B, C) on the surface of cells.

5.4. Discussion

In vitro investigation of IFN γ treatment on GBM cell lines allows for a rudimentary understanding of how GBM tumours might respond to immunotherapy which will need to be taken into consideration for future immunotherapy. These analyses indicate that GBM cells actively adapt to IFN γ exposure enhancing their immune escape. However, vaccines are likely to be given after the majority of the tumour cells have been removed by surgery and therefore the small number of remaining cells might then be killed by a large number of vaccine-induced high avidity T-cells. It is also important however to note that as well as these deleterious effects IFN γ can in fact also result in an increase of MHC class I and class II molecules and therefore increased antigen presentation (Zhou 2009, Steimle, Siegrist et al. 1994), a finding which the HLA-A, B, C staining corroborates. Indeed, IFN γ leads to adaptation of the proteasome with replacement of the β 1, β 2 and β 5 hydrolytic subunits of the 20S core (within the 26S proteasome) with LMP2, LMP7 and MECL-1 resulting in formation of the immunoproteasome (Kloetzel, Ossendorp 2004). This shift results in increased proteolytic peptide processing and presentation via the increased MHC expressed, ultimately resulting in increased generation of immune epitopes and resultant anti-tumour T-cell activity (Kloetzel, Ossendorp 2004).

The upregulation of many of these immunosuppressive antigens provides a rationale for combining checkpoint blockade with active immunotherapy, this would help dampen the immune nullifying effects of IFN γ and help enhance its immune stimulating properties, helping to boost the immune response to vaccination.

These analyses show a clear increase in IDO expression in the two cell lines studied. What is of even more interest is that in both the SF-188 and SEBTA-027 cell lines this IDO is active leading to the catabolism of tryptophan to kynurenine. IDO expression by antigen presenting cells after IFN γ

exposure is a counter measure to maintain immune balance after activation of these cells by IFN γ . Unfortunately it also appears that cancer cells react to IFN γ in the same manner. IDO is a key enzyme in the kynurenine pathway along with TDO (see *Figure 39*). Several of the metabolites produced by the tryptophan pathway lead to a reduction of proliferation and apoptosis of TH1 T-helper cells. These metabolites also have anti-proliferative effects on other cell types such as B and NK cells. The kynurenine pathway appears to have a globally immunosuppressive effect and not just an effect limited to individual immune cell populations. IFN γ was shown to increase the levels of kynurenine within the culture media of GBM cells. Kynurenine specifically has been shown to affect antigen-specific T-cells reducing their proliferation (Mandi, Vecsei 2012). It is also thought that IDO activation can result in increased TH2 cell immune responses. Kynurenine also leads to conversion of CD4 T-cells into regulatory T-cells; a well-defined immune inhibitory T-cell subset (Mandi, Vecsei 2012). Due to the immune inhibitory effects of IDO its inhibition has been studied in the clinical setting for multiple malignancies. IDO has been previously shown to be a viable target for the therapy of GBM, with its expression being linked with poorer patient survival (Miyazaki, Moritake et al. 2009, Wainwright, Balyasnikova et al. 2012). IDO inhibition has been explored pre-clinically in GBM mouse models (Wainwright, Chang et al. 2014, Hanihara, Kawataki et al. 2016). As of writing this thesis (2019) there are five clinical trials listed as recruiting or completed utilising IDO blockade for brain tumours on clinicaltrials.gov.

Not only does IFN γ induce the expression of immune inhibitory IDO in GBM tumour cells, it also induces/increases expression of several immune inhibitory cell-surface proteins. Whilst it appears that IFN γ leads to the upregulation of MHC class I (HLA-A, B, C) unfortunately it also appears that IFN γ leads to up-regulation of the non-classical MHC class I molecules HLA-E and HLA-G. As detailed previously HLA-E and HLA-G have immune dampening effects enabling GBM cells to escape NK-cell mediated lysis. The upregulation of these molecules on the surface of GBM cells provides a rationale for combining potential blockade of HLA-E and/or HLA-G with active immunotherapy as a means for overcoming the IFN γ induced immunosuppression. Whilst there are no clinical trials blocking HLA-E or –G in glioblastoma multiforme several methods for targeting these checkpoints are being developed. RNA interference of the HLA-G gene has been shown to increase NK mediated lysis of tumour cells (Zidi, Ben Amor 2012). Antibodies that block the interaction of HLA-E with the NK cell inhibitory receptor NKG2A have been developed to enhance NK mediated tumour cells lysis; monalizumab is an NKG2A blocking antibody and has been tested in clinical trials for cancer (Guillerey, Huntington et al. 2016). No results have been published about the use of monalizumab in the GBM setting but previous research has found that monalizumab shows promise for head and neck cancer and ovarian cancer (Carotta 2016). The immune suppressive checkpoint PD-L1 was also upregulated after IFN γ exposure. This increased PD-L1 expression on the surface of GBM cells is

potentially problematic, however this opens up the opportunity to use PD1/PD-L1 blockade in combination with immunotherapy even in cases where the patient's tumour does not express PD-L1.

IFN γ was also found to increase the expression of CD40 on the surface of the SF-188 GBM cell line. CD40 is a member of the tumour necrosis factor receptor family. CD40 has previously been shown to be expressed on a variety of cancers including GBM. The interaction of CD40 with its ligand (CD40L) has been shown to be vital for induction of T-cell help for CTL mediated lysis, this is due to ligation of CD40 on dendritic cells with CD40L on stimulated T-helper cells (Schoenberger, Toes et al. 1998). CD40 stimulation has also been shown to lead to increased antigen presentation by tumour cells. Ligation of CD40L on NK cells with CD40 on tumour cells also leads to NK cell activation and tumour cell killing (Eliopoulos, Young 2004). CD40 ligation to CD40L provides strong co-stimulatory signals to T-cells. *In vitro* experiments have shown that ligation of CD40L with CD40 on cancer cells leads to upregulation of Fas and FasL by these cells. There is also increased secretion of the cytokines IL-6, IL-8, GM-CSF and TNF α by tumour cells upon CD40 ligation. These changes promote cancer cell-death and immune cell attraction. What is also of interest is that CD40 ligation reduces the growth of cancer cells. Transfection of CD40 into cancer cells that do not express CD40 results in greater T-cell activation, revealing the important role of CD40 in tumour specific immune responses (Alexandroff, Jackson et al. 2000). CD40 is an attractive target for anti-cancer therapy and its upregulation by IFN γ increases the susceptibility of GBM cells to potential immune attack. This could provide a rationale for the use of CD40 agonists in conjunction with active immunotherapy.

Whilst IFN γ is essential for immune signalling and immune cell function it also acts to prevent over-activity of the immune system, and thus it also acts to dampen the immune system and prevent over-activation of immune cells and therefore prevent deleterious immune activity in the normal setting. GBM cells also appear to react to interferon gamma in a similar manner, with tumour cells upregulating many immune inhibitory molecules. These results suggest that combinatorial immunotherapy would be the most effective way to approach GBM therapy in the clinic. Interestingly in a pre-clinical GBM model combined blockade of IDO, PD-L1 and CTLA-4 has been shown to result in 100 % long-term survival in mice bearing GL261 tumours (Wainwright, Chang et al. 2014). This combinatorial therapy was shown to significantly reduce regulatory T-cell infiltrate into these experimental brain tumours whilst increasing the presence of activated CD8⁺ T-cells (Wainwright, Chang et al. 2014). Combinatorial therapy utilising IDO inhibition, PD-1 blockade and radiotherapy has also shown great promise in the therapy of intracranial GL261 and CT-2A GBM like tumours (Ladomersky, Zhai et al. 2018). These results highlight the necessity for combined immunotherapy when targeting cancer, especially GBM.

5.5. Conclusion

These preliminary analyses reveal that GBM tumour cells actively respond to the presence of the immune-related cytokine IFN γ . Exposure to IFN γ resulted in the increase of both immune inhibitory and immune-stimulatory molecules, with a more predominant increase in the inhibitory factors. Under normal circumstances these changes take place to protect the body from auto-immune attack however in the case of GBM these changes enable these tumours to escape immune surveillance. As a result, the active adaptation of the tumour in response to immune therapy needs to be accounted for when utilising ImmunoBody[®] immunotherapy. These results indicate that combining checkpoint blockade and potentially IDO blockade with vaccine therapy would help overcome the immune escape mechanisms employed by GBM cells.

CHAPTER 6: PRE-CLINICAL ANTI-TUMOUR ASSESSMENT OF THE COMBINED IMMUNOBODY® VACCINES

6.1. Introduction

Cancer immunotherapy was heralded as Science magazine's breakthrough of the year 2013 (Couzin-Frankel 2013). The utilisation of the immune system to target cancer has garnered great interest and the utilisation of immune therapies for cancer treatment have progressed in leaps and bounds. Sipuleucel-T was the first FDA approved immunotherapy for the treatment of prostate cancer. Sipuleucel-T is generated by co-culturing *in vitro* the patient's PBMCs with a recombinant fusion protein of PAP and granulocyte-macrophage colony-stimulating factor. After activation the stimulated PBMCs are then reintroduced back into the patient (Higano, Small et al. 2010). As understanding of the interactions between the immune system and cancer has increased so have differing methods of augmenting the immune system. With this understanding came the development of immune checkpoint inhibition. Immune checkpoints function to dampen the immune response and prevent immune over activation. Some tissues also express immune inhibitory checkpoints on their surface to prevent them from generating an immune response, and one example is the placenta that expresses the PD-L1 checkpoint inhibitor. One of the first major steps towards the development of immune checkpoint inhibitors was the discovery of cytotoxic T-lymphocyte-associated protein 4 (CTLA-4). Upon T-cell receptor engagement CTLA-4 translocates to the surface of T-cells where it out competes CD28 for binding to its ligands CD80/86 preventing important costimulatory signals. The binding of CTLA-4 to CD80/86 has also been shown to lead to the transfer of CD80 and CD86 to CTLA-4 expressing cells, these CTLA-4 expressing cells then degrade these CD80 and CD86 molecules. This results in decreased immune cell activity and stunts the immune cell activation capabilities of dendritic cells (Qureshi, Zheng et al. 2011). Pre-clinical studies in mice showed that treating tumour bearing mice with a CTLA-4 blocking antibody led to durable regression (Leach, Krummel et al. 1996). As a result, two fully human anti-CTLA-4 antibodies: Ipilimumab and Tremelimumab were developed and entered clinical trials. Early results revealed that CTLA-4 blockade could on rare occasions result in tumour regression however these occurrences were accompanied by toxicities due to tissue-specific inflammation. Anti-CTLA-4 therapy was shown to increase survival of patients suffering with metastatic melanoma and as a result Ipilimumab was approved by the FDA in 2011 (Ribas, Wolchok 2018). It is important to note that the response to ipilimumab was not 100% and only around 20-30% of patients displayed improved survival (Ledford 2011). Another important immune checkpoint that has been discovered and targeted is programmed death-1 (PD-1). PD-1 is expressed on activated T-cells and it binds to its ligands PD-L1 (frequently expressed on tumour cells) or PD-L2; this binding results in apoptosis of activated T-cells. PD-1 blockade has been shown to have less toxic side effects than CTLA-4

blockade (Callahan, Wolchok 2013), this is thought to be due to its activity being more specific for anti-tumour T-cells due to their chronic stimulation. Currently there are two FDA approved anti-PD-1 and three approved PD-L1 blocking antibodies for use in the cancer setting. Unfortunately, no immune-checkpoint blocking antibodies have been approved for glioblastoma multiforme, however their use is being explored in late stage clinical trials (Ribas, Wolchok 2018). As of 2017 there were 62 clinical trials investigating the use of immune checkpoint blockade in the GBM setting either alone or in combination with other treatment modalities, with even more combinations being explored subsequently. The use of these immune checkpoints is also being explored in the adjuvant and neoadjuvant setting. With neoadjuvant treatment the checkpoint blockade is administered prior to surgical excision of the tumour, the aim of this is to try and minimise the tumour prior to surgery. This also allows for the expansion and activation of tumour specific T-cells before resection. In phase III clinical trials Ipilimumab (anti-CTLA4) and Nivolumab (anti-PD-1) therapies have been combined for the treatment of melanoma, this was shown to prolong patient progression free survival compared to either antibody alone, unfortunately this treatment is also accompanied with adverse events with 55% of patients studied experiencing high-grade adverse events (Maxwell, Jackson et al. 2017). Nivolumab and Ipilimumab have also been combined in the recurrent GBM setting, with a high proportion of patients experiencing adverse events much like in the melanoma setting (Maxwell, Jackson et al. 2017). Unfortunately, in the recurrent GBM setting Nivolumab therapy was found to be ineffective at improving patient survival in a phase III trial (Fillee, Henriquez et al. 2017).

The main issues that can arise from using these immune checkpoint antibodies is the potential for adverse inflammatory events to occur and potential autoimmune reactions. These side effects are commonly managed via the use of corticosteroids. The CNS actively interacts with the immune system so checkpoint inhibitors are attractive avenues for therapies. PD-L1 expression has been shown to be prevalent in GBM tumours with as many as 88% of cases from newly diagnosed GBM expressing PD-L1 and 72% of recurrent GBM expressing PD-L1 (Preusser, Lim et al. 2015). The analyses performed in chapter 3 have also confirmed that PD-L1 expression appears to be a hallmark of GBM tumours. Glioma cells have also been shown to secrete IL-10 which induces PD-L1 expression on tumour infiltrating macrophages and circulating monocytes. PD-1 positive T-cells are found in 33% of GBM samples, as a result blockade of the PD-1/PD-L1 axis represents an attractive avenue for the therapeutic treatment of GBM. Pre-clinical blockade of this axis in animal models of GBM has shown great promise and as a result the use of these checkpoint blockade antibodies has progressed into clinical trials for GBM. What is of great interest is the combination of immune checkpoint blockade with other therapies, the utilisation of PD-1/PD-L1 blockade as a monotherapy has shown moderate success but the idea of combining these therapies with other therapies to

further boost patient anti-tumour response is an exciting prospect for the field of cancer immunotherapy (Preusser, Lim et al. 2015).

Combining immune checkpoint blockade with vaccination therapy presents an attractive avenue for immunotherapy, with the active vaccination educating T-cells and homing them in on tumours, and checkpoint blockade removing the 'breaks' applied by the tumour on the activated immune cells. It has already been demonstrated that ImmunoBody[®] vaccination generates a strong immune response directed towards the tumour antigens TRP-2 and WT-1. Synergising ImmunoBody[®] vaccination with PD-1/PD-L1 blockade represents an attractive avenue for GBM therapy. Previous pre-clinical research has shown that combining SCIB-1 (TRP-2/gp100) ImmunoBody[®] vaccination with anti-PD-1 antibody blockade has immune boosting effects. Xue W. et al. (2016) combined SCIB-1 ImmunoBody[®] vaccination with PD-1 blockade for the treatment of humanised B16 murine melanoma in a humanised mouse model. Vaccination with SCIB-1 resulted in increased T-cell infiltration into the tumour and combination of SCIB-1 with anti-PD-1 improved CD-8 T-cell infiltration. This increased T-cell infiltration also led to improved survival, with 80% of mice showing long term survival compared to 40% of SCIB-1 and 50% of anti-PD-1 treated mice (Xue, W., Brentville, Symonds, Cook, Yagita, Metheringham, and Durrant 2016). In a phase II clinical trial utilising an autologous heat shock protein vaccination to treat GBM patients PD-L1 expression on myeloid cells was a predictor of survival when patients received this vaccine. Examining the expression of PD-L1 on circulating myeloid cells revealed that patients with high PD-L1 expression had a median overall survival of 18 months after treatment compared to 44.7 months for patients with low PD-L1 expression on their circulating myeloid cells (Bloch, Lim et al. 2017). These results highlight the influence of these immune checkpoints on immunotherapeutic modalities.

The combination of an anti-cancer vaccine with immune checkpoint inhibition has previously been shown to improve survival in tumour bearing animals. In a study utilising a dendritic cell vaccination it was found that vaccination increased T-cell infiltration into established intracranial GL261 murine GBM tumours, however in animals with elevated tumour burden this increased T-cell infiltrate was not associated with a significant increase in survival. This indicates that vaccination generates an immune response leading to increased immune cell infiltrate, however factors within the tumour microenvironment are preventing these cells from mounting an effective anti-tumour immune response (Antonios, Soto et al. 2016). Analysis of tumour infiltrating lymphocytes revealed that there was an increased expression of PD-1 on these cells, as a result it was hypothesised that the failure of the vaccine to improve survival was due to immune suppression mediated by the PD-1/PD-L1 pathway. Dendritic cell vaccination was administered in conjunction with anti-PD-1 antibody to treat established intracranial GL261 glioblastoma, this regime significantly improved the survival of mice, with 40% long-term survival observed (Antonios, Soto et al. 2016).

6.1.1. The intracranial B16 HHDII/DR1 proof of concept model

As discussed in chapter 4 the HHDII/DR1 mouse provides a mouse model that helps to closely emulate the human immune system in a pre-clinical mouse model. Previous research from chapter 4 has shown that the combined ImmunoBody[®] vaccines generates a strong anti-WT-1 and TRP-2 response. When SCIB1 and WT-1 ImmunoBody[®] vaccines are given together they generate splenocytes that are reactive to both WT-1 and TRP-2 to the same extent as singly vaccinated splenocytes. The B16 HHDII/DR1 cell line is a murine melanoma cell line that has been genetically modified to lack murine class I and II molecules, these class I and class II molecules have been replaced by a chimeric version of the human HLA-A2.1 class I molecule and the human HLA-DR1 class two molecule. What is also vital is that this cell line also expressed the TRP-2 and WT-1 antigens that were found to be expressed in human GBM tumours, and the antigenic targets of choice for ImmunoBody[®] vaccine therapy. What is also of great importance is that there is high homology between the murine and human TRP-2 and WT-1 peptide sequences. The TRP-2 180-188 (SVYDFFVWL) peptide sequence encoded in the SCIB1 ImmunoBody[®] is identical between both the human and mouse TRP-2 protein. Whilst the human and murine WT-1 peptide sequences are highly homologous between mouse and man, the sequence encoded by the WT-1 ImmunoBody[®] vaccine (5-19) is one amino acid different from the human sequence, the human sequence is VRDLNALLPAVPSLG whereas the murine sequence is VRDLNALLPAVSSLG. What is even more important is that the most stimulating class I peptide is one amino acid different between mouse and human. Gp100 does not have high sequence homology between mouse and humans, however this is of little concern as the ImmunoBody[®] vaccination did not generate a strong anti gp100 response and only one of the GBM tumours studied in chapter 3 expressed gp100.

6.2. Aims and hypothesis

The aim of this chapter is to see how efficient dual SCIB1 and WT-1 ImmunoBody[®] vaccination is at preventing and treating intracranial B16 HHDII/DR1 tumours in the C57BL6 HHDII/DR1 humanised mouse model. The addition of checkpoint blockade to the vaccination schedule will also be studied to see if the immune response can be boosted.

6.3. Results

6.3.1. Prophylactic vaccination with dual SCIB1 and WT-1 ImmunoBody® vaccination prolongs survival in mice bearing intracranial B16 HHDII/DR1 Luc2 tumours

In chapter 4 the use of the WT-1 and SCIB1 ImmunoBody® vaccines was shown to result in a peptide specific response to the TRP-2 and WT-1 peptides encoded within the ImmunoBody® construct. This dual vaccination also generated splenocytes that responded to GBM cells in an HLA-A2 restricted manner. The ability of this dual ImmunoBody® vaccination regime to prevent/delay the growth of intracranially implanted B16 HHDII/DR1 cells was then tested to see if these *in vitro* results translated into *in vivo* results. Mice were vaccinated as detailed in the methods section (chapter 2 section 2.2.) and seven days after the last vaccination 5×10^3 B16HHDII/DR1 Luc2 cells in 3 μ L PBS were implanted into the brains of these mice. This dosage of cells was previously shown to result in intracranial tumour development in 100 % of animals during optimisation experiments. The B16 HHDII/DR1 Luc2 cells had been transfected with the luciferase enzyme, this enzyme breaks down luciferin resulting in bioluminescence. This allowed for monitoring of *in vivo* tumour growth via intraperitoneal injection of luciferin followed by imaging on an IVIS machine (Perkin Elmer). Not only were the tumours monitored but the mice themselves were monitored to ensure their well-being. If mice experienced bodyweight loss (of more than 15% from baseline) or displayed any clinical signs they were humanely euthanised and their tissues were collected for analysis.

The B16HHDII/DR1 intracranial tumour model was chosen to act as a proof of concept model to prove that immune cells generated by the ImmunoBody® vaccine can affect tumours located within the brain. B16 is a murine melanoma cell line, but it displays aggressive growth much like GBM tumours. What was of even more importance was that *in vitro* analysis performed in chapter 3 revealed that these B16 HHDII/DR1 cells express both the TRP-2 and WT-1 antigens making them suitable targets. What is of even more importance is that these cells express the chimeric HLA-A2 molecule HHDII and the chimeric HLA-DR1 MHC class II molecule.

The prophylactic treatment of C57BL/6 HHDII/DR1 mice with dual ImmunoBody® vaccination significantly increased their symptom free survival after being challenged with intracranial B16 HHDII/DR1 tumours in comparison to sham (empty bullet) vaccinated mice. This result highlights the anti-tumour activity of the combined SCIB1 and WT-1 ImmunoBody® vaccines is sufficient to generate immune cells that can reach the brain and delay tumour formation.

Survival analysis

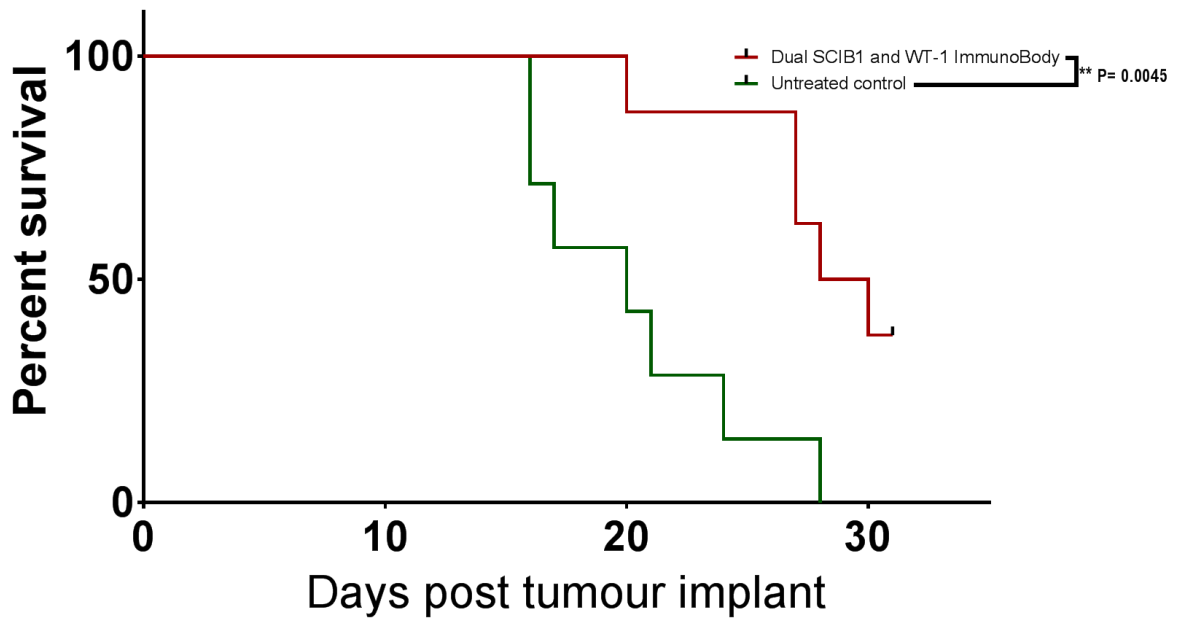


Figure 50. Kaplan-Meier survival analysis of mice prophylactically vaccinated with SCIB1 and WT-1 ImmunoBody[®] vaccination compared to unvaccinated mice. The green line represents the sham vaccinated control group, and the red line represents dually vaccinated mice. Control group n=7, treatment group n=8, ** = $P \leq 0.01$ as determined by the log rank test.

6.3.2. Addition of checkpoint blockade into the ImmunoBody[®] vaccination strategy effects on tumour bearing animal survival

Prophylactic analysis revealed that dual ImmunoBody[®] vaccination delayed the growth of intracranial B16HHDII/DR1 tumours. As a result, it was decided to see if the dual ImmunoBody[®] vaccination could affect the survival of mice bearing established intracranial B16 HHDII/DR1 Luc2 tumours. It was also decided to study if adding anti-PD-1 antibody checkpoint blockade to the vaccination regime could further increase survival of mice bearing established tumours. PD-1 was selected for targeting due to the interferon gamma induced expression of PD-L1 on tumour cells (see Chapter 5), this enables PD-1 blockade to counteract the active response of tumour cells to activated immune cells within the local environment. Clinical trialling of PD-1 blockade with pembrolizumab and CTLA-4 blockade with ipilimumab revealed in melanoma patients that ipilimumab is associated with increased high-grade treatment-related adverse effects when compared to pembrolizumab. Pembrolizumab was also shown to increase overall survival of patients with malignant melanoma when compared to ipilimumab (Robert, Schachter et al. 2015). Blockade of CTLA-4 has also been linked to an increased rate of liver damage when compared to anti-PD-1 therapies (Nishida, Kudo 2019). Whilst PD-1 blockade has some potential negative side effects its side effects appear to be less damaging than those associated with CTLA-4 blockade as a result the combination of ImmunoBody[®] vaccination with anti-PD-1 therapy was investigated.

Due to the aggressive growth of intracranial B16 HHDII/DR1 the vaccination schedule had to be altered to try and provide optimum protection before these tumours become fatal. During optimisation it was found that these tumours were usually fatal after around 21 days, meaning that the normal vaccination schedule may not be completed for many animals. Mice were immunised on days 3-, 7- and 10-days post tumour implant. This shortened vaccination regime has been previously used with ImmunoBody[®] vaccination in pre-clinical tumour models and it has shown to still provide anti-tumour benefits (Xue, W., Brentville, Symonds, Cook, Yagita, Metheringham, and Durrant 2016, Xue, W., Metheringham et al. 2016). As before tumours were monitored using luciferin and the mice were monitored for signs of malaise.

Dual ImmunoBody[®] vaccination combined with anti-PD-1 appeared to provide a moderate survival advantage for mice bearing intracranial B16 HHDII/DR1 tumours when compared to the dual ImmunoBody[®] vaccination with PD-1 isotype control, however when comparing both groups with the control there is no significant difference in survival (see *Figure 50*). There may be several reasons for this, one such reason is the undesired spread of the tumours within the brain (see *Figure 51*).

Survival analysis

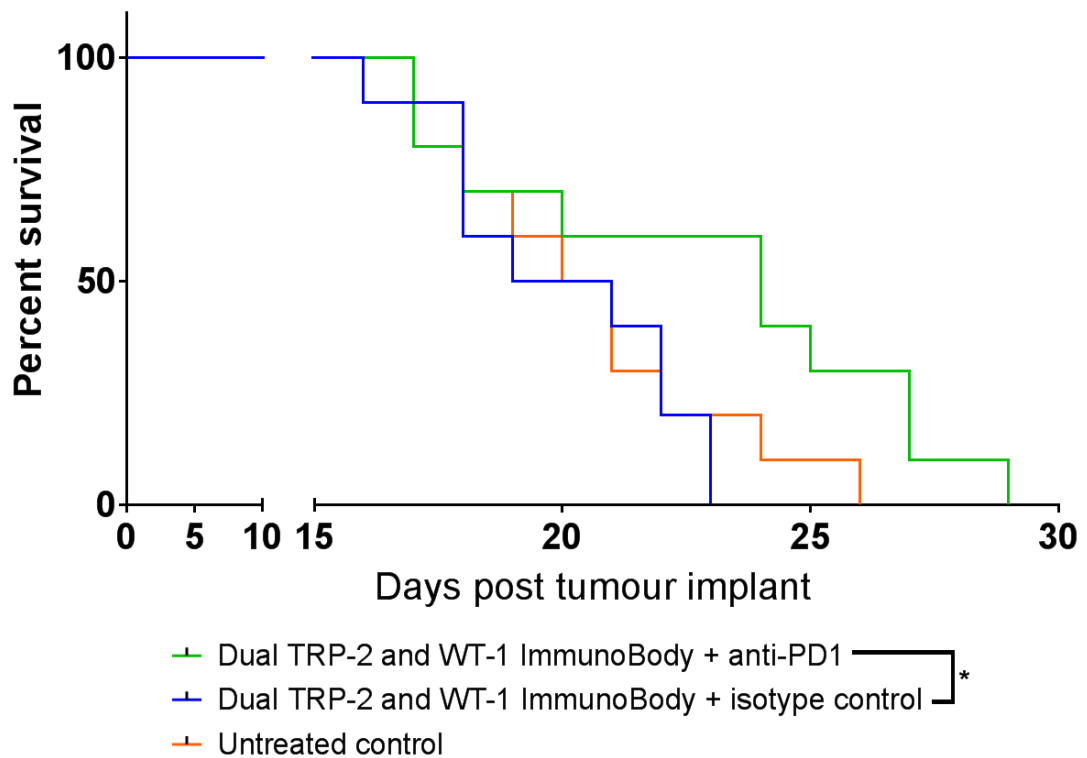


Figure 51. Kaplan-Meier survival analysis of intracranial B16 bearing HHDII/DR1 mice treated with dual SCIB1 and WT-1 ImmunoBody® vaccination either in combination with anti-PD-1 or PD-1 isotype control and untreated mice. N= 10. * = $P \leq 0.05$ as determined by the log rank test. The green line represents dually vaccinated mice that received anti-PD-1 antibody therapy, the blue line represents dually vaccinated mice that received isotype control antibody and the orange line represents the sham vaccinated control group.

In Figure 52 one can see that the injected tumours have spread to the cerebellum, whilst these tumours are relatively small, they are located within a vital area of the brain (in this case the cerebellum). The main reason for culling the animal was weight loss, the cerebellum has previously been linked to feeding control (Zhu, J. N., Wang 2008) and this may explain the weight loss observed. The cerebellum is also important for motor control and therefore tumours located within this region can cause serious clinical symptoms. Whilst brain tumours are highly invasive pre-clinical models of the disease are usually well contained and spread outside the area of implantation is uncommon. The spread of tumours from the site of injection is often as a result of tumour cells being injected into the cerebrospinal fluid located within the ventricles, this then leads to tumour spread down the cerebellum and spinal cord (Baumann, Dorsey et al. 2012).

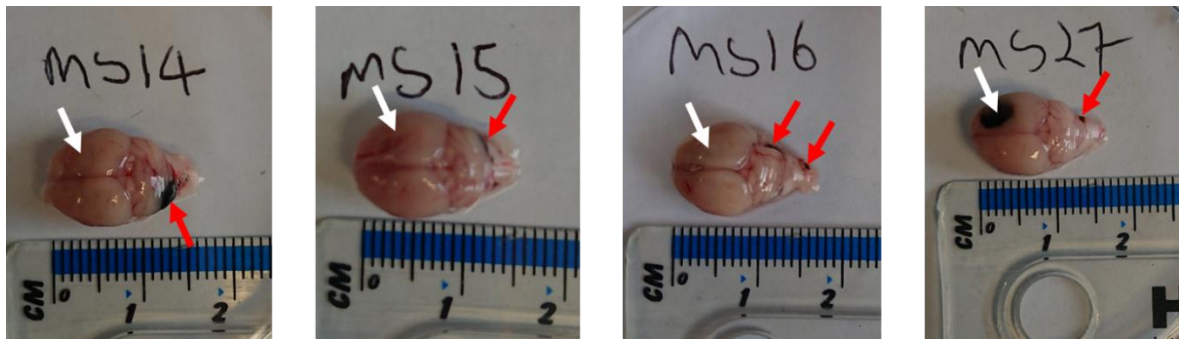


Figure 52. Some examples of the cerebellar spread of intracranially implanted tumours observed in the therapeutic study; cerebellar tumours are highlighted by the red arrows, the white arrow represents the site of cell injection. Mice 14-16 are from the dual ImmunoBody® + anti-PD-1 group and mouse 27 is from the untreated control group.

6.3.3. Flow cytometric analysis of brain tumour infiltrating lymphocytes from mice given therapeutic ImmunoBody® and anti-PD-1 treatment

Once mice displayed clinical symptoms or showed over fifteen percent body weight loss they were humanely euthanised and their brains were collected. The brains were then processed (as detailed in chapter 2 section 2.2.) allowing for the flow cytometric analysis of the brain tumour infiltrating lymphocytes. The gating strategy utilised is also detailed in chapter 2. CD3, CD4 and CD8 cell surface staining allowed for the identification of different T-cell subsets located within the tumour and these subsets were further analysed (an example of this flow cytometric analysis can be seen in appendix 3). Mice were split into three groups, group 1 had received dual TRP-2 and WT-1 vaccination with PD-1 isotype control antibody, group 2 received dual TRP-2 and WT-1 vaccination with anti-PD-1 blockade and finally group 3 represents untreated control mice. Dual ImmunoBody® vaccination increases the number of CD3, CD8 positive cells within the tumour infiltrating lymphocyte population (see *Figure 53*). The addition of anti-PD-1 immune checkpoint blockade to the vaccine regime does not appear to significantly alter the number of tumour infiltrating CD8⁺ cells so this indicates that the dual ImmunoBody® vaccination causes the increased CD8⁺ T-cell infiltrate observed.

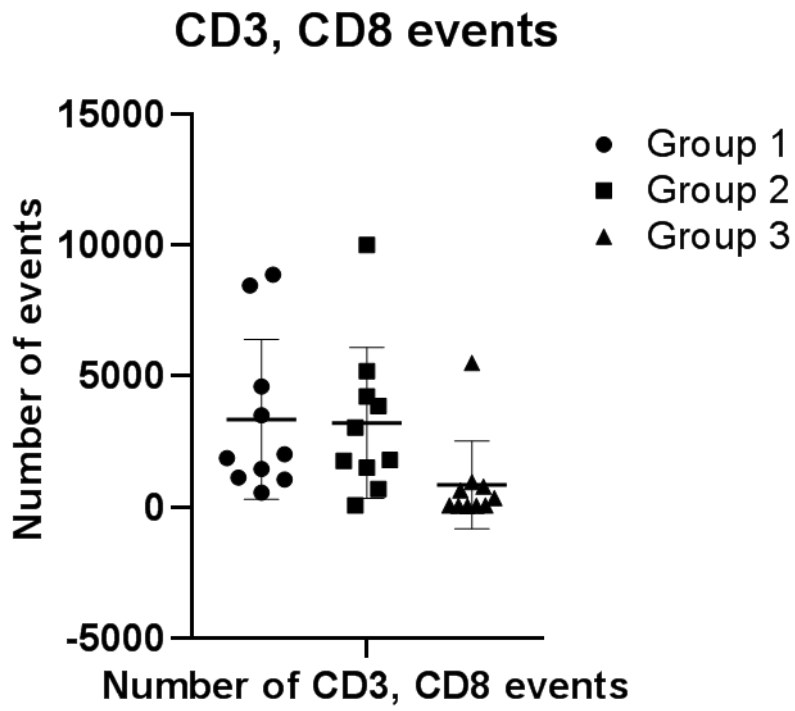


Figure 53. Number of CD3, CD8⁺ positive TILs obtained from intracranial B16HHDII/DR1 tumours. Group 1= Dual vaccination + PD-1 isotype control, Group 2= Dual vaccination + anti-PD1, Group 3= Untreated controls. N= 10.

Further analyses were only performed on runs in which over 500 CD3, CD8⁺ events were measured. Dual ImmunoBody[®] vaccination in combination with anti-PD-1 immune checkpoint blockade increases the percentage of CD8⁺ and CD4⁺ positive CD3 cells within the TIL population (see *Figure 54*). Dual ImmunoBody[®] vaccination with PD-1 isotype control also led to a slight increase in the percentage of CD4 and CD8 positive CD3 cells within the tumour. The increase in CD4 and CD8 T-cells is promising and indicates an active immune cell infiltration in the brain tumours of immunised mice.

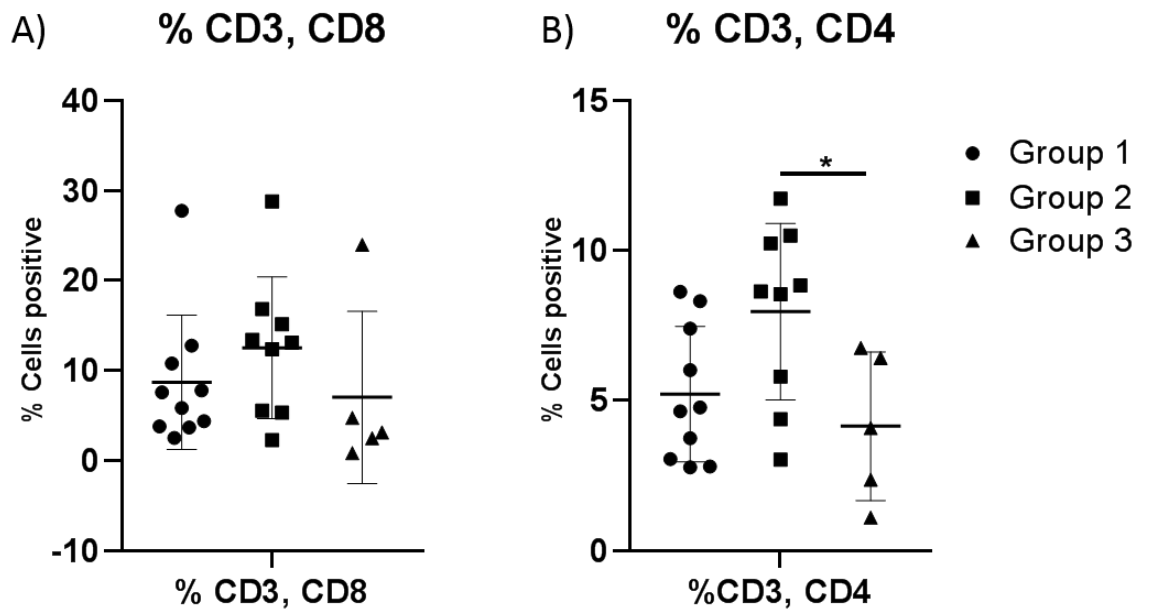


Figure 54. Percentage of A) CD3,CD4 and B) CD3,CD8 positive cells obtained from B16HHDII/DR1 brain tumour TILs. Group 1= Dual vaccination + PD-1 isotype control, Group 2= Dual vaccination + anti-PD1, Group 3= Untreated controls. N= 5-10. * = $P \leq 0.05$ as deemed by one way ANOVA followed by Tukey's ad hoc test.

When further studying the CD8 T-cell TIL population it can be seen that dual ImmunoBody® vaccination (with and without anti-PD-1) leads to an increased percentage of CD25 and CD69 positive CD8 T-cells (see *Figure 55*). CD25 and CD69 are T-cell activation markers indicating that the TIL populations from the vaccinated mice are actively responding to tumours. However there is also a high level of PD-1. This PD-1 expression is also indicative of activation, however the interaction of this PD-1 with PD-L1 on tumour cells can abrogate the anti-tumour response.

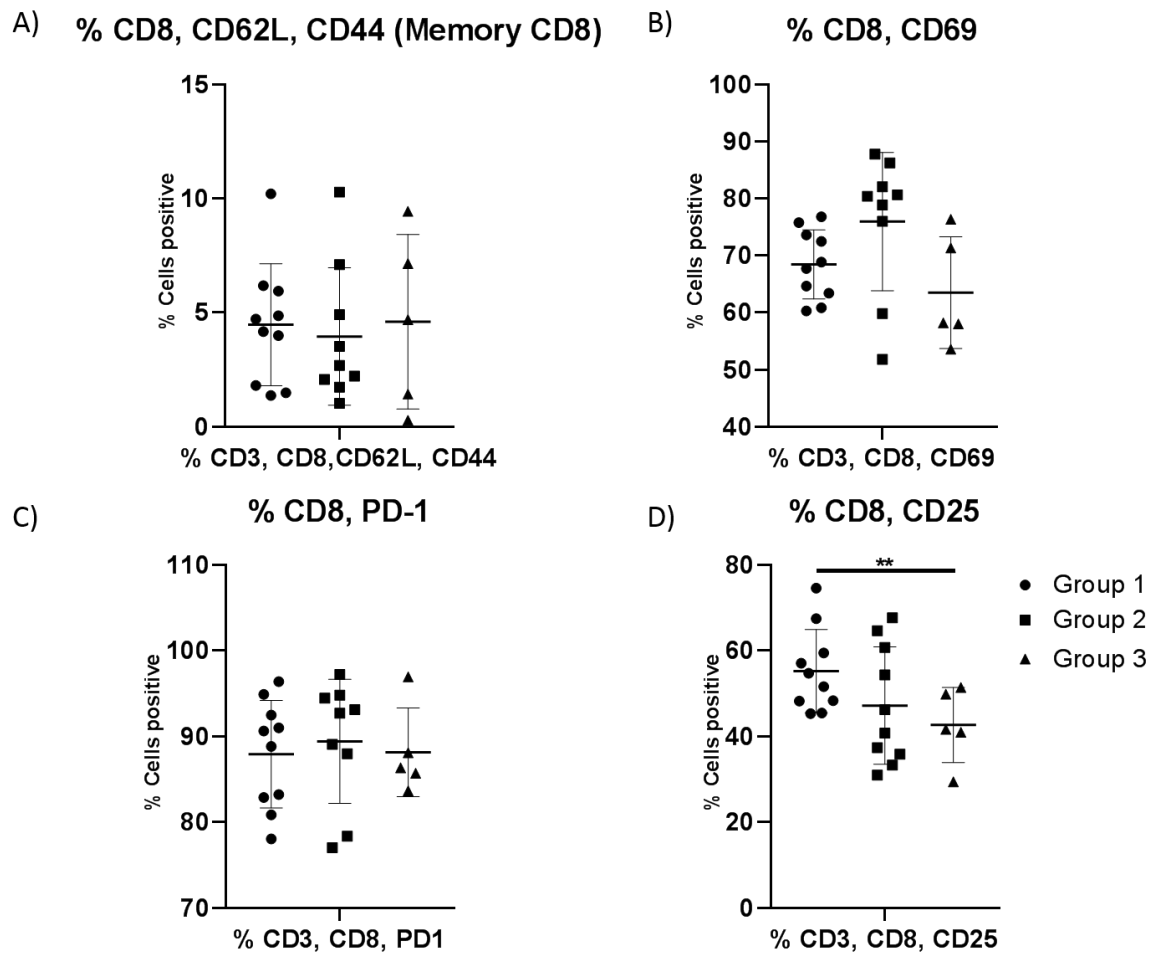


Figure 55. Flow cytometric analysis of CD3,CD8 positive cells obtained from B16HHDII/DR1 brain tumour TILs. A) CD62L and CD44 double positive cells (memory cells) B) CD69 positive cells C) PD-1 positive cells D) CD25 positive cells. Group 1= Dual vaccination + PD-1 isotype control, Group 2= Dual vaccination + anti-PD1, Group 3= Untreated controls. N = 5-10. ** = $P \leq 0.01$ as deemed by one way ANOVA followed by Tukey's ad hoc test.

When the CD4 T-cell population was further probed mice given the dual SCIB1 and WT-1 ImmunoBody® with anti-PD-1 blockade had increases in the number of CD25, CD69 and PD-1 CD4 T-cells. These markers indicate that there is also an active response from the CD4 T-cells as well as the CD8 T-cells in mice given ImmunoBody® vaccination and anti-PD-1. Unfortunately, these changes are not observed in mice given dual vaccination with the PD-1 isotype control (see *Figure 56*).

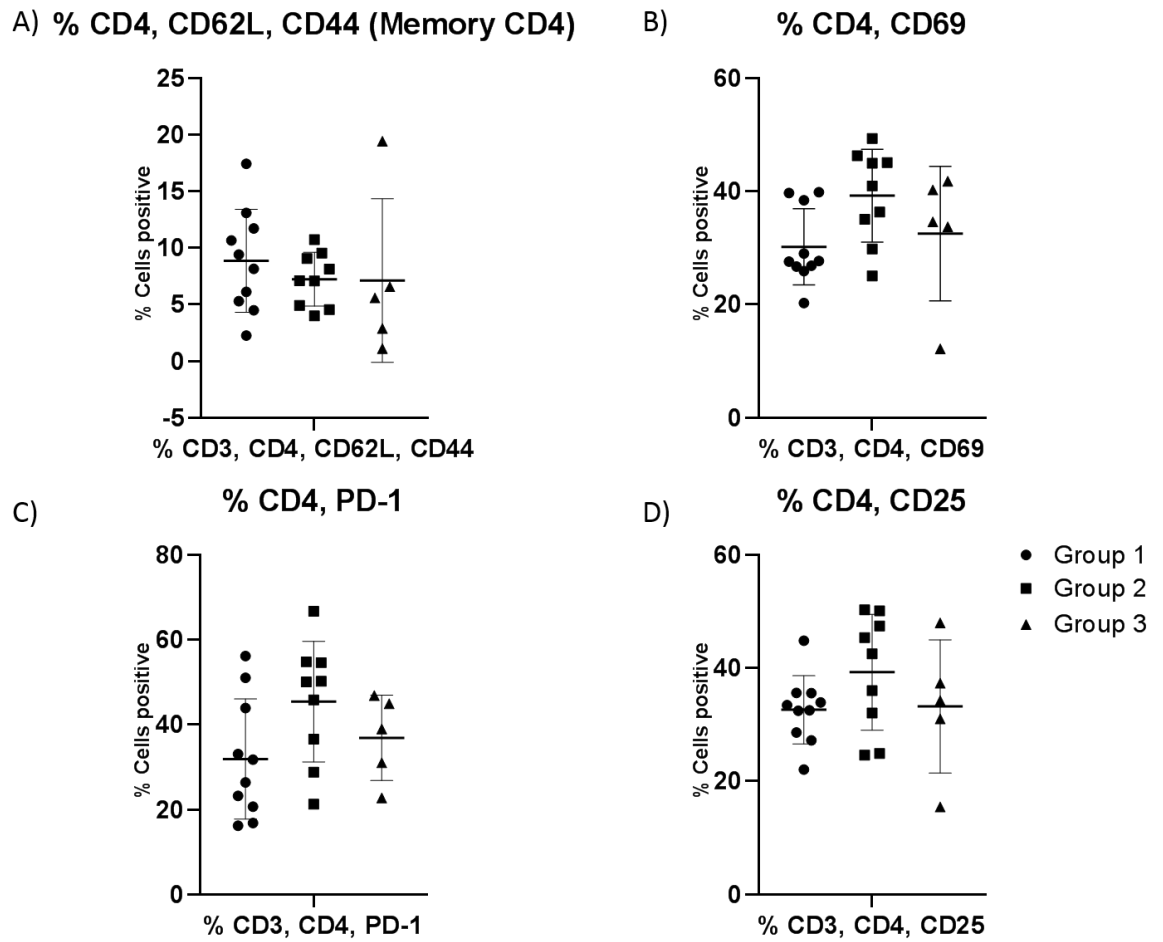


Figure 56. Flow cytometric analysis of CD3,CD4 positive cells obtained from B16HHDII/DR1 brain tumour TILs. A) CD62L and CD44 double positive cells (memory cells) B) CD69 positive cells C) PD-1 positive cells D) CD25 positive cells. Group 1= Dual vaccination + PD-1 isotype control, Group 2= Dual vaccination + anti-PD1, Group 3= Untreated controls. N = 5-10.

When looking at the regulatory T-cell populations, dual vaccination in conjunction with anti-PD-1 antibody leads to a marginally higher CD8 T-reg infiltrate into tumours compared to the dually vaccinated and untreated control groups (see *Figure 57*). Dual vaccination with PD-1 isotype control also appears to lead to an increase in the percentage of CD4 regulatory T-cells in the TIL population. The mice given anti-PD-1 in combination with dual vaccination did not seem to have the same CD4 T-reg cell infiltrate. Combination of vaccination with anti-PD-1 therapy has previously been shown to decrease the number of regulatory T-cells within B16 tumours (Curran, Montalvo et al. 2010). Whilst an increase in regulatory T-cells is undesirable it does indicate an active immune response within the TIL population.

6.4. Discussion

Whilst the survival of intracranial B16 HHDII/DR1 tumour bearing mice is not significantly improved by ImmunoBody[®] vaccine in combination with PD-1 blockade (when compared to unvaccinated mice) there is an increase in tumour infiltrating CD8 and CD4 cells. This increased immune infiltrate is promising and highlights that T-cells are actively entering the brain and accessing the tumour. What is even more promising is that since there is increased immune cell infiltration into the tumour there are ways of potentially boosting the anti-tumour immune effect. Tumours are highly immunosuppressive hence these infiltrating immune cells are not increasing the survival of tumour bearing mice. Whilst PD-1 blockade aims to improve the activity of these tumour cells there are a few limitations to this modality when treating tumours located within the brain. Previous research has found anti-PD-1 therapy to be ineffective at treating recurrent GBM (Filley, Henriquez et al. 2017). Failure may be due to the relative impairment that the blood brain barrier puts upon antibody penetration. The blood brain barrier usually prohibits entry of compounds that are larger than 400-600 Da, in the case of anti-PD-1 antibodies these are over 100 KDa in size so are excluded by the blood brain barrier. As a result, these anti-PD-1 antibodies bind to T-cells in the periphery, not those located within the tumour, this means that the majority of T-cells targeted by PD-1 blockade are not tumour specific (Filley, Henriquez et al. 2017). Antibody penetration into the brain is very low with only around 0.1% of peripherally administered antibodies entering the brain under normal conditions (Thom, Hatcher et al. 2018). As a result of this poor brain penetrance the blood brain barrier's effects need to be taken into account. The blood brain barrier functions to prevent the passage of large molecules into the brain parenchyma. Systemically administered antibodies have been shown to be present at much lower levels in the cerebrospinal fluid than the serum (the cerebrospinal fluid is a surrogate indicator of brain penetration by antibodies) (Wang, Q., Delva et al. 2018). The delivery of immune checkpoint blockade to the tumour may help to improve objective responses. One main advantage of locally delivering checkpoint blockade is that it can help minimise the off-target side effects sometimes observed. In a pre-clinical murine melanoma model localised delivery of anti-PD-1 using a locally applied biodegradable microneedle system was shown to be more efficient than systemically administered anti-PD-1 (Wang, C., Ye et al. 2017). In the GBM settings tumours are not as accessible as in the melanoma setting so as a result an alternative method for accessing these tumours needs to be considered. One highly invasive method that could potentially be utilised is an Ommaya reservoir, this is a catheter system that can be implanted within the brain with a subcutaneous injection site under the scalp that can be used to inject therapeutics down the catheter positioned within the brain. Unfortunately, the Ommaya reservoir creates some complications; improper placement of the catheter can cause serious damage to the brain and can even result in death of the patient. Due to the nature of the Ommaya reservoir patients are also at risk of developing infections, and in some cases these infections can also be

fatal due to the location of the reservoir within the brain (Mechleb, Khater et al. 2003, Perrin, Lishner et al. 1990). Another alternative method for delivering antibodies directly to the tumour is to simply administer anti-PD-1 into the surgical cavity of patients after tumour removal, one problem with this method is that only one dose can be given and therefore the anti-PD-1 may only have a short-term effect. Biodegradable wafers impregnated with anti-PD-1 could also be utilised to gradually dose the tumour bed post-surgically. Gliadel wafers are one such example of slow release biodegradable polymers used to directly deliver drugs into the surgical resection cavity of GBM tumours. Gliadel wafers are comprised of a polymer known as polifeproan20 combined with carmustine chemotherapy. This chemotherapy can access the brain when administered systemically however much like antibody therapy accumulation within the brain is fairly low. As a result biodegradable wafers were developed to directly deliver therapy to the tumour site (Kleinberg 2016). It would be of great interest to try and develop a biodegradable wafer that can slowly release IgG antibodies in the tumour resection cavity. An alternative less invasive method to improve antibody brain penetrance is to engineer antibodies so that they can cross the blood brain barrier. The ultimate aim is to get antibodies to penetrate the blood brain barrier without altering the structural integrity of the blood brain barrier. One such method may be to develop molecular Trojan horses; these are antibodies that are linked to protein ligands for receptors on the blood brain barrier. One such example of a receptor that can be used to cross the blood brain barrier is the transferrin receptor; OX26 is an antibody that binds to the rat transferrin receptor without affecting its ligand binding. Conjugation of peptides with this antibody has allowed for their therapeutic delivery to the brain (Neves, Aires-da-Silva et al. 2016). The affinity of these anti-transferrin receptor antibodies was altered via genetic engineering and antibodies with a lower binding affinity demonstrated better brain distribution due to their improved detachment from the transferrin receptors (Neves, Aires-da-Silva et al. 2016). The anti-transferrin antibodies are an effective way to deliver conjugated therapeutics across the blood brain barrier, but the interest of this project is to deliver therapeutic antibodies to the brain. This can be done by engineering bi-specific antibodies, so that one arm of the antibody is specific for the transferrin receptor, enabling antibody crossing and the other arm can be specific for PD-1 in this case (Neves, Aires-da-Silva et al. 2016).

It is also worth considering the application of neoadjuvant therapy, this is the administration of vaccination and anti-PD-1 prior to the surgical removal of the GBM tumour. Previous research indicates that neoadjuvant therapy may be the optimal way of utilising immunotherapy in the GBM setting. In an early phase clinical trial utilising the anti-PD-1 antibody Pemrolizumab in the neoadjuvant setting for patients with recurrent GBM Pemrolizumab therapy was found to lead to a significant increase in overall survival when compared to adjuvant Pemrolizumab therapy

(Cloughesy, Mochizuki et al. 2019). Neoadjuvant therapy is believed to lead to an expansion of tumour specific T-cells that can target any tumour cells that may have spread from the primary tumour site. The presence of the tumour also leads to up-regulation of PD-1 by the immune cells, making anti-PD-1 more effective (Melero, Berraondo et al. 2016).

One key factor that needs to be taken into account is the aggressiveness and rapid growth rate of the B16 melanoma cell line compared to other cell lines used to test GBM immunotherapy such as the GL261 cell line. Previous research has found that intracranial B16 tumours are more lethal than intracranial GL261 with mice dying at a much faster rate (Wainwright, Chang et al. 2014). PD-1 blockade has previously been paired with active immunotherapy in pre-clinical murine models to great effect. Antonios et al. (2016) demonstrated that vaccination with dendritic cells pulsed with GL261 lysate, in the established GL261 murine model of GBM increased the infiltration of T-cells into the brain tumour, however there was no significant increase in survival of these mice with established tumours. Tumour infiltrating lymphocytes appeared to express PD-1 on their surface to a much higher level than splenic lymphocytes as a result anti-PD-1 antibody therapy was combined with dendritic cell vaccination for the treatment of established GL261 tumours. This combination resulted in significant survival improvement, however 100% long term survival was not achieved. Both dendritic cell vaccination and anti-PD-1 alone did not improve the survival of mice with established tumours (Antonios, Soto et al. 2016). Part of the issues observed with animal survival in this thesis may be due to the tumour burden being too large to effectively target with dual ImmunoBody[®] and anti-PD-1 therapy, this may be remedied by injecting fewer tumour cells intracranially. Previous research has found that combinatorial immunotherapy combining CTLA-4, IDO and PD-L1 blockade is effective at treating the intracranial murine GBM cell line GL261 however this same efficacy was not observed when this regime is used to treat intracranial B16 melanoma (Wainwright, Chang et al. 2014). These tumours are highly aggressive and as a result therapy was commenced rapidly in these studies, with treatment being given three days after implantation of tumours. This triple therapy did expand the survival of mice, but this survival benefit was minimal compared to that witnessed in intracranial GL261. These differences are thought to be due to the presence of regulatory T cells within the tumours. Intracranial GL261 tumours were found to contain over ten times the amount of regulatory T-cells as intracranial B16 tumours (Wainwright, Chang et al. 2014).

This study utilised gene gun administration of the ImmunoBody[®] vaccination to the stomach of experimental animals. Whilst this location is fairly central with regards to the anatomy of the mouse, this is not the ideal location for targeting tumours located within the brain of these mice. Pre-clinical assessment of vaccine therapy for intracranial murine GBM has revealed that the vaccination site can affect the efficacy of the vaccine (Ohlfest, Andersen et al. 2013). Utilising an autologous tumour

lysate vaccine, mice were either vaccinated in the scruff of the neck, the foreleg and the hind leg; mice vaccinated in the hind leg were shown to have significantly increased long-term survival compared to mice vaccinated in the neck and foreleg. When staining for antigen specific T-cells with a dextramer, the frequency of dextramer positive CD8 T-cells decreased when T-cells were analysed from lymph nodes closest to the tumour. There was a threefold increase in dextramer staining when the TILs were analysed from mice vaccinated in the hind leg vs those in the neck. Vaccination closer to the tumour site resulted in suppressed effector function, with cytotoxic T-lymphocytes isolated from mice vaccinated the neck showing less *ex vivo* tumour cell killing than cytotoxic lymphocytes taken from mice vaccinated in the hind leg. These results indicate that immunosuppressive cells/cytokines drain from the tumours to their closest local lymph nodes impairing the function of immune cells within the vicinity of the tumour (Ohlfest, Andersen et al. 2013).

It is of importance to use a multi-faceted approach when tackling cancer, even pre-clinical animal models have shown that combination of vaccine therapy with checkpoint blockade does not lead to 100% survival. This indicates there are probably other factors worthy of consideration when treating cancers with combinatorial immunotherapy (Ali, Lewin et al. 2016, Xue, W., Brentville, Symonds, Cook, Yagita, Metheringham, and Durrant 2016). One issue with combining multiple immunotherapeutic modalities is the potential for immune over-activation, as a result it is worth looking at combining other treatment methods with immunotherapy to enhance the anti-tumour immune response. This may simply be in the form of dietary and lifestyle changes, or even by supplementation with natural anti-cancer therapeutics that are well tolerated and relatively cancer specific, one such example is the dipeptide carnosine.

6.5. Conclusion

Dual ImmunoBody® vaccination generates an anti-tumour effect that leads to a modest increase in T-cell infiltration into the intracranial tumours. This increased infiltrate unfortunately does not improve survival of mice with established tumours. Previous research has found that addition of immune checkpoint blockade with vaccination can help these infiltrating TILs overcome the immunosuppressive effects within the tumour microenvironment and generate an efficient anti-tumour response. Unfortunately combination of dual ImmunoBody® vaccination with anti-PD-1 antibody therapy did not increase the survival of these mice when compared to untreated mice. This failure of anti-PD-1 to rescue the anti-tumour immune response may be due to the intracranial location of these tumours. As a result it would be of great interest in future to look at local administration of checkpoint blockade or it would be useful to explore other potential combinations of therapy.

CHAPTER 7: CARNOSINE AS A NATURAL THERAPY FOR GLIOBLASTOMA MULTIFORME

7.1. Introduction

Carnosine is a dipeptide composed of β -alanine and L-histidine; it is a pleiotropic compound in that it has varying effects on different cell types. Carnosine increases the longevity of human fibroblast cells whereas on the other hand it seems to inhibit tumour cell growth. This tumour specificity is thought to be due to the metabolic changes that occur in tumour cells, with most cancers relying on glycolysis for their energy rather than oxidative phosphorylation (a phenomenon known as the Warburg effect) (Gaunitz, Hipkiss 2012). Carnosine has previously been shown to have anti-GBM properties, with carnosine treatment being shown to inhibit the growth of patient derived GBM tumour cells (Renner, Asperger et al. 2010). Numerous studies have revealed that carnosine has effects on many different cancer cell types and these effects are attributed to numerous different cell-signalling pathways and functions. These varied effects contribute to carnosine's enigmatic nature. Carnosine has numerous properties such as reactive oxygen species (ROS) scavenging and pH buffering. Carnosine has been shown to suppress ROS production in activated neurons (Boldyrev, Bulygina et al. 2004). Carnosine appears to inhibit anaerobic glycolysis in glioblastoma multiforme cells, reducing their levels of ATP production. This reduction in ATP production occurs as soon as 30 minutes after carnosine addition. Inhibition of mitochondrial oxidative phosphorylation with potassium cyanide did not alter GBM cellular ATP production and this did not affect the ability of carnosine to reduce ATP levels. However, inhibition of glycolytic activity with oxamate reduced ATP production greatly, carnosine had no effect on ATP levels of these cells. These results indicate that carnosine is an inhibitor of glycolysis in GBM cells (Renner, Asperger et al. 2010). Carnosine treatment of GBM cells appears to induce the expression of pyruvate dehydrogenase 4 (PDK4). PDK4 inhibits pyruvate dehydrogenase, this in turn results in reduced conversion of pyruvate into acetyl-CoA (Renner, Asperger et al. 2010).

One of the hallmarks of cancer is altered metabolism, this altered metabolism is acquired via numerous mutations and enables cancer cells to survive under the metabolic burden that is put upon them by their rapid growth. The Warburg effect is a phenomenon commonly seen in cancer, cancer cells prefer to generate their ATP via aerobic glycolysis rather than mitochondrial oxidative phosphorylation, and this enables these cells to thrive in a low oxygen environment. Brain tumours generate three times the amount of ATP by aerobic glycolysis than normal brain tissue (Wolf, Agnihotri et al. 2010). The proliferation of cancer cells requires more than just ATP. As a result cancer cells shift their metabolic patterns in order to produce many of the required macromolecules required such as nucleotides, lipids, proteins and fatty acids. The favouring of aerobic glycolysis

produces the metabolic intermediates required for production of the necessary macromolecules (Wolf, Agnihotri et al. 2010). Not only does aerobic glycolysis enable production of vital macromolecules it also results in production of lower levels of potentially harmful reactive oxygen species. Aerobic glycolysis also produces lactic and carbonic acid that is pumped out of cells into the tumour microenvironment, this acidic environment enhances tumour immune escape and increases tumour invasion (Wolf, Agnihotri et al. 2010). As mentioned above tumours rely on aerobic glycolysis for their energy production, producing lactic acid. Cancer patients have been shown to have elevated lactate levels within their serum and the level of lactate increases with tumour burden. Incubation of human cytotoxic T-lymphocytes with lactic acid after antigen-specific stimulation resulted in reduced proliferation and after long term exposure (24h) lactic acid induced CTL death. Lactic acid not only reduced proliferation of these cells it also effected their function, with reduced cytotoxicity observed and impaired IL-2 and IFN γ production observed (Fischer, Hoffmann et al. 2007).

Due to its ability to buffer pH and alter energy production in cancer cells carnosine offers a safe method for potentially aiding with the treatment of GBM. Whilst it has been shown that carnosine alters the metabolism and growth of GBM it provides an attractive method for making these cells easier to target immunotherapeutically.

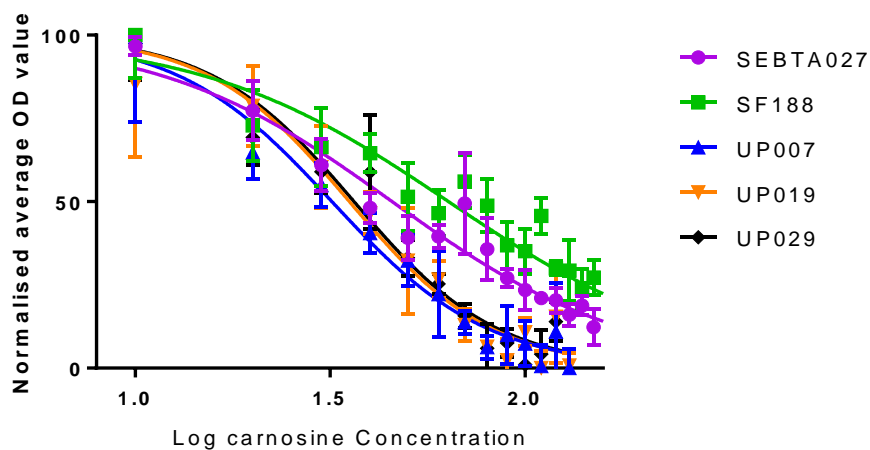
7.2. Aims and hypothesis

The aim of this chapter was to discover whether carnosine exerts anti-tumour effects against the human GBM cell lines SEBTA-027, SF188, UP-007, UP-019 and UP-029 and the murine GBM cell line GL261Luc2 by altering their mitochondrial metabolism, this was assessed via a 3-(4,5-dimethylthiazol-2-yl)-2,5-diphenyltetrazolium bromide (MTT) assay. Carnosine's use will then be explored *in vivo* to see if any effects *in vitro* translate into an anti-tumour effect *in vivo*.

7.3. Results

7.3.1. Effects of carnosine on the mitochondrial activity of glioblastoma multiforme cell lines

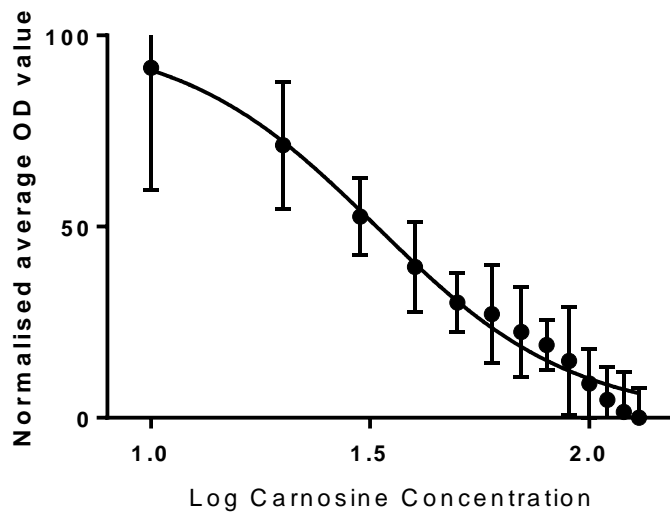
Due to the previously reported activity carnosine has on the metabolic activity of GBM cells it was decided to test this activity on several GBM cell lines which have not been previously treated with carnosine. An MTT assay was used to measure the mitochondrial activity of carnosine treated GBM cells.



	SEBTA027	SF188	UP007	UP019	UP029
Sigmoidal dose-response (variable slope)					
Best-fit values					
Bottom	= 0	= 0	= 0	= 0	= 0
Top	= 100	= 100	= 100	= 100	= 100
LogEC50	1.659	1.804	1.504	1.549	1.561
HillSlope	-1.452	-1.363	-2.177	-2.382	-2.363
EC50	45.6	63.63	31.94	35.43	36.39

Figure 58. MTT dose response curves for human GBM cells treated with carnosine. The EC50 for each cell line is displayed in the table below the dose response curves, with the value shown representing the mM concentration. Carnosine was applied to cells for 24 hours prior to performing the MTT assay. N=3.

The MTT assay results reveal that carnosine appears to reduce the metabolic activity of human GBM cell lines in a dose dependent manner. Dose response curves reveal that the EC50 for all of these cell lines is within a similar dose (30-65 mM carnosine) with the SF-188 cell line requiring the highest concentration of carnosine (63.63 mM) and the UP-007 cell line requiring the least (31.94 mM). The effects of carnosine were also tested on the murine GL261 Luc2 cell line to see if the metabolic changes observed were ubiquitous across murine and human GBMs, enabling pre clinical modelling to be performed.



	GL261 Luc 2
Sigmoidal dose-response (variable slope)	
Best-fit values	
Bottom	= 0
Top	= 100
LogEC50	1.515
HillSlope	-1.943
EC50	32.72

Figure 59. The MTT dose response curve for the murine GBM cell line GL261 treated with carnosine. The EC50 value is shown below the dose response curve, with the number being shown representing the mM concentration. Carnosine was applied to cells for 24 hours prior to performing the MTT assay. N= 3.

The MTT assay results reveal that carnosine appears to reduce the metabolic activity of the murine GL261 Luc2 GBM cell line with it having an EC50 of 32.72 mM.

7.3.2. Effects of carnosine on the migration of glioblastoma multiforme cells

Due to the invasive nature of GBM it was decided to test how carnosine affects the migration of GBM cell lines in order to see if it could be potentially used to prevent the invasion and migration of GBM cells post-surgically. In order to test if carnosine affected GBM cell line migration scratch assays were performed. In order to do this cells were grown on a 96-well plate to almost 100 % confluence, once confluent a scratch was made using an Essen bioscience wound maker. Once the scratch was made the media was removed from the cells and they were gently rinsed with PBS twice. After rinsing the media was replaced and in the case of carnosine treated cells carnosine containing media was added (at a ctrl 0 mM and EC75 dose). The plate containing cells was then placed into an IncuCyte machine which took pictures every 2 hours. The IncuCyte software was then used to measure the relative wound density giving a representation of wound closure. The SF-188 and SEBTA-027 cell lines were examined due to their antigen expression profile and their potential use in future tumour modelling experiments. Below in *Figure 60* and *61* are the results from the SF-188 cell line.

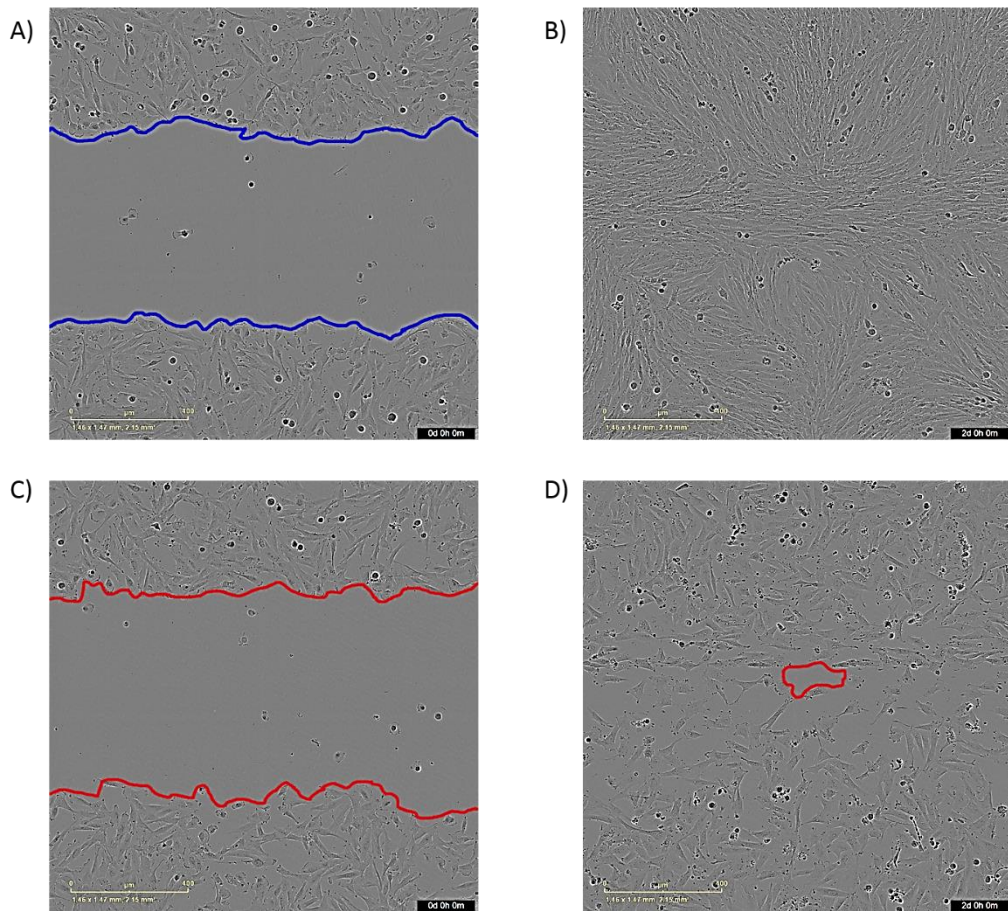


Figure 60. Microscope images of SF-188 scratch closure A) 0h control B) 48h Ctrl C) 0h EC75 D) 48h EC75. Scale bar = 400 μ m.

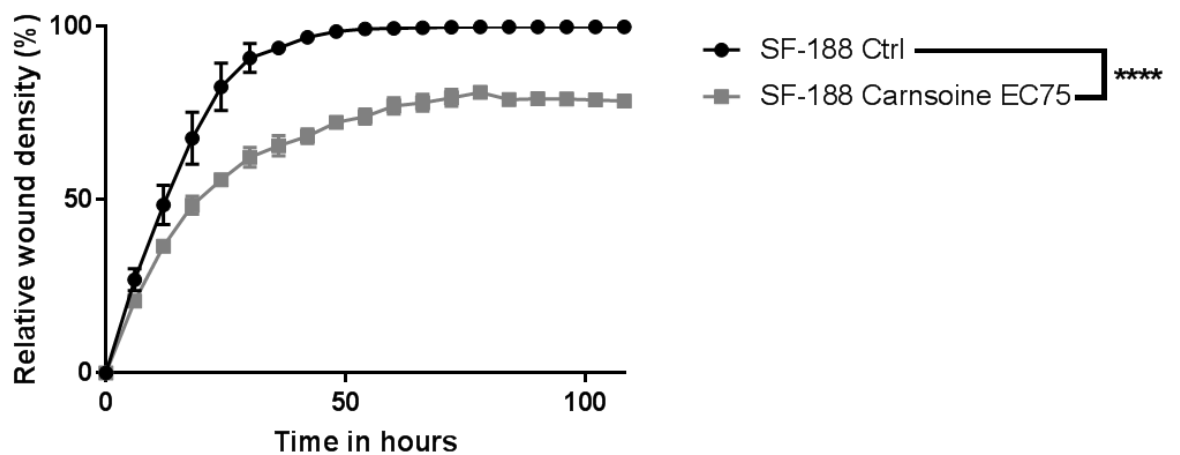


Figure 61. Scratch assay results from SF-188 cells with and without carnosine. Control cells were grown in normal media and carnosine treated cells were given the EC75 dosage as calculated by the MTT dose response curves. N = 3 **** = $P \leq 0.0001$ as deemed by a paired T-test.

Carnosine was shown to significantly reduce the migration of SF-188 cells (see *Figure 62* and *63*) in scratch assays. Control untreated cells appear to close the wound after around 40 hours, with regards to cell treated with the carnosine EC75 they never fully closed the wound after a period of 96 hours. When studying the wound closure microscopically the SF-188 cells can be seen to migrate at a slower rate when treated with carnosine, also of interest was the fact that these cells do not appear to be dying (there are very few cells seen floating or rounded). These results taken with the MTT results indicate that carnosine's anti-cancer activity is mediated by its ability to alter the metabolic function of these cells and not via the direct induction of cell death.

It was also decided to see if carnosine had the same effects on the SEBTA-027 cell line since the SF-188 and SEBTA-027 cell lines are of interest due to their antigen expression profiles. As a result, scratch assays were performed in the same manner as they were for the SF-188 cell line. The results are shown below in *Figure 62* and *63*.

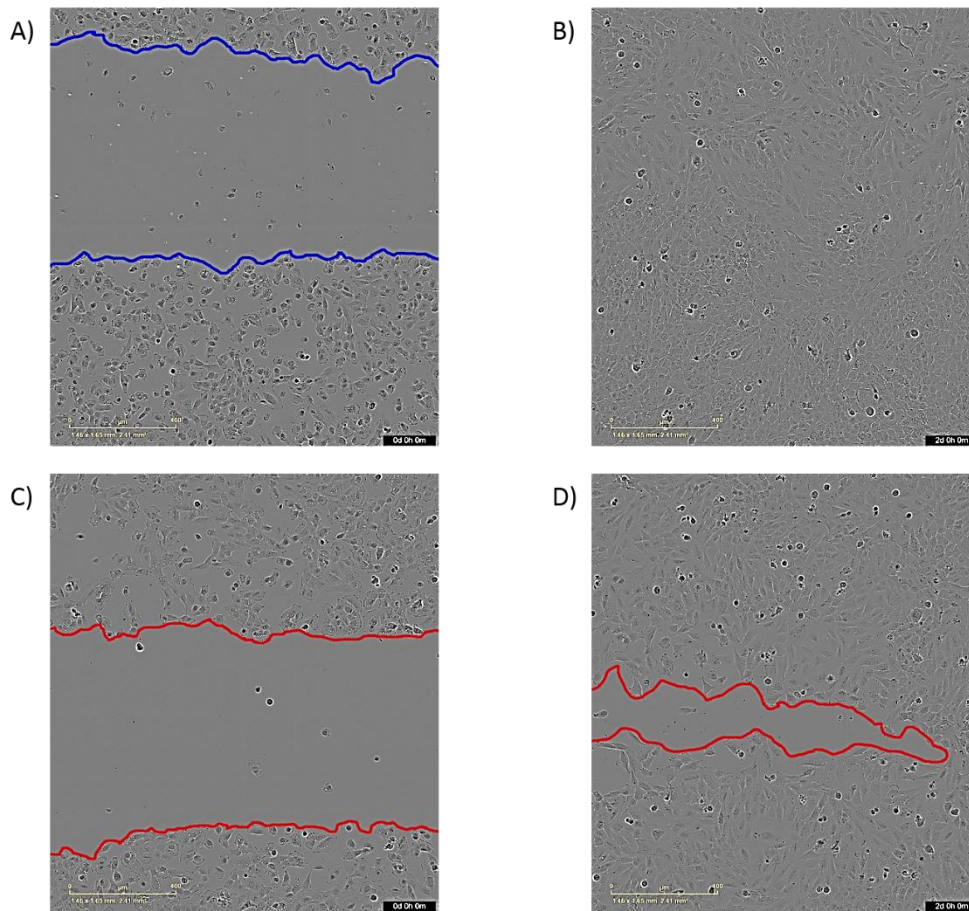


Figure 62. Microscope images of SEBTA-027 scratch closure A) 0h control B) 48h Ctrl C) 0h EC75 D) 48h EC75. Scale bar = 400 μ m.

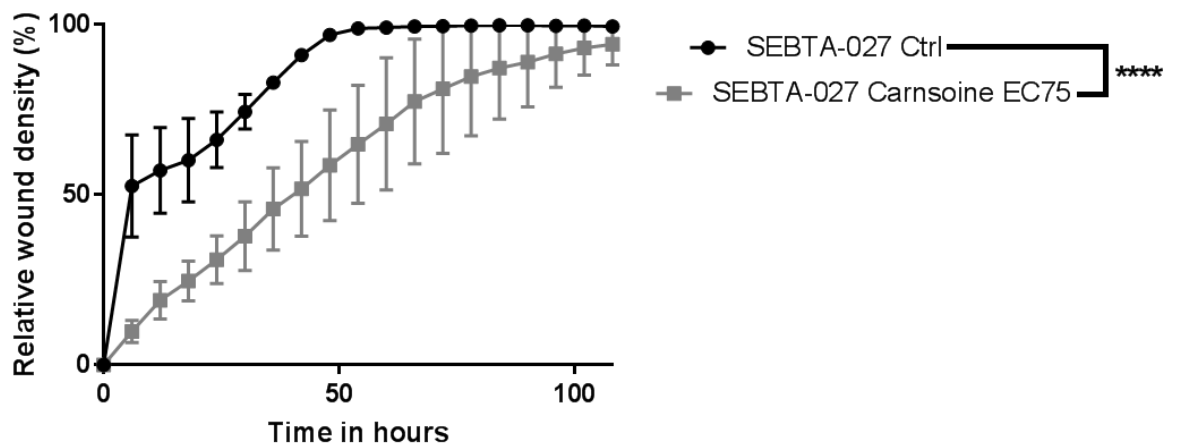


Figure 63. Scratch assay results from SEBTA-027 cells with and without carnosine. Control cells were grown in normal media and carnosine treated cells were given the EC75 dosage as calculated by the MTT dose response curves. $N = 3$ **** = $P \leq 0.0001$ as deemed by a paired T-test.

Carnosine appears to have the same effect on wound closure for the SEBTA-027 cell line as it did for the SF-188 cell line. Carnosine treated cells showed a slower wound closure compared to control cells grown with normal media (see *Figure 62*). Microscopic analysis reveals the same trend as that seen in the SF-188 cell line with the cells appearing to show reduced migration and very little cell death being observed.

Seeing as the effects of carnosine were studied in human cell lines it was also decided to test the effects of carnosine on the murine GBM like cell line GL261 Luc2. Scratch assays were performed in exactly the same manner as they were for both of the human cell lines. The results are shown below in *Figure 64* and *65*.

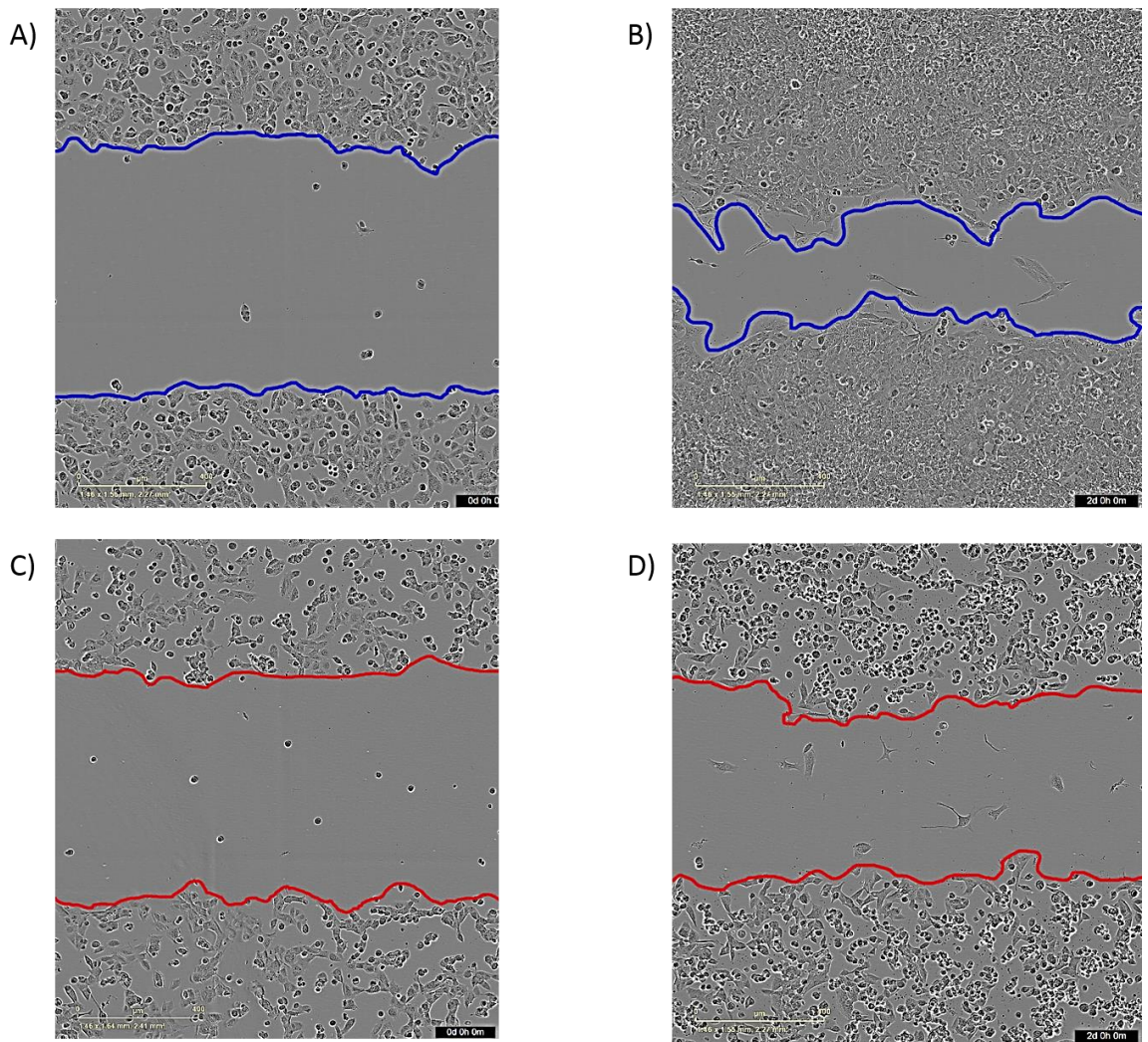


Figure 64. Microscope images of GL261 Luc2 scratch closure A) 0h control B) 48h Ctrl C) 0h EC75 D) 48h EC75. Scale bar = 400 μ m.

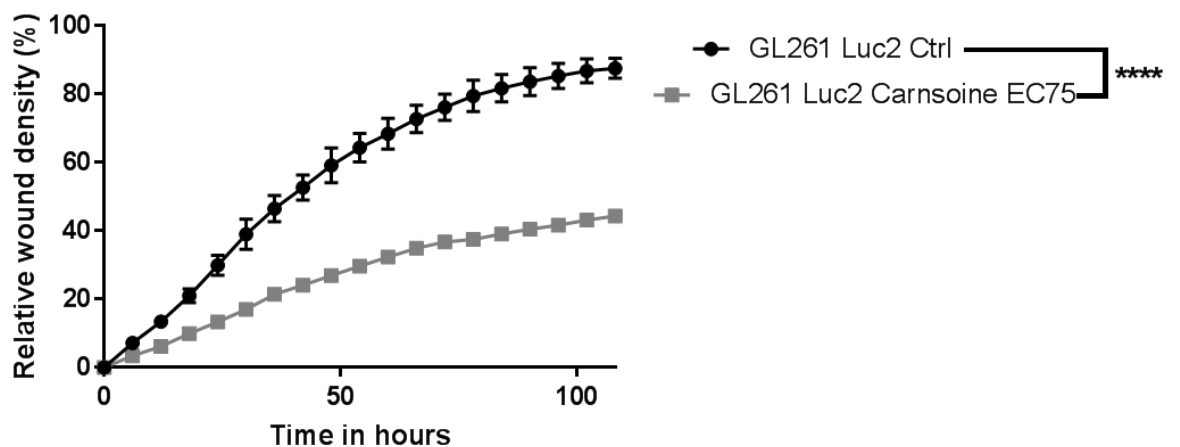


Figure 65. Scratch assay results from GL261 Luc 2 cells with and without carnosine. Control cells were grown in normal media and carnosine treated cells were given the EC75 dosage as calculated by the MTT dose response curves. $N = 3$ **** = $P \leq 0.0001$ as deemed by a paired T-test.

Carnosine seems to have a much greater effect on the migration of the GL261 Luc2 cell line than the human GBM cell lines studied. After 96 hours of carnosine treatment the wound density of carnosine treated GL261 Luc2 cells was never higher than 40%. When looking at the GL261 Luc2 cells microscopically carnosine appears to have a marked effect with a large number of cells appearing rounded. The murine GL261 Luc2 cell line appears to have a more visible response to carnosine therapy than the human cell lines studied. Previous research and the MTT results reveal that carnosine has an effect on the metabolism of GBM cells (Renner, Asperger et al. 2010, Oppermann, Faust et al. 2019). The differences observed between the human and murine GBM cell lines may be due to the metabolic differences between the two species that these cells originate from. Mice have a higher metabolic rate than humans due to their smaller size and greater surface area to volume ratio (Demetrius 2005). Because carnosine effects mitochondrial metabolism its effects would be expected to be heightened in a murine cell line due to the increased metabolism, these results support this hypothesis.

7.3.3. *In vivo* effects of carnosine GL261 Luc2 bearing NOD-SCID mice

After studying the effects of carnosine *in vitro* it was decided to see what effects carnosine could have on the *in vivo* growth of GL261 Luc2 tumours. A single 20 μ L of 1M dose of carnosine dissolved in PBS was injected intratumourally into subcutaneous GL261 Luc2 cells grown in the flank of NOD-SCID mice. A control group of mice received the same volume (20 μ L) of PBS without carnosine.

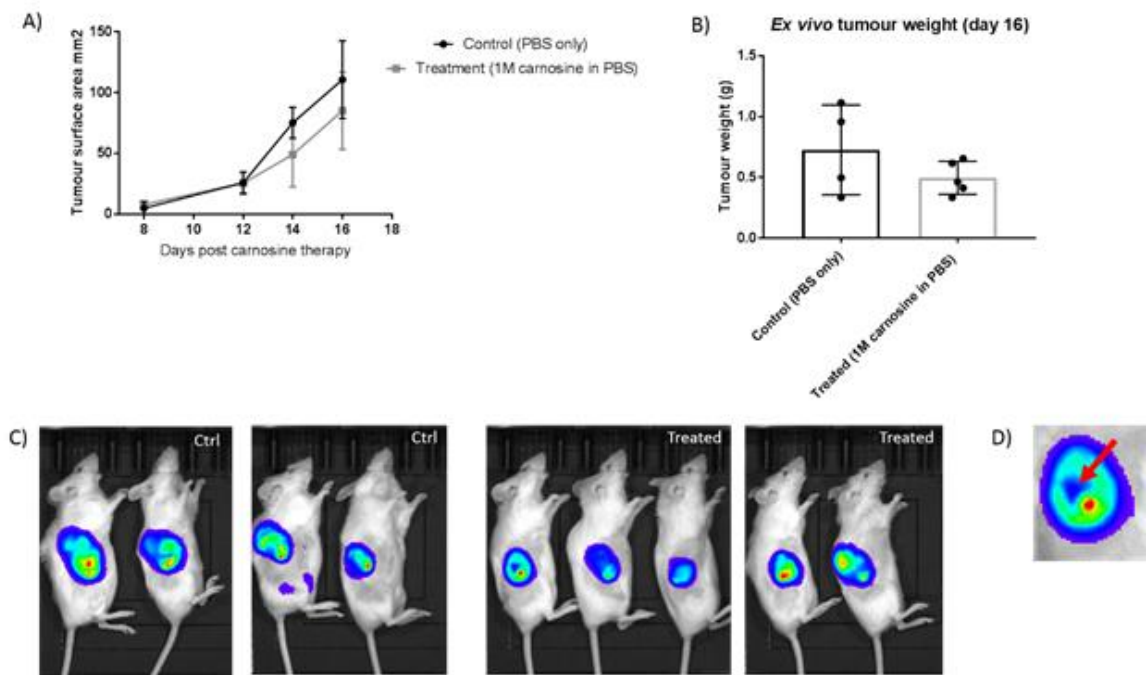


Figure 66. A) Tumour surface area measurements of GL261 Luc2 tumours taken from carnosine and PBS treated mice. B) Weights of tumours excised 16 days after carnosine treatment. C) In vivo bioluminescent images taken on day 16 post carnosine therapy, the left 4 mice are control mice and the 5 on the right are carnosine treated. D) Close up of an in vivo image of a carnosine treated tumour, the red arrow highlights an area of reduced tumour growth at the site of injection. Red indicates high luciferase activity (indicative of greater tumour size), and blue represents areas of less luminescence.

Intratumoural injection of a single dose of 1M carnosine reduces the size of GL261 Luc2 tumours implanted in the flank of NOD-SCID mice (See *Figure 66. A) and B)*), what is also of interest is that there appears to be an area of specific tumour reduction in the area of injection (see *Figure 66. D)*). These results indicate that a single intratumoural dose of carnosine can reduce the size of GL261 Luc2 tumours.

7.4. Discussion

The MTT assay results reveal that carnosine has anti-metabolic activity on the GBM cells studied, and this anti-metabolic activity is also evident in the murine GL261 Luc2 GBM cell line. The MTT assay relies on mitochondria converting MTT into formazan resulting in a colour change that is a surrogate marker for mitochondrial activity. Not only does carnosine appear to alter the metabolism of these cells it also appears to alter their motility with the scratch assay revealing that carnosine slowed down scratch closure in both a human and murine GBM cell lines. This result is highly promising for the prospect of carnosine as a GBM therapeutic, as these tumours are renowned for their migration and invasion within the brain with recurrence being inevitable after roughly 32 – 36 weeks (Hou, Veeravagu et al. 2006). Carnosine also appears to reduce tumour growth in a NOD-SCID GL261 Luc2 subcutaneous model. This *in vivo* action of carnosine can be attributed to the direct activity of carnosine on the cells seeing as the NOD-SCID mouse is an immunocompromised mouse, ruling out the contribution of the immune compartment in the anti-tumour activity of carnosine.

Previous research has shown that in an *in vitro* co-culture system with T98G GBM cells and normal fibroblast cells, T98G cells were grown within a cloning ring and fibroblasts were grown outside of the cloning ring, addition of carnosine to this co-culture system was then studied. When the cloning ring is removed T98G cells invade the fibroblast layer and form multiple colonies, when carnosine was added to the co-culture system the T98G cells formed less colonies and had a reduced invasion of the surrounding fibroblast layer (Oppermann, Dietherle et al. 2018). This selective inhibition of the GBM cells whilst the surrounding normal fibroblast cells are left intact is what makes carnosine such an attractive therapy. These findings clearly indicate that carnosine has a cancer specific effect. Furthermore, carnosine could also be of use for its protective effects especially when combined with radiotherapy and chemotherapy by reducing the bystander effects that these therapies have on normal cells within the body, especially when dealing with a sensitive organ such as the brain. Radiotherapy results in the generation of radical species and the release of pro-inflammatory cytokines that result in cellular death (Alan Mitteer, Wang et al. 2015, Tabatabaei, Visse et al. 2017).

Due to the reactive species scavenging and anti-oxidant effects of carnosine it can protect tissues from the deleterious effects that reactive species and inflammation can have. Carnosine has been shown to improve the survival of mice receiving whole body irradiation. One concern may be that these protective effects may impede the anti-tumour effect of radiotherapy. In humans the use of a carnosine-zinc complex for head and neck cancer patients was shown to reduce oral mucositis whilst no negative effects on the radiotherapy were observed (Gaunitz, Hipkiss 2012).

One key factor to take into account when using carnosine is the presence of the enzyme carnosinase. This enzyme actively breaks down carnosine into its constitutive peptides potentially nullifying its effects (Sauerhofer, Yuan et al. 2007). If L-carnosine is systemically administered carnosinase breaks down carnosine preventing it from reaching tumours and exerting its effects. As a result, it is of great interest to synthesise biosimilar chemicals that have the same activity as carnosine but overcome the cleavage by carnosinase. In the GBM setting it may be worth examining the use of L-carnosine in the surgical resection cavity or implanting slow release devices to administer carnosine temporally. Carnosine naturally occurs at a high level in the brain where it is believed to play a protective role (Stvolinsky, Kukley et al. 1999). Carnosine is synthesised by the enzyme carnosine synthase, this enzyme combines β -alanine and L-histidine to produce carnosine, this enzyme was found to be at high levels within the murine brain (Harding, O'Fallon 1979). Carnosine is also abundant in skeletal muscle where it has been shown to regulate the intramuscular pH and prevent fatigue. Carnosine synthase is responsible for the synthesis of carnosine within the muscle and β -alanine has been shown to be the limiting factor with regards to carnosine synthesis. As a result, β -alanine supplementation is utilised to improve exercise performance and reduce muscular fatigue via an increase in intramuscular carnosine concentration and therefore lactic acid buffering capacity (Artioli, Gualano et al. 2010). Due to the presence of carnosine synthase in the brain and carnosinase in the serum it may be worth considering systemic administration of β -alanine as opposed to carnosine as a method for increasing levels of intracerebral carnosine in GBM patients.

The clear anti-migratory effects that carnosine has on GBM cells would make it a useful first line therapeutic, it would be of great benefit to administer carnosine to the resection cavity of GBM tumours post-surgery, prior to the potential application of immunotherapy; this carnosine would act to prevent the invasion of any residual cells into the surrounding brain. Seeing as the focus of this thesis is on immunotherapy it would be of great interest to study the effects of carnosine on the immune cells. Previously carnosine has been shown to extend the *in vitro* lifespan of CD4 T-cells. This longevity was attributed to the reactive species scavenging properties of carnosine reducing levels of oxidative DNA damage within these cells (Hyland, Duggan et al. 2000). This provides great promise for combining carnosine therapy with immunotherapy. The *in vivo* data presented here reveals that intratumoural carnosine slows the growth of GBM tumours, this effect

was studied in NOD-SCID mice so the effects seen can be attributed to carnosine's direct activity on tumour cells. It would be of great interest to see how carnosine effects tumours in immunocompetent mice, this would reveal the potential interaction between the immune compartment and carnosine.

7.5. Conclusion

Carnosine was shown to alter the mitochondrial metabolism of GBM cells, and to reduce the growth and migration of these cells. Intratumoural delivery of carnosine was also able to slow tumour growth *in vivo* as well as *in vitro*. As a result of these findings carnosine shows great promise as an adjunct therapy for GBM. Whilst carnosine does not appear to kill GBM cells it does slow their migration which is of great therapeutic benefit in the GBM setting, especially when considering the combination of immunotherapy with carnosine therapy. The tumour specificity and lack of serious side effects make carnosine a treatment worth considering in the GBM setting.

CHAPTER 8: DISCUSSION AND FUTURE WORK

Glioblastoma multiforme remains one of the cancers with the worst prognosis and poorest patient survival. Despite decades of research very little has changed with regards to the therapeutic landscape of GBM. Radiotherapy, temozolomide chemotherapy and surgical interventions remain the current 'gold standard' for GBM therapy. Immunotherapy provides an attractive therapy modality for this type of cancer due to its high specificity and the ability of activated immune cells to activate the brain parenchyma, traversing the blood brain barrier (a hindrance for many molecular therapies). Whilst immunotherapy has garnered significant interest for the treatment of GBM many immunotherapeutic approaches have failed during clinical trial testing (Weller, Butowski et al. 2017, Filley, Henriquez et al. 2017). As a result, alternative immunotherapeutic approaches need to be explored in order to discover an effective therapy. Glioblastoma multiforme is also known to be highly immunosuppressive and this may be a reason for the failure of immunotherapeutic modalities, therefore future clinical trials using immunotherapeutic approaches will need to take this into consideration, combining active immunotherapy with checkpoint blockade.

The aim of this thesis was to try and develop a new immunotherapeutic approach for the treatment of glioblastoma multiforme tumours. This involved the identification and targeting of immunotherapeutic antigens expressed by GBM. In order to try and overcome the immunosuppressive nature of GBM a novel vaccine platform known as the ImmunoBody[®] has been utilised to generate an immune response. ImmunoBody[®] is a DNA plasmid vaccine that encodes an IgG molecule with the peptides of interest engrafted into its complementarity determining regions. This method of vaccination has shown great pre-clinical promise and can generate a strong anti-tumour immune response that has shown efficacy as a monotherapy for the treatment of pre-clinical melanoma (Pudney, Metherringham et al. 2010). GBM is notoriously immunosuppressive with GBM cancers being shown to express immunosuppressive cytokines such as TGF β and IL-10, not only do GBMS secrete immunosuppressive cytokines they have also been shown to express the immunosuppressive ligand PD-L1 on their surface (Nduom, Weller et al. 2015). PD-L1 on GBM cells binds to the PD-1 receptor on activated T-cells, this binding leads to inhibition of T-cell activity. What is also of great importance is that the pro-inflammatory cytokine IFN γ leads to induction of PD-L1 on tumour cells meaning that activated immune cells releasing IFN γ within the tumour microenvironment can cause cancers to actively adapt to the immune pressure put upon them (Topalian, Drake et al. 2012). This PD-1/PD-L1 interaction has been blocked in the clinical setting with the aim of boosting the anti-tumour response. Due to the immunosuppressive nature of GBM it would be of great interest to combine ImmunoBody[®] vaccination with PD-1/PD-L1 blockade. The

rationale for combining these two treatment modalities is to generate an anti-tumour immune response via vaccination and then boost this response by preventing the immune dampening PD-1/PD-L1 interaction.

8.1. GBM tumours express immunogenic antigens that make them targetable with immunotherapy however they also have an immunosuppressive phenotype

Analysis of GBM cell lines and tumours tissue sections from GBM patients revealed that these tumours express a variety of antigens that could be targeted with immunotherapeutic approaches. The WT-1 and TRP-2 antigens were identified as potential immunotherapeutic targets worth further study due to their prevalence in both tumour tissues and cell lines. TRP-2 is a well-known immunogenic antigen commonly targeted in the melanoma setting (Patel, P. M., Ottensmeier et al. 2018, Bronte, Apolloni et al. 2000). Melanocytes in the skin and glial cells within the brain are both derived from the neuroectoderm during embryogenesis, as a result tumours of the brain and tumours of the skin express many of the same antigens. As a result of this shared lineage the expression of many melanoma antigens has been explored in GBM tumours. TRP-2 expression has previously been shown to be in a relatively high percentage of GBM cases (62- 34%), however its expression is not ubiquitous across all GBM cases (Chi, Merchant et al. 1997, Saikali, Avril et al. 2007, Liu, G., Khong et al. 2003). In addition, in order to avoid the risk of seeing the emergence of a clone of cells resistant to the vaccine due to antigen loss (immune escape variant), it was thought wise to target two independent antigens. The WT-1 antigen was chosen due to its known immunogenicity and due to its previously reported expression in GBM tumours (Rushing, Sandberg et al. 2010, Chiba, Hashimoto et al. 2010). An ideal vaccine should target antigens that are expressed primarily by cancer cells or at least expressed in significantly higher quantity compared to healthy tissues. It would also be of great benefit to target antigens that are expressed by many different tumours so that the vaccine could be applicable to other cancer types broadening the scope for the therapy. An ideal target antigen should be immunogenic and if it is required for tumour cell survival and tumorigenicity it makes an even more attractive target (Cheever, Allison et al. 2009). This last characteristic reduces the chances for the antigen to be silenced by the tumour under immunological pressure as it is essential for the cancer's survival. An analysis of 75 cancer antigens revealed that WT-1 was the top antigen to target in the pancreatic cancer setting. The WT-1 antigen was the top antigen due to its importance in proliferation, invasion and metastases (Koido, Okamoto et al. 2017), previous research has shown that knockdown of the WT-1 gene slowed the growth of human GBM cells and slowed their *in vivo* growth in nude mice (Clark, Ware et al. 2010). WT-1 has also been shown to be involved in the regulation of apoptosis of GBM cell lines with WT-1 silenced GBM cell lines expressing more pro-apoptotic genes than WT-1 expressing GBM cell lines

(Kijima, Hosen et al. 2014). Therefore, both TRP2 and WT1 antigens were judged good antigens and therefore chosen for the development of a vaccine to treat GBM.

GBM is also renowned for its immunosuppressive phenotype, GBM is primarily a disease associated with old age with the majority of cases occurring in patients aged between 55 and 60 years of age (Hanif, Muzaffar et al. 2017). It has been shown that the increasing age of GBM patients is associated with an increased immunosuppressive gene expression profile. PD-L1 and IDO mRNA expression is increased in the GBM tumours of older patients (aged 60-69) (Ladomersky, Scholtens et al. 2019). It was decided to analyse the immune phenotype of several GBM cell lines using flow cytometry. This technique was used to look at the cell surface expression of several immune activating and inhibiting ligands. These analyses revealed that there were high levels of the immune inhibitory ligand PD-L1 on the surface of cultured GBM cell lines. PD-L1 is an immunosuppressive ligand for the PD-1 receptor expressed by T-cells. Ligation of PD-1 on T-cells with PD-L1 results in a reduction in the activity of T-cells and an increase in immunosuppression (Ohaegbulam, Assal et al. 2015). PD-L1 expression is usually restricted to immune privileged tissues however numerous cancers have co-opted this inhibitory ligand as a means to prevent immune attack. PTEN loss is frequent in many cancers, with GBM being no exception, this loss of PTEN results in expression of PD-L1 by GBM cancers (Parsa, Waldron et al. 2007). Whilst this expression of PD-L1 enhances the immune escape of tumours it can also be targeted using antibodies to try and prevent the immune escape of tumours enabling their immune recognition. Interestingly the non-classical MHC class I molecule HLA-G was also discovered on the surface of cultured GBM cells. HLA-G expression is usually restricted to the trophoblasts protecting the embryo from immune attack (Kovats, Main et al. 1990). HLA-G has previously been shown to prevent cytotoxic CD8 T-cell lysis of HLA-G expressing cells (Le Gal, Riteau et al. 1999). HLA-G has also previously been shown to protect GBM cells from lysis by alloreactive PBMCs, blockade of HLA-G using antibodies was shown to rescue the lysis of tumour cells by alloreactive PBMCs (Wiendl, Mitsdoerffer et al. 2002).

Whilst the cell lines studied appeared to express immunosuppressive proteins, they also appear to express some immune activating proteins. The GBM cells studied all appear to express the MHC class I antigen (HLA-A, B, C) on their surface. These MHC class I molecules are responsible for presenting immunogenic peptides to cytotoxic T-cells, these MHC class I molecules also protect tumour cells from NK cell mediated lysis however this antigen presentation via MHC class I targets cells for killing by CD8 T-cells (Garcia-Lora, Algarra et al. 2003). Tumour cells sometimes down regulate MHC class I expression to prevent immune cell recognition, this loss of MHC class I therefore makes them susceptible to NK cell mediated lysis, however it would appear that whilst tumour cells down regulate classical MHC class I they also appear to upregulate non-classical class I molecules such as HLA-G that protect them from NK cells. Fortunately, the cell lines studied appear

to express HLA-A, B, C so they are susceptible to cytotoxic T-cell attack. The GBM cell lines studied also appear to express CD40 on their surface. CD40L is expressed by activated T-cells and it binds to CD40, a costimulatory receptor contributing to cell-mediated immunity (Elgueta, Benson et al. 2009). CD40 ligation on B cells and dendritic cells results in an upregulation of MHC molecules on their surfaces and improved antigen presentation. CD40 ligation on tumours has been shown to result in the direct death of tumour cells independent of the immune compartment, this CD40 also leads to CD8 T-cell activation (Vonderheide 2007).

These results taken together indicate that GBM expresses immunogenic antigens that can be targeted via immunotherapy however the immune profile of these tumours needs to be accounted for, such as the apparent expression of the anti-immune PD-L1 and expression of MHC class I. Once these antigens were discovered it was decided to utilise a WT-1 and TRP-2 directed ImmunoBody[®] vaccine to generate an anti-tumour immune response in a pre-clinical murine model of GBM.

8.2. ImmunoBody[®] vaccination generates a strong anti-tumour immune response and the addition of checkpoint blockade appears to help tumour infiltrating immune cells overcome intratumoural immunosuppression

The ImmunoBody[®] vaccination provides an exciting new immunotherapeutic approach for the treatment of intracranial tumours. The ability of ImmunoBody[®] to generate a strong immune response and its ability to prophylactically prevent tumour occurrence make it a viable therapy for the treatment of brain tumours. The ImmunoBody[®] vaccine platform provides an attractive method for generating an anti-tumour immune response due to its ability to generate an immune response via direct and cross presentation of tumour antigens using an IgG antibody as a carrier protein. As previously mentioned, it was decided to target the WT-1 and TRP-2 antigens immunotherapeutically due to their prevalence and importance in GBM. Targeting multiple antigens prevents immune escape from occurring, this is the phenomenon where cancers will adapt their antigen expression profile to enable them to evade immune eradication (Dunn, G. P., Old et al. 2004). One issue to consider when vaccinating against multiple antigens is the presence of epitope dominance, this is where the response to one immunogenic antigen overrides the response to the co-administered antigen. Due to the desire to target both the WT-1 and TRP-2 antigens it was decided to see if there was any immunodominance to either of these antigens when both TRP-2 and WT-1 ImmunoBody[®] vaccines were given simultaneously. When given together the SCIB1 (TRP-2 directed) and WT-1 ImmunoBody[®] vaccines did not display any immunodominance with the TRP-2 and WT-1 immune response being of similar frequency and avidity when the vaccines were given alone and simultaneously. Due to these findings it was decided to test this dual ImmunoBody[®] regime in a prophylactic setting with the dual vaccination regime being administered followed by

intracranial tumour implantation. In the prophylactic setting dual WT-1 and SCIB-1 ImmunoBody® vaccination resulted in a significant improvement of survival when compared to sham vaccinated mice, confirming the anti-tumour activity of dual ImmunoBody® vaccination. When treating established intracranial tumours ImmunoBody® vaccination failed to significantly improve the survival of tumour bearing mice, however ImmunoBody® vaccination lead to an increased cytotoxic T-cell infiltrate into brain tumours. It was hypothesised that adding immune checkpoint blockade to the ImmunoBody® vaccination schedule would boost the anti-tumour immune response and improve survival of tumour bearing mice, when anti-PD-1 antibody was added to dual WT-1 and SCIB1 ImmunoBody® vaccination it lead to a significant improvement in survival compared to mice given dual ImmunoBody® vaccination with PD-1 isotype control however this treatment was not curative. Established intracranial tumours are notoriously difficult to treat and there are several methods that could be employed to try and improve the response to combinatorial therapy. Whilst there appears to be some promise for the use of immunotherapy in the GBM setting there are several issues that need to be addressed in order to achieve a robust anti-tumour response. The preclinical data presented within this thesis reveals that ImmunoBody® vaccination generates an increase in the number of T-cells infiltrating intracranial tumours however this increase was not linked to an increased in survival, similar findings have been found using a dendritic cell vaccine (Antonios, Soto et al. 2016). Previous research has found that addition of anti-PD-1 to vaccine therapy boosted the anti-tumour response of these TILs resulting in improved survival (Antonios, Soto et al. 2016). As mentioned previously GBM cells respond to IFN γ in their microenvironment therefore it was decided to analyse the response of GBM cells to IFN γ .

8.3. GBM cells can respond to IFN γ in their local environment and adapt their immune-related antigen expression profile

ELISpot results reveal that ImmunoBody® vaccination generates IFN γ release from splenocytes when exposed to the target peptides. As a result, it was of great interest to see how GBM cells react to IFN γ in their environment. *In vitro* analyses reveal that GBM cells appear to actively alter their phenotype when in the presence of IFN γ indicating that activated immune cells within the tumour may alter the tumour's phenotype and alter its immune profile altering the anti-tumour efficacy of these cells. Tumours are known to escape the immune pressures put upon them, so antigens that can enhance their immune escape are likely to be upregulated. In a late stage aggressive cancer like GBM the tumour mass is likely to be comprised of cells that have escaped the immune pressures put upon them and therefore these tumours are highly likely to be immune evasive and suppressive.

IFN γ is a pleiotropic cytokine that acts on both innate and adaptive immune regulation. IFN γ is known to lead to increased MHC expression and therefore antigen presentation. IFN γ has been

utilised as a therapeutic in the cancer setting (Zaidi, Merlino 2011). IFN γ has been shown to inhibit GBM cell growth *in vitro* as a result its direct administration intratumourally has been studied as a therapy for GBM. Recombinant IFN γ was given in conjunction with radiotherapy for newly diagnosed GBM patients, this therapy was well tolerated with the only side effect observed being a raised body temperature post injection. Whilst this therapy was well tolerated it failed to result in a survival benefit when compared to radiation alone (Farkkila, Jaaskelainen et al. 1994). IFN γ is known to induce IL-6 expression in GBM (Iwami, Natsume et al. 2011) IL-6 is associated with invasion of GBM cells and as tumour grade increases so does the level of IL-6 (Shan, He et al. 2015). Due to the pleiotropic nature of IFN γ its role in the immune response needs to be considered as part of a combinatorial approach.

In vitro analyses conducted for this thesis revealed that when GBM cells were exposed to IFN γ they upregulate several immune related cell surface antigens. IFN γ treatment led to an increase of the immunosuppressive non-classical class I MHC molecules HLA-G and -E. Expression of these molecules on the surface of tumour cells will potentially prevent lysis of tumour cells by T-cells and NK cells, providing them with a means by which to circumvent the immune system (Le Gal, Riteau et al. 1999, Wischhusen, Friese et al. 2005). The GBM cells studied also appear to upregulate the expression of PD-L1 on their surface after IFN γ treatment which would also contribute towards their immune escape via ligation to PD-1 on the surface of activated T-cells. The expression of PD-L1 by GBM tumours has been linked to shorter survival times with high PD-L1 expression leading to a significant reduction in patient survival times (Nduom, Wei et al. 2016). The upregulation of these molecules presents a significant challenge to the success of any vaccine used to treat GBM, however the identification of their presence provides further molecules to target when utilising immunotherapy.

However, the cell lines studied also upregulated classical MHC class I (HLA-A, B, C) on their surface when exposed to IFN γ . The upregulation of MHC class I is known to improve antigen presentation and T-cell recognition of tumours making them more susceptible to cytotoxic T-cell killing. Cancers can lose expression of MHC class I and this is a method that enables them to escape immune recognition, the loss of MHC class I prevents recognition of tumour cells by cytotoxic T-cells and leads to the development of immune escape variants (Garrido, Aptsiauri et al. 2016). Moreover, the expression of immune stimulatory CD40 on the surface of the cell lines studied was also upregulated after IFN γ exposure. CD40 is an important regulator of the immune response, binding of CD40 to its ligand (CD40L) leads to amplification of the immune response via the upregulation of costimulatory molecules and MHC class I (Costello, Gastaut et al. 1999).

IFN γ also increased the level of immune inhibitory enzyme IDO in the GBM cell lines studied. IDO is a well-known immune inhibitor and its expression in GBM has been linked to worsened survival

(Wainwright, Balyasnikova et al. 2012). The expression of IDO by cancer cells implanted into immunocompetent mice prevents their rejection when prophylactically vaccinated, the rejection of these tumours could be rescued by inhibiting IDO with 1MT. These findings point to IDO being an important modulator of the anti-tumour immune response (Munn, Mellor 2004). IDO expression within tumours is linked with an increase in the presence of immune inhibitory regulatory T-cells. IDO also leads to depletion of tryptophan, a critical amino-acid for the survival of T-cells, in the tumour microenvironment, resulting in the reduction of T-cell growth and thereby contributing to an immunosuppressive environment (Zhai, Lauing et al. 2015).

GBM cell lines adapt to the presence of IFN γ in their environment and this can help reveal the response of these cells to immunotherapy. GBM is highly immunosuppressive as evidenced by PD-L1, GLA-E and HLA-G expression, this immunosuppression is exacerbated when these cells are exposed to IFN γ . It is also important to note that these cells also upregulate some immune stimulatory molecules such as MHC class I and CD40, so IFN γ represents a potential 'double-edged sword' for immunotherapy. These findings provide a rationale for combining immune checkpoint blockade with active immunotherapy.

8.4. Carnosine represents an attractive natural therapy for GBM

Long term survival in GBM is extremely rare and despite aggressive surgery and radio chemo therapy tumours nearly always recur. GBM cells are highly invasive and have been shown to penetrate brain tissue and travel along the vasculature, this makes complete surgical resection of these tumours almost impossible (Paw, Carpenter et al. 2015). Upon recurrence the prognosis of GBM patients is extremely poor with median survival only being just under 7 months (van Linde, Brahm et al. 2017). Due to the highly invasive nature of GBM it would be of great benefit to try and prevent the proliferation and migration of any cells that remain post-surgery providing a window of opportunity for vaccine induced immune cells to target this reduced number of tumour cells before they can spread and grow.

Carnosine a di-peptide composed of β -alanine and L-histidine has been shown to significantly inhibit colony formation and migration of GBM cells co-cultured with normal fibroblast cells, without affecting the fibroblasts. This tumour specificity and ability of carnosine to prevent colony formation make it an attractive therapeutic option (Oppermann, Dietterle et al. 2018). The effects of carnosine on GBM cells was studied in this thesis, with carnosine being shown to reduce the migration of GBM cells. Carnosine also alters the mitochondrial activity of all of the GBM cell lines studied (as indicated by an MTT assay). This ability of carnosine to reduce the migration of GBM cells in a selective manner make it an attractive therapeutic option in combination with

immunotherapy. Carnosine has been shown to increase the longevity of CD4⁺T-cells *in vitro* (Hyland, Duggan et al. 2000), carnosine is also a pH buffer which would be beneficial when combined with immunotherapy. Tumours frequently have an acidic microenvironment due to increased glycolysis within the tumour producing lactic acid, this acidic pH inhibits immune cell function and reduces immune cell killing of tumour cells (Lardner 2001). The prospect of delivering carnosine directly into the post-surgical cavity of GBM patients (either directly or by using carnosine impregnated biodegradable wafers) provides great promise, this therapy would reduce migration of any remaining tumour cells whilst buffering the local pH enabling efficient anti-tumour immune cell activity. Due to the pH buffering capabilities of carnosine it would be of great benefit to combine it with immunotherapy for the aforementioned reasons.

8.5. Issues with brain tumour immunotherapy

Unfortunately, as evidenced by our findings and those of others GBM tumours are highly immunosuppressive and adapt to immune pressures put upon them. What further impedes the efficacy of immunotherapy in the GBM context is the unique interaction between the brain and the immune system and the unusual immune environment of the brain. Even though the brain is unique in immunological terms it is not devoid of an active immune response and activated immune cells can access tumours within the brain (Prins, Shu et al. 2008). Results obtained in this study have revealed that ImmunoBody[®] vaccination did generate an antigen-specific immune response that provided tumour protection in a prophylactic brain tumour model. When ImmunoBody[®] vaccination was used to treat established intracranial tumours, it didn't convey a survival advantage for mice bearing intracranial tumours. Combination of anti-PD-1 with ImmunoBody[®] vaccination did appear to result in a significant survival advantage however all mice still succumb quickly to the disease. There are many reasons for why therapy may have failed to completely cure the mice. Flow cytometric analysis of TILs did indicate an increased T-cell infiltrate after vaccination. However, the immune cells penetrating the tumour may have been locally suppressed, as a result combination of PD-1 blockade with vaccination helped to rescue this immune response. The addition of PD-1 seemed to improve survival of mice harbouring intracranial tumours when compared to mice receiving dual vaccination with isotype control. However the fact that mice die in a short period of time indicates that perhaps the ability of anti-PD-1 to penetrate the tumour and the blood brain barrier is limited. It would be of great interest to use labelled anti-PD-1 antibody to examine its trafficking throughout the body, when injected intravenously and when administered intranasally. Whilst the antibody can still exert its effects extracranially it would be most beneficial if it were delivered to the tumour so that it can boost the immune cells within the tumour. This may be improved by directly delivering the antibody using an Ommaya reservoir or gliadel wafers

impregnated with anti-PD-1 into the tumour resection cavity. Previous research has shown that only around 0.1% of peripherally administered IgG antibodies penetrate the brain under normal conditions (Thom, Hatcher et al. 2018). In GBM cases the blood brain barrier is compromised and 'leakier' than that of a healthy brain however antibody penetrance isn't increased due to the large size of antibodies (Razpotnik, Novak et al. 2017). Interestingly, a small clinical trial found that it was better for the patients to receive anti-PD-1 before surgery rather than after surgery probably due to the fact that most anti-GBM T-cells were already inside the tumour at the time of surgery and therefore adding anti-PD-1 did very little to relieve the break of T-cells that were no longer there (Cloughesy, Mochizuki et al. 2019).

The blood brain barrier (BBB) is a significant obstacle to overcome with regards to treating brain diseases with GBM being no exception. Many drugs and molecules that show promise *in vitro* often fail to have the same effects *in vivo* due their inability to penetrate the blood brain barrier and access the brain parenchyma. There are numerous reasons for the highly selective nature of the BBB and it works to prevent entry and exit of undesirable substances that could affect the highly sensitive brain. The BBB helps to maintain an ideal environment for brain function by regulating ion, nutrient, macromolecule and neurotransmitter levels whilst also excluding harmful toxins (Abbott, Patabendige et al. 2010). IgG penetration into the brain parenchyma is relatively low and there is active efflux of IgG molecules from the brain via the Fc region of these antibodies when they are introduced intracerebrally (Zhang, Y., Pardridge 2001). In the cancer setting the blood-tumour barrier is far more disorganised than the intact blood brain barrier, this enables larger molecules to penetrate the tumour than would be permitted by the blood brain barrier, however this permeability is not homogeneous with high amounts of tumour variation observed. Native lung cancer has been seen to have a higher level of T-cell infiltrate compared to brain metastases, indicating that the intracerebral location of these tumours impedes T-cell penetration (Berghoff, Preusser 2018). Systemically administered antibodies can access the brain parenchyma however the brain accumulation is dismally low, with only around 0.1 % of the serum concentration being detected in the brain. This low accumulation has been attributed to the blood brain barrier and the rapid clearance of antibodies from the CSF (Iwasaki 2017). Mouse studies have shown that the site of vaccination can alter the immune response to glioblastoma multiforme tumours, mice vaccinated in regions further from the site of the tumour displayed a stronger anti-tumour response. This indicates that the lymph nodes located closest to the tumour are being altered by factors that are draining from the tumour, T-cell priming appears to be impaired in the cervical lymph nodes (located within the neck) (Ohlfest, Andersen et al. 2013).

8.6. Improving future immune therapy for glioblastoma multiforme

Due to the issues with antibody penetrance of brain tumours several avenues can be utilised to improve blood brain barrier crossing and brain penetrance of therapeutic antibodies. One of the most basic methods for enabling antibody penetration into the brain is to utilise focused ultrasound, this relies on high frequency ultrasonic waves to disrupt the tight junctions within the blood brain barrier allowing molecules otherwise not permitted to cross the blood brain barrier. Previous research has shown that the application of focused ultrasound with gas-filled microbubbles can permit the entrance of therapeutic antibodies into the brain without any damage to the brain parenchyma (Kinoshita, McDannold et al. 2006). One concern may be that ultrasound may affect gap junctions within the brain altering cell-cell communication, fortunately gap junctions are not destroyed it is their assembly that is affected, however these changes were reversed 24 hours after ultrasound exposure (Alonso, Reinz et al. 2010).

There are two main methods that molecules use to cross the blood brain barrier: adsorption-mediated transcytosis and receptor-mediated transcytosis. Adsorption-mediated transcytosis simply relies on positively charged molecules interacting with the negatively charged phospholipids within the membrane of endothelial cells, this then results in internalisation of the positively charged molecules and their shuttling across the membrane into the brain parenchyma (Razpotnik, Novak et al. 2017). Receptor-mediated transcytosis relies on the binding of molecules to their specific receptor on the endothelium of the BBB, resulting in their internalisation and shuttling across the endothelial cells. There are several receptors that mediate this form of transcytosis across the BBB, these are the insulin, LDL-related protein type I and transferrin receptors. These receptors can be targeted to improve the delivery of antibodies across the BBB (Razpotnik, Novak et al. 2017). Unfortunately, due to the presence of neonatal Fc receptors on the blood brain barrier antibodies are actively removed from the brain via reverse transcytosis.

Altering the structure of antibodies can afford the opportunity to overcome the active efflux of antibodies from the brain parenchyma by these neonatal Fc receptors (Razpotnik, Novak et al. 2017). Antibodies can be engineered to improve their crossing of the blood brain barrier and this can be done by piggybacking on the receptors that allow receptor mediated transcytosis. The transferrin receptor was an early target for receptor mediated delivery across the BBB, it is highly expressed in the brain vasculature and functions to shuttle iron into the brain. A mouse anti-rat transferrin receptor antibody known as OX26 was developed with the aim of crossing the BBB, this antibody binds to the receptor without altering its ability to bind iron, allowing it to perform its normal function. Conjugation of this antibody with therapeutic peptides was shown to improve their delivery to the brain (Jones, Shusta 2007). One issue that arose when using antibodies to target the transferrin receptor is the affinity of these antibodies for the receptor prevented their

release from the receptor preventing therapeutic delivery to the brain. In order to improve the delivery of potential payloads attached to the transferrin antibody the antibody affinity was altered by genetic engineering, reducing the affinity of these antibodies improved their delivery throughout the brain. These antibodies can be engineered to have one arm specific for the transferrin receptor and the other arm can be specific for an antigenic target of choice, creating a bispecific antibody (Watts, Dennis 2013). The insulin receptor is also a viable target for crossing the blood brain barrier, a bispecific antibody targeting amyloid beta and the human insulin receptor has previously been developed and tested in monkeys (Stanimirovic, Kemmerich et al. 2014). This method would be of great use to shuttle an antibody specific for PD-1/PD-L1 directly into the brain allowing it to improve its tumour penetration and activity. Single chain variable fragments (scFvs) are fusion proteins composed of the variable regions of the heavy and light chains of immunoglobulins joined by a peptide linker. Previously a scFvs has been developed with a cell penetrating peptide (CPP) as the linker between the light and heavy variable regions. These scFv-CPP molecules were shown to cross the blood brain barrier and penetrate the brain parenchyma in mice given I.V. doses of scFv-CPP (Skrlj, Drevensek et al. 2013).

Another alternative way to deliver therapeutic antibodies across the blood brain barrier is the utilisation of nanoparticles or liposomes. These liposomes and nanoparticles can be altered to improve their blood brain barrier crossing, this can be done by giving the nanoparticles a positive charge increasing their adsorption mediated transcytosis. These nanoparticles can also be synthesised to hijack the receptor mediated transcytosis systems, either by incorporating antibodies directed against the receptors, or ligands for these receptors on the surface of these nanoparticles. Liposomes can be used to encapsulate and deliver antibodies, this encapsulation prevents the enclosed antibodies binding to their targets outside of the tumour location, preventing potential off target effects and enhancing tumour delivery (Razpotnik, Novak et al. 2017). Magnetoliposomes are magnetic nanoparticles that can be physically directed using magnetic fields, this can enable specific delivery to the brain and even aid tumour targeting of the therapeutic payload (Razpotnik, Novak et al. 2017). It is also important to note that not just antibodies can be loaded into these nanoparticles, other therapeutics such as carnosine can be loaded preventing their degradation and enhancing their tumour delivery.

Stem cells can also be used to deliver therapeutic antibodies to tumours located within the brain. Stem cells display a tropism towards tumour sites, stem cells can actively penetrate tumours and can inhabit hypoxic regions within tumours even crossing the blood brain barrier to access intracranial tumours. Stem cells can be genetically modified to express antibodies or scFvs, previous research has found that these stem cells can penetrate tumours and locally deliver therapeutic antibodies. Whilst these stem cells show promise they also have some down sides; stem cells have

been shown to produce anti-inflammatory cytokines which aren't conducive for their use in the immunotherapy setting (Frank, Najbauer et al. 2010). One major concern associated with the use of stem cells is the potential of stem cells to become tumorigenic exacerbating the problem they are designed to remedy. It has been shown that mixing bone marrow derived stem cells with breast cancer cells leads to induction of xenografts with increased metastatic potential, this was attributed to secretion of the chemokine CCL5 by the stem cells. Bone marrow derived stem cells have also been shown to spontaneously transform into cells with a malignant phenotype when cultured *in vitro*, however these results have been refuted and transformation has been attributed to culture environments (Zhang, C. L., Huang et al. 2017). Despite the fear of tumorigenesis steps can be taken to prevent this being a concern and a rigorous stem cell selection process can stop potentially tumorigenic stem cells being administered (Zhang, C. L., Huang et al. 2017).

8.7. Improving immune cell transit into the brain of vaccinated mice

Much like antibody therapies; focused ultrasound can be used to improve immune cell entry into tumours located within the brain. NK-92 is a human NK cell line that can be transduced with chimeric antigen receptors enabling it to specifically target tumours. In a pre-clinical model of breast cancer brain metastases NK-92 cells were transduced with a HER2 receptor enabling them to target MB-231-HER2 cells located within the brains of athymic nude mice. Focused ultrasound was applied to the brain of tumour bearing mice injected with these HER2 specific NK-92 cells. Focused ultrasound was shown to result in a 5-fold increase in the number of NK-92 cells within the tumour, these NK-92 cells maintain their function and these cells cause the apoptosis of tumour cells, meaning that ultrasound does not appear to affect their activity (Alkins, Burgess et al. 2013). Unlike NK cells, T-cells can actively cross the blood brain barrier however this entry is tightly controlled. In order for T-cells to traverse the blood brain barrier they need to make direct contact with it, resulting in the 'capture' of the T-cell. The ligand P-selectin glycoprotein ligand-1 on the surface of T-cells binds to selectins on the surface of the blood brain barrier endothelial cells alternatively α 4-integrins on the surface of T-cells can bind vascular cell adhesion molecule (VCAM) and mucosal addressin cell adhesion molecule (MAdCAM-1). Once T-cells are 'captured' they roll along the blood brain barrier endothelial cells at a slowed rate, resulting in increased cell adhesion to the endothelial cells. Once T-cells have been sufficiently slowed they start to protrude into the endothelium. Cells can then migrate across the endothelium in two distinct manners: transcellular diapedesis where immune cells travel through the endothelial cells directly and paracellular diapedesis where cells pass through the junctions between the endothelial cells (Banks, Erickson 2010, Engelhardt, Ransohoff 2012). Once T-cells have penetrated the endothelial layer they need to breach the underlying glia limitans in order to reach the brain parenchyma. Matrix

metalloproteinases (MMPs) regulate the crossing of T-cells across the glia limitans, MMP-2 and MMP-9 activity is necessary for this to occur. MMP2 and MMP-9 cleave β -dystroglycan on astrocyte end feet enabling immune cell penetration of the parenchyma (Engelhardt, Ransohoff 2012). Antigen specific CD8 T-cells have been shown to specifically shuttle across the blood brain barrier to access peptides located within the brain. The presence of immunogenic peptide in the brain results in up regulation of MHC class I on the luminal side of endothelial cells within blood vessels. This increased MHC class I expression results in increased peptide specific CD8 T-cell crossing of the blood brain barrier (Galea, Bernardes-Silva et al. 2007). The presence of the blood brain barrier protects the brain from unnecessary T-cell infiltration and potential inflammation of the brain. In GBM the blood brain barrier is compromised and is 'leaky' compared to the healthy blood brain barrier, there are high levels of heterogeneity of this disruption and it varies from case to case. Not only does the blood brain barrier pose a challenge for immunotherapy there is also the blood tumour barrier to consider. Blood vessels associated with glioblastoma upregulate the adhesion molecule tenascin C (TNC), this captures T-cells and prevents their crossing of the blood vessels (Quail, Joyce 2017). Previous research has shown that T-cells can be engineered to express ligands for adhesion molecules on endothelial cells improving their capture and crossing of the blood brain barrier, enabling more efficient tumour targeting (Platten 2018). One of the oldest methods used for increasing penetration of the blood brain barrier is osmotic disruption using mannitol. Infusion of hyperosmotic mannitol results in endothelial cell shrinking and the subsequent opening of the gap junctions. Unfortunately, osmotic disruption of the blood brain barrier is non-specific and as a result a variety of molecules can leave and enter the brain resulting in potentially fatal oedema and toxicity (van Tellingen, Yetkin-Arik et al. 2015).

It is important to note that there is dysfunction of the blood brain barrier in GBM with down regulation of the proteins that form the tight junctions in the BBB (Wolburg, Wolburg-Buchholz et al. 2003). This dysfunction of the blood brain barrier explains the cerebral oedema frequently observed in GBM patients. *In vitro* experiments have revealed that GBM cells secrete factors that lead to the increase in the leakiness of an *in vitro* model of the BBB as indicated by transepithelial electrical resistance (Schneider, Ludwig et al. 2004). Invading glioblastoma cells can also lead to a physical disruption of the architecture of the blood brain and blood tumour barriers. GBM cells utilise blood vessels as a route for invasion and they co-opt blood vessels to aid their growth. These GBM cells displace astrocyte end feet from their perivascular location, the presence of just a small number of cells in these perivascular locations is enough to increase the permeability of the blood brain barrier. This finding was confirmed to be due to the tumour implanted within the brains of mice and not due to the surgical procedure used to implant tumours, control mice underwent the same surgical procedure but rather than having GBM cells injected into their brains non-malignant

glial cells were implanted. These animals didn't have the same leakiness as that observed in GBM harbouring mice (as indicated by Evans blue dye exclusion) (Watkins, Robel et al. 2014).

8.8. Incorporation of immunotherapy into standard therapy

When utilising immunotherapy for the treatment of GBM it would be of great benefit to combine immunotherapy with standard therapy. Unfortunately, some of the therapeutics utilised for GBM are known to have immunosuppressive properties. Dexamethasone is a steroidal anti-inflammatory drug that is used to control oedema in GBM patients. Due to its anti-inflammatory properties dexamethasone is immunosuppressive, it is quite common for dexamethasone to be utilised to control adverse responses to immunotherapy dampening potentially deleterious immune over activation. Dexamethasone is a well-known immunosuppressor and as a result if patients receive immunotherapy they should cease dexamethasone therapy (Platten 2019). *In vitro* experiments have shown that dexamethasone inhibits healthy CD8 and CD4 T-cell division (Giles, Hutchinson et al. 2018). Dexamethasone also appears to alter the maturation of dendritic cells *in vitro*; these dendritic cells also seem to secrete higher levels of anti-inflammatory cytokines whereas dendritic cells that weren't exposed to dexamethasone secreted more pro-inflammatory cytokines. Dexamethasone also seems to decrease the CD4 T-cell priming by dendritic cells (Falcon-Beas, Tittarelli et al. 2019). Seeing as dexamethasone has immunosuppressive effects an alternative method for reducing oedema in GBM patients' needs to be explored. Bevacizumab is an anti-VEGF antibody that can potentially be used to reduce oedema in GBM patients without generating any immunosuppressive side effects. However as mentioned previously antibodies aren't very good at penetrating intracranial tumours therefore their penetrance would need to be improved using the aforementioned methods. Studies using Bevacizumab for GBM patients have revealed that it reduces oedema in a durable manner (Ananthnarayan, Bahng et al. 2008, Ellingson, Cloughesy et al. 2012).

GBM patients are also treated with radiotherapy and temozolomide chemotherapy, the current 'gold standard' for GBM therapy. Temozolomide and radiotherapy can have both immune suppressive and immune activating effects and when utilising immunotherapy an optimum dosing schedule needs to be used when combining standard therapy with immunotherapy. When studying patients receiving standard radiotherapy and TMZ chemotherapy their CD4 T-cell count can be seen to reduce post therapy and this reduced CD4 count was shown to be linked with reduced survival (Grossman, Ye et al. 2011). Whilst CD4 T-cell count is seen to go down it is important to note that some of these CD4 cells may potentially be CD4 regulatory T-cells, these can be negative regulators of the anti-tumour immune response. In a pre-clinical rat model harbouring subcutaneous GBM cells it was shown that low dose metronomic (frequent low doses) temozolomide chemotherapy

results in a decrease in the number of regulatory T-cells located within the spleens and tumours of these rats (Banissi, Ghiringhelli et al. 2009). Pre-clinical murine work has revealed that when the standard temozolomide dosing regime is employed, the anti-tumour effects of PD-1 blockade are abrogated, however when utilising metronomic dosing (frequent low doses) of temozolomide the anti-tumour effects of anti-PD-1 therapy remain (Platten 2019). Radiotherapy appears to enhance anti-tumour immunity so its combination with immunotherapy is very enticing. Radiotherapy can increase tumour immune recognition by increasing the expression of MHC class I, irradiation also leads to increased immune cell infiltrate into tumours and increased antigen recognition (Chow, Hara et al. 2015). Another important phenomenon to take into account is the abscopal effect, this is when radiation applied to one tumour site leads to regression of tumours at a distal site, and this indicates that the irradiation of the tumours results in increased T-cell activation that can result in eradication of tumours located throughout the body (Chow, Hara et al. 2015). Combination of radiotherapy with anti-PD-1 immune checkpoint blockade has been shown to improve long term survival in an orthotopic mouse model of GBM. This combinatorial therapy resulted in a reduced number of regulatory T-cells and an increase in the number of CD8 effector cells within the brain tumours (Zeng, See et al. 2013). Radiotherapy combined with IDO blockade and anti-PD-1 therapy has been shown to have a similar synergistic effect with mice given combinatorial IDO blockade, anti-PD-1 and radiotherapy resulted in long term survival, the addition of temozolomide to this treatment regime reduced the number of long term survivors to a third of that when utilising the treatments without chemotherapy (Ladomersky, Zhai et al. 2018). Radiotherapy leads to an increase in IFN γ secretion by tumour cells and this may help to explain why PD-1 blockade and anti-IDO therapy combine so well with this method of therapy. Combined chemotherapy and radiotherapy has been shown to lead to an upregulation of IFN γ by murine melanoma (B16-F10) and GBM (GL261 Luc2) cell lines, this was linked to increased PD-L1 expression on the surface of these cell lines (Derer, Spiljar et al. 2016). The effects of standard radio-chemotherapy were studied by analysing the PBMCs of GBM patients before and after therapy. Standard therapy resulted in a significant decrease in the white blood cell count of patients, decreases were observed in the CD3 and CD4 cell count however there was no significant decrease in the number of CD8 cells. Treatment was also shown to lead to a significant increase in the number of regulatory T-cells within the PBMCs of GBM patients (Fadul, Fisher et al. 2011).

These data indicate that there needs to be an optimisation of the usage of standard therapy when combining it with immunotherapy, simple adjustments can help the two modalities work in a beneficial manner, however this will need further research. It is also important to take into account the fact that some patients are resistant to temozolomide chemotherapy due to expression of the MGMT protein.

8.9. Concluding remarks

In order to develop an effective therapy for glioblastoma multiforme numerous factors need to be taken into account. Just in the context of immune evasion GBM cells adaptively upregulate immune escape ligands and cytokines. It is also important to take into account other factors that affect the immune system, a patient's mental status can affect the efficacy of immune therapies. A diagnosis of cancer can be highly stressful especially with a terminal cancer such as glioblastoma multiforme. The hypothalamic-pituitary-adrenal (HPA) axis and the sympathetic-adrenal medullary (SAM) axis are two major neuronal-hormonal axes that can affect the immune system; these axes lead to secretion of cortisol and catecholamine that can interact with immune cells and alter their activity. Stress can lead to a shift from a Th1 CD4 T-cell profile to a Th2 CD4 T-cell profile, result in a reduced antibody response to vaccination and lead to increased incidence of illness (Padgett, Glaser 2003). Immunotherapy definitely represents an attractive therapeutic option for the treatment of GBM, and the ImmunoBody[®] vaccine represents an attractive method of generating tumour specific T-cells. In order to treat established tumours the combination of ImmunoBody[®] vaccination with other treatment modalities needs to be explored. The addition of an anti-PD-1 antibody to the ImmunoBody[®] vaccination schedule resulted in a marginal increase in the survival of intracranial tumour bearing mice however this was not deemed significant. One issue that needs to be taken into account is the ability of the anti-PD-1 antibody to access the tumour as a result it would be of great interest to examine methods for improving antibody penetrance of the blood brain barrier. Addition of this therapy to standard therapy is also worthy of further investigation, it may be worth considering the combination of this approach with radiotherapy. It is also worth considering cessation of TMZ and dexamethasone therapy due to their immunosuppressive nature. It is also worth noting that TMZ is not efficacious in all cases due to the presence of the MGMT protein in some patients' tumours.

REFERENCES

clinicaltrials.gov-PubMed-NCBI.Available:

<https://www.ncbi.nlm.nih.gov/pubmed/?term=clinicaltrials.gov> [5/15/2020, 2020].

ABBOTT, N.J., PATABENDIGE, A.A., DOLMAN, D.E., YUSOF, S.R. and BEGLEY, D.J., 2010. Structure and function of the blood-brain barrier. *Neurobiology of disease*, **37**(1), pp. 13-25.

AKIYAMA, Y., KOMIYAMA, M., MIYATA, H., YAGOTO, M., ASHIZAWA, T., IIZUKA, A., OSHITA, C., KUME, A., NOGAMI, M., ITO, I., WATANABE, R., SUGINO, T., MITSUYA, K., HAYASHI, N., NAKASU, Y. and YAMAGUCHI, K., 2014. Novel cancer-testis antigen expression on glioma cell lines derived from high-grade glioma patients. *Oncology reports*, **31**(4), pp. 1683-1690.

ALAN MITTEER, R., WANG, Y., SHAH, J., GORDON, S., FAGER, M., BUTTER, P.P., JUN KIM, H., GUARDIOLA-SALMERON, C., CARABE-FERNANDEZ, A. and FAN, Y., 2015. Proton beam radiation induces DNA damage and cell apoptosis in glioma stem cells through reactive oxygen species. *Scientific reports*, **5**, pp. 13961.

ALEXANDROFF, A.B., JACKSON, A.M., PATERSON, T., HALEY, J.L., ROSS, J.A., LONGO, D.L., MURPHY, W.J., JAMES, K. and TAUB, D.D., 2000. Role for CD40-CD40 ligand interactions in the immune response to solid tumours. *Molecular immunology*, **37**(9), pp. 515-526.

ALI, O.A., LEWIN, S.A., DRANOFF, G. and MOONEY, D.J., 2016. Vaccines Combined with Immune Checkpoint Antibodies Promote Cytotoxic T-cell Activity and Tumor Eradication. *Cancer immunology research*, **4**(2), pp. 95-100.

ALKINS, R., BURGESS, A., GANGULY, M., FRANCIA, G., KERBEL, R., WELS, W.S. and HYNYNEN, K., 2013. Focused ultrasound delivers targeted immune cells to metastatic brain tumors. *Cancer research*, **73**(6), pp. 1892-1899.

ALLARD, M., OGER, R., VIGNARD, V., PERCIER, J.M., FREGNI, G., PERIER, A., CAIGNARD, A., CHARREAU, B., BERNARDEAU, K., KHAMMARI, A., DRENO, B. and GERVOIS, N., 2011. Serum soluble HLA-E in melanoma: a new potential immune-related marker in cancer. *PloS one*, **6**(6), pp. e21118.

ALONSO, A., REINZ, E., JENNE, J.W., FATAR, M., SCHMIDT-GLENEWINKEL, H., HENNERICI, M.G. and MEAIRS, S., 2010. Reorganization of gap junctions after focused ultrasound blood-brain barrier opening in the rat brain. *Journal of cerebral blood flow and metabolism : official journal of the International Society of Cerebral Blood Flow and Metabolism*, **30**(7), pp. 1394-1402.

ANANTHNARAYAN, S., BAHNG, J., RORING, J., NGHIEMPHU, P., LAI, A., CLOUGHESY, T. and POPE, W.B., 2008. Time course of imaging changes of GBM during extended bevacizumab treatment. *Journal of neuro-oncology*, **88**(3), pp. 339-347.

ANTONIOS, J.P., SOTO, H., EVERSON, R.G., ORPILLA, J., MOUGHON, D., SHIN, N., SEDIGHIM, S., YONG, W.H., LI, G., CLOUGHESY, T.F., LIAU, L.M. and PRINS, R.M., 2016. PD-1 blockade enhances the vaccination-induced immune response in glioma. *JCI insight*, **1**(10), pp. 10.1172/jci.insight.87059.

ARTIOLI, G.G., GUALANO, B., SMITH, A., STOUT, J. and LANCHI, A.H., Jr, 2010. Role of beta-alanine supplementation on muscle carnosine and exercise performance. *Medicine and science in sports and exercise*, **42**(6), pp. 1162-1173.

- ASPELUND, A., ANTILA, S., PROULX, S.T., KARLSEN, T.V., KARAMAN, S., DETMAR, M., WIIG, H. and ALITALO, K., 2015. A dural lymphatic vascular system that drains brain interstitial fluid and macromolecules. *The Journal of experimental medicine*, **212**(7), pp. 991-999.
- AUTHIER, A., FARRAND, K.J., BROADLEY, K.W., ANCELET, L.R., HUNN, M.K., STONE, S., MCCONNELL, M.J. and HERMANS, I.F., 2015. Enhanced immunosuppression by therapy-exposed glioblastoma multiforme tumor cells. *International journal of cancer*, **136**(11), pp. 2566-2578.
- BAGLEY, S.J., DESAI, A.S., LINETTE, G.P., JUNE, C.H. and O'ROURKE, D.M., 2018. CAR T-cell therapy for glioblastoma: recent clinical advances and future challenges. *Neuro-oncology*, **20**(11), pp. 1429-1438.
- BANISSI, C., GHIRINGHELLI, F., CHEN, L. and CARPENTIER, A.F., 2009. Treg depletion with a low-dose metronomic temozolomide regimen in a rat glioma model. *Cancer immunology, immunotherapy : CII*, **58**(10), pp. 1627-1634.
- BANKS, W.A. and ERICKSON, M.A., 2010. The blood-brain barrier and immune function and dysfunction. *Neurobiology of disease*, **37**(1), pp. 26-32.
- BARTH, R.J., Jr, MULE, J.J., SPIESS, P.J. and ROSENBERG, S.A., 1991. Interferon gamma and tumor necrosis factor have a role in tumor regressions mediated by murine CD8+ tumor-infiltrating lymphocytes. *The Journal of experimental medicine*, **173**(3), pp. 647-658.
- BASLER, M., KIRK, C.J. and GROETTRUP, M., 2013. The immunoproteasome in antigen processing and other immunological functions. *Current opinion in immunology*, **25**(1), pp. 74-80.
- BAUMANN, B.C., DORSEY, J.F., BENCI, J.L., JOH, D.Y. and KAO, G.D., 2012. Stereotactic intracranial implantation and in vivo bioluminescent imaging of tumor xenografts in a mouse model system of glioblastoma multiforme. *Journal of visualized experiments : JoVE*, **(67)**. pii: 4089. doi(67), pp. 10.3791/4089.
- BERGHOFF, A.S., KIESEL, B., WIDHALM, G., RAJKY, O., RICKEN, G., WOHRER, A., DIECKMANN, K., FILIPITS, M., BRANDSTETTER, A., WELLER, M., KURSCHIED, S., HEGI, M.E., ZIELINSKI, C.C., MAROSI, C., HAINFELLNER, J.A., PREUSSER, M. and WICK, W., 2015a. Programmed death ligand 1 expression and tumor-infiltrating lymphocytes in glioblastoma. *Neuro-oncology*, **17**(8), pp. 1064-1075.
- BERGHOFF, A.S., KIESEL, B., WIDHALM, G., RAJKY, O., RICKEN, G., WOHRER, A., DIECKMANN, K., FILIPITS, M., BRANDSTETTER, A., WELLER, M., KURSCHIED, S., HEGI, M.E., ZIELINSKI, C.C., MAROSI, C., HAINFELLNER, J.A., PREUSSER, M. and WICK, W., 2015b. Programmed death ligand 1 expression and tumor-infiltrating lymphocytes in glioblastoma. *Neuro-oncology*, **17**(8), pp. 1064-1075.
- BERGHOFF, A.S. and PREUSSER, M., 2018. Role of the blood-brain barrier in metastatic disease of the central nervous system. *Handbook of clinical neurology*, **149**, pp. 57-66.
- BIGNER, D.D., FRIEDMAN, A.H., FRIEDMAN, H.S. and MCLENDON, R., 2016. *The Duke Glioma Handbook: Pathology, Diagnosis, and Management*. Cambridge: Cambridge University Press.
- BIRNER, P., TOUMANGELOVA-UZEIR, K., NATCHEV, S. and GUENTCHEV, M., 2010. STAT3 tyrosine phosphorylation influences survival in glioblastoma. *Journal of neuro-oncology*, **100**(3), pp. 339-343.
- BLEEKER, F.E., MOLENAAR, R.J. and LEENSTRA, S., 2012. Recent advances in the molecular understanding of glioblastoma. *Journal of neuro-oncology*, **108**(1), pp. 11-27.

BLOCH, O., LIM, M., SUGHRUE, M.E., KOMOTAR, R.J., ABRAHAMS, J.M., O'ROURKE, D.M., D'AMBROSIO, A., BRUCE, J.N. and PARSA, A.T., 2017. Autologous Heat Shock Protein Peptide Vaccination for Newly Diagnosed Glioblastoma: Impact of Peripheral PD-L1 Expression on Response to Therapy. *Clinical cancer research : an official journal of the American Association for Cancer Research*, **23**(14), pp. 3575-3584.

BLOOM, M.B., PERRY-LALLEY, D., ROBBINS, P.F., LI, Y., EL-GAMIL, M., ROSENBERG, S.A. and YANG, J.C., 1997. Identification of tyrosinase-related protein 2 as a tumor rejection antigen for the B16 melanoma. *The Journal of experimental medicine*, **185**(3), pp. 453-459.

BODMER, S., STROMMER, K., FREI, K., SIEPL, C., DE TRIBOLET, N., HEID, I. and FONTANA, A., 1989. Immunosuppression and transforming growth factor-beta in glioblastoma. Preferential production of transforming growth factor-beta 2. *Journal of immunology (Baltimore, Md.: 1950)*, **143**(10), pp. 3222-3229.

BOEHM, U., KLAMP, T., GROOT, M. and HOWARD, J.C., 1997. Cellular responses to interferon-gamma. *Annual Review of Immunology*, **15**, pp. 749-795.

BOLDYREV, A., BULYGINA, E., LEINSOO, T., PETRUSHANKO, I., TSUBONE, S. and ABE, H., 2004. Protection of neuronal cells against reactive oxygen species by carnosine and related compounds. *Comparative biochemistry and physiology. Part B, Biochemistry & molecular biology*, **137**(1), pp. 81-88.

BOWLES, A.P., Jr and PERKINS, E., 1999. Long-term remission of malignant brain tumors after intracranial infection: a report of four cases. *Neurosurgery*, **44**(3), pp. 636-42; discussion 642-3.

BRENTVILLE, V.A., METHERINGHAM, R.L., GUNN, B. and DURRANT, L.G., 2012. High avidity cytotoxic T lymphocytes can be selected into the memory pool but they are exquisitely sensitive to functional impairment. *PLoS one*, **7**(7), pp. e41112.

BRONTE, V., APOLLONI, E., RONCA, R., ZAMBONI, P., OVERWIJK, W.W., SURMAN, D.R., RESTIFO, N.P. and ZANOVELLO, P., 2000. Genetic vaccination with "self" tyrosinase-related protein 2 causes melanoma eradication but not vitiligo. *Cancer research*, **60**(2), pp. 253-258.

BROWN, C.E., ALIZADEH, D., STARR, R., WENG, L., WAGNER, J.R., NARANJO, A., OSTBERG, J.R., BLANCHARD, M.S., KILPATRICK, J., SIMPSON, J., KURIEN, A., PRICEMAN, S.J., WANG, X., HARSHBARGER, T.L., D'APUZZO, M., RESSLER, J.A., JENSEN, M.C., BARISH, M.E., CHEN, M., PORTNOW, J., FORMAN, S.J. and BADIE, B., 2016. Regression of Glioblastoma after Chimeric Antigen Receptor T-Cell Therapy. *The New England journal of medicine*, **375**(26), pp. 2561-2569.

BROWN, N.F., CARTER, T.J., OTTAVIANI, D. and MULHOLLAND, P., 2018. Harnessing the immune system in glioblastoma. *British journal of cancer*, **119**(10), pp. 1171-1181.

CALLAHAN, M.K. and WOLCHOK, J.D., 2013. At the bedside: CTLA-4- and PD-1-blocking antibodies in cancer immunotherapy. *Journal of leukocyte biology*, **94**(1), pp. 41-53.

CANDOLFI, M., CURTIN, J.F., YAGIZ, K., ASSI, H., WIBOWO, M.K., ALZADEH, G.E., FOULAD, D., MUHAMMAD, A.K., SALEHI, S., KEECH, N., PUNTEL, M., LIU, C., SANDERSON, N.R., KROEGER, K.M., DUNN, R., MARTINS, G., LOWENSTEIN, P.R. and CASTRO, M.G., 2011. B cells are critical to T-cell-mediated antitumor immunity induced by a combined immune-stimulatory/conditionally cytotoxic therapy for glioblastoma. *Neoplasia (New York, N.Y.)*, **13**(10), pp. 947-960.

- CAROSELLA, E.D., ROUAS-FREISS, N., TRONIK-LE ROUX, D., MOREAU, P. and LEMAULT, J., 2015. HLA-G: An Immune Checkpoint Molecule. *Advances in Immunology*, **127**, pp. 33-144.
- CAROTTA, S., 2016. Targeting NK Cells for Anticancer Immunotherapy: Clinical and Preclinical Approaches. *Frontiers in immunology*, **7**, pp. 152.
- CARTER, T., SHAW, H., COHN-BROWN, D., CHESTER, K. and MULHOLLAND, P., 2016. Ipilimumab and Bevacizumab in Glioblastoma. *Clinical oncology (Royal College of Radiologists (Great Britain))*, **28**(10), pp. 622-626.
- CHAHLAVI, A., RAYMAN, P., RICHMOND, A.L., BISWAS, K., ZHANG, R., VOGELBAUM, M., TANNENBAUM, C., BARNETT, G. and FINKE, J.H., 2005. Glioblastomas induce T-lymphocyte death by two distinct pathways involving gangliosides and CD70. *Cancer research*, **65**(12), pp. 5428-5438.
- CHAMP, C.E., PALMER, J.D., VOLEK, J.S., WERNER-WASIK, M., ANDREWS, D.W., EVANS, J.J., GLASS, J., KIM, L. and SHI, W., 2014. Targeting metabolism with a ketogenic diet during the treatment of glioblastoma multiforme. *Journal of neuro-oncology*, **117**(1), pp. 125-131.
- CHANG, W.L. and BARRY, P.A., 2010. Attenuation of innate immunity by cytomegalovirus IL-10 establishes a long-term deficit of adaptive antiviral immunity. *Proceedings of the National Academy of Sciences of the United States of America*, **107**(52), pp. 22647-22652.
- CHEEVER, M.A., ALLISON, J.P., FERRIS, A.S., FINN, O.J., HASTINGS, B.M., HECHT, T.T., MELLMAN, I., PRINDIVILLE, S.A., VINER, J.L., WEINER, L.M. and MATRISIAN, L.M., 2009. The prioritization of cancer antigens: a national cancer institute pilot project for the acceleration of translational research. *Clinical cancer research : an official journal of the American Association for Cancer Research*, **15**(17), pp. 5323-5337.
- CHEEVER, M.A. and HIGANO, C.S., 2011. PROVENGE (Sipuleucel-T) in prostate cancer: the first FDA-approved therapeutic cancer vaccine. *Clinical cancer research : an official journal of the American Association for Cancer Research*, **17**(11), pp. 3520-3526.
- CHEN, D.S., IRVING, B.A. and HODI, F.S., 2012. Molecular pathways: next-generation immunotherapy--inhibiting programmed death-ligand 1 and programmed death-1. *Clinical cancer research : an official journal of the American Association for Cancer Research*, **18**(24), pp. 6580-6587.
- CHEN, W. and MCCLUSKEY, J., 2006. Immunodominance and immunodomination: critical factors in developing effective CD8+ T-cell-based cancer vaccines. *Advances in Cancer Research*, **95**, pp. 203-247.
- CHI, D.D., MERCHANT, R.E., RAND, R., CONRAD, A.J., GARRISON, D., TURNER, R., MORTON, D.L. and HOON, D.S., 1997. Molecular detection of tumor-associated antigens shared by human cutaneous melanomas and gliomas. *The American journal of pathology*, **150**(6), pp. 2143-2152.
- CHIBA, Y., HASHIMOTO, N., TSUBOI, A., RABO, C., OKA, Y., KINOSHITA, M., KAGAWA, N., OJI, Y., SUGIYAMA, H. and YOSHIMINE, T., 2010. Prognostic value of WT1 protein expression level and MIB-1 staining index as predictor of response to WT1 immunotherapy in glioblastoma patients. *Brain tumor pathology*, **27**(1), pp. 29-34.
- CHOW, K.K., HARA, W., LIM, M. and LI, G., 2015. Combining immunotherapy with radiation for the treatment of glioblastoma. *Journal of neuro-oncology*, **123**(3), pp. 459-464.

CLARK, A.J., WARE, J.L., CHEN, M.Y., GRAF, M.R., VAN METER, T.E., DOS SANTOS, W.G., FILLMORE, H.L. and BROADDUS, W.C., 2010. Effect of WT1 gene silencing on the tumorigenicity of human glioblastoma multiforme cells. *Journal of neurosurgery*, **112**(1), pp. 18-25.

CLOUGHESY, T.F., MOCHIZUKI, A.Y., ORPILLA, J.R., HUGO, W., LEE, A.H., DAVIDSON, T.B., WANG, A.C., ELLINGSON, B.M., RYTLEWSKI, J.A., SANDERS, C.M., KAWAGUCHI, E.S., DU, L., LI, G., YONG, W.H., GAFFEY, S.C., COHEN, A.L., MELLINGHOFF, I.K., LEE, E.Q., REARDON, D.A., O'BRIEN, B.J., BUTOWSKI, N.A., NGHIEMPHU, P.L., CLARKE, J.L., ARRILLAGA-ROMANY, I.C., COLMAN, H., KALEY, T.J., DE GROOT, J.F., LIAU, L.M., WEN, P.Y. and PRINS, R.M., 2019. Neoadjuvant anti-PD-1 immunotherapy promotes a survival benefit with intratumoral and systemic immune responses in recurrent glioblastoma. *Nature medicine*, **25**(3), pp. 477-486.

COBBS, C.S., HARKINS, L., SAMANTA, M., GILLESPIE, G.Y., BHARARA, S., KING, P.H., NABORS, L.B., COBBS, C.G. and BRITT, W.J., 2002. Human cytomegalovirus infection and expression in human malignant glioma. *Cancer research*, **62**(12), pp. 3347-3350.

COHEN, M.H., SHEN, Y.L., KEEGAN, P. and PAZDUR, R., 2009. FDA drug approval summary: bevacizumab (Avastin) as treatment of recurrent glioblastoma multiforme. *The oncologist*, **14**(11), pp. 1131-1138.

COLEY, W.B., 1891. II. Contribution to the Knowledge of Sarcoma. *Annals of Surgery*, **14**(3), pp. 199-220.

COSTELLO, R.T., GASTAUT, J.A. and OLIVE, D., 1999. What is the real role of CD40 in cancer immunotherapy? *Immunology today*, **20**(11), pp. 488-493.

COUZIN-FRANKEL, J., 2013. Breakthrough of the year 2013. Cancer immunotherapy. *Science (New York, N.Y.)*, **342**(6165), pp. 1432-1433.

COX, J.C. and COULTER, A.R., 1997. Adjuvants--a classification and review of their modes of action. *Vaccine*, **15**(3), pp. 248-256.

CRANE, C.A., AHN, B.J., HAN, S.J. and PARSA, A.T., 2012. Soluble factors secreted by glioblastoma cell lines facilitate recruitment, survival, and expansion of regulatory T cells: implications for immunotherapy. *Neuro-oncology*, **14**(5), pp. 584-595.

CRESSWELL, P., 1996. Invariant chain structure and MHC class II function. *Cell*, **84**(4), pp. 505-507.

CURRAN, M.A., MONTALVO, W., YAGITA, H. and ALLISON, J.P., 2010. PD-1 and CTLA-4 combination blockade expands infiltrating T cells and reduces regulatory T and myeloid cells within B16 melanoma tumors. *Proceedings of the National Academy of Sciences of the United States of America*, **107**(9), pp. 4275-4280.

D. CAPONEGRO, M., TETSUO MIYAUCHI, J. and E. TSIRKA, S., 2018. Contributions of immune cell populations in the maintenance, progression, and therapeutic modalities of glioma. **2**(1), pp. 24-44.

DE GRUIJL, T.D., VAN DEN EERTWEGH, A.J., PINEDO, H.M. and SCHEPER, R.J., 2008. Whole-cell cancer vaccination: from autologous to allogeneic tumor- and dendritic cell-based vaccines. *Cancer immunology, immunotherapy : CII*, **57**(10), pp. 1569-1577.

DEMETRIUS, L., 2005. Of mice and men. When it comes to studying ageing and the means to slow it down, mice are not just small humans. *EMBO reports*, **6 Spec No**, pp. S39-44.

DERER, A., SPILJAR, M., BAUMLER, M., HECHT, M., FIETKAU, R., FREY, B. and GAIPL, U.S., 2016. Chemoradiation Increases PD-L1 Expression in Certain Melanoma and Glioblastoma Cells. *Frontiers in immunology*, **7**, pp. 610.

DIDENKO, V.V., NGO, H.N., MINCHEW, C. and BASKIN, D.S., 2002a. Apoptosis of T lymphocytes invading glioblastomas multiforme: a possible tumor defense mechanism. *Journal of neurosurgery*, **96**(3), pp. 580-584.

DITTE, Z., DITTE, P., LABUDOVA, M., SIMKO, V., IULIANO, F., ZATOVICOVA, M., CSADEROVA, L., PASTOREKOVA, S. and PASTOREK, J., 2014. Carnosine inhibits carbonic anhydrase IX-mediated extracellular acidosis and suppresses growth of HeLa tumor xenografts. *BMC cancer*, **14**, pp. 358-2407-14-358.

DUNN, G.P., OLD, L.J. and SCHREIBER, R.D., 2004. The three Es of cancer immunoediting. *Annual Review of Immunology*, **22**, pp. 329-360.

DUNN, J., BABORIE, A., ALAM, F., JOYCE, K., MOXHAM, M., SIBSON, R., CROOKS, D., HUSBAND, D., SHENOY, A., BRODBELT, A., WONG, H., LILOGLOU, T., HAYLOCK, B. and WALKER, C., 2009. Extent of MGMT promoter methylation correlates with outcome in glioblastomas given temozolomide and radiotherapy. *British journal of cancer*, **101**(1), pp. 124-131.

DURRANT, L.G., PARSONS, T., MOSS, R., SPENDLOVE, I., CARTER, G. and CARR, F., 2001. Human anti-idiotypic antibodies can be good immunogens as they target FC receptors on antigen-presenting cells allowing efficient stimulation of both helper and cytotoxic T-cell responses. *International journal of cancer*, **92**(3), pp. 414-420.

EHTESHAM, M., SAMOTO, K., KABOS, P., ACOSTA, F.L., GUTIERREZ, M.A., BLACK, K.L. and YU, J.S., 2002. Treatment of intracranial glioma with in situ interferon-gamma and tumor necrosis factor-alpha gene transfer. *Cancer gene therapy*, **9**(11), pp. 925-934.

EISENBERG, G., MACHLENKIN, A., FRANKENBURG, S., MANSURA, A., PITCOVSKI, J., YEFENOF, E., PERETZ, T. and LOTEM, M., 2010. Transcutaneous immunization with hydrophilic recombinant gp100 protein induces antigen-specific cellular immune response. *Cellular immunology*, **266**(1), pp. 98-103.

ELGUETA, R., BENSON, M.J., DE VRIES, V.C., WASIUK, A., GUO, Y. and NOELLE, R.J., 2009. Molecular mechanism and function of CD40/CD40L engagement in the immune system. *Immunological reviews*, **229**(1), pp. 152-172.

ELIOPOULOS, A.G. and YOUNG, L.S., 2004. The role of the CD40 pathway in the pathogenesis and treatment of cancer. *Current opinion in pharmacology*, **4**(4), pp. 360-367.

ELLINGSON, B.M., CLOUGHESY, T.F., LAI, A., NGHIEMPHU, P.L., LALEZARI, S., ZAW, T., MOTEVALIBASHINAEINI, K., MISCHER, P.S. and POPE, W.B., 2012. Quantification of edema reduction using differential quantitative T2 (DQT2) relaxometry mapping in recurrent glioblastoma treated with bevacizumab. *Journal of neuro-oncology*, **106**(1), pp. 111-119.

ENGELHARDT, B. and RANSOHOFF, R.M., 2012. Capture, crawl, cross: the T cell code to breach the blood-brain barriers. *Trends in immunology*, **33**(12), pp. 579-589.

FADUL, C.E., FISHER, J.L., GUI, J., HAMPTON, T.H., COTE, A.L. and ERNSTOFF, M.S., 2011. Immune modulation effects of concomitant temozolomide and radiation therapy on peripheral blood mononuclear cells in patients with glioblastoma multiforme. *Neuro-oncology*, **13**(4), pp. 393-400.

FALCON-BEAS, C., TITTARELLI, A., MORA-BAU, G., TEMPIO, F., PEREZ, C., HEVIA, D., BEHRENS, C., FLORES, I., FALCON-BEAS, F., GARRIDO, P., ASCUI, G., PEREDA, C., GONZALEZ, F.E., SALAZAR-ONFRAY, F. and LOPEZ, M.N., 2019. Dexamethasone turns tumor antigen-presenting cells into tolerogenic dendritic cells with T cell inhibitory functions. *Immunobiology*, **224**(5), pp. 697-705.

FANNI, D., FANOS, V., MONGA, G., GEROSA, C., LOCCI, A., NEMOLATO, S., VAN EYKEN, P. and FAA, G., 2011. Expression of WT1 during normal human kidney development. *The journal of maternal-fetal & neonatal medicine : the official journal of the European Association of Perinatal Medicine, the Federation of Asia and Oceania Perinatal Societies, the International Society of Perinatal Obstetricians*, **24 Suppl 2**, pp. 44-47.

FARKKILA, M., JAASKELAINEN, J., KALLIO, M., BLOMSTEDT, G., RAININKO, R., VIRKKUNEN, P., PAETAU, A., SARELIN, H. and MANTYLA, M., 1994. Randomised, controlled study of intratumoral recombinant gamma-interferon treatment in newly diagnosed glioblastoma. *British journal of cancer*, **70**(1), pp. 138-141.

FILLEY, A.C., HENRIQUEZ, M. and DEY, M., 2017. Recurrent glioma clinical trial, CheckMate-143: the game is not over yet. *Oncotarget*, **8**(53), pp. 91779-91794.

FIGLIORE, E., FUSCO, C., ROMERO, P. and STAMENKOVIC, I., 2002. Matrix metalloproteinase 9 (MMP-9/gelatinase B) proteolytically cleaves ICAM-1 and participates in tumor cell resistance to natural killer cell-mediated cytotoxicity. *Oncogene*, **21**(34), pp. 5213-5223.

FISCHER, K., HOFFMANN, P., VOELKL, S., MEIDENBAUER, N., AMMER, J., EDINGER, M., GOTTFRIED, E., SCHWARZ, S., ROTHE, G., HOVES, S., RENNER, K., TIMISCHL, B., MACKENSEN, A., KUNZ-SCHUGHART, L., ANDREESEN, R., KRAUSE, S.W. and KREUTZ, M., 2007. Inhibitory effect of tumor cell-derived lactic acid on human T cells. *Blood*, **109**(9), pp. 3812-3819.

FRANK, R.T., NAJBAUER, J. and ABOODY, K.S., 2010. Concise review: stem cells as an emerging platform for antibody therapy of cancer. *Stem cells (Dayton, Ohio)*, **28**(11), pp. 2084-2087.

FREMD, C., SCHUETZ, F., SOHN, C., BECKHOVE, P. and DOMSCHKE, C., 2013. B cell-regulated immune responses in tumor models and cancer patients. *Oncoimmunology*, **2**(7), pp. e25443.

FRIESE, M.A., PLATTEN, M., LUTZ, S.Z., NAUMANN, U., AULWURM, S., BISCHOF, F., BUHRING, H.J., DICHGANS, J., RAMMENSEE, H.G., STEINLE, A. and WELLER, M., 2003. MICA/NKG2D-mediated immunogene therapy of experimental gliomas. *Cancer research*, **63**(24), pp. 8996-9006.

GALEA, I., BERNARDES-SILVA, M., FORSE, P.A., VAN ROOIJEN, N., LIBLAU, R.S. and PERRY, V.H., 2007. An antigen-specific pathway for CD8 T cells across the blood-brain barrier. *The Journal of experimental medicine*, **204**(9), pp. 2023-2030.

GARCIA-DIAZ, A., SHIN, D.S., MORENO, B.H., SACO, J., ESCUIN-ORDINAS, H., RODRIGUEZ, G.A., ZARETSKY, J.M., SUN, L., HUGO, W., WANG, X., PARISI, G., SAUS, C.P., TORREJON, D.Y., GRAEBER, T.G., COMIN-ANDUIX, B., HU-LIESKOVAN, S., DAMOISEAUX, R., LO, R.S. and RIBAS, A., 2019. Interferon Receptor Signaling Pathways Regulating PD-L1 and PD-L2 Expression. *Cell reports*, **29**(11), pp. 3766.

GARCIA-LORA, A., ALGARRA, I. and GARRIDO, F., 2003. MHC class I antigens, immune surveillance, and tumor immune escape. *Journal of cellular physiology*, **195**(3), pp. 346-355.

GARRIDO, F., APTSIAURI, N., DOORDUIJN, E.M., GARCIA LORA, A.M. and VAN HALL, T., 2016. The urgent need to recover MHC class I in cancers for effective immunotherapy. *Current opinion in immunology*, **39**, pp. 44-51.

GAUNITZ, F. and HIPKISS, A.R., 2012. Carnosine and cancer: a perspective. *Amino acids*, **43**(1), pp. 135-142.

GAUTAM, P., NAIR, S.C., GUPTA, M.K., SHARMA, R., POLISETTY, R.V., UPPIN, M.S., SUNDARAM, C., PULIGOPU, A.K., ANKATHI, P., PUROHIT, A.K., CHANDAK, G.R., HARSHA, H.C. and SIRDESHMUKH, R., 2012. Proteins with altered levels in plasma from glioblastoma patients as revealed by iTRAQ-based quantitative proteomic analysis. *PLoS one*, **7**(9), pp. e46153.

GILBERT, M.R., DIGNAM, J.J., ARMSTRONG, T.S., WEFEL, J.S., BLUMENTHAL, D.T., VOGELBAUM, M.A., COLMAN, H., CHAKRAVARTI, A., PUGH, S., WON, M., JERAJ, R., BROWN, P.D., JAECKLE, K.A., SCHIFF, D., STIEBER, V.W., BRACHMAN, D.G., WERNER-WASIK, M., TREMONT-LUKATS, I.W., SULMAN, E.P., ALDAPE, K.D., CURRAN, W.J., Jr and MEHTA, M.P., 2014. A randomized trial of bevacizumab for newly diagnosed glioblastoma. *The New England journal of medicine*, **370**(8), pp. 699-708.

GILES, A.J., HUTCHINSON, M.N.D., SONNEMANN, H.M., JUNG, J., FECCI, P.E., RATNAM, N.M., ZHANG, W., SONG, H., BAILEY, R., DAVIS, D., REID, C.M., PARK, D.M. and GILBERT, M.R., 2018. Dexamethasone-induced immunosuppression: mechanisms and implications for immunotherapy. *Journal for immunotherapy of cancer*, **6**(1), pp. 51-018-0371-5.

GINGRAS, M.C., ROUSSEL, E., BRUNER, J.M., BRANCH, C.D. and MOSER, R.P., 1995. Comparison of cell adhesion molecule expression between glioblastoma multiforme and autologous normal brain tissue. *Journal of neuroimmunology*, **57**(1-2), pp. 143-153.

GROSSMAN, S.A., YE, X., LESSER, G., SLOAN, A., CARRAWAY, H., DESIDERI, S., PIANTADOSI, S. and NABTT CNS CONSORTIUM, 2011. Immunosuppression in patients with high-grade gliomas treated with radiation and temozolomide. *Clinical cancer research : an official journal of the American Association for Cancer Research*, **17**(16), pp. 5473-5480.

GUERMONPREZ, P., VALLADEAU, J., ZITVOGEL, L., THERY, C. and AMIGORENA, S., 2002. Antigen presentation and T cell stimulation by dendritic cells. *Annual Review of Immunology*, **20**, pp. 621-667.

GUILLEREY, C., HUNTINGTON, N.D. and SMYTH, M.J., 2016. Targeting natural killer cells in cancer immunotherapy. *Nature immunology*, **17**(9), pp. 1025-1036.

GUO, F.F. and CUI, J.W., 2019. The Role of Tumor-Infiltrating B Cells in Tumor Immunity. *Journal of oncology*, **2019**, pp. 2592419.

GUO, L., SANG, M., LIU, Q., FAN, X., ZHANG, X. and SHAN, B., 2013. The expression and clinical significance of melanoma-associated antigen-A1, -A3 and -A11 in glioma. *Oncology letters*, **6**(1), pp. 55-62.

HAN, S., ZHANG, C., LI, Q., DONG, J., LIU, Y., HUANG, Y., JIANG, T. and WU, A., 2014. Tumour-infiltrating CD4(+) and CD8(+) lymphocytes as predictors of clinical outcome in glioma. *British journal of cancer*, **110**(10), pp. 2560-2568.

HANAHAHAN, D. and WEINBERG, R.A., 2011. Hallmarks of cancer: the next generation. *Cell*, **144**(5), pp. 646-674.

HANIF, F., MUZAFFAR, K., PERVEEN, K., MALHI, S.M. and SIMJEE, S., 2017. Glioblastoma Multiforme: A Review of its Epidemiology and Pathogenesis through Clinical Presentation and Treatment. *Asian Pacific journal of cancer prevention : APJCP*, **18**(1), pp. 3-9.

HANIHARA, M., KAWATAKI, T., OH-OKA, K., MITSUKA, K., NAKAO, A. and KINOUCI, H., 2016. Synergistic antitumor effect with indoleamine 2,3-dioxygenase inhibition and temozolomide in a murine glioma model. *Journal of neurosurgery*, **124**(6), pp. 1594-1601.

HARDING, J.W. and O'FALLON, J.V., 1979. The subcellular distribution of carnosine, carnosine synthetase, and carnosinase in mouse olfactory tissues. *Brain research*, **173**(1), pp. 99-109.

HASSEL, J.C., HEINZERLING, L., ABERLE, J., BAHR, O., EIGENTLER, T.K., GRIMM, M.O., GRUNWALD, V., LEIPE, J., REINMUTH, N., TIETZE, J.K., TROJAN, J., ZIMMER, L. and GUTZMER, R., 2017. Combined immune checkpoint blockade (anti-PD-1/anti-CTLA-4): Evaluation and management of adverse drug reactions. *Cancer treatment reviews*, **57**, pp. 36-49.

HDEIB, A. and SLOAN, A.E., 2015. Dendritic cell immunotherapy for solid tumors: evaluation of the DCVax(R) platform in the treatment of glioblastoma multiforme. *CNS oncology*, **4**(2), pp. 63-69.

HIGANO, C.S., SMALL, E.J., SCHELLHAMMER, P., YASOTHAN, U., GUBERNICK, S., KIRKPATRICK, P. and KANTOFF, P.W., 2010. Sipuleucel-T. *Nature reviews. Drug discovery*, **9**(7), pp. 513-514.

HIPKISS, A.R., PRESTON, J.E., HIMSWORTH, D.T., WORTHINGTON, V.C., KEOWN, M., MICHAELIS, J., LAWRENCE, J., MATEEN, A., ALLENDE, L., EAGLES, P.A. and ABBOTT, N.J., 1998. Pluripotent protective effects of carnosine, a naturally occurring dipeptide. *Annals of the New York Academy of Sciences*, **854**, pp. 37-53.

HOLLAND, E.C., 2000. Glioblastoma multiforme: the terminator. *Proceedings of the National Academy of Sciences of the United States of America*, **97**(12), pp. 6242-6244.

HOTTINGER, A.F., PACHECO, P. and STUPP, R., 2016. Tumor treating fields: a novel treatment modality and its use in brain tumors. *Neuro-oncology*, **18**(10), pp. 1338-1349.

HOU, L.C., VEERAVAGU, A., HSU, A.R. and TSE, V.C., 2006. Recurrent glioblastoma multiforme: a review of natural history and management options. *Neurosurgical focus*, **20**(4), pp. E5.

HUETTNER, C., PAULUS, W. and ROGGENDORF, W., 1995. Messenger RNA expression of the immunosuppressive cytokine IL-10 in human gliomas. *The American journal of pathology*, **146**(2), pp. 317-322.

HUNG, K., HAYASHI, R., LAFOND-WALKER, A., LOWENSTEIN, C., PARDOLL, D. and LEVITSKY, H., 1998. The central role of CD4(+) T cells in the antitumor immune response. *The Journal of experimental medicine*, **188**(12), pp. 2357-2368.

HYLAND, P., DUGGAN, O., HIPKISS, A., BARNETT, C. and BARNETT, Y., 2000. The effects of carnosine on oxidative DNA damage levels and in vitro lifespan in human peripheral blood derived CD4+T cell clones. *Mechanisms of ageing and development*, **121**(1-3), pp. 203-215.

IANNELLO, A. and AHMAD, A., 2005. Role of antibody-dependent cell-mediated cytotoxicity in the efficacy of therapeutic anti-cancer monoclonal antibodies. *Cancer metastasis reviews*, **24**(4), pp. 487-499.

- INOUE, S., LEITNER, W.W., GOLDING, B. and SCOTT, D., 2006. Inhibitory effects of B cells on antitumor immunity. *Cancer research*, **66**(15), pp. 7741-7747.
- IOVINE, B., GUARDIA, F., IRACE, C. and BEVILACQUA, M.A., 2016. l-carnosine dipeptide overcomes acquired resistance to 5-fluorouracil in HT29 human colon cancer cells via downregulation of HIF1-alpha and induction of apoptosis. *Biochimie*, **127**, pp. 196-204.
- ITO, H., NAKASHIMA, H. and CHIOCCA, E.A., 2019. Molecular responses to immune checkpoint blockade in glioblastoma. *Nature medicine*, **25**(3), pp. 359-361.
- IWAMI, K., NATSUME, A. and WAKABAYASHI, T., 2011. Cytokine networks in glioma. *Neurosurgical review*, **34**(3), pp. 253-63; discussion 263-4.
- IWASAKI, A., 2017. Immune Regulation of Antibody Access to Neuronal Tissues. *Trends in molecular medicine*, **23**(3), pp. 227-245.
- JACKSON, C., RUZEVICK, J., PHALLEN, J., BELCAID, Z. and LIM, M., 2011. Challenges in immunotherapy presented by the glioblastoma multiforme microenvironment. *Clinical & developmental immunology*, **2011**, pp. 732413.
- JAGER, E., GNJATIC, S., NAGATA, Y., STOCKERT, E., JAGER, D., KARBACH, J., NEUMANN, A., RIECKENBERG, J., CHEN, Y.T., RITTER, G., HOFFMAN, E., ARAND, M., OLD, L.J. and KNUTH, A., 2000. Induction of primary NY-ESO-1 immunity: CD8+ T lymphocyte and antibody responses in peptide-vaccinated patients with NY-ESO-1+ cancers. *Proceedings of the National Academy of Sciences of the United States of America*, **97**(22), pp. 12198-12203.
- JANEWAY, C.A., CAPRA, J.D., TRAVERS, P. AND WALPORT M., 2001. *Immunobiology 5 : the immune system in health and disease*. 5th edn. New York; Edinburgh: Garland; Churchill Livingstone.
- JONES, A.R. and SHUSTA, E.V., 2007. Blood-brain barrier transport of therapeutics via receptor-mediation. *Pharmaceutical research*, **24**(9), pp. 1759-1771.
- JOSEPHS, S.F., ICHIM, T.E., PRINCE, S.M., KESARI, S., MARINCOLA, F.M., ESCOBEDO, A.R. and JAFRI, A., 2018. Unleashing endogenous TNF-alpha as a cancer immunotherapeutic. *Journal of translational medicine*, **16**(1), pp. 242-018-1611-7.
- KAINA, B., CHRISTMANN, M., NAUMANN, S. and ROOS, W.P., 2007. MGMT: key node in the battle against genotoxicity, carcinogenicity and apoptosis induced by alkylating agents. *DNA repair*, **6**(8), pp. 1079-1099.
- KANE, A. and YANG, I., 2010. Interferon-gamma in brain tumor immunotherapy. *Neurosurgery clinics of North America*, **21**(1), pp. 77-86.
- KEDL, R.M., KAPPLER, J.W. and MARRACK, P., 2003. Epitope dominance, competition and T cell affinity maturation. *Current opinion in immunology*, **15**(1), pp. 120-127.
- KENNEDY, B.C., SHOWERS, C.R., ANDERSON, D.E., ANDERSON, L., CANOLL, P., BRUCE, J.N. and ANDERSON, R.C., 2013. Tumor-associated macrophages in glioma: friend or foe? *Journal of oncology*, **2013**, pp. 486912.
- KHONG, H. and OVERWIJK, W.W., 2016. Adjuvants for peptide-based cancer vaccines. *Journal for immunotherapy of cancer*, **4**, pp. 56-016-0160-y. eCollection 2016.

KIJIMA, N., HOSEN, N., KAGAWA, N., HASHIMOTO, N., KINOSHITA, M., OJI, Y., SUGIYAMA, H. and YOSHIMINE, T., 2014. Wilms' tumor 1 is involved in tumorigenicity of glioblastoma by regulating cell proliferation and apoptosis. *Anticancer Research*, **34**(1), pp. 61-67.

KINOSHITA, M., MCDANNOLD, N., JOLESZ, F.A. and HYNYNEN, K., 2006. Noninvasive localized delivery of Herceptin to the mouse brain by MRI-guided focused ultrasound-induced blood-brain barrier disruption. *Proceedings of the National Academy of Sciences of the United States of America*, **103**(31), pp. 11719-11723.

KLEINBERG, L., 2016. Polifeprosan 20, 3.85% carmustine slow release wafer in malignant glioma: patient selection and perspectives on a low-burden therapy. *Patient preference and adherence*, **10**, pp. 2397-2406.

KLOETZEL, P.M. and OSSENDORP, F., 2004. Proteasome and peptidase function in MHC-class-I-mediated antigen presentation. *Current opinion in immunology*, **16**(1), pp. 76-81.

KNUTSON, K.L. and DISIS, M.L., 2005. Tumor antigen-specific T helper cells in cancer immunity and immunotherapy. *Cancer immunology, immunotherapy : CII*, **54**(8), pp. 721-728.

KOIDO, S., OKAMOTO, M., KOBAYASHI, M., SHIMODAIRA, S. and SUGIYAMA, H., 2017. Significance of Wilms' tumor 1 antigen as a cancer vaccine for pancreatic cancer. *Discovery medicine*, **24**(130), pp. 41-49.

KONIG, R., HUANG, L.Y. and GERMAIN, R.N., 1992. MHC class II interaction with CD4 mediated by a region analogous to the MHC class I binding site for CD8. *Nature*, **356**(6372), pp. 796-798.

KORE, R.A. and ABRAHAM, E.C., 2014. Inflammatory cytokines, interleukin-1 beta and tumor necrosis factor-alpha, upregulated in glioblastoma multiforme, raise the levels of CRYAB in exosomes secreted by U373 glioma cells. *Biochemical and biophysical research communications*, **453**(3), pp. 326-331.

KOVACS-SOLYOM, F., BLASKO, A., FAJKA-BOJA, R., KATONA, R.L., VEGH, L., NOVAK, J., SZEKENI, G.J., KRENACS, L., UHER, F., TUBAK, V., KISS, R. and MONOSTORI, E., 2010. Mechanism of tumor cell-induced T-cell apoptosis mediated by galectin-1. *Immunology letters*, **127**(2), pp. 108-118.

KOVATS, S., MAIN, E.K., LIBRACH, C., STUBBLEBINE, M., FISHER, S.J. and DEMARS, R., 1990. A class I antigen, HLA-G, expressed in human trophoblasts. *Science (New York, N.Y.)*, **248**(4952), pp. 220-223.

LADOMERSKY, E., SCHOLTENS, D.M., KOCHERGINSKY, M., HIBLER, E.A., BARTOM, E.T., OTTO-MEYER, S., ZHAI, L., LAUING, K.L., CHOI, J., SOSMAN, J.A., WU, J.D., ZHANG, B., LUKAS, R.V. and WAINWRIGHT, D.A., 2019. The Coincidence Between Increasing Age, Immunosuppression, and the Incidence of Patients With Glioblastoma. *Frontiers in pharmacology*, **10**, pp. 200.

LADOMERSKY, E., ZHAI, L., LENZEN, A., LAUING, K.L., QIAN, J., SCHOLTENS, D.M., GRITSINA, G., SUN, X., LIU, Y., YU, F., GONG, W., LIU, Y., JIANG, B., TANG, T., PATEL, R., PLATANIAS, L.C., JAMES, C.D., STUPP, R., LUKAS, R.V., BINDER, D.C. and WAINWRIGHT, D.A., 2018. IDO1 Inhibition Synergizes with Radiation and PD-1 Blockade to Durably Increase Survival Against Advanced Glioblastoma. *Clinical cancer research : an official journal of the American Association for Cancer Research*, **24**(11), pp. 2559-2573.

LANZAVECCHIA, A. and SALLUSTO, F., 2001. Regulation of T cell immunity by dendritic cells. *Cell*, **106**(3), pp. 263-266.

LAPOINTE, R., BELLEMARE-PELLETIER, A., HOUSSEAU, F., THIBODEAU, J. and HWU, P., 2003. CD40-stimulated B lymphocytes pulsed with tumor antigens are effective antigen-presenting cells that can generate specific T cells. *Cancer research*, **63**(11), pp. 2836-2843.

LARDNER, A., 2001. The effects of extracellular pH on immune function. *Journal of leukocyte biology*, **69**(4), pp. 522-530.

LE GAL, F.A., RITEAU, B., SEDLIK, C., KHALIL-DAHER, I., MENIER, C., DAUSSET, J., GUILLET, J.G., CAROSELLA, E.D. and ROUAS-FREISS, N., 1999. HLA-G-mediated inhibition of antigen-specific cytotoxic T lymphocytes. *International immunology*, **11**(8), pp. 1351-1356.

LEACH, D.R., KRUMMEL, M.F. and ALLISON, J.P., 1996. Enhancement of antitumor immunity by CTLA-4 blockade. *Science (New York, N.Y.)*, **271**(5256), pp. 1734-1736.

LEDFORD, H., 2011. Melanoma drug wins US approval. *Nature*, **471**(7340), pp. 561.

LEE, S.Y., 2016. Temozolomide resistance in glioblastoma multiforme. *Genes & diseases*, **3**(3), pp. 198-210.

LI, B., SEVERSON, E., PIGNON, J.C., ZHAO, H., LI, T., NOVAK, J., JIANG, P., SHEN, H., ASTER, J.C., RODIG, S., SIGNORETTI, S., LIU, J.S. and LIU, X.S., 2016. Comprehensive analyses of tumor immunity: implications for cancer immunotherapy. *Genome biology*, **17**(1), pp. 174-016-1028-7.

LI, M., BOLDUC, A.R., HODA, M.N., GAMBLE, D.N., DOLISCA, S.B., BOLDUC, A.K., HOANG, K., ASHLEY, C., MCCALL, D., ROJANI, A.M., MARIA, B.L., RIXE, O., MACDONALD, T.J., HEEGER, P.S., MELLOR, A.L., MUNN, D.H. and JOHNSON, T.S., 2014. The indoleamine 2,3-dioxygenase pathway controls complement-dependent enhancement of chemo-radiation therapy against murine glioblastoma. *Journal for immunotherapy of cancer*, **2**, pp. 21-1426-2-21. eCollection 2014.

LI, W., JOSHI, M.D., SINGHANIA, S., RAMSEY, K.H. and MURTHY, A.K., 2014. Peptide Vaccine: Progress and Challenges. *Vaccines*, **2**(3), pp. 515-536.

LIAU, L.M., ASHKAN, K., TRAN, D.D., CAMPION, J.L., TRUSHEIM, J.E., COBBS, C.S., HETH, J.A., SALACZ, M., TAYLOR, S., D'ANDRE, S.D., IWAMOTO, F.M., DROPCHO, E.J., MOSHEL, Y.A., WALTER, K.A., PILLAINAYAGAM, C.P., AIKEN, R., CHAUDHARY, R., GOLDLUST, S.A., BOTA, D.A., DUIC, P., GREWAL, J., ELINZANO, H., TOMS, S.A., LILLEHEI, K.O., MIKKELSEN, T., WALBERT, T., ABRAM, S.R., BRENNER, A.J., BREM, S., EWEND, M.G., KHAGI, S., PORTNOW, J., KIM, L.J., LOUDON, W.G., THOMPSON, R.C., AVIGAN, D.E., FINK, K.L., GEOFFROY, F.J., LINDHORST, S., LUTZKY, J., SLOAN, A.E., SCHACKERT, G., KREX, D., MEISEL, H.J., WU, J., DAVIS, R.P., DUMA, C., ETAME, A.B., MATHIEU, D., KESARI, S., PICCIONI, D., WESTPHAL, M., BASKIN, D.S., NEW, P.Z., LACROIX, M., MAY, S.A., PLUARD, T.J., TSE, V., GREEN, R.M., VILLANO, J.L., PEARLMAN, M., PETRECCA, K., SCHULDER, M., TAYLOR, L.P., MAIDA, A.E., PRINS, R.M., CLOUGHESY, T.F., MULHOLLAND, P. and BOSCH, M.L., 2018. First results on survival from a large Phase 3 clinical trial of an autologous dendritic cell vaccine in newly diagnosed glioblastoma. *Journal of translational medicine*, **16**(1), pp. 142-018-1507-6.

LIM, J.P. and GLEESON, P.A., 2011. Macropinocytosis: an endocytic pathway for internalising large gulps. *Immunology and cell biology*, **89**(8), pp. 836-843.

LINDENCORONA, J.A., PREISS, S., KAMMERTOENS, T., SCHULER, T., PIECHOCKI, M., WEI, W.Z., SELIGER, B., BLANKENSTEIN, T. and KIESSLING, R., 2004. CD4+ T cell-mediated HER-2/neu-specific tumor rejection in the absence of B cells. *International journal of cancer*, **109**(2), pp. 259-264.

LIU, G., AKASAKI, Y., KHONG, H.T., WHEELER, C.J., DAS, A., BLACK, K.L. and YU, J.S., 2005. Cytotoxic T cell targeting of TRP-2 sensitizes human malignant glioma to chemotherapy. *Oncogene*, **24**(33), pp. 5226-5234.

LIU, G., KHONG, H.T., WHEELER, C.J., YU, J.S., BLACK, K.L. and YING, H., 2003. Molecular and functional analysis of tyrosinase-related protein (TRP)-2 as a cytotoxic T lymphocyte target in patients with malignant glioma. *Journal of immunotherapy (Hagerstown, Md.: 1997)*, **26**(4), pp. 301-312.

LIU, G., YING, H., ZENG, G., WHEELER, C.J., BLACK, K.L. and YU, J.S., 2004. HER-2, gp100, and MAGE-1 are expressed in human glioblastoma and recognized by cytotoxic T cells. *Cancer research*, **64**(14), pp. 4980-4986.

LIU, Y., CARLSSON, R., AMBJORN, M., HASAN, M., BADN, W., DARABI, A., SIESJO, P. and ISSAZADEH-NAVIKAS, S., 2013. PD-L1 expression by neurons nearby tumors indicates better prognosis in glioblastoma patients. *The Journal of neuroscience : the official journal of the Society for Neuroscience*, **33**(35), pp. 14231-14245.

LOHR, J., RATLIFF, T., HUPPERTZ, A., GE, Y., DICTUS, C., AHMADI, R., GRAU, S., HIRAOKA, N., ECKSTEIN, V., ECKER, R.C., KORFF, T., VON DEIMLING, A., UNTERBERG, A., BECKHOVE, P. and HEROLD-MENDE, C., 2011. Effector T-cell infiltration positively impacts survival of glioblastoma patients and is impaired by tumor-derived TGF-beta. *Clinical cancer research : an official journal of the American Association for Cancer Research*, **17**(13), pp. 4296-4308.

LOUVEAU, A., PLOG, B.A., ANTILA, S., ALITALO, K., NEDERGAARD, M. and KIPNIS, J., 2017. Understanding the functions and relationships of the glymphatic system and meningeal lymphatics. *The Journal of clinical investigation*, **127**(9), pp. 3210-3219.

LOUVEAU, A., SMIRNOV, I., KEYES, T.J., ECCLES, J.D., ROUHANI, S.J., PESKE, J.D., DERECKI, N.C., CASTLE, D., MANDELL, J.W., LEE, K.S., HARRIS, T.H. and KIPNIS, J., 2015. Structural and functional features of central nervous system lymphatic vessels. *Nature*, **523**(7560), pp. 337-341.

LUCAS, K.G., BAO, L., BRUGGEMAN, R., DUNHAM, K. and SPECHT, C., 2011. The detection of CMV pp65 and IE1 in glioblastoma multiforme. *Journal of neuro-oncology*, **103**(2), pp. 231-238.

L UWOR, R.B., STYLLI, S.S. and KAYE, A.H., 2013. The role of Stat3 in glioblastoma multiforme. *Journal of clinical neuroscience : official journal of the Neurosurgical Society of Australasia*, **20**(7), pp. 907-911.

MAENAKA, K. and JONES, E.Y., 1999. MHC superfamily structure and the immune system. *Current opinion in structural biology*, **9**(6), pp. 745-753.

MAIER, S., GERAGHTY, D.E. and WEISS, E.H., 1999. Expression and regulation of HLA-G in human glioma cell lines. *Transplantation proceedings*, **31**(4), pp. 1849-1853.

MANDI, Y. and VECSEI, L., 2012. The kynurenine system and immunoregulation. *Journal of neural transmission (Vienna, Austria : 1996)*, **119**(2), pp. 197-209.

MASTELIC-GAVILLET, B., BALINT, K., BOUDOUSQUIE, C., GANNON, P.O. and KANDALAFT, L.E., 2019. Personalized Dendritic Cell Vaccines-Recent Breakthroughs and Encouraging Clinical Results. *Frontiers in immunology*, **10**, pp. 766.

- MAXWELL, R., JACKSON, C.M. and LIM, M., 2017. Clinical Trials Investigating Immune Checkpoint Blockade in Glioblastoma. *Current treatment options in oncology*, **18**(8), pp. 51-017-0492-y.
- MBONGUE, J.C., NICHOLAS, D.A., TORREZ, T.W., KIM, N.S., FIREK, A.F. and LANGRIDGE, W.H., 2015. The Role of Indoleamine 2, 3-Dioxygenase in Immune Suppression and Autoimmunity. *Vaccines*, **3**(3), pp. 703-729.
- MCGRANAHAN, T., THERKELSEN, K.E., AHMAD, S. and NAGPAL, S., 2019. Current State of Immunotherapy for Treatment of Glioblastoma. *Current treatment options in oncology*, **20**(3), pp. 24-019-0619-4.
- MCLAREN, J.E. and RAMJI, D.P., 2009. Interferon gamma: a master regulator of atherosclerosis. *Cytokine & growth factor reviews*, **20**(2), pp. 125-135.
- MECHLEB, B., KHATER, F., EID, A., DAVID, G. and MOORMAN, J.P., 2003. Late onset Ommaya reservoir infection due to Staphylococcus aureus: case report and review of Ommaya Infections. *The Journal of infection*, **46**(3), pp. 196-198.
- MEDAWAR, P.B., 1948. Immunity to homologous grafted skin; the fate of skin homografts transplanted to the brain, to subcutaneous tissue, and to the anterior chamber of the eye. *British journal of experimental pathology*, **29**(1), pp. 58-69.
- MELERO, I., BERRAONDO, P., RODRIGUEZ-RUIZ, M.E. and PEREZ-GRACIA, J.L., 2016. Making the Most of Cancer Surgery with Neoadjuvant Immunotherapy. *Cancer discovery*, **6**(12), pp. 1312-1314.
- MENSSEN, H.D., BERTELMANN, E., BARTELT, S., SCHMIDT, R.A., PECHER, G., SCHRAMM, K. and THIEL, E., 2000. Wilms' tumor gene (WT1) expression in lung cancer, colon cancer and glioblastoma cell lines compared to freshly isolated tumor specimens. *Journal of cancer research and clinical oncology*, **126**(4), pp. 226-232.
- METHERINGHAM, R.L., PUDNEY, V.A., GUNN, B., TOWEY, M., SPENDLOVE, I. and DURRANT, L.G., 2009. Antibodies designed as effective cancer vaccines. *mAbs*, **1**(1), pp. 71-85.
- MINEO, J.F., BORDRON, A., QUINTIN-ROUE, I., LOISEL, S., STER, K.L., BUHE, V., LAGARDE, N. and BERTHOUE, C., 2004. Recombinant humanised anti-HER2/neu antibody (Herceptin) induces cellular death of glioblastomas. *British journal of cancer*, **91**(6), pp. 1195-1199.
- MITSUKA, K., KAWATAKI, T., SATOH, E., ASAHARA, T., HORIKOSHI, T. and KINOUCHE, H., 2013. Expression of indoleamine 2,3-dioxygenase and correlation with pathological malignancy in gliomas. *Neurosurgery*, **72**(6), pp. 1031-8; discussion 1038-9.
- MITTAL, S., KLINGER, N.V., MICHELHAUGH, S.K., BARGER, G.R., PANNULLO, S.C. and JUHASZ, C., 2018. Alternating electric tumor treating fields for treatment of glioblastoma: rationale, preclinical, and clinical studies. *Journal of neurosurgery*, **128**(2), pp. 414-421.
- MITTELBRONN, M., PLATTEN, M., ZEINER, P., DOMBROWSKI, Y., FRANK, B., ZACHSKORN, C., HARTEP, P.N., WELLER, M. and WISCHHUSEN, J., 2011. Macrophage migration inhibitory factor (MIF) expression in human malignant gliomas contributes to immune escape and tumour progression. *Acta Neuropathologica*, **122**(3), pp. 353-365.
- MITTELBRONN, M., SIMON, P., LOFFLER, C., CAPPER, D., BUNZ, B., HARTEP, P., SCHLASZUS, H., SCHLEICH, A., TABATABAI, G., GOEPPERT, B., MEYERMANN, R., WELLER, M. and WISCHHUSEN, J.,

2007. Elevated HLA-E levels in human glioblastomas but not in grade I to III astrocytomas correlate with infiltrating CD8+ cells. *Journal of neuroimmunology*, **189**(1-2), pp. 50-58.
- MIYAZAKI, T., MORITAKE, K., YAMADA, K., HARA, N., OSAGO, H., SHIBATA, T., AKIYAMA, Y. and TSUCHIYA, M., 2009. Indoleamine 2,3-dioxygenase as a new target for malignant glioma therapy. Laboratory investigation. *Journal of neurosurgery*, **111**(2), pp. 230-237.
- MUNN, D.H. and MELLOR, A.L., 2004. IDO and tolerance to tumors. *Trends in molecular medicine*, **10**(1), pp. 15-18.
- NAHTA, R. and ESTEVA, F.J., 2006. Herceptin: mechanisms of action and resistance. *Cancer letters*, **232**(2), pp. 123-138.
- NAKAHARA, Y., OKAMOTO, H., MINETA, T. and TABUCHI, K., 2004. Expression of the Wilms' tumor gene product WT1 in glioblastomas and medulloblastomas. *Brain tumor pathology*, **21**(3), pp. 113-116.
- NDUOM, E.K., WEI, J., YAGHI, N.K., HUANG, N., KONG, L.Y., GABRUSIEWICZ, K., LING, X., ZHOU, S., IVAN, C., CHEN, J.Q., BURKS, J.K., FULLER, G.N., CALIN, G.A., CONRAD, C.A., CREAMY, C., RITTHIPICHAI, K., RADVANYI, L. and HEIMBERGER, A.B., 2016. PD-L1 expression and prognostic impact in glioblastoma. *Neuro-oncology*, **18**(2), pp. 195-205.
- NDUOM, E.K., WELLER, M. and HEIMBERGER, A.B., 2015. Immunosuppressive mechanisms in glioblastoma. *Neuro-oncology*, **17 Suppl 7**, pp. vii9-vii14.
- NEVES, V., AIRES-DA-SILVA, F., CORTE-REAL, S. and CASTANHO, M.A.R.B., 2016. *Antibody Approaches To Treat Brain Diseases*.
- NGUYEN, S., BEZIAT, V., DHEDIN, N., KUENTZ, M., VERNANT, J.P., DEBRE, P. and VIEILLARD, V., 2009. HLA-E upregulation on IFN-gamma-activated AML blasts impairs CD94/NKG2A-dependent NK cytotoxicity after haplo-mismatched hematopoietic SCT. *Bone marrow transplantation*, **43**(9), pp. 693-699.
- NIMMERJAHN, F. and RAVETCH, J.V., 2008. Fcγ receptors as regulators of immune responses. *Nature reviews.Immunology*, **8**(1), pp. 34-47.
- NISHIDA, N. and KUDO, M., 2019. Liver damage related to immune checkpoint inhibitors. *Hepatology international*, **13**(3), pp. 248-252.
- NOROXE, D.S., POULSEN, H.S. and LASSEN, U., 2017. Hallmarks of glioblastoma: a systematic review. *ESMO open*, **1**(6), pp. e000144-2016-000144. eCollection 2016.
- OHAEGBULAM, K.C., ASSAL, A., LAZAR-MOLNAR, E., YAO, Y. and ZANG, X., 2015. Human cancer immunotherapy with antibodies to the PD-1 and PD-L1 pathway. *Trends in molecular medicine*, **21**(1), pp. 24-33.
- OHLFEST, J.R., ANDERSEN, B.M., LITTELMAN, A.J., XIA, J., PENNELL, C.A., SWIER, L.E., SALAZAR, A.M. and OLIN, M.R., 2013. Vaccine injection site matters: qualitative and quantitative defects in CD8 T cells primed as a function of proximity to the tumor in a murine glioma model. *Journal of immunology (Baltimore, Md.: 1950)*, **190**(2), pp. 613-620.
- OKAZAKI, T. and HONJO, T., 2006. The PD-1-PD-L pathway in immunological tolerance. *Trends in immunology*, **27**(4), pp. 195-201.

- OKURA, H., SMITH, C.A. and RUTKA, J.T., 2014. Gene therapy for malignant glioma. *Molecular and cellular therapies*, **2**, pp. 21-8426-2-21. eCollection 2014.
- OPPERMANN, H., DIETTERLE, J., PURCZ, K., MORAWSKI, M., EISENLOFFEL, C., MULLER, W., MEIXENSBERGER, J. and GAUNITZ, F., 2018. Carnosine selectively inhibits migration of IDH-wildtype glioblastoma cells in a co-culture model with fibroblasts. *Cancer cell international*, **18**, pp. 111-018-0611-2. eCollection 2018.
- OPPERMANN, H., FAUST, H., YAMANISHI, U., MEIXENSBERGER, J. and GAUNITZ, F., 2019. Carnosine inhibits glioblastoma growth independent from PI3K/Akt/mTOR signaling. *PloS one*, **14**(6), pp. e0218972.
- O'ROURKE, D.M., NASRALLAH, M.P., DESAI, A., MELENHORST, J.J., MANSFIELD, K., MORRISSETTE, J.J.D., MARTINEZ-LAGE, M., BREM, S., MALONEY, E., SHEN, A., ISAACS, R., MOHAN, S., PLESA, G., LACEY, S.F., NAVENOT, J.M., ZHENG, Z., LEVINE, B.L., OKADA, H., JUNE, C.H., BROGDON, J.L. and MAUS, M.V., 2017. A single dose of peripherally infused EGFRvIII-directed CAR T cells mediates antigen loss and induces adaptive resistance in patients with recurrent glioblastoma. *Science translational medicine*, **9**(399), pp. 10.1126/scitranslmed.aaa0984.
- OSTROM, Q.T., GITTLEMAN, H., LIAO, P., VECCHIONE-KOVAL, T., WOLINSKY, Y., KRUCHKO, C. and BARNHOLTZ-SLOAN, J.S., 2017. CBTRUS Statistical Report: Primary brain and other central nervous system tumors diagnosed in the United States in 2010-2014. *Neuro-oncology*, **19**(suppl_5), pp. v1-v88.
- PADGETT, D.A. and GLASER, R., 2003. How stress influences the immune response. *Trends in immunology*, **24**(8), pp. 444-448.
- PALLINI, R., CASALBORE, P., MERCANTI, D., MAGGIANO, N. and LAROCCA, L., M., 2000. Phenotypic Change of Human Cultured Meningioma Cells. *Journal of neurooncology*, **49**(1), pp. 9-17.
- PANDURANGAN, M., MISTRY, B., ENKHATAIVAN, G. and KIM, D.H., 2016. Efficacy of carnosine on activation of caspase 3 and human renal carcinoma cell inhibition. *International journal of biological macromolecules*, **92**, pp. 377-382.
- PARKHURST, M.R., FITZGERALD, E.B., SOUTHWOOD, S., SETTE, A., ROSENBERG, S.A. and KAWAKAMI, Y., 1998. Identification of a shared HLA-A*0201-restricted T-cell epitope from the melanoma antigen tyrosinase-related protein 2 (TRP2). *Cancer research*, **58**(21), pp. 4895-4901.
- PARSA, A.T., WALDRON, J.S., PANNER, A., CRANE, C.A., PARNEY, I.F., BARRY, J.J., CACHOLA, K.E., MURRAY, J.C., TIHAN, T., JENSEN, M.C., MISCHER, P.S., STOKOE, D. and PIEPER, R.O., 2007. Loss of tumor suppressor PTEN function increases B7-H1 expression and immunoresistance in glioma. *Nature medicine*, **13**(1), pp. 84-88.
- PASCOLO, S., BERVAS, N., URE, J.M., SMITH, A.G., LEMONNIER, F.A. and PERARNAU, B., 1997. HLA-A2.1-restricted education and cytolytic activity of CD8(+) T lymphocytes from beta2 microglobulin (beta2m) HLA-A2.1 monochain transgenic H-2Db beta2m double knockout mice. *The Journal of experimental medicine*, **185**(12), pp. 2043-2051.
- PATEL, P.M., OTTENSMEIER, C.H., MULATERO, C., LORIGAN, P., PLUMMER, R., PANDHA, H., ELSHEIKH, S., HADJIMICHAEL, E., VILLASANTI, N., ADAMS, S.E., CUNNELL, M., METHERINGHAM, R.L., BRENTVILLE, V.A., MACHADO, L., DANIELS, I., GIJON, M., HANNAMAN, D. and DURRANT, L.G., 2018. Targeting gp100 and TRP-2 with a DNA vaccine: Incorporating T cell epitopes with a human IgG1

- antibody induces potent T cell responses that are associated with favourable clinical outcome in a phase I/II trial. *Oncoimmunology*, **7**(6), pp. e1433516.
- PATEL, P.M., DURRANT, L.G., OTTENSMEIER, C., MULATERO, C., LORIGAN, P., PLUMMER, R., CUNNELL, M., METHERINGHAM, R., BRENTVILLE, V., MACHADO, L., DANIELS, I. and HANNAMAN, D., 2014. Phase I trial of ImmunoBody in melanoma patients. *JCO*, **32**(15), pp. 3061-3061.
- PAW, I., CARPENTER, R.C., WATABE, K., DEBINSKI, W. and LO, H.W., 2015. Mechanisms regulating glioma invasion. *Cancer letters*, **362**(1), pp. 1-7.
- PERRIN, R.G., LISHNER, M., GUHA, A., CURTIS, J., FELD, R. and MESSNER, H., 1990. Experience with Ommaya reservoir in 120 consecutive patients with meningeal malignancy. *The Canadian journal of neurological sciences. Le journal canadien des sciences neurologiques*, **17**(2), pp. 190-192.
- PIAO, Y., HENRY, V., TIAO, N., PARK, S.Y., MARTINEZ-LEDESMA, J., DONG, J.W., BALASUBRAMANIAN, V. and DE GROOT, J.F., 2017. Targeting intercellular adhesion molecule-1 prolongs survival in mice bearing bevacizumab-resistant glioblastoma. *Oncotarget*, **8**(57), pp. 96970-96983.
- PLATTEN, M., 2019. How to integrate immunotherapy into standard of care in glioblastoma. *Neuro-oncology*, **21**(6), pp. 699-700.
- PLATTEN, M., 2018. T cells engineered to home in on brain cancer. *Nature*, **561**(7723), pp. 319-320.
- PLATTEN, M., WICK, W. and WELLER, M., 2001. Malignant glioma biology: role for TGF-beta in growth, motility, angiogenesis, and immune escape. *Microscopy research and technique*, **52**(4), pp. 401-410.
- POLYZOIDIS, S. and ASHKAN, K., 2014. DCVax(R)-L--developed by Northwest Biotherapeutics. *Human vaccines & immunotherapeutics*, **10**(11), pp. 3139-3145.
- POSTOW, M.A., CALLAHAN, M.K. and WOLCHOK, J.D., 2015. Immune Checkpoint Blockade in Cancer Therapy. *Journal of clinical oncology : official journal of the American Society of Clinical Oncology*, **33**(17), pp. 1974-1982.
- PRESICCE, P., TADDEO, A., CONTI, A., VILLA, M.L. and DELLA BELLA, S., 2008. Keyhole limpet hemocyanin induces the activation and maturation of human dendritic cells through the involvement of mannose receptor. *Molecular immunology*, **45**(4), pp. 1136-1145.
- PREUSSER, M., LIM, M., HAFLER, D.A., REARDON, D.A. and SAMPSON, J.H., 2015. Prospects of immune checkpoint modulators in the treatment of glioblastoma. *Nature reviews. Neurology*, **11**(9), pp. 504-514.
- PRINS, R.M., SHU, C.J., RADU, C.G., VO, D.D., KHAN-FAROOQI, H., SOTO, H., YANG, M.Y., LIN, M.S., SHELLY, S., WITTE, O.N., RIBAS, A. and LIAU, L.M., 2008. Anti-tumor activity and trafficking of self, tumor-specific T cells against tumors located in the brain. *Cancer immunology, immunotherapy : CII*, **57**(9), pp. 1279-1289.
- PUDNEY, V.A., METHERINGHAM, R.L., GUNN, B., SPENDLOVE, I., RAMAGE, J.M. and DURRANT, L.G., 2010. DNA vaccination with T-cell epitopes encoded within Ab molecules induces high-avidity anti-tumor CD8+ T cells. *European journal of immunology*, **40**(3), pp. 899-910.

QIU, X.Y., HU, D.X., CHEN, W.Q., CHEN, R.Q., QIAN, S.R., LI, C.Y., LI, Y.J., XIONG, X.X., LIU, D., PAN, F., YU, S.B. and CHEN, X.Q., 2018. PD-L1 confers glioblastoma multiforme malignancy via Ras binding and Ras/Erk/EMT activation. *Biochimica et biophysica acta.Molecular basis of disease*, **1864**(5 Pt A), pp. 1754-1769.

QUAIL, D.F. and JOYCE, J.A., 2017. The Microenvironmental Landscape of Brain Tumors. *Cancer cell*, **31**(3), pp. 326-341.

QURESHI, O.S., ZHENG, Y., NAKAMURA, K., ATTRIDGE, K., MANZOTTI, C., SCHMIDT, E.M., BAKER, J., JEFFERY, L.E., KAUR, S., BRIGGS, Z., HOU, T.Z., FUTTER, C.E., ANDERSON, G., WALKER, L.S. and SANSOM, D.M., 2011. Trans-endocytosis of CD80 and CD86: a molecular basis for the cell-extrinsic function of CTLA-4. *Science (New York, N.Y.)*, **332**(6029), pp. 600-603.

RAZPOTNIK, R., NOVAK, N., CURIN SERBEC, V. and RAJCEVIC, U., 2017. Targeting Malignant Brain Tumors with Antibodies. *Frontiers in immunology*, **8**, pp. 1181.

REARDON, D.A., FREEMAN, G., WU, C., CHIOCCA, E.A., WUCHERPFENNIG, K.W., WEN, P.Y., FRITSCH, E.F., CURRY, W.T., Jr, SAMPSON, J.H. and DRANOFF, G., 2014. Immunotherapy advances for glioblastoma. *Neuro-oncology*, **16**(11), pp. 1441-1458.

REARDON, D.A., GILBERT, M.R., WICK, W. and LIAU, L., 2015. Immunotherapy for neuro-oncology: the critical rationale for combinatorial therapy. *Neuro-oncology*, **17 Suppl 7**, pp. vii32-vii40.

RENNER, C., ASPERGER, A., SEYFFARTH, A., MEIXENSBERGER, J., GEBHARDT, R. and GAUNITZ, F., 2010. Carnosine inhibits ATP production in cells from malignant glioma. *Neurological research*, **32**(1), pp. 101-105.

RIBAS, A. and WOLCHOK, J.D., 2018. Cancer immunotherapy using checkpoint blockade. *Science (New York, N.Y.)*, **359**(6382), pp. 1350-1355.

ROBERT, C., SCHACHTER, J., LONG, G.V., ARANCE, A., GROB, J.J., MORTIER, L., DAUD, A., CARLINO, M.S., MCNEIL, C., LOTEM, M., LARKIN, J., LORIGAN, P., NEYNS, B., BLANK, C.U., HAMID, O., MATEUS, C., SHAPIRA-FROMMER, R., KOSH, M., ZHOU, H., IBRAHIM, N., EBBINGHAUS, S., RIBAS, A. and KEYNOTE-006 INVESTIGATORS, 2015. Pembrolizumab versus Ipilimumab in Advanced Melanoma. *The New England journal of medicine*, **372**(26), pp. 2521-2532.

ROCHE, P.A. and FURUTA, K., 2015. The ins and outs of MHC class II-mediated antigen processing and presentation. *Nature reviews.Immunology*, **15**(4), pp. 203-216.

ROCK, K.L., BENACERRAF, B. and ABBAS, A.K., 1984. Antigen presentation by hapten-specific B lymphocytes. I. Role of surface immunoglobulin receptors. *The Journal of experimental medicine*, **160**(4), pp. 1102-1113.

ROOS, W.P. and KAINA, B., 2013. DNA damage-induced cell death: from specific DNA lesions to the DNA damage response and apoptosis. *Cancer letters*, **332**(2), pp. 237-248.

RUSHING, E.J., SANDBERG, G.D. and HORKAYNE-SZAKALY, I., 2010. High-grade astrocytomas show increased Nestin and Wilms's tumor gene (WT1) protein expression. *International journal of surgical pathology*, **18**(4), pp. 255-259.

SAIKALI, S., AVRIL, T., COLLET, B., HAMLAT, A., BANSARD, J.Y., DRENOU, B., GUEGAN, Y. and QUILLIEN, V., 2007. Expression of nine tumour antigens in a series of human glioblastoma

- multiforme: interest of EGFRvIII, IL-13Ralpha2, gp100 and TRP-2 for immunotherapy. *Journal of neuro-oncology*, **81**(2), pp. 139-148.
- SAKAI, K., SHIMODAIRA, S., MAEJIMA, S., UDAGAWA, N., SANO, K., HIGUCHI, Y., KOYA, T., OCHIAI, T., KOIDE, M., UEHARA, S., NAKAMURA, M., SUGIYAMA, H., YONEMITSU, Y., OKAMOTO, M. and HONGO, K., 2015. Dendritic cell-based immunotherapy targeting Wilms' tumor 1 in patients with recurrent malignant glioma. *Journal of neurosurgery*, **123**(4), pp. 989-997.
- SAMPSON, J.H., HEIMBERGER, A.B., ARCHER, G.E., ALDAPE, K.D., FRIEDMAN, A.H., FRIEDMAN, H.S., GILBERT, M.R., HERNDON, J.E., 2nd, MCLENDON, R.E., MITCHELL, D.A., REARDON, D.A., SAWAYA, R., SCHMITTLING, R.J., SHI, W., VREDENBURGH, J.J. and BIGNER, D.D., 2010. Immunologic escape after prolonged progression-free survival with epidermal growth factor receptor variant III peptide vaccination in patients with newly diagnosed glioblastoma. *Journal of clinical oncology : official journal of the American Society of Clinical Oncology*, **28**(31), pp. 4722-4729.
- SANCHEZ-PAULETE, A.R., TEJEIRA, A., CUETO, F.J., GARASA, S., PEREZ-GRACIA, J.L., SANCHEZ-ARRAEZ, A., SANCHO, D. and MELERO, I., 2017. Antigen cross-presentation and T-cell cross-priming in cancer immunology and immunotherapy. *Annals of oncology : official journal of the European Society for Medical Oncology*, **28**(suppl_12), pp. xii44-xii55.
- SANDBERG, J.K., GRUFMAN, P., WOLPERT, E.Z., FRANKSSON, L., CHAMBERS, B.J. and KARRE, K., 1998. Superdominance among immunodominant H-2Kb-restricted epitopes and reversal by dendritic cell-mediated antigen delivery. *Journal of immunology (Baltimore, Md.: 1950)*, **160**(7), pp. 3163-3169.
- SAUERHOFER, S., YUAN, G., BRAUN, G.S., DEINZER, M., NEUMAIER, M., GRETZ, N., FLOEGE, J., KRIZ, W., VAN DER WOUDE, F. and MOELLER, M.J., 2007. L-carnosine, a substrate of carnosinase-1, influences glucose metabolism. *Diabetes*, **56**(10), pp. 2425-2432.
- SCHNEIDER, S.W., LUDWIG, T., TATENHORST, L., BRAUNE, S., OBERLEITHNER, H., SENNER, V. and PAULUS, W., 2004. Glioblastoma cells release factors that disrupt blood-brain barrier features. *Acta Neuropathologica*, **107**(3), pp. 272-276.
- SCHOENBERGER, S.P., TOES, R.E., VAN DER VOORT, E.I., OFFRINGA, R. and MELIEF, C.J., 1998. T-cell help for cytotoxic T lymphocytes is mediated by CD40-CD40L interactions. *Nature*, **393**(6684), pp. 480-483.
- SCHREIBER, H., WU, T.H., NACHMAN, J. and KAST, W.M., 2002. Immunodominance and tumor escape. *Seminars in cancer biology*, **12**(1), pp. 25-31.
- SHAN, Y., HE, X., SONG, W., HAN, D., NIU, J. and WANG, J., 2015. Role of IL-6 in the invasiveness and prognosis of glioma. *International journal of clinical and experimental medicine*, **8**(6), pp. 9114-9120.
- SHEN, Y., YANG, J., LI, J., SHI, X., OUYANG, L., TIAN, Y. and LU, J., 2014. Carnosine inhibits the proliferation of human gastric cancer SGC-7901 cells through both of the mitochondrial respiration and glycolysis pathways. *PloS one*, **9**(8), pp. e104632.
- SHEU, J. and SHIH, I., 2010. HLA-G and immune evasion in cancer cells. *Journal of the Formosan Medical Association = Taiwan yi zhi*, **109**(4), pp. 248-257.
- SILVER, D.J., SINYUK, M., VOGELBAUM, M.A., AHLUWALIA, M.S. and LATHIA, J.D., 2016. The intersection of cancer, cancer stem cells, and the immune system: therapeutic opportunities. *Neuro-oncology*, **18**(2), pp. 153-159.

- SKRLJ, N., DREVENSEK, G., HUDOKLIN, S., ROMIH, R., CURIN SERBEC, V. and DOLINAR, M., 2013. Recombinant single-chain antibody with the Trojan peptide penetratin positioned in the linker region enables cargo transfer across the blood-brain barrier. *Applied Biochemistry and Biotechnology*, **169**(1), pp. 159-169.
- SPEAR, P., WU, M.R., SENTMAN, M.L. and SENTMAN, C.L., 2013. NKG2D ligands as therapeutic targets. *Cancer immunity*, **13**, pp. 8.
- STANIMIROVIC, D., KEMMERICH, K., HAQQANI, A.S. and FARRINGTON, G.K., 2014. Engineering and pharmacology of blood-brain barrier-permeable bispecific antibodies. *Advances in Pharmacology (San Diego, Calif.)*, **71**, pp. 301-335.
- STEIMLE, V., SIEGRIST, C.A., MOTTET, A., LISOWSKA-GROSPIERRE, B. and MACH, B., 1994. Regulation of MHC class II expression by interferon-gamma mediated by the transactivator gene CIITA. *Science (New York, N.Y.)*, **265**(5168), pp. 106-109.
- STUPP, R., MASON, W.P., VAN DEN BENT, M.J., WELLER, M., FISHER, B., TAPHOORN, M.J., BELANGER, K., BRANDES, A.A., MAROSI, C., BOGDAHN, U., CURSCHMANN, J., JANZER, R.C., LUDWIN, S.K., GORLIA, T., ALLGEIER, A., LACOMBE, D., CAIRNCROSS, J.G., EISENHAEUER, E., MIRIMANOFF, R.O., EUROPEAN ORGANISATION FOR RESEARCH AND TREATMENT OF CANCER BRAIN TUMOR AND RADIOTHERAPY GROUPS and NATIONAL CANCER INSTITUTE OF CANADA CLINICAL TRIALS GROUP, 2005. Radiotherapy plus concomitant and adjuvant temozolomide for glioblastoma. *The New England journal of medicine*, **352**(10), pp. 987-996.
- STVOLINSKY, S.L., KUKLEY, M.L., DOBROTA, D., MATEJOVICOVA, M., TKAC, I. and BOLDYREV, A.A., 1999. Carnosine: an endogenous neuroprotector in the ischemic brain. *Cellular and molecular neurobiology*, **19**(1), pp. 45-56.
- SWARTZ, A.M., LI, Q.J. and SAMPSON, J.H., 2014. Rindopepimut: a promising immunotherapeutic for the treatment of glioblastoma multiforme. *Immunotherapy*, **6**(6), pp. 679-690.
- SWARTZ, A.M., SHEN, S.H., SALGADO, M.A., CONGDON, K.L. and SANCHEZ-PEREZ, L., 2018. Promising vaccines for treating glioblastoma. *Expert opinion on biological therapy*, **18**(11), pp. 1159-1170.
- TABATABAEI, P., VISSE, E., BERGSTROM, P., BRANNSTROM, T., SIESJO, P. and BERGENHEIM, A.T., 2017. Radiotherapy induces an immediate inflammatory reaction in malignant glioma: a clinical microdialysis study. *Journal of neuro-oncology*, **131**(1), pp. 83-92.
- TAN, T.T. and COUSSENS, L.M., 2007. Humoral immunity, inflammation and cancer. *Current opinion in immunology*, **19**(2), pp. 209-216.
- TANG, J., FLOMENBERG, P., HARSHYNE, L., KENYON, L. and ANDREWS, D.W., 2005. Glioblastoma patients exhibit circulating tumor-specific CD8+ T cells. *Clinical cancer research : an official journal of the American Association for Cancer Research*, **11**(14), pp. 5292-5299.
- THOM, G., HATCHER, J., HEARN, A., PATERSON, J., RODRIGO, N., BELJEAN, A., GURRELL, I. and WEBSTER, C., 2018. Isolation of blood-brain barrier-crossing antibodies from a phage display library by competitive elution and their ability to penetrate the central nervous system. *mAbs*, **10**(2), pp. 304-314.
- TONG, A.W. and STONE, M.J., 2003a. Prospects for CD40-directed experimental therapy of human cancer. *Cancer gene therapy*, **10**(1), pp. 1-13.

- TONG, A.W. and STONE, M.J., 2003b. Prospects for CD40-directed experimental therapy of human cancer. *Cancer gene therapy*, **10**(1), pp. 1-13.
- TOPALIAN, S.L., DRAKE, C.G. and PARDOLL, D.M., 2012. Targeting the PD-1/B7-H1(PD-L1) pathway to activate anti-tumor immunity. *Current opinion in immunology*, **24**(2), pp. 207-212.
- UJIFUKU, K., MITSUTAKE, N., TAKAKURA, S., MATSUSE, M., SAENKO, V., SUZUKI, K., HAYASHI, K., MATSUO, T., KAMADA, K., NAGATA, I. and YAMASHITA, S., 2010. miR-195, miR-455-3p and miR-10a(*) are implicated in acquired temozolomide resistance in glioblastoma multiforme cells. *Cancer letters*, **296**(2), pp. 241-248.
- VAN LINDE, M.E., BRAHM, C.G., DE WITT HAMER, P.C., REIJNEVELD, J.C., BRUYNZEEL, A.M.E., VANDERTOP, W.P., VAN DE VEN, P.M., WAGEMAKERS, M., VAN DER WEIDE, H.L., ENTING, R.H., WALENKAMP, A.M.E. and VERHEUL, H.M.W., 2017. Treatment outcome of patients with recurrent glioblastoma multiforme: a retrospective multicenter analysis. *Journal of neuro-oncology*, **135**(1), pp. 183-192.
- VAN TELLINGEN, O., YETKIN-ARIK, B., DE GOOIJER, M.C., WESSELING, P., WURDINGER, T. and DE VRIES, H.E., 2015. Overcoming the blood-brain tumor barrier for effective glioblastoma treatment. *Drug resistance updates : reviews and commentaries in antimicrobial and anticancer chemotherapy*, **19**, pp. 1-12.
- VERHAAK, R.G., HOADLEY, K.A., PURDOM, E., WANG, V., QI, Y., WILKERSON, M.D., MILLER, C.R., DING, L., GOLUB, T., MESIROV, J.P., ALEXE, G., LAWRENCE, M., O'KELLY, M., TAMAYO, P., WEIR, B.A., GABRIEL, S., WINCKLER, W., GUPTA, S., JAKKULA, L., FEILER, H.S., HODGSON, J.G., JAMES, C.D., SARKARIA, J.N., BRENNAN, C., KAHN, A., SPELLMAN, P.T., WILSON, R.K., SPEED, T.P., GRAY, J.W., MEYERSON, M., GETZ, G., PEROU, C.M., HAYES, D.N. and CANCER GENOME ATLAS RESEARCH NETWORK, 2010. Integrated genomic analysis identifies clinically relevant subtypes of glioblastoma characterized by abnormalities in PDGFRA, IDH1, EGFR, and NF1. *Cancer cell*, **17**(1), pp. 98-110.
- VLAHOVIC, G., FECCI, P.E., REARDON, D. and SAMPSON, J.H., 2015. Programmed death ligand 1 (PD-L1) as an immunotherapy target in patients with glioblastoma. *Neuro-oncology*, **17**(8), pp. 1043-1045.
- VONDERHEIDE, R.H., 2007. Prospect of targeting the CD40 pathway for cancer therapy. *Clinical cancer research : an official journal of the American Association for Cancer Research*, **13**(4), pp. 1083-1088.
- WAGNER, S., CZUB, S., GREIF, M., VINCE, G.H., SUSS, N., KERKAU, S., RIECKMANN, P., ROGGENDORF, W., ROOSEN, K. and TONN, J.C., 1999. Microglial/macrophage expression of interleukin 10 in human glioblastomas. *International journal of cancer*, **82**(1), pp. 12-16.
- WAINWRIGHT, D.A., BALYASNIKOVA, I.V., CHANG, A.L., AHMED, A.U., MOON, K.S., AUFFINGER, B., TOBIAS, A.L., HAN, Y. and LESNIAK, M.S., 2012. IDO expression in brain tumors increases the recruitment of regulatory T cells and negatively impacts survival. *Clinical cancer research : an official journal of the American Association for Cancer Research*, **18**(22), pp. 6110-6121.
- WAINWRIGHT, D.A., CHANG, A.L., DEY, M., BALYASNIKOVA, I.V., KIM, C.K., TOBIAS, A., CHENG, Y., KIM, J.W., QIAO, J., ZHANG, L., HAN, Y. and LESNIAK, M.S., 2014. Durable therapeutic efficacy utilizing combinatorial blockade against IDO, CTLA-4, and PD-L1 in mice with brain tumors. *Clinical cancer research : an official journal of the American Association for Cancer Research*, **20**(20), pp. 5290-5301.

- WALKER, L.S. and SANSOM, D.M., 2015. Confusing signals: recent progress in CTLA-4 biology. *Trends in immunology*, **36**(2), pp. 63-70.
- WANG, C., YE, Y. and GU, Z., 2017. Local delivery of checkpoints antibodies. *Human vaccines & immunotherapeutics*, **13**(1), pp. 245-248.
- WANG, Q., DELVA, L., WEINREB, P.H., PEPINSKY, R.B., GRAHAM, D., VEIZAJ, E., CHEUNG, A.E., CHEN, W., NESTOROV, I., ROHDE, E., CAPUTO, R., KUESTERS, G.M., BOHNERT, T. and GAN, L.S., 2018. Monoclonal antibody exposure in rat and cynomolgus monkey cerebrospinal fluid following systemic administration. *Fluids and barriers of the CNS*, **15**(1), pp. 10-018-0093-6.
- WASTOWSKI, I.J., SIMOES, R.T., YAGHI, L., DONADI, E.A., PANCOTO, J.T., PORAS, I., LECHAPT-ZALCMAN, E., BERNAUDIN, M., VALABLE, S., CARLOTTI, C.G., Jr, FLAJOLLET, S., JENSEN, S.S., FERRONE, S., CAROSELLA, E.D., KRISTENSEN, B.W. and MOREAU, P., 2013. Human leukocyte antigen-G is frequently expressed in glioblastoma and may be induced in vitro by combined 5-aza-2'-deoxycytidine and interferon-gamma treatments: results from a multicentric study. *The American journal of pathology*, **182**(2), pp. 540-552.
- WATKINS, S., ROBEL, S., KIMBROUGH, I.F., ROBERT, S.M., ELLIS-DAVIES, G. and SONTHEIMER, H., 2014. Disruption of astrocyte-vascular coupling and the blood-brain barrier by invading glioma cells. *Nature communications*, **5**, pp. 4196.
- WATTS, R.J. and DENNIS, M.S., 2013. Bispecific antibodies for delivery into the brain. *Current opinion in chemical biology*, **17**(3), pp. 393-399.
- WEARSCH, P.A. and CRESSWELL, P., 2008. The quality control of MHC class I peptide loading. *Current opinion in cell biology*, **20**(6), pp. 624-631.
- WEI, J., BARR, J., KONG, L.Y., WANG, Y., WU, A., SHARMA, A.K., GUMIN, J., HENRY, V., COLMAN, H., PRIEBE, W., SAWAYA, R., LANG, F.F. and HEIMBERGER, A.B., 2010. Glioblastoma cancer-initiating cells inhibit T-cell proliferation and effector responses by the signal transducers and activators of transcription 3 pathway. *Molecular cancer therapeutics*, **9**(1), pp. 67-78.
- WELLER, M., BUTOWSKI, N., TRAN, D.D., RECHT, L.D., LIM, M., HIRTE, H., ASHBY, L., MECHTLER, L., GOLDLUST, S.A., IWAMOTO, F., DRAPPATZ, J., O'ROURKE, D.M., WONG, M., HAMILTON, M.G., FINOCCHIARO, G., PERRY, J., WICK, W., GREEN, J., HE, Y., TURNER, C.D., YELLIN, M.J., KELER, T., DAVIS, T.A., STUPP, R., SAMPSON, J.H. and ACT IV TRIAL INVESTIGATORS, 2017. Rindopepimut with temozolomide for patients with newly diagnosed, EGFRvIII-expressing glioblastoma (ACT IV): a randomised, double-blind, international phase 3 trial. *The Lancet. Oncology*, **18**(10), pp. 1373-1385.
- WEN, P.Y., REARDON, D.A., ARMSTRONG, T.S., PHUPHANICH, S., AIKEN, R.D., LANDOLFI, J.C., CURRY, W.T., ZHU, J.J., GLANTZ, M., PEEREBOOM, D.M., MARKERT, J.M., LARocca, R., O'ROURKE, D.M., FINK, K., KIM, L., GRUBER, M., LESSER, G.J., PAN, E., KESARI, S., MUZIKANSKY, A., PINILLA, C., SANTOS, R.G. and YU, J.S., 2019. A Randomized Double-Blind Placebo-Controlled Phase II Trial of Dendritic Cell Vaccine ICT-107 in Newly Diagnosed Patients with Glioblastoma. *Clinical cancer research : an official journal of the American Association for Cancer Research*, .
- WIENDL, H., MITSDOERFFER, M., HOFMEISTER, V., WISCHHUSEN, J., BORNEMANN, A., MEYERMANN, R., WEISS, E.H., MELMS, A. and WELLER, M., 2002. A functional role of HLA-G expression in human gliomas: an alternative strategy of immune escape. *Journal of immunology (Baltimore, Md.: 1950)*, **168**(9), pp. 4772-4780.

WISCHHUSEN, J., FRIESE, M.A., MITTELBRONN, M., MEYERMANN, R. and WELLER, M., 2005a. HLA-E protects glioma cells from NKG2D-mediated immune responses in vitro: implications for immune escape in vivo. *Journal of neuropathology and experimental neurology*, **64**(6), pp. 523-528.

WOLBURG, H., WOLBURG-BUCHHOLZ, K., KRAUS, J., RASCHER-EGGSTEIN, G., LIEBNER, S., HAMM, S., DUFFNER, F., GROTE, E.H., RISAU, W. and ENGELHARDT, B., 2003. Localization of claudin-3 in tight junctions of the blood-brain barrier is selectively lost during experimental autoimmune encephalomyelitis and human glioblastoma multiforme. *Acta Neuropathologica*, **105**(6), pp. 586-592.

WOLF, A., AGNIHOTRI, S. and GUHA, A., 2010. Targeting metabolic remodeling in glioblastoma multiforme. *Oncotarget*, **1**(7), pp. 552-562.

WOLPERT, F., ROTH, P., LAMSZUS, K., TABATABAI, G., WELLER, M. and EISELE, G., 2012. HLA-E contributes to an immune-inhibitory phenotype of glioblastoma stem-like cells. *Journal of neuroimmunology*, **250**(1-2), pp. 27-34.

WU, A., WEI, J., KONG, L.Y., WANG, Y., PRIEBE, W., QIAO, W., SAWAYA, R. and HEIMBERGER, A.B., 2010. Glioma cancer stem cells induce immunosuppressive macrophages/microglia. *Neuro-oncology*, **12**(11), pp. 1113-1125.

XUE, S., SONG, G. and YU, J., 2017. The prognostic significance of PD-L1 expression in patients with glioma: A meta-analysis. *Scientific reports*, **7**(1), pp. 4231-017-04023-x.

XUE, W., BRENTVILLE, V.A., SYMONDS, P., COOK, K.W., YAGITA, H., METHERINGHAM, R.L. and DURRANT, L.G., 2016. SCIB1, a huIgG1 antibody DNA vaccination, combined with PD-1 blockade induced efficient therapy of poorly immunogenic tumors. *Oncotarget*, **7**(50), pp. 83088-83100.

XUE, W., METHERINGHAM, R.L., BRENTVILLE, V.A., GUNN, B., SYMONDS, P., YAGITA, H., RAMAGE, J.M. and DURRANT, L.G., 2016. SCIB2, an antibody DNA vaccine encoding NY-ESO-1 epitopes, induces potent antitumor immunity which is further enhanced by checkpoint blockade. *Oncoimmunology*, **5**(6), pp. e1169353.

YEUNG, Y.T., MCDONALD, K.L., GREWAL, T. and MUNOZ, L., 2013. Interleukins in glioblastoma pathophysiology: implications for therapy. *British journal of pharmacology*, **168**(3), pp. 591-606.

YOUNG, R.M., JAMSHIDI, A., DAVIS, G. and SHERMAN, J.H., 2015. Current trends in the surgical management and treatment of adult glioblastoma. *Annals of translational medicine*, **3**(9), pp. 121-5839.2015.05.10.

YUEN, G.J., DEMISSIE, E. and PILLAI, S., 2016. B lymphocytes and cancer: a love-hate relationship. *Trends in cancer*, **2**(12), pp. 747-757.

ZAGZAG, D., SALNIKOW, K., CHIRIBOGA, L., YEE, H., LAN, L., ALI, M.A., GARCIA, R., DEMARIA, S. and NEWCOMB, E.W., 2005. Downregulation of major histocompatibility complex antigens in invading glioma cells: stealth invasion of the brain. *Laboratory investigation; a journal of technical methods and pathology*, **85**(3), pp. 328-341.

ZAIDI, M.R. and MERLINO, G., 2011. The two faces of interferon-gamma in cancer. *Clinical cancer research : an official journal of the American Association for Cancer Research*, **17**(19), pp. 6118-6124.

ZENG, J., SEE, A.P., PHALLEN, J., JACKSON, C.M., BELCAID, Z., RUZEVICK, J., DURHAM, N., MEYER, C., HARRIS, T.J., ALBESIANO, E., PRADILLA, G., FORD, E., WONG, J., HAMMERS, H.J., MATHIOS, D., TYLER,

B., BREM, H., TRAN, P.T., PARDOLL, D., DRAKE, C.G. and LIM, M., 2013. Anti-PD-1 blockade and stereotactic radiation produce long-term survival in mice with intracranial gliomas. *International journal of radiation oncology, biology, physics*, **86**(2), pp. 343-349.

ZHAI, L., LAUING, K.L., CHANG, A.L., DEY, M., QIAN, J., CHENG, Y., LESNIAK, M.S. and WAINWRIGHT, D.A., 2015. The role of IDO in brain tumor immunotherapy. *Journal of neuro-oncology*, **123**(3), pp. 395-403.

ZHANG, C.L., HUANG, T., WU, B.L., HE, W.X. and LIU, D., 2017. Stem cells in cancer therapy: opportunities and challenges. *Oncotarget*, **8**(43), pp. 75756-75766.

ZHANG, J., STEVENS, M.F. and BRADSHAW, T.D., 2012. Temozolomide: mechanisms of action, repair and resistance. *Current molecular pharmacology*, **5**(1), pp. 102-114.

ZHANG, K., WANG, X.Q., ZHOU, B. and ZHANG, L., 2013. The prognostic value of MGMT promoter methylation in Glioblastoma multiforme: a meta-analysis. *Familial cancer*, **12**(3), pp. 449-458.

ZHANG, M., KLEBER, S., ROHRICH, M., TIMKE, C., HAN, N., TUETTENBERG, J., MARTIN-VILLALBA, A., DEBUS, J., PESCHKE, P., WIRKNER, U., LAHN, M. and HUBER, P.E., 2011. Blockade of TGF-beta signaling by the TGFbetaR-I kinase inhibitor LY2109761 enhances radiation response and prolongs survival in glioblastoma. *Cancer research*, **71**(23), pp. 7155-7167.

ZHANG, Y. and PARDRIDGE, W.M., 2001. Mediated efflux of IgG molecules from brain to blood across the blood-brain barrier. *Journal of neuroimmunology*, **114**(1-2), pp. 168-172.

ZHAO, J., CHEN, A.X., GARTRELL, R.D., SILVERMAN, A.M., APARICIO, L., CHU, T., BORDBAR, D., SHAN, D., SAMANAMUD, J., MAHAJAN, A., FILIP, I., ORENBUCH, R., GOETZ, M., YAMAGUCHI, J.T., CLONEY, M., HORBINSKI, C., LUKAS, R.V., RAIZER, J., RAE, A.I., YUAN, J., CANOLL, P., BRUCE, J.N., SAENGER, Y.M., SIMS, P., IWAMOTO, F.M., SONABEND, A.M. and RABADAN, R., 2019. Immune and genomic correlates of response to anti-PD-1 immunotherapy in glioblastoma. *Nature medicine*, **25**(3), pp. 462-469.

ZHENG, P.P., KROS, J.M. and LI, J., 2018. Approved CAR T cell therapies: ice bucket challenges on glaring safety risks and long-term impacts. *Drug discovery today*, **23**(6), pp. 1175-1182.

ZHOU, F., 2009. Molecular mechanisms of IFN-gamma to up-regulate MHC class I antigen processing and presentation. *International reviews of immunology*, **28**(3-4), pp. 239-260.

ZHU, J.N. and WANG, J.J., 2008. The cerebellum in feeding control: possible function and mechanism. *Cellular and molecular neurobiology*, **28**(4), pp. 469-478.

ZHU, V.F., YANG, J., LEBRUN, D.G. and LI, M., 2012. Understanding the role of cytokines in Glioblastoma Multiforme pathogenesis. *Cancer letters*, **316**(2), pp. 139-150.

ZHU, X., PRASAD, S., GAEDICKE, S., HETTICH, M., FIRAT, E. and NIEDERMANN, G., 2015. Patient-derived glioblastoma stem cells are killed by CD133-specific CAR T cells but induce the T cell aging marker CD57. *Oncotarget*, **6**(1), pp. 171-184.

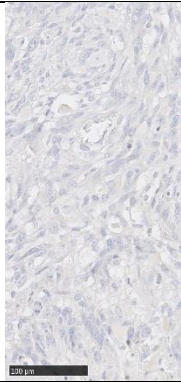
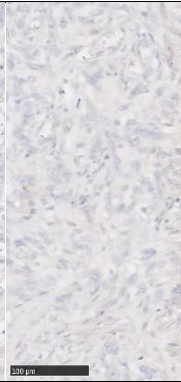
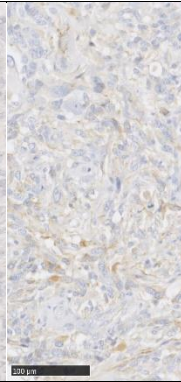
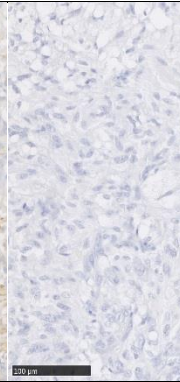
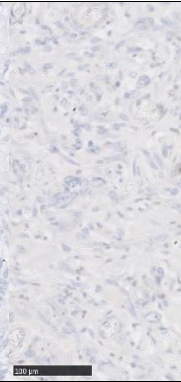
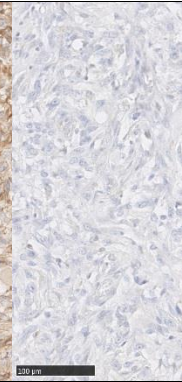
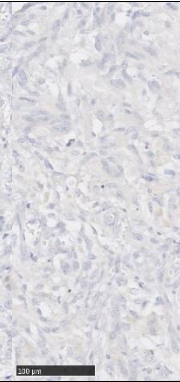
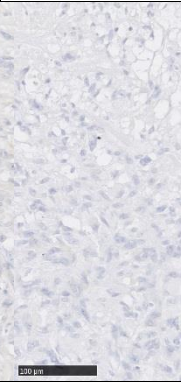
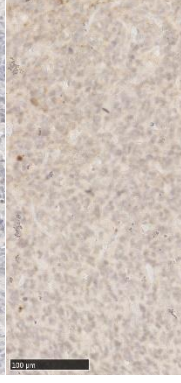
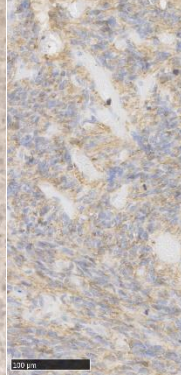
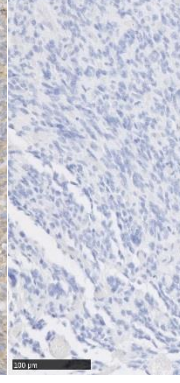
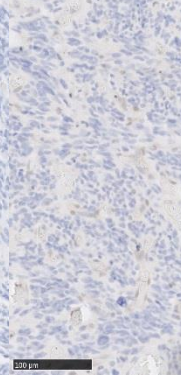
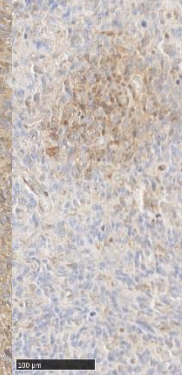
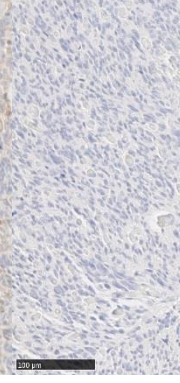
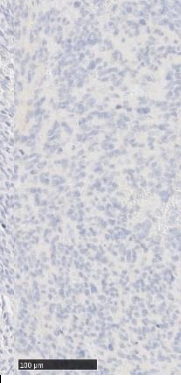
ZIDI, I. and BEN AMOR, N., 2012. Nanoparticles targeting HLA-G for gene therapy in cancer. *Medical oncology (Northwood, London, England)*, **29**(2), pp. 1384-1390.

ZUCCOLI, G., MARCELLO, N., PISANELLO, A., SERVADEI, F., VACCARO, S., MUKHERJEE, P. and SEYFRIED, T.N., 2010. Metabolic management of glioblastoma multiforme using standard therapy

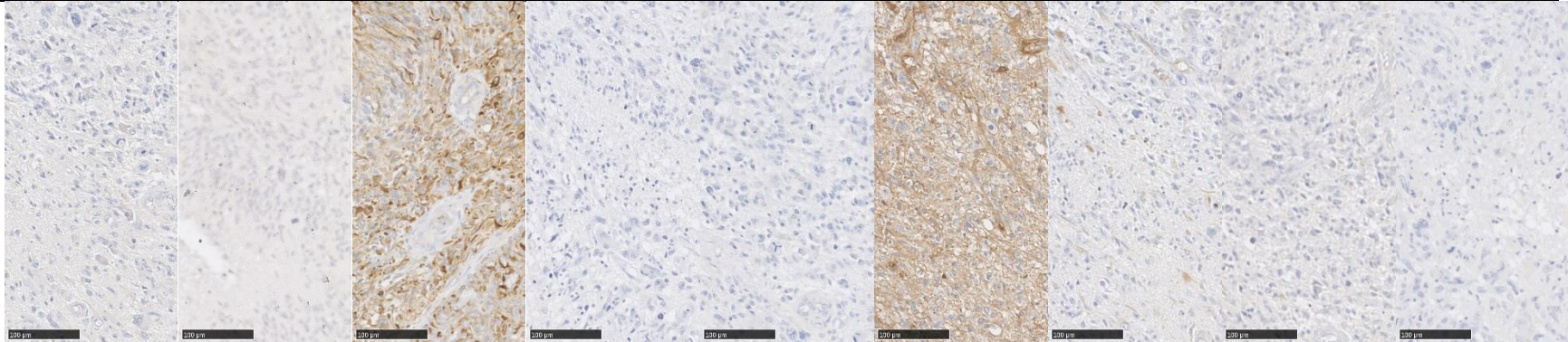
together with a restricted ketogenic diet: Case Report. *Nutrition & metabolism*, **7**, pp. 33-7075-7-33.

APPENDICES

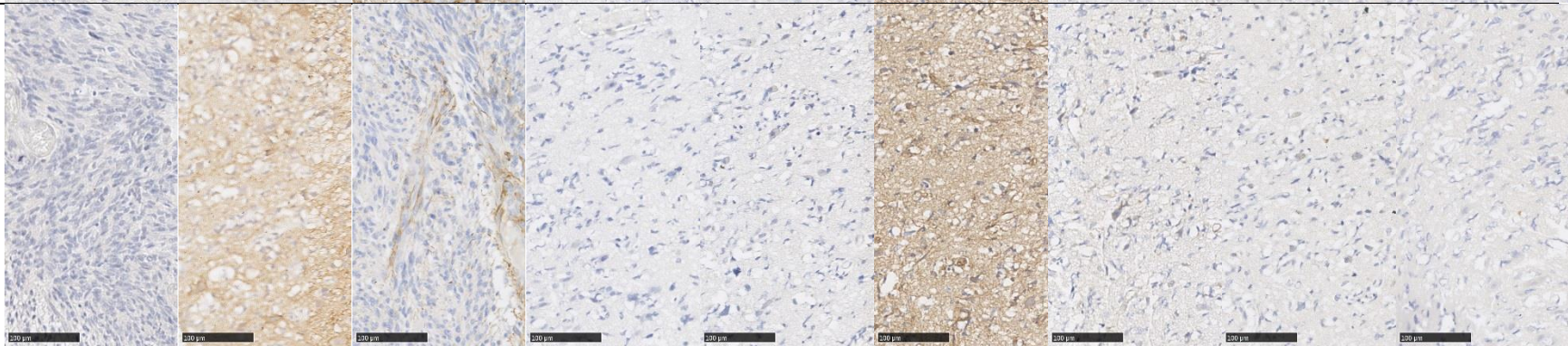
Appendix 1. IHC staining breakdown of GBM tissues

	Antigen									
	HAGE	TRP-2	WT-1	gp100	MGMT	HLA-ABC	HLA-E	HLA-G	PD-L1	
Case 1 Male 38 GBM										
Case 2 Male 31 GBM										

Case 3
Male 20
GBM

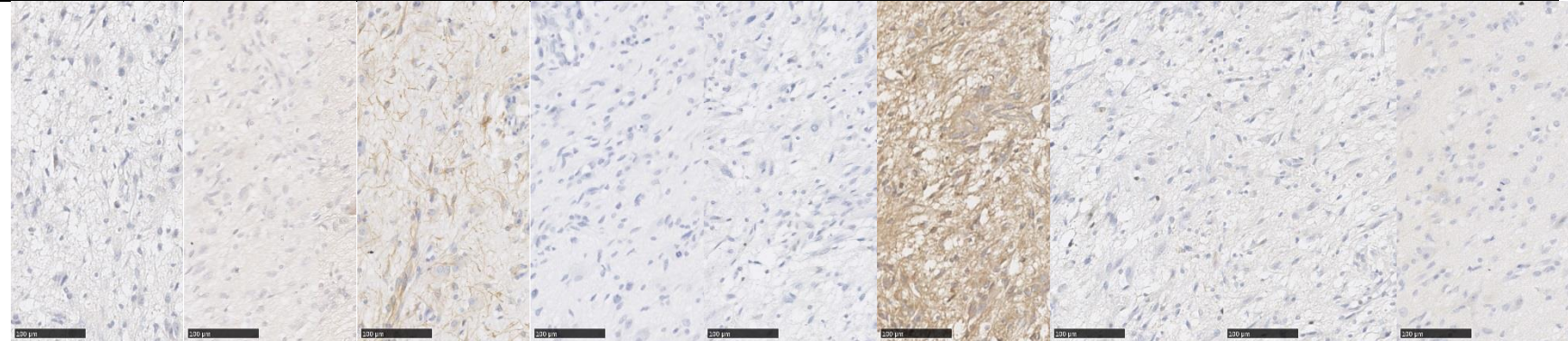


Case 4
Female 19
GBM

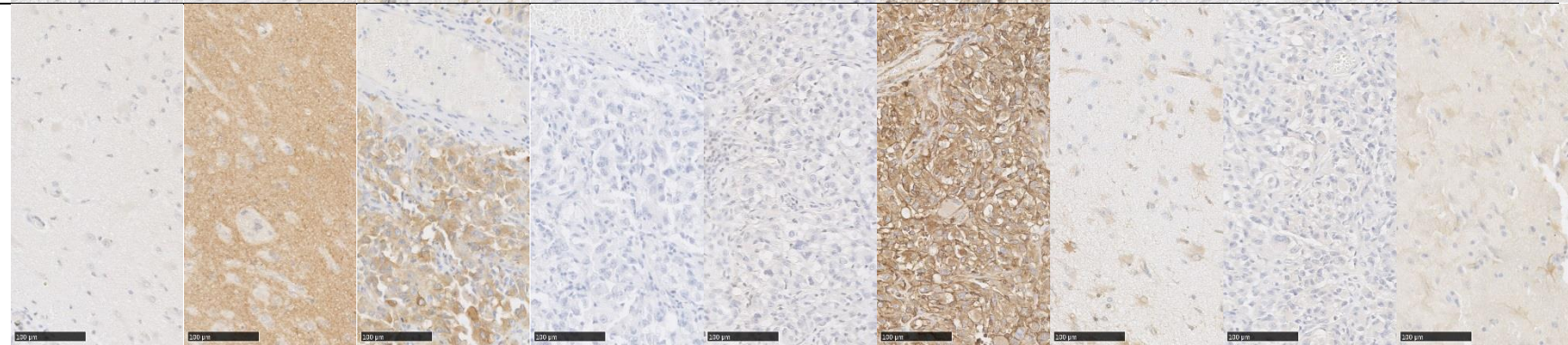


--	--	--	--	--	--	--	--	--	--

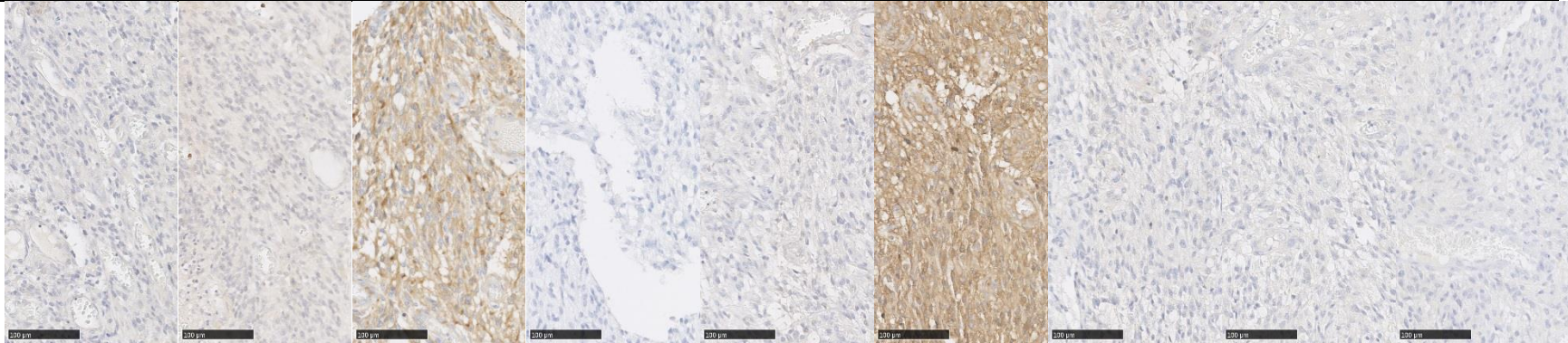
Case 5
Male 43
AA



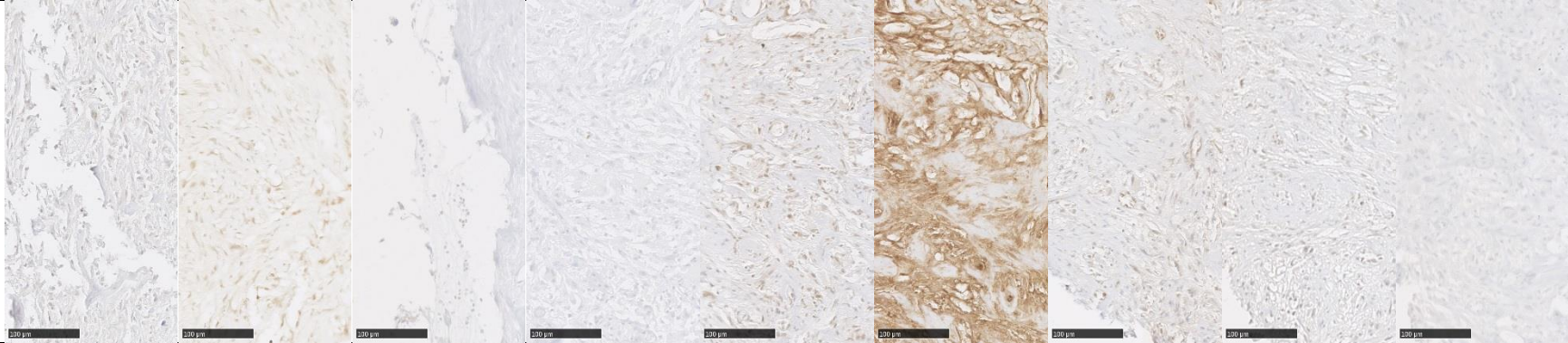
Case 6
Female
59 GBM



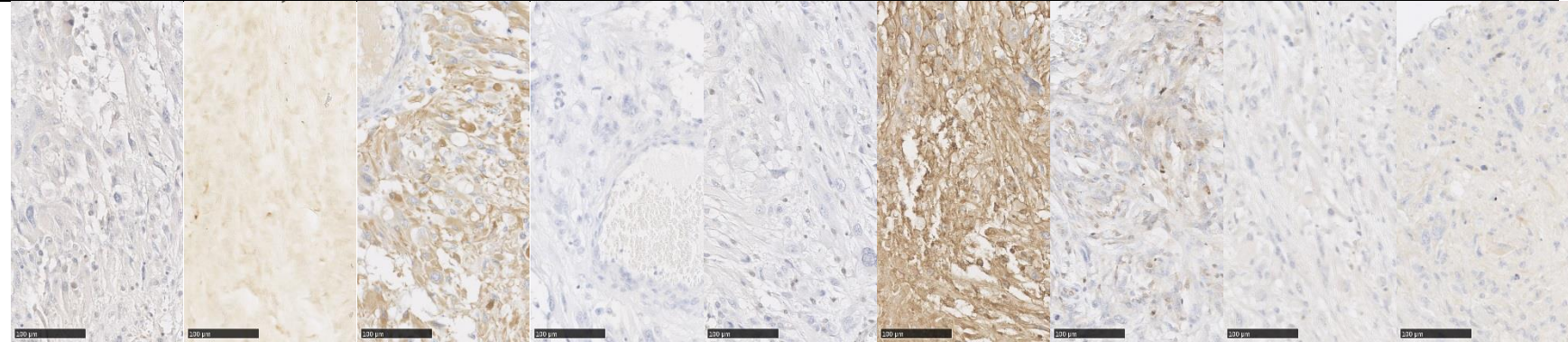
Case 7
Male 40
GBM



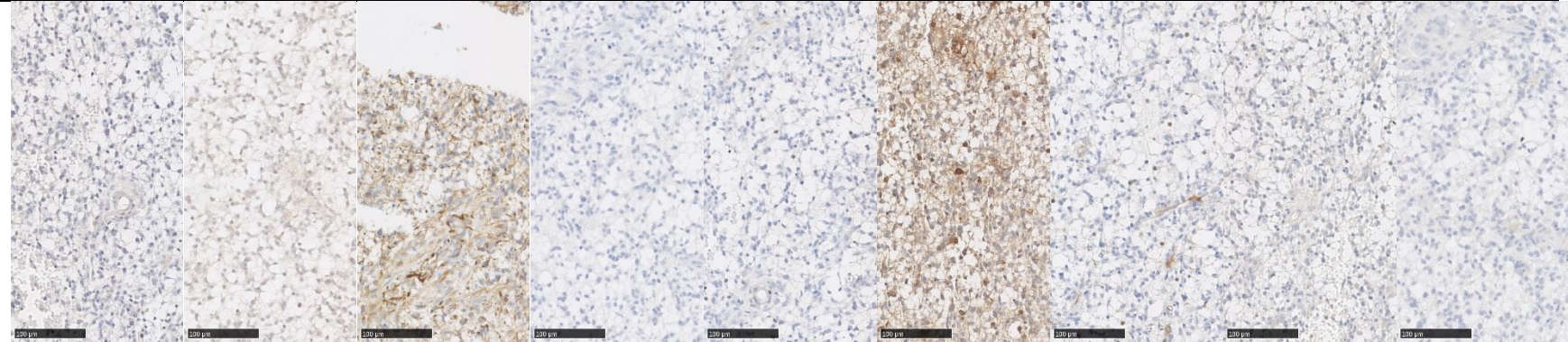
Case 8
Male 24
GBM



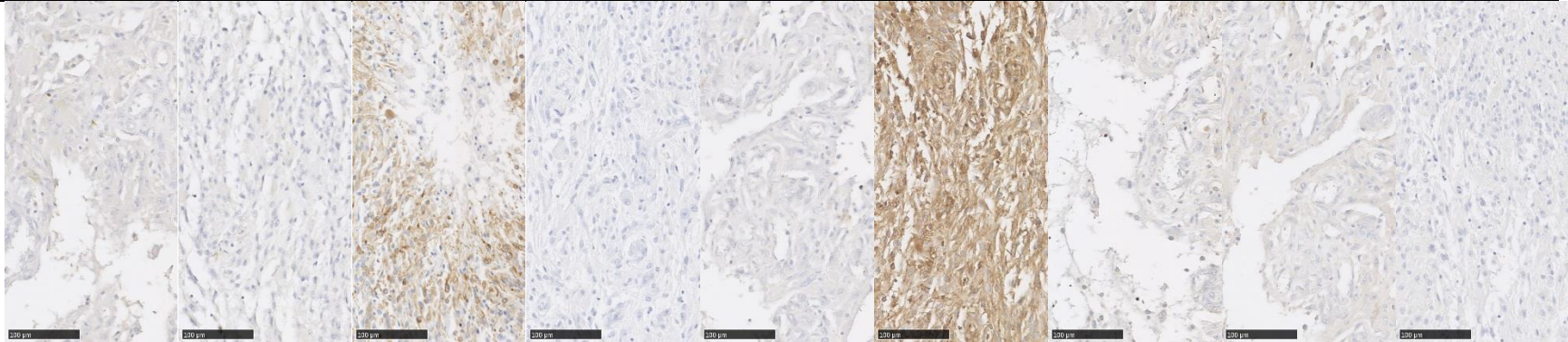
Case 9
Male 1
GBM



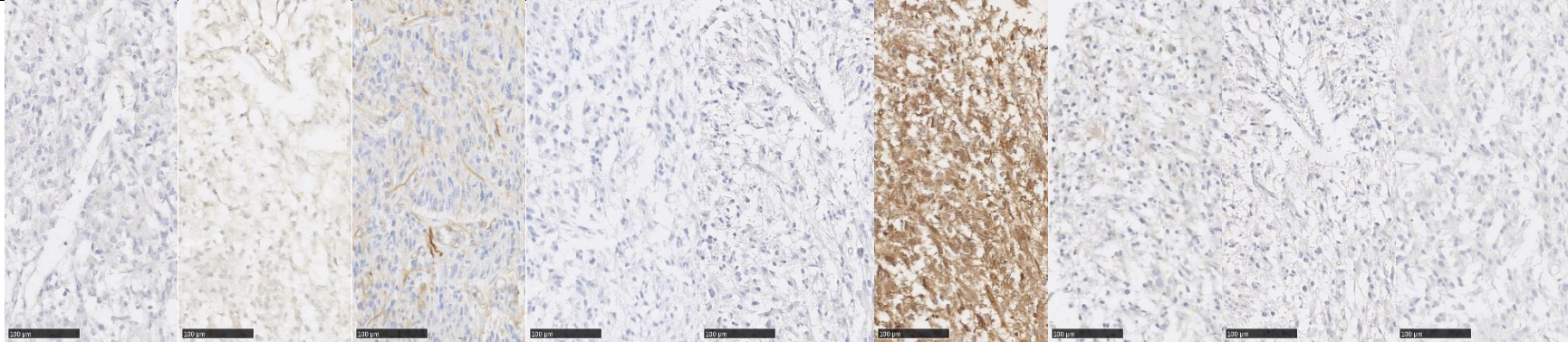
Case 10
Male 75
GBM



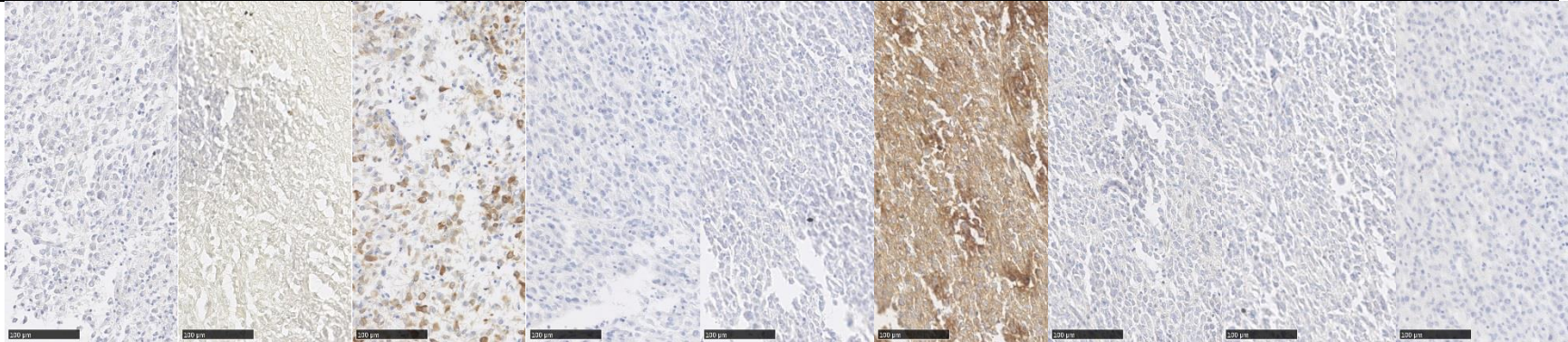
Case 11
Female
41 GBM



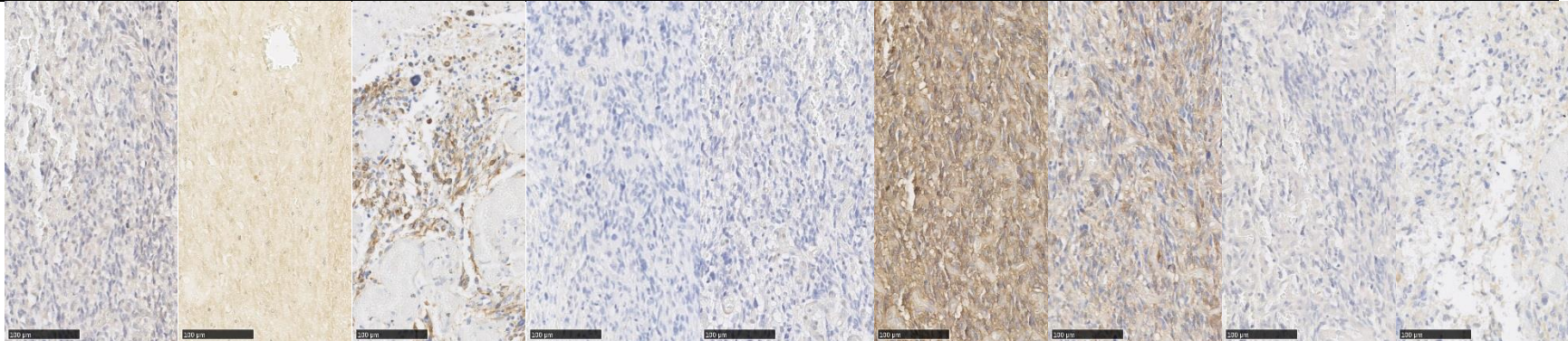
Case 12
Male 51
GBM



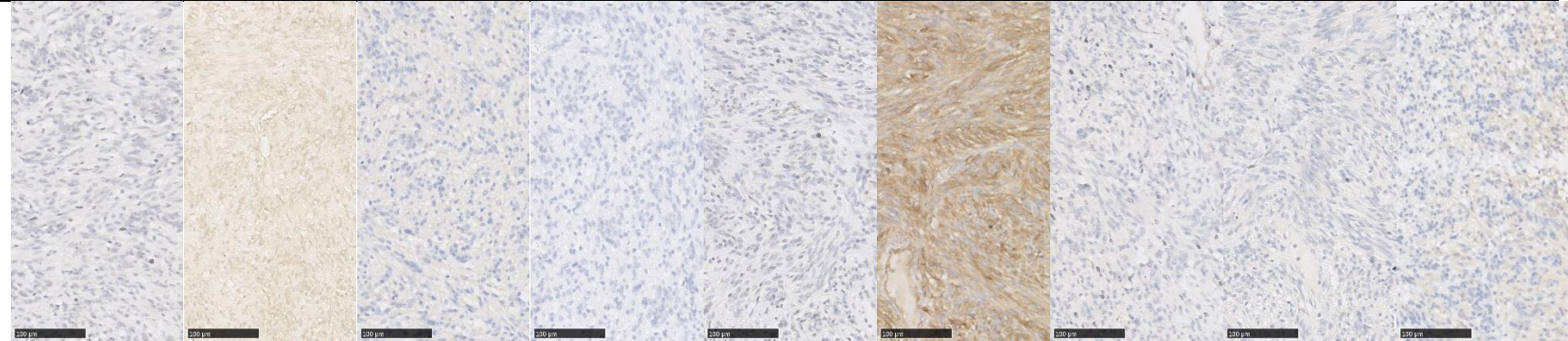
Case 13
Female
58 GBM



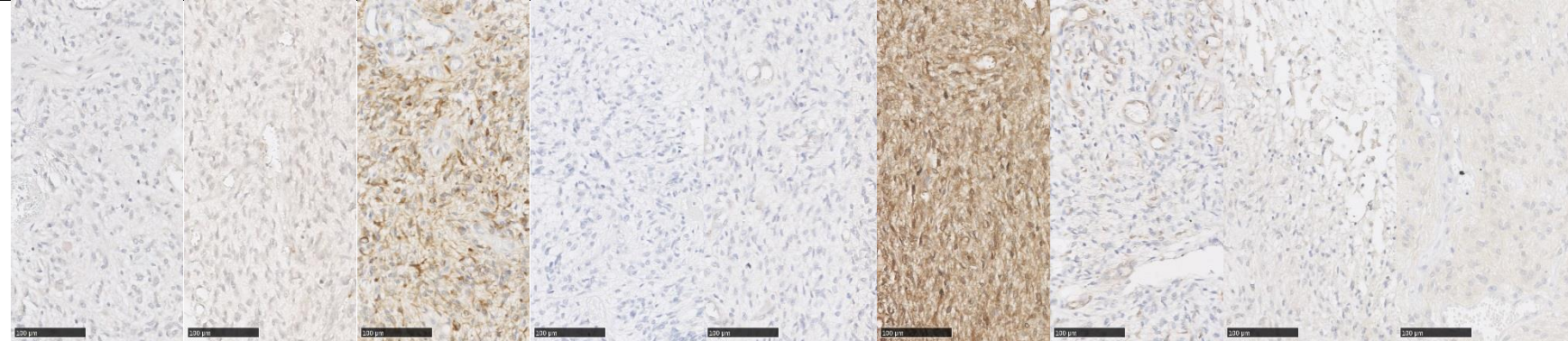
Case 14
Female
31 GBM



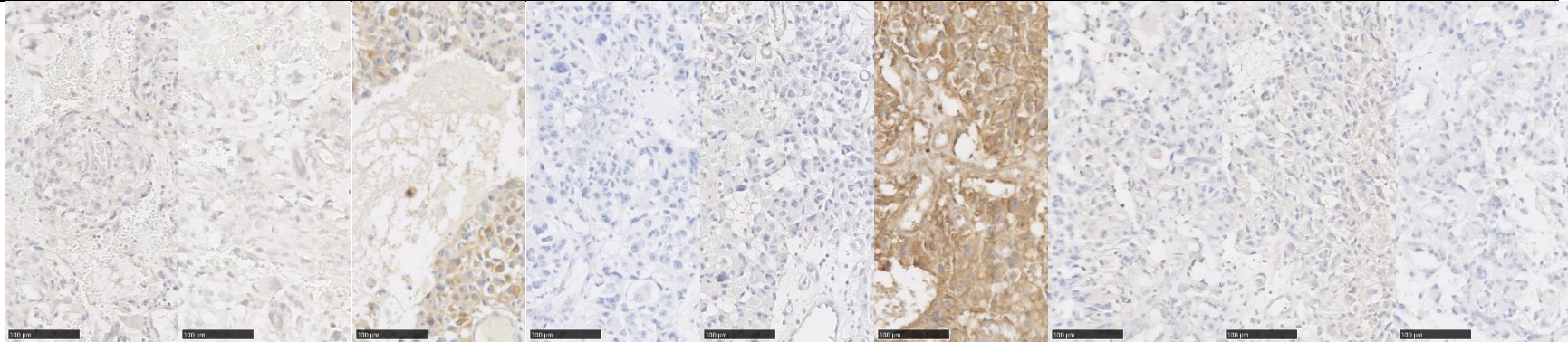
Case 15
Female
11 GBM



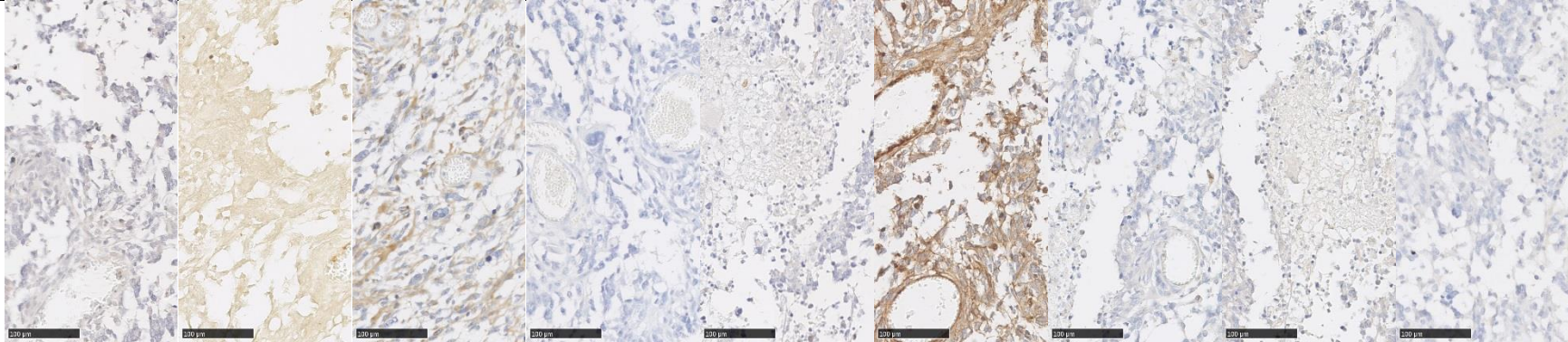
Case 16
Female
51 GBM



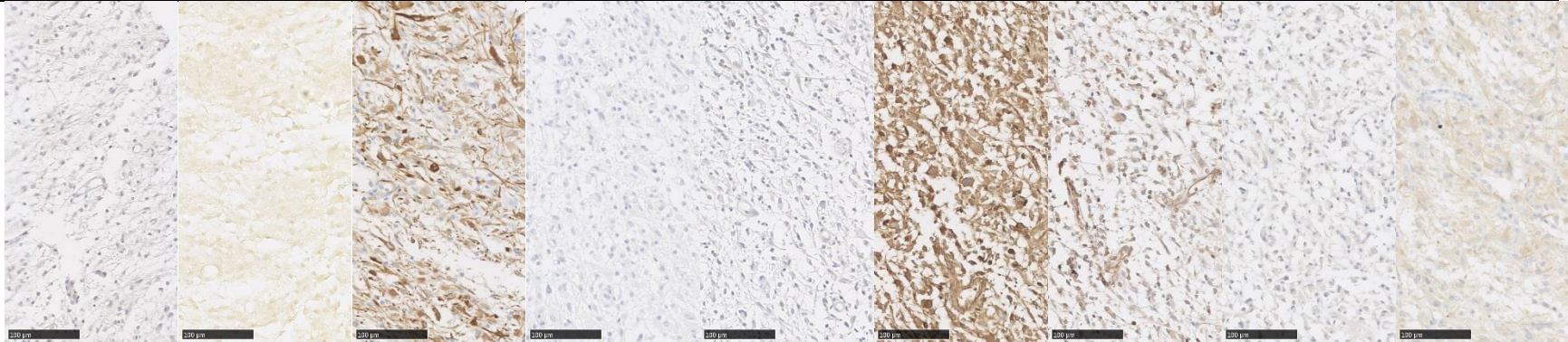
Case 17
Female
22 GBM



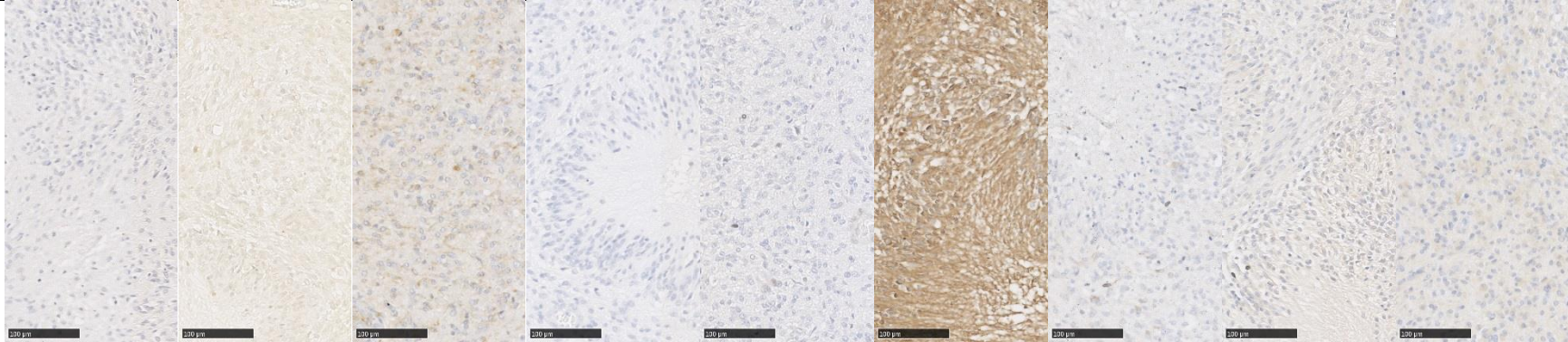
Case 18
Male 33
GBM



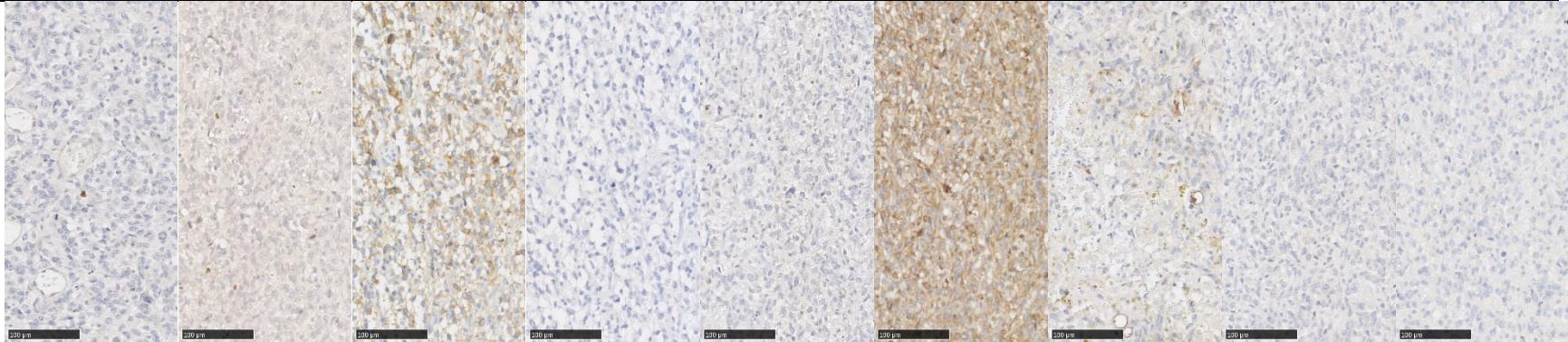
Case 19
Male 73
GBM



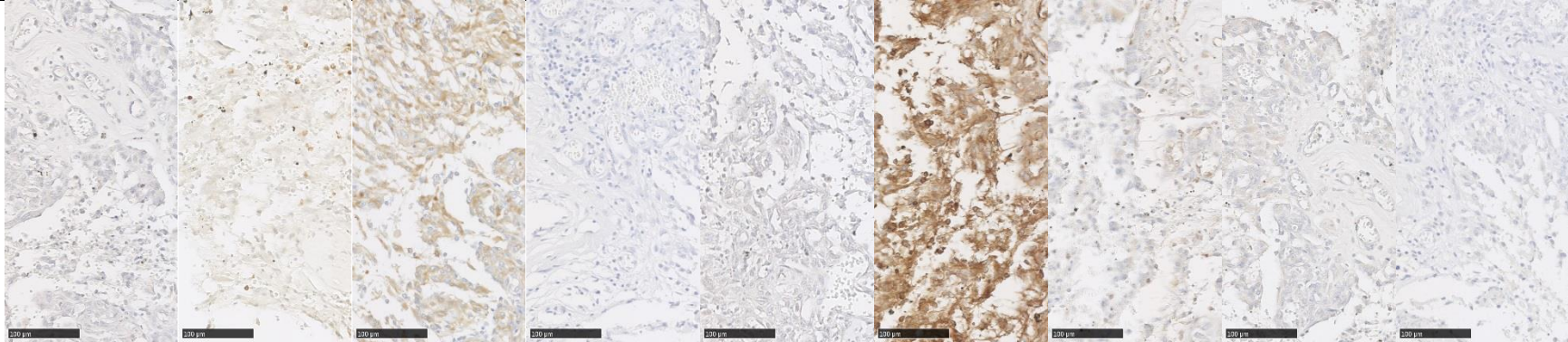
Case 20
Male 43
GBM



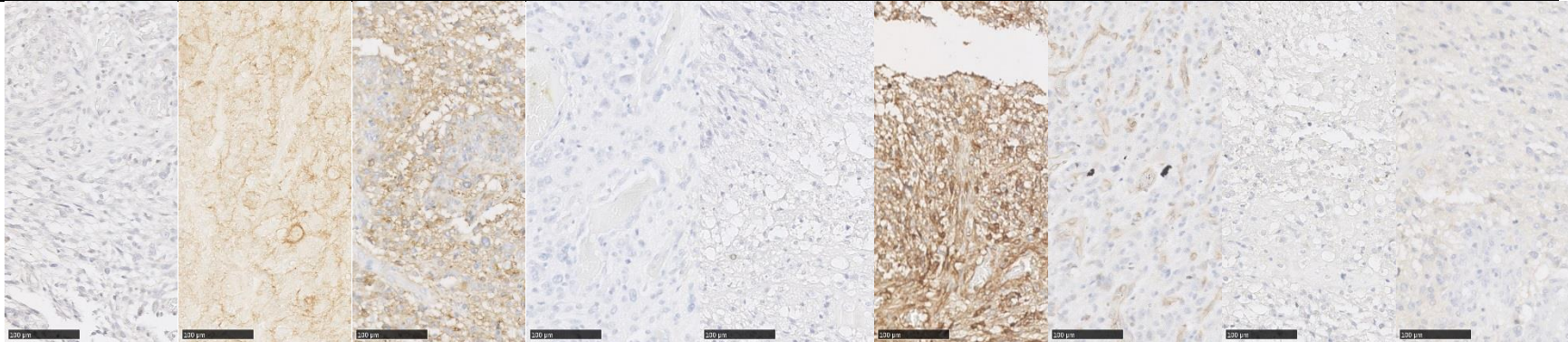
Case 21
Female
61 GBM



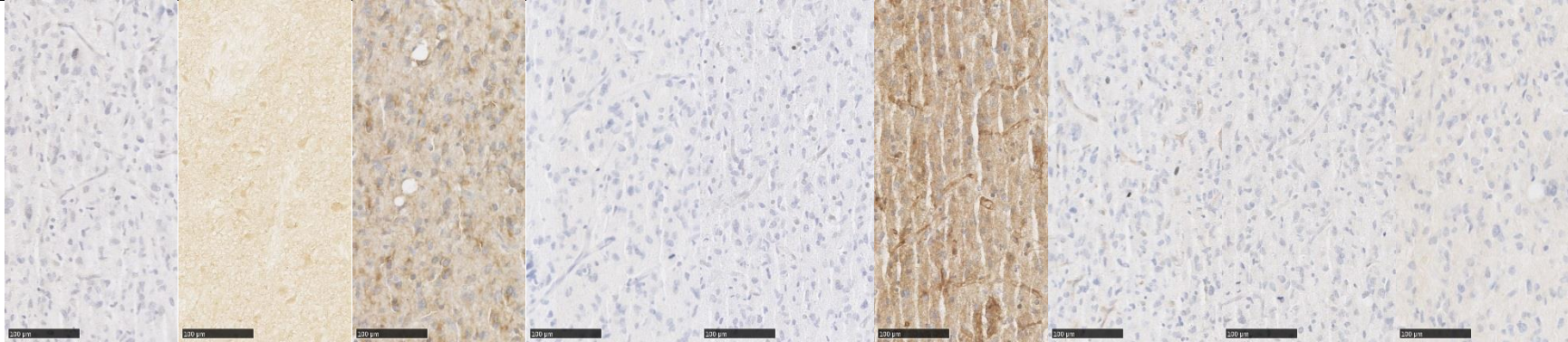
Case 22
Male 26
GBM



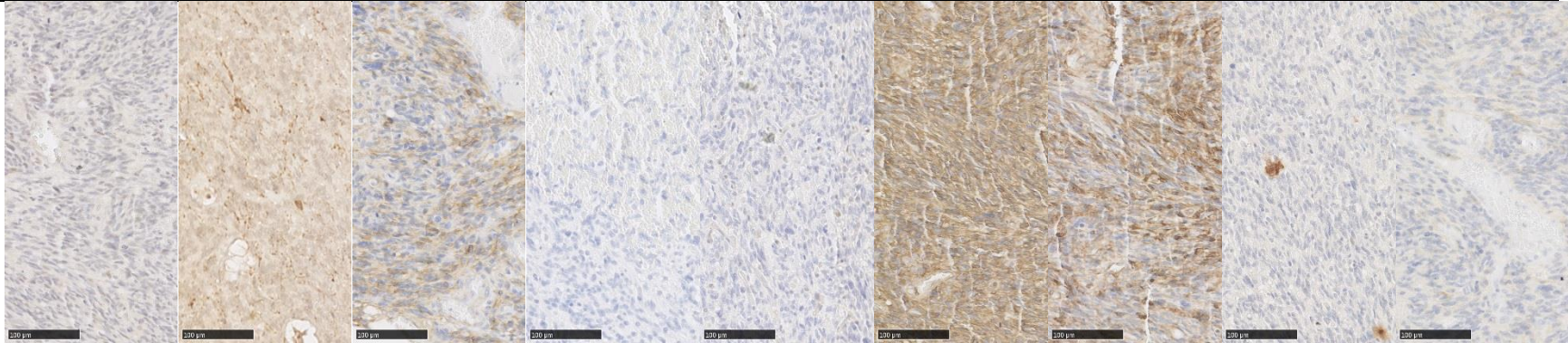
Case 23
Male 59
GBM



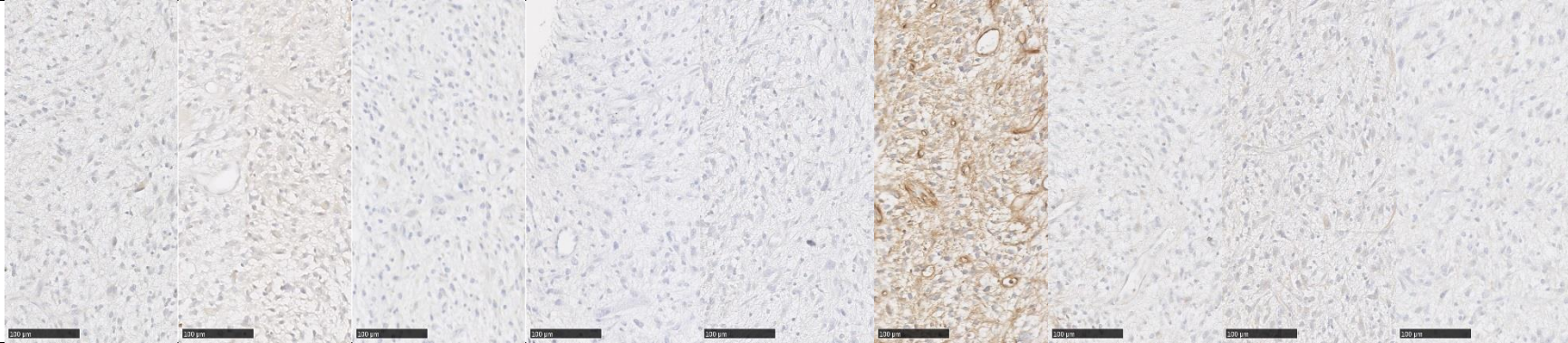
Case 24
Female
40 AA



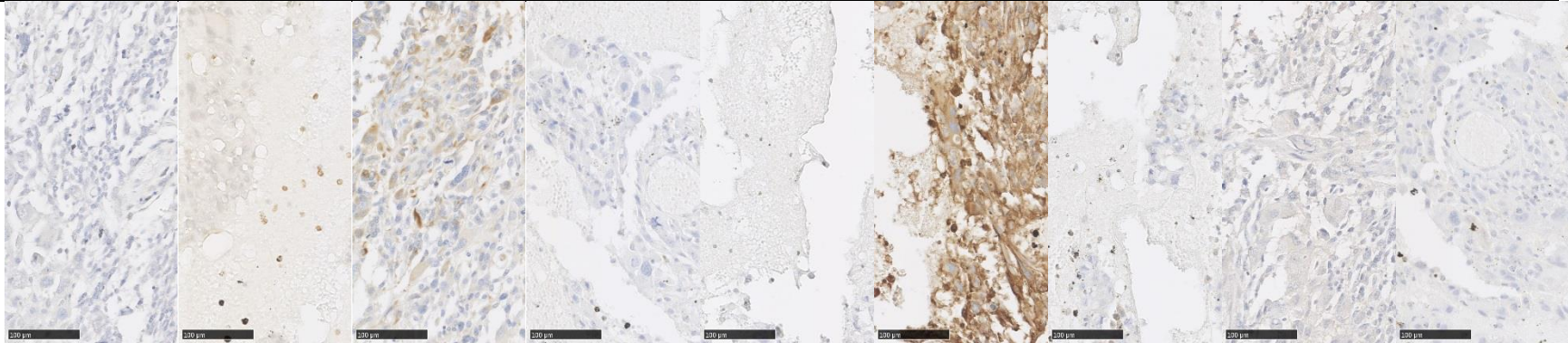
Case 25
Male 34
GBM



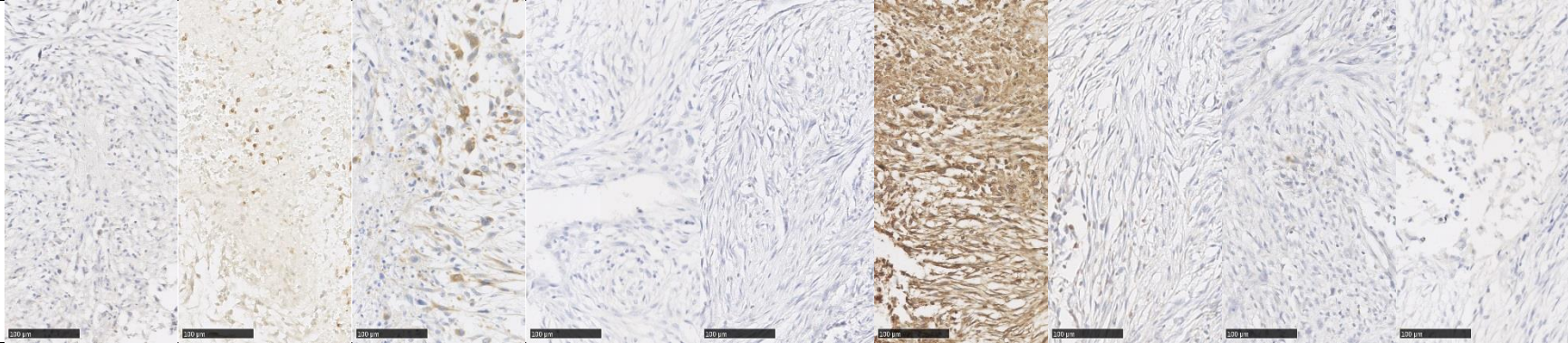
Case 26
Female
33 AA



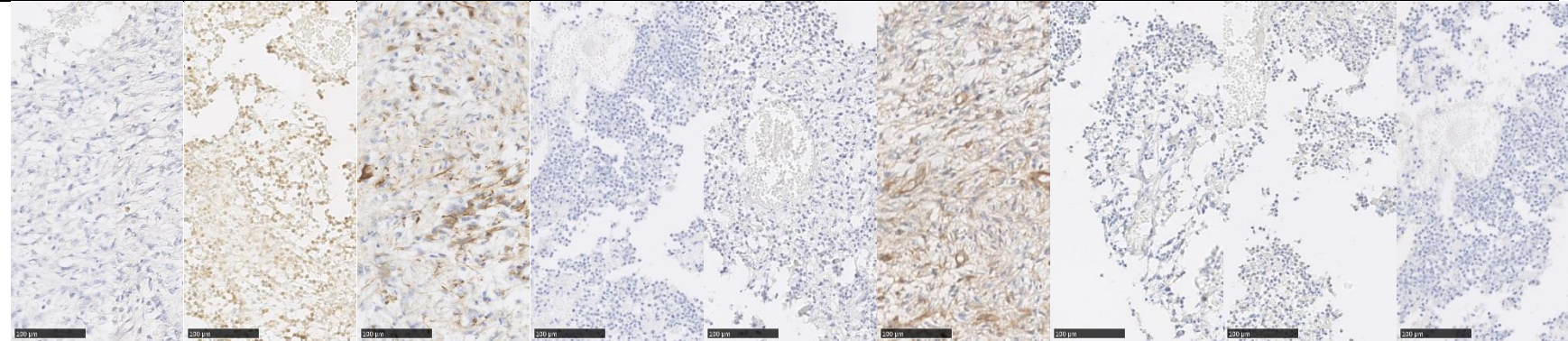
Case 27
Male 40
GBM



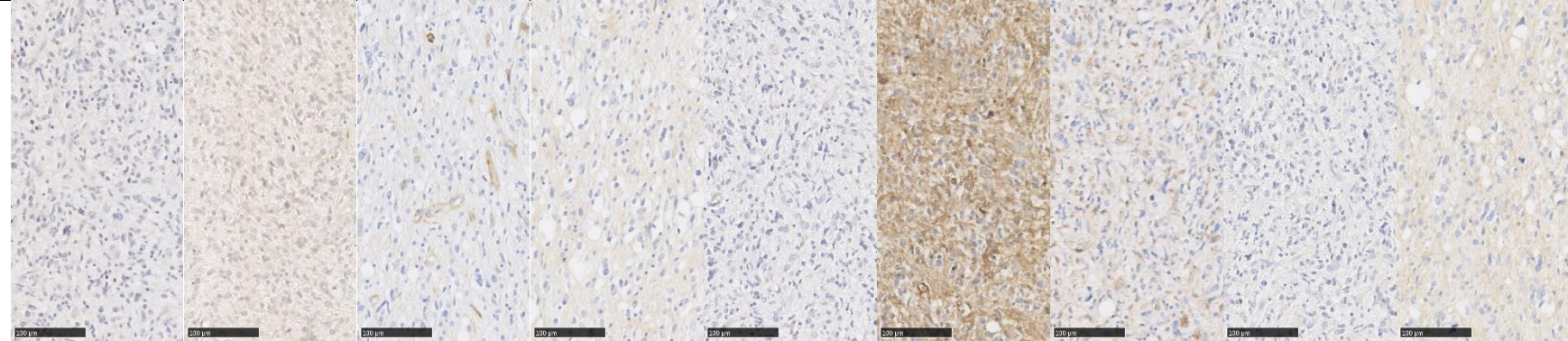
Case 28
Female
58 GBM



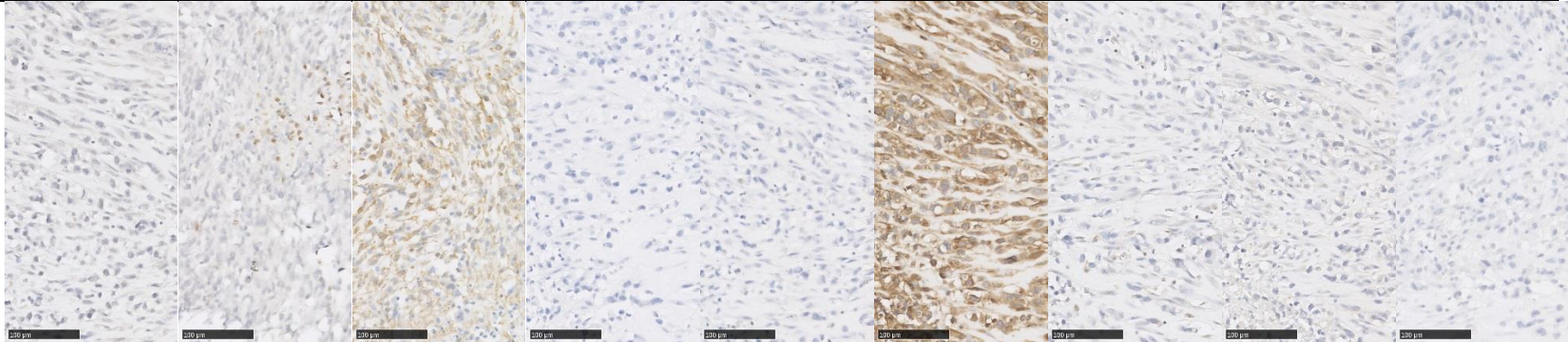
Case 29
Female
33 GBM



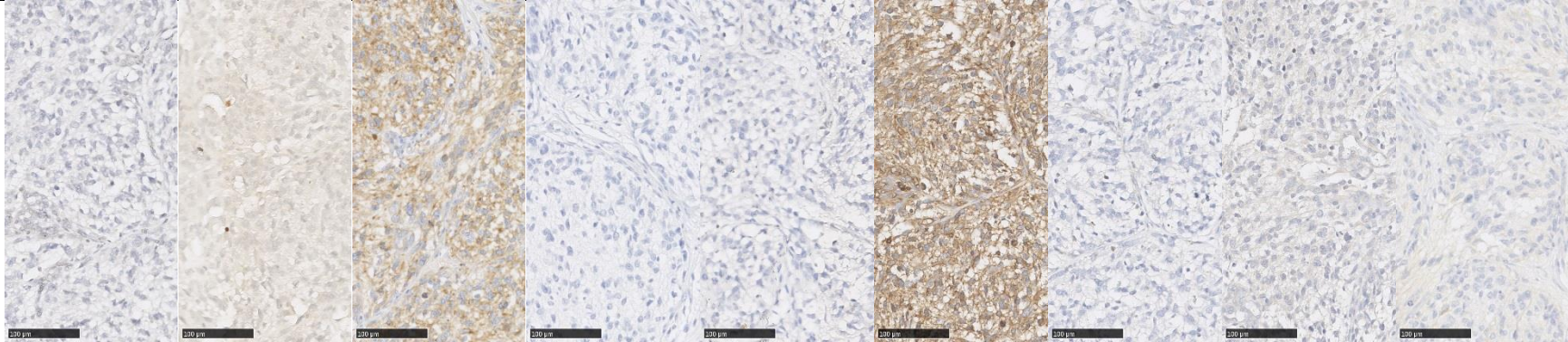
Case 30
Female
44 GBM



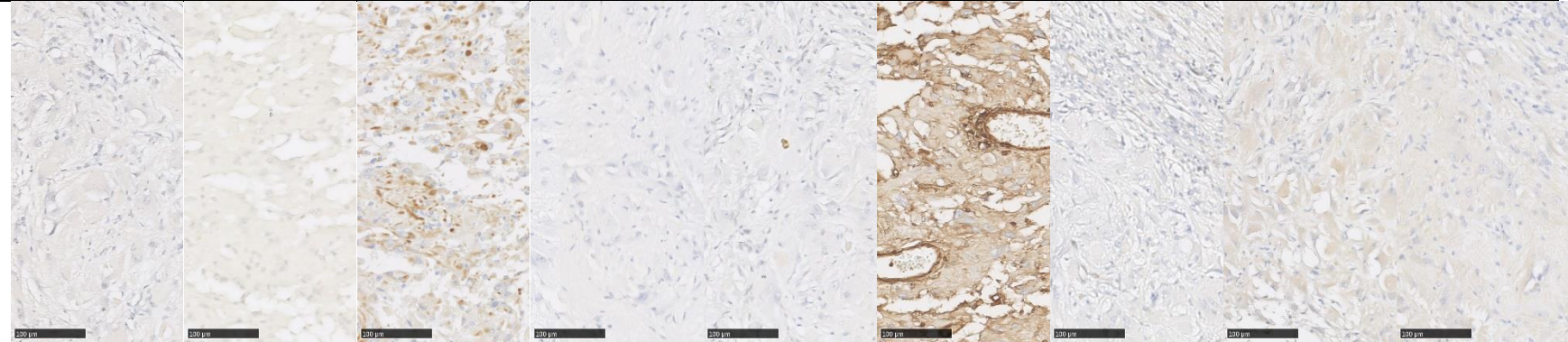
Case 31
Male 26
GBM



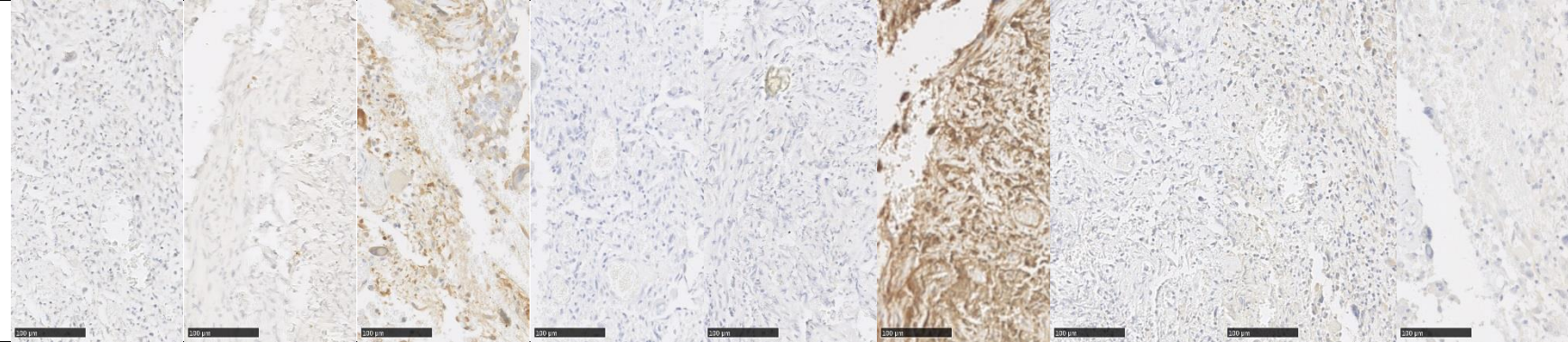
Case 32
Female 48
GBM



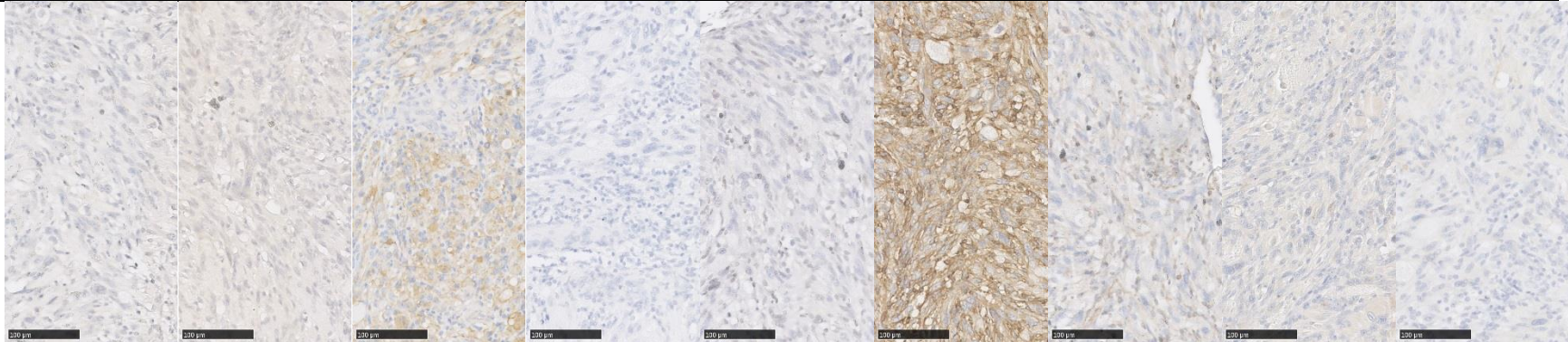
Case 33
Male 43
GBM



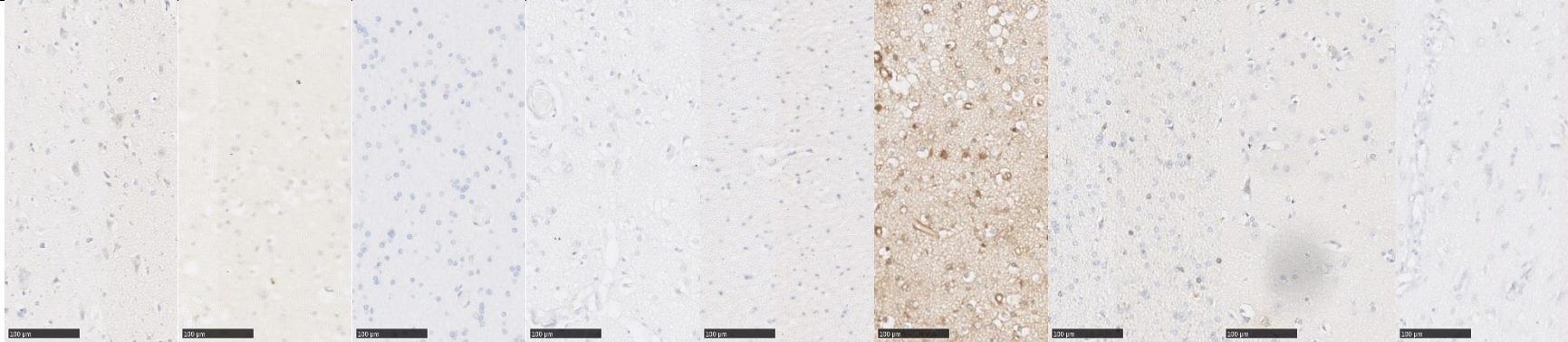
Case 34
Female
30 GBM



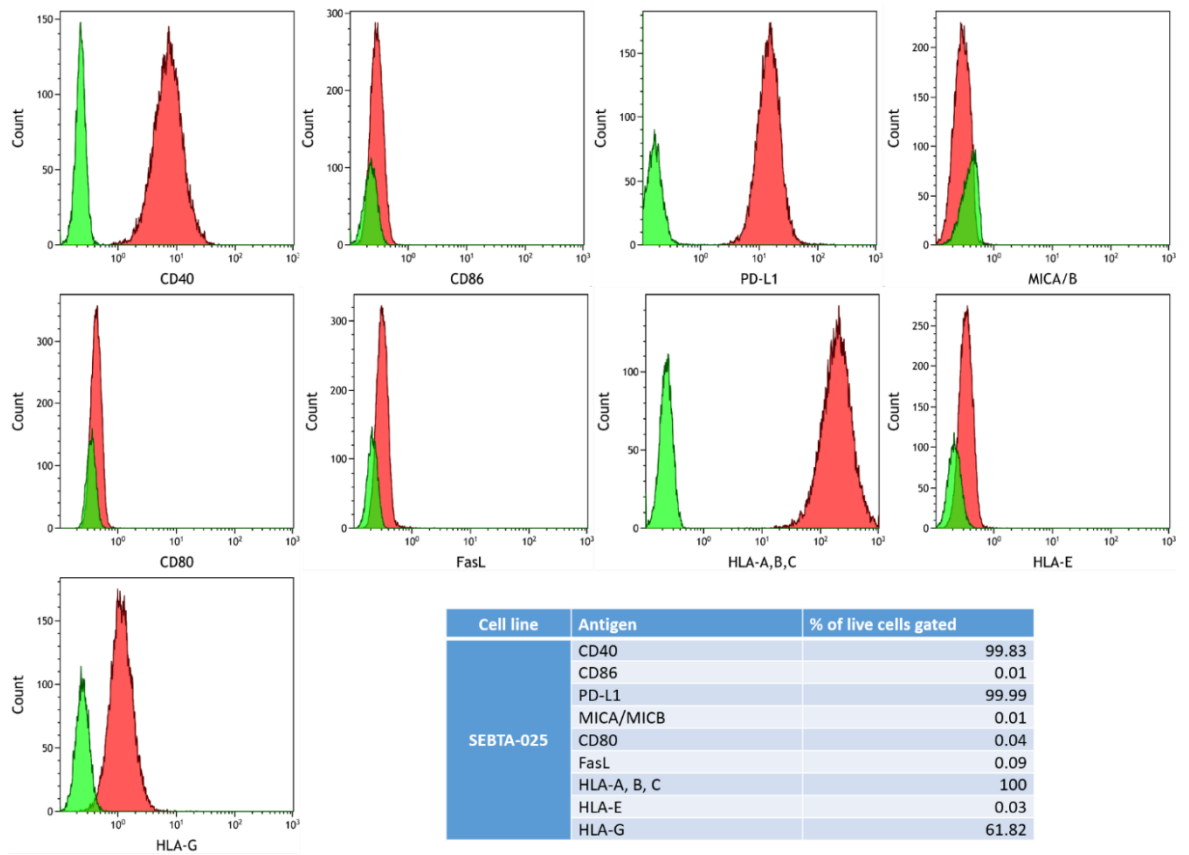
**Case 35
Female
42 GBM**



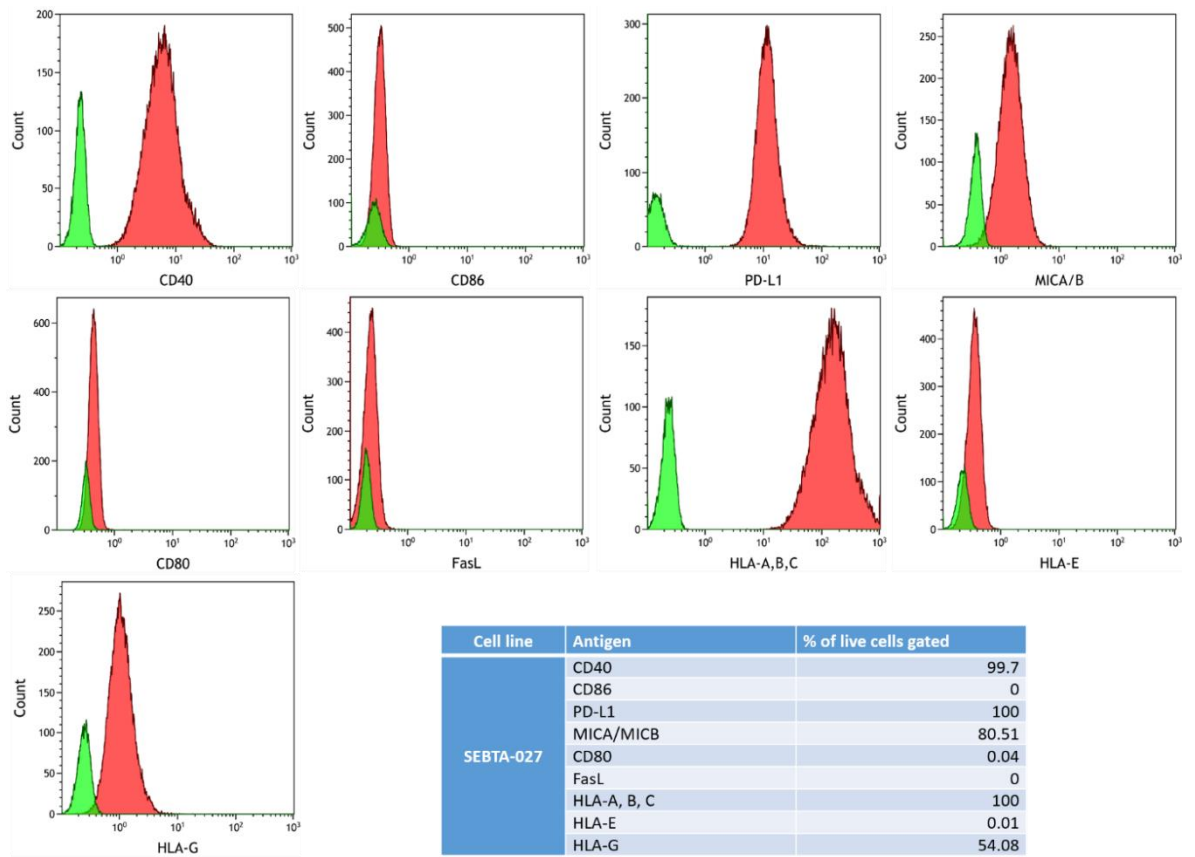
**Normal
brain**



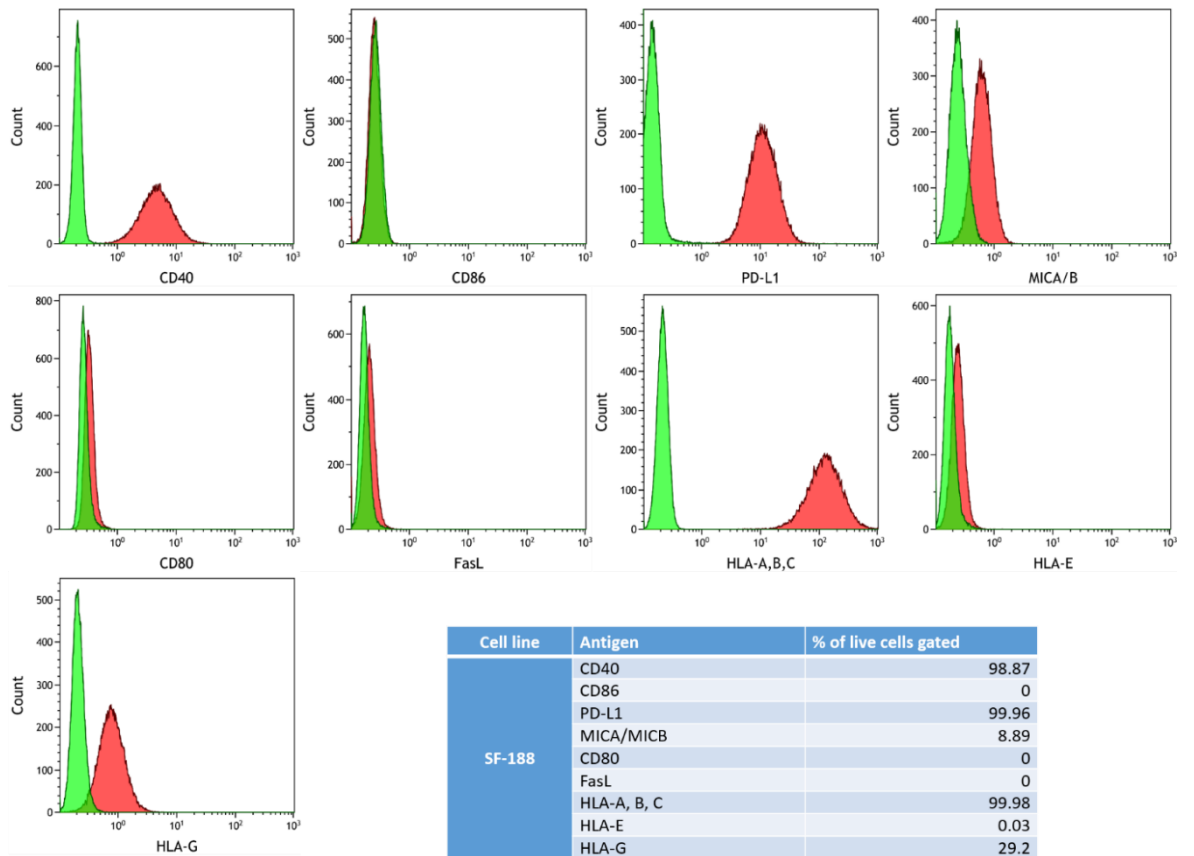
Appendix 2. Break down of the flow cytometry histograms for each GBM cell line



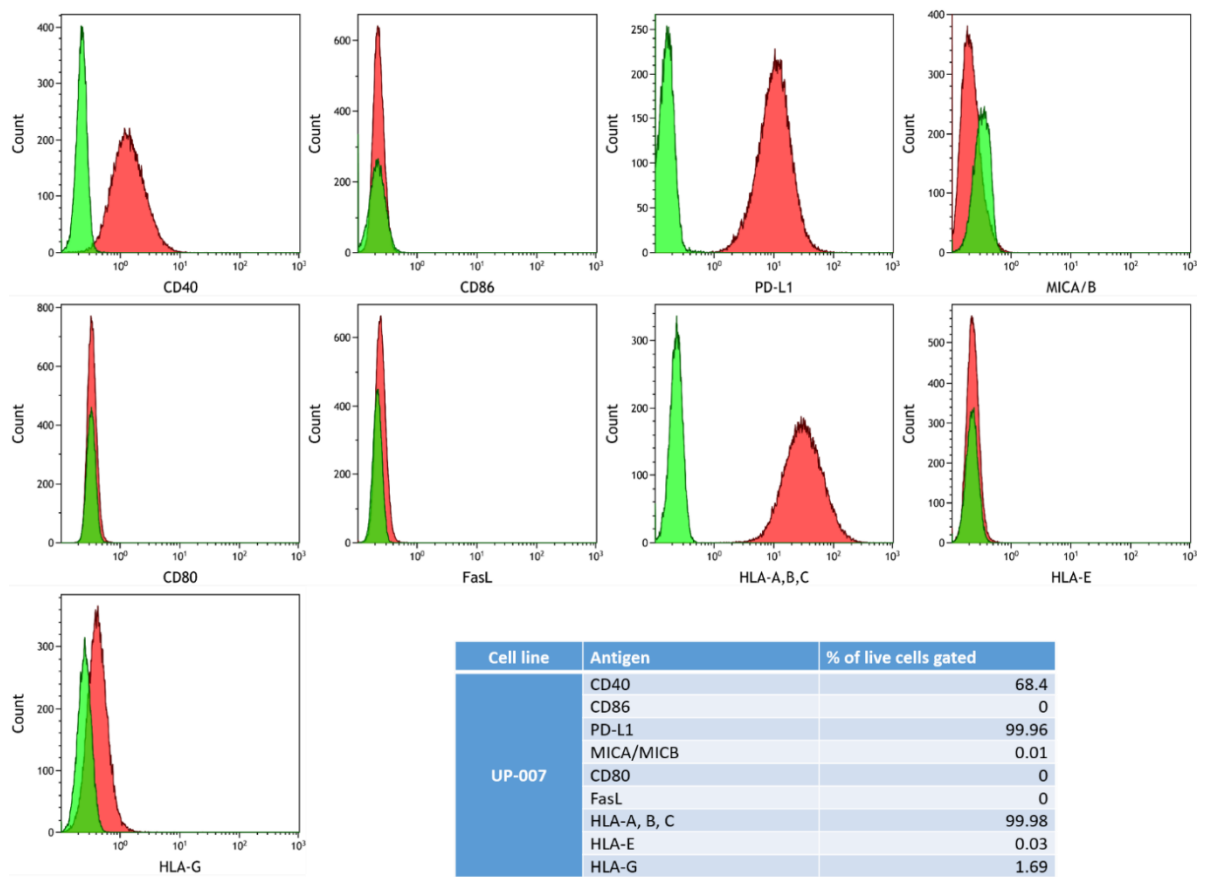
Appendix 2 Figure 1. SEBTA-025 the green peaks represent unstained cells whereas the red peaks represent stained cells



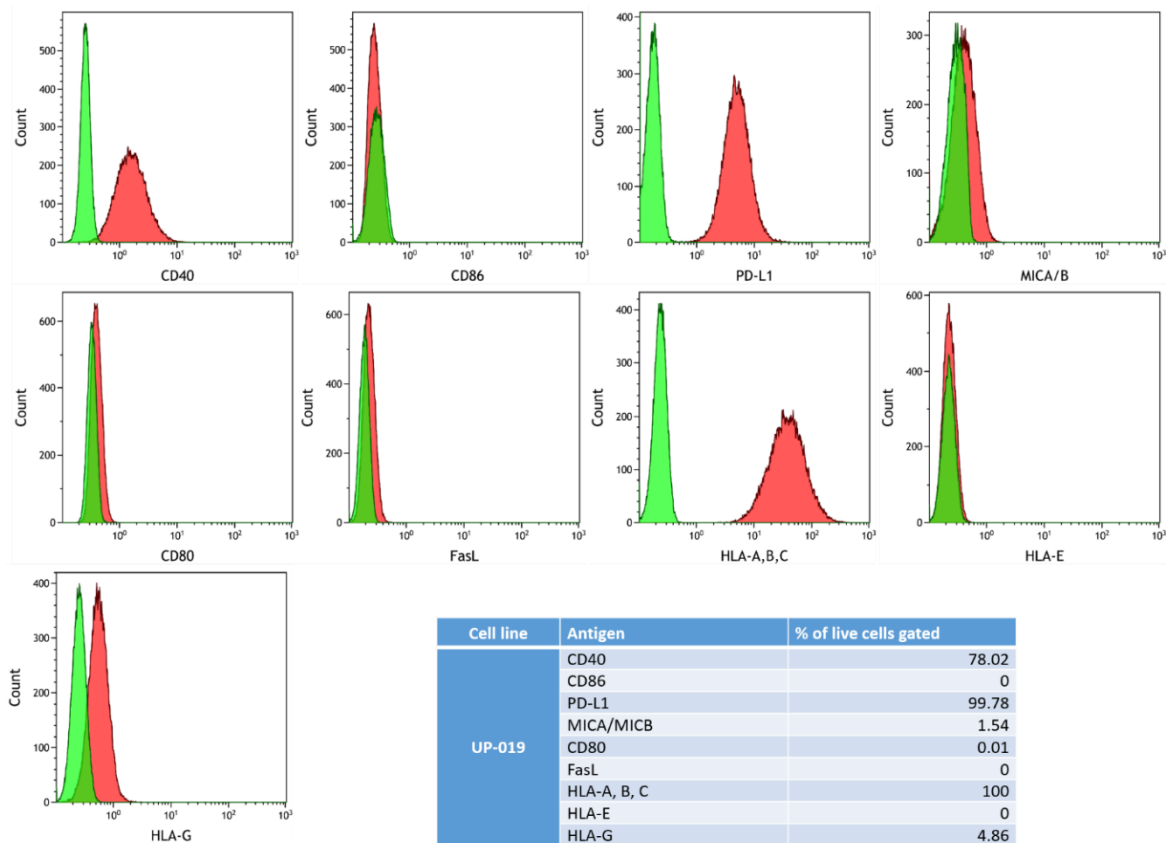
Appendix 2 Figure 2. SEBTA-027 the green peaks represent unstained cells whereas the red peaks represent stained cells



Appendix 2 Figure 3. SF-188 the green peaks represent unstained cells whereas the red peaks represent stained cells

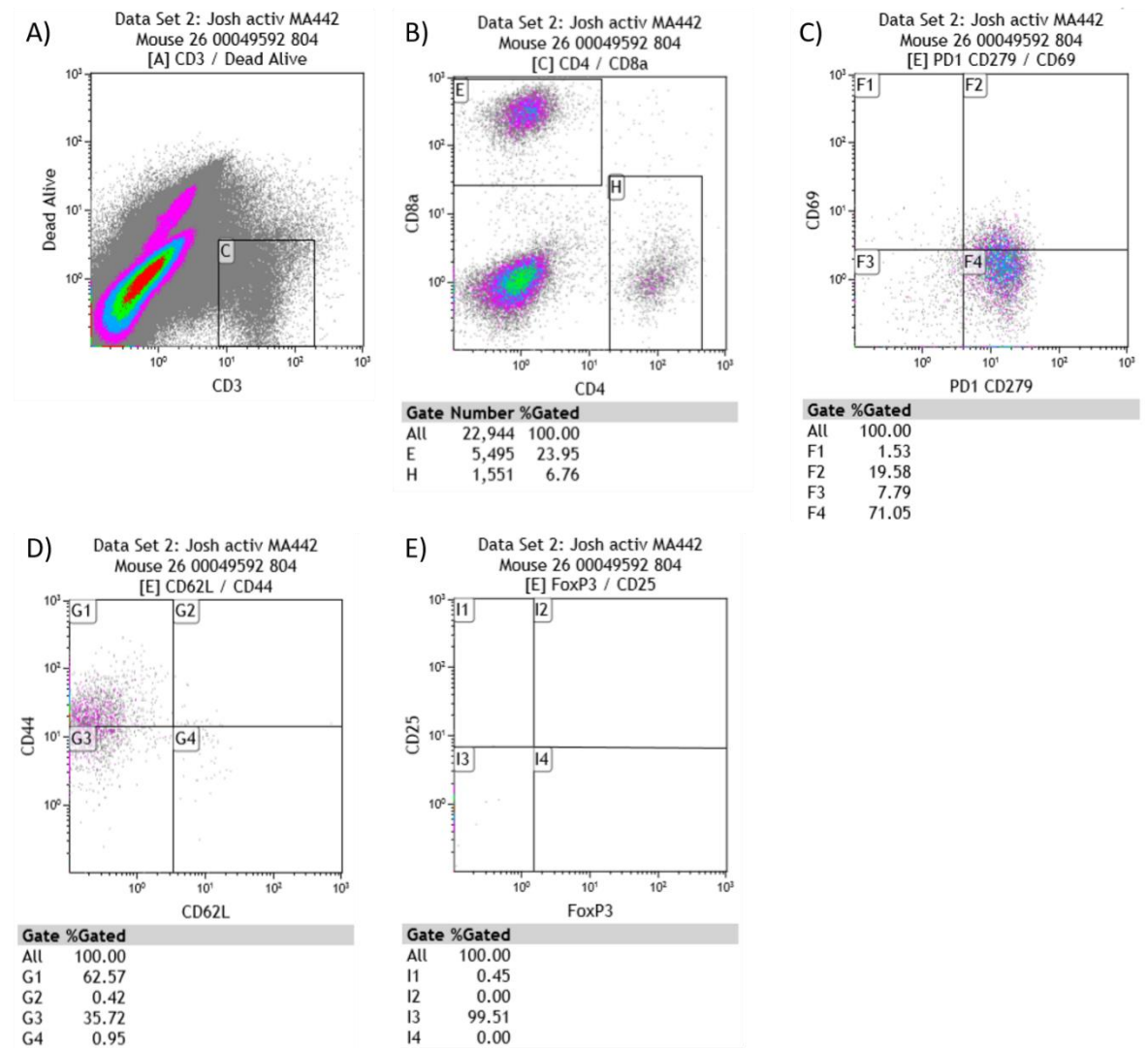


Appendix 2 Figure 4. UP-007 the green peaks represent unstained cells whereas the red peaks represent stained cells

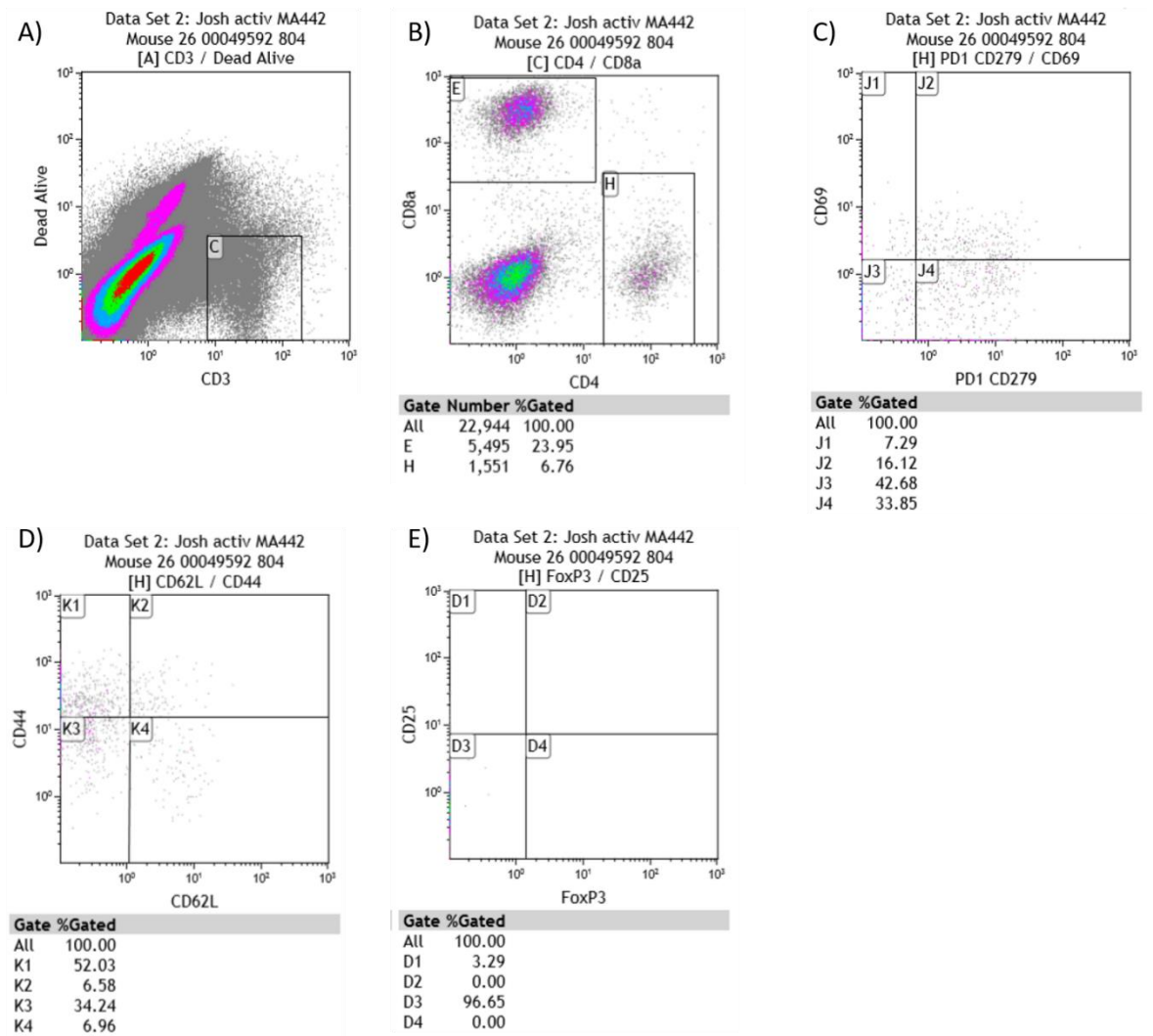


Appendix 2 Figure 5. UP-019 the green peaks represent unstained cells whereas the red peaks represent stained cells

Appendix 3. An example flow cytometry plot obtained from B16HHDII intracranial tumour infiltrating lymphocytes



Appendix 3 Figure 1. Breakdown of flow cytometry staining of CD8⁺ TILs. A) Live CD3⁺ cells were gated out of the TIL population and then in B) CD3⁺ cells were then split into CD4⁺ and CD8⁺ cells which were then further probed. C) Dot plot of CD69 and PD-1 stained CD8⁺ cells D) Dot plot of CD44 and CD62L stained CD8⁺ cells E) Dot plot of CD25 and FoxP3 stained CD8⁺ cells.



Appendix 3 Figure 2. Breakdown of flow cytometry staining of CD4⁺ TILs. A) Live CD3⁺ cells were gated out of the TIL population and then in B) CD3⁺ cells were then split into CD4⁺ and CD8⁺ cells which were then further probed. C) Dot plot of CD69 and PD-1 stained CD4⁺ cells D) Dot plot of CD44 and CD62L stained CD4⁺ cells E) Dot plot of CD25 and FoxP3 stained CD4⁺ cells.